

Fabian Hansmann

The Missing Link between Asset Data and Asset Management

RR 2

MONOGRAPHIC SERIES TU GRAZ
RAILWAY RESEARCH



Fabian Hansmann

**The Missing Link between Asset Data
and Asset Management**

Monographic Series TU Graz

Railway Research RR

Series Editor

Univ.-Prof. Dipl.-Ing. Dr.techn. Peter Veit

Monographic Series TU Graz

Railway Research

Volume 2

Fabian Hansmann

The Missing Link between Asset Data and Asset Management

This work is based on the PhD thesis “Innovative Messdatenanalyse – ein Beitrag für ein nachhaltiges Anlagenmanagement Gleis”, presented at Graz University of Technology; submitted to the Faculty of Civil Engineering, in 2015.
Assessor A (internal) Peter Veit (Graz University of Technology)
Assessor B (external) Stephan Freudenstein (Technische Universität München)

© 2018 Verlag der Technischen Universität Graz

Cover photo	Stefan Marschnig
Layout	Christina Fraueneder, TU Graz Stefan Schleich, TU Graz
Print	Medienfabrik Graz mfg.at

Verlag der Technischen Universität Graz
www.ub.tugraz.at/Verlag

Print

ISBN 978-3-85125-567-6

E-Book

ISBN 978-3-85125-568-3

DOI 10.3217/978-3-85125-567-6



<https://creativecommons.org/licenses/by/4.0/>

Vorwort zur Schriftenreihe Railway Research

Das Institut für Eisenbahnwesen und Verkehrswirtschaft der Technischen Universität Graz beschäftigt sich als Institut der Fakultät für Bauingenieurwissenschaften mit der Eisenbahninfrastruktur, und zwar den bautechnischen Fragen des Errichtens des Fahrwegs, des Betrieb der Strecken und damit eng verknüpft seiner Wartung und Instandsetzung. Damit sind sämtliche für eine Betrachtung des gesamten Lebenszyklus der Infrastruktur erforderlichen Bausteine abgedeckt.

Das Einbeziehen wirtschaftlicher Bewertungen der Lebenszyklen erlaubt den Schwerpunkt „Nachhaltigkeit“ umfassend in technischer, betrieblicher und wirtschaftlicher Sicht abzudecken. Die Forschungsfragen betreffen dabei das Gleislageverhalten, mit der Zielsetzung dieses prognostizierbar zu machen und damit die Voraussetzung für präventive Instandhaltung zu schaffen. Die Forschung des Instituts in betrieblicher Hinsicht umfasst Fahrplangestaltung und eine auf Nachfrageprognosen aufbauende Netzentwicklung sowie Auswirkungen unterschiedlicher Verfügbarkeiten. Alle diese Themen werden im Forschungsbereich Life Cycle Management einer umfassenden wirtschaftlichen Bewertung zugeführt.

Mit diesem Ansatz versucht das Institut für Eisenbahnwesen und Verkehrswirtschaft seinem Anspruch das System Eisenbahn in Forschung und Lehre zu vertreten gerecht zu werden.

The Missing Link between Asset Data and Asset Management

Durch die Digitalisierung des Fahrwegs der Eisenbahn steht eine wachsende Menge an Daten zur Verfügung. Die Messdaten – meist einzelne Komponenten betreffend – stellen für sich jedoch keine Information dar. Sie sind eine Momentaufnahme eines Teils des Fahrwegs und somit für das Asset Management kaum verwendbar. Das „Missing Link“ zwischen Daten und Asset Management liegt nicht im Datenumfang sondern ist dem Bereich der Analyse zuzuordnen. Die Stoßrichtungen sind dabei die Einzeldaten im Systemkontext „Fahrweg und seine Belastung“ zu analysieren womit auch zusätzliche Information aus bekannten Daten ableitbar werden. Zudem gründen sich Entscheidungen des Asset Managements auf Prognosen des Verhaltens des Fahrwegs. Dazu werden Trendanalysen vorgestellt, auf deren Basis präventive Instandhaltung möglich wird, und somit die Frage Re-Investieren oder Instandhalten, aus technisch-wirtschaftlicher Sicht beantwortet werden kann. Die vorliegende Forschungsarbeit stellt Datenanalysen von Messdaten unter Berücksichtigung der Systemzusammenhänge im Gleis ebenso vor wie die dazugehörigen Trendanalysen und behandelt damit die wesentlichen Bausteine eines effektiven Asset Managements.

Peter Veit

To my family and Marion!

Leider läßt sich eine wahrhafte Dankbarkeit mit Worten nicht ausdrücken.

Johann Wolfgang von Goethe (1749-1832)

Abstract

Various loads on the railway track superstructure lead to continuous wear on the track components. As a result, the service life of single components and eventually of the whole system is limited. In order to create sustainable, fact-based maintenance plans, it is necessary to capture the condition of the track and the individual components in a reproducible, continuous fashion. Evaluating the asset based on measurement data, typically signals from track geometry cars, thus makes long-term budget planning possible and provides a solid basis for a sustainable asset management strategy.

Maintenance operations in Austria are typically reactive, based on the experience of local track engineers and fixed time intervals. However, it is possible to identify a shift during recent years, away from expensive reactive maintenance planning and towards more sustainable preventive strategies. The updated version of the European standard EN13848-4 (2014) is the first standard which distinguishes between different quality classes, focusing on classifying the track geometry.

Based on these facts, this thesis tackles the challenge of classifying the track geometry by considering its evolution over its service life in terms of its quality, based on measurement data. This measurement signal analysis will then be extended to describe the condition of individual components and an attempt made to classify signal features for specifically occurring damage patterns. This new analysis establishes both a load-based classification of track geometry and component-specific condition monitoring. The investigation is based on a database containing recording data and additional asset information for 3,800 track kilometres of the main Austrian network.

By calculating key statistical indicators, it is possible to develop objective asset monitoring based on a proven correlation between the recorded measurement signals and the track deterioration. This correlation is confirmed by local inspections. The condition monitoring hereby established estimates the remaining service life of each component, focusing on the ballast and sleepers. These form a basis for lifecycle-cost-based decision making, and enable medium-term budget planning.

Kurzfassung

Die in den Eisenbahnoberbau eingebrachten Lasten führen zu einem wachsenden Verschleiß unterschiedlichen Komponenten. Dieser Versagensmechanismus limitiert die Nutzungsdauer der einzelnen Komponenten und folglich jene des Gesamtsystems. Die Planung von zustandsabhängigen und verursachungsorientierten Maßnahmen erfordert eine reproduzierbare und kontinuierliche Erfassung des Anlagenzustands. Ein Anlagenmanagement, basierend auf der Auswertung von Messdaten, bildet dafür die mögliche Entscheidungsgrundlage. Es ermöglicht dem Infrastrukturbetreiber die Evaluierung des Netzzustandes und eine langfristige Planung seines Mitteleinsatzes.

Die Planung von Maschineneinsätzen erfolgt in Österreich durch den Infrastrukturbetreiber und beruht auf Erfahrungen, Gleisbegehungen, zeitlichen Intervallen und der Auswertung von Messsignalen. Die nationale Normung erwähnte bislang lediglich Schwellenwerte zur reaktiven Planung von Maßnahmen. Erst die kürzlich aktualisierte Fassung der EN13848-4 erlaubt es zum ersten Mal Messsignale in Qualitätsklassen einzustufen, legt das Hauptaugenmerk jedoch auf die Betrachtung der Gleislage.

Die vorliegende Forschungsarbeit verfolgt das Ziel die Gleislage unter Berücksichtigung ihrer zeitlichen Entwicklung über die Nutzungsdauer hinsichtlich ihrer Qualität zu klassifizieren. Darüber hinaus wird die Messsignalanalyse durch eine komponentenspezifische Zustandsbeschreibung erweitert, wobei versucht wird einzelne Signalcharakteristika eindeutig auftretenden Schadensbildern zuzuordnen. Die Herausforderung besteht in einer kontinuierlichen Beschreibung des Anlagenzustands, sowie der Interpretation der historischen Entwicklung zur Abschätzung zukünftiger Aufwände. Als Datengrundlage für die vorliegende Forschungsarbeit dient eine am Institut entwickelte Datenbank, welche 3.800 Gleiskilometer umfasst und sowohl Mess- als auch Oberbaudaten enthält.

Die aus der Berechnung der statistischen Kennziffern gewonnenen Erkenntnisse erlauben es dem Infrastrukturbetreiber so den Anlagenzustand zu erfassen und zu bewerten. Vor-Ort-Untersuchungen bestätigen die Korrelation zwischen unterschiedliche Versagensmechanismen und unterschiedlichen Signalen bzw. deren Charakteristik. Die zeitliche Entwicklung der statistischen Kennziffern erlaubt somit die komponentenspezifische Erfassung des Anlagenzustandes und dessen Bewertung hinsichtlich seiner vorhandenen Restsubstanz für Schwelle und Schotter. Diese bildet die Grundvoraussetzung für lebenszykluskostenbasierte Entscheidungen und erlauben eine mittelfristige Budgetplanung.

Content

Abstract.....	6
Kurzfassung	7
1 Introduction.....	11
1.1 Asset management.....	12
1.2 Objective and approach	14
2 Calculation of cumulative Load	17
2.1 Objective	17
2.2 Load Data	18
2.2.1 Underlying Data	19
2.2.2 The average section-specific Load as Indicator for the temporal Traffic Evolution.....	21
2.3 The estimation Function	25
2.4 Validation Process	31
3 Track Geometry	35
3.1 Introduction	36
3.2 On the Relationship between the Track Geometry Quality and Tamping Measures.....	38
3.2.1 Temporal Evolution of the Standard Deviation of the vertical Track Geometry	39
3.2.2 Evolution of the Standard Deviation of the horizontal Track Geometry	41
3.2.3 Evolution of the MDZ-a Indicator.....	42
3.3 Installation Quality and Removal Quality	43
3.4 On the Relationship between the Track Geometry and cumulative Loads	49
3.4.1 Definition of Terms	50
3.4.2 The Relationship between Q_n , b_n and Q_{ult}	51
3.4.3 Different Parameter Sets	53
3.4.4 Evolution of the Track Geometry in straight Sections ($R>600m$).....	55
3.4.5 The Relationship between consecutive Maintenance Periods.....	72
3.4.6 Sensitivity Analysis.....	74
3.5 Summary of the Classification Algorithm	76
3.5.1 Model Construction	76
3.5.2 Primary Classification.....	77
3.5.3 Secondary Classification.....	79
3.5.4 Comparison between fully and partially logarithmic evaluations.....	80
3.5.5 Implementation of the Classification in the TUG Network.....	81
3.5.6 Summary and Discussion of Results.....	85
3.6 The Connection between Wavelengths and Damage Characteristics	87
3.6.1 Historical Development of Fractal Analysis	90
3.6.2 Application of Fractal Analysis to the Track Geometry in the TUG Network	94
3.6.3 Network Analysis.....	98
3.6.4 Effects of ballast bed breakdown from a fractal analysis viewpoint.....	104
3.6.5 From Theory to Practice – visual Track Inspection	106
3.6.6 Construction of a Regression Model and its Possibilities	112
3.6.7 Summary and Future Developments	119

4	Sleeper condition monitoring.....	121
4.1	Introduction	122
4.2	Roughness of the track gauge.....	124
4.2.1	The Discontinuity Algorithm	126
4.2.2	Value Distribution	129
4.2.3	Installation Quality and Removal Quality	132
4.3	ProgMod Prediction Model.....	135
4.3.1	Construction of the Algorithm	135
4.3.2	Results of the Regression Model	136
4.4	Effects of Maintenance Actions and different Superstructure on the Quality Signal.....	140
4.5	Evolution of the standard deviation over the cumulative load	144
4.6	Network-wide Evaluation.....	148
4.7	Summary.....	150
5	Epilogue.....	151
	Bibliography	155
Annex 1	Glimpses into the TUG database.....	145
Annex 2	Construction of the TUG database	146
Annex 3	Recording signals, quality signals and quality values	147
Annex 4	The origins of recording signals – track geometry cars	146
Annex 5	Recording track geometry	147
Annex 6	Measuring rail profiles and abrasion.....	150

1

Introduction

In 2013, Deutsche Bahn Netz AG had 1.48 billion euros available for maintenance expenditure. A closer look at the allocation of this sum reveals that 720 million euros were attributed to track superstructure. Investment in the existing network cost the German taxpayer 1.3 billion euros for track superstructure. [Hempe 2014]

In 2013, ÖBB-Infrastruktur AG spent 487.5 million euros on maintaining track, although as the precise division of the costs into individual sectors is not available, it is not possible to make any statements about the investment ratios at this juncture. [Bundesministerium für Wissenschaft und Verkehr 2013]

In the 2009/10 business year, Network Rail spent 464 million pounds on track maintenance, and a further 698 million pounds on laying new track. [Audley, Andrews 2013]

Railway infrastructures require a huge capital commitment to operate. One of the important tasks railway infrastructure manager must carry out is the development of a strategy that balances maintenance and reinvestment, avoiding potential security risks or non-availability risks while reducing growing cost pressures. To develop such a strategy, an accurate report of the current state of the railway lines is required, which can then be used to determine suitable future measures. These measures, which may be preventive or corrective (reactive), will focus on improving the state of the track, enabling it to reach or even exceed its expected service life. A preventive maintenance plan based on meaningful track monitoring not only enables sustainable usage of the infrastructure, but also, among

other things, makes it possible to reduce the costs of corrective maintenance. [Hansmann, Marschnig 2012]

DB-Netz AG achieved a 47% reduction in track maintenance costs through preventive measures on the rails (grinding, milling and planing). The higher costs for preventive work were outweighed by the savings made as a result of the reduction in the number of rail sections that had to be replaced. The preventive maintenance reduced the extent of the damage, thereby prolonging the service life of the rails. [Hempe 2014]

1.1 Asset management

"Systematic and coordinated activities and practices through which an organization optimally manages its assets and their associated performance, risks and expenditures over their lifecycle for the purpose of delivering the organization's business objectives."

"coordinated activities of an organization to realize value from assets"

[Woodhouse 2014]

The International Union of Railways (UIC) defines the primary objective of an asset strategy as being to optimize decisions on inspection, maintenance, renewal and enhancement of the infrastructure, so as to minimize the overall lifetime costs. To this end, an asset management strategy has the following outline [UIC 2010]:

- Inspection regime
- Maintenance and renewal intervention criteria
- Equipment obsolescence assumptions
- Technical strategies
- Redundancy
- Cost of inspection, maintenance and renewal

A sustainable asset management strategy is founded upon an objective survey of the current state of the assets and the resulting evaluation of their quality. Based on this evaluation, it is possible to identify possible developments and time-critical measures which aim to achieve set goals. The sooner the state of the assets can be assessed – for example, observing the changes over time helps to determine necessary long-term measures – the sooner an efficient, sustainable resource allocation plan can be developed. The asset strategy for infrastructure manager includes a large number of diverse assets with a wide range of service lives and differing inspection and maintenance requirements. The track system itself, comprised of diverse interdependent components which are exposed to significant

loads, sits at the core of the following work. A simplified breakdown into the following components can be made:

- Rails
- Fasteners
- Sleepers
- Ballast
- Substructure

The malfunctioning of a single component not only threatens the availability of the entire system, but also affects the service life of the entire track.

As demonstrated by the example of the Austrian Federal Railways (cf. [ÖBB Infrastruktur AG 2012]), railway network infrastructure organizations determine the state of their equipment through a combination of inspections by experts and the operation of track recording cars on main routes. Both of these techniques have advantages and disadvantages, only some of which will be briefly noted at this point.

The track recording car makes it possible to obtain an overview of various different measurements in a short time. The difficulty lies in associating these measurements with the wear of distinct components. By contrast, during a track inspection it is possible to observe and assess the wear of individual components at a particular location. However, track inspections are both expensive and time-consuming. They are only worthwhile when carried out by specialist experts; furthermore, the results will still be subjective to some extent. Consequently, it is difficult to reproducibly assess the complete network on different occasions throughout the year. Combining both techniques gives the infrastructure organization maximum utility.

Many railways simplify the evaluations to individual signals, which can then be compared with certain thresholds – either standard or internally defined – from which potential future measures can be defined. The principal focus is often on observation of the track geometry, while other components and even temporal evolution are frequently not considered (cf. [Pace 2012]). However, the diverse measurements captured by track geometry cars offer possibilities far beyond simply assessing the track geometry; they can be used to construct additional information concerning the condition of specific components.

1.2 Objective and approach

In recent years, research has shown a relationship between the value of particular recording signals and the damage patterns manifested in the track system or the resulting measures adopted. (cf. [Auer 2004], [Auer et al. 2007], [Auer 2013], [Bocciolone et al. 2007], [Selig et al. 2008], [Faiz, Singh 2009], [Matsuda et al. 2011]).

Various IT solutions have been developed around the intersection between recording signals and asset management. These solutions facilitate the evaluation of the recording signals and make it possible to observe developments over time in combination with additional information, such as track superstructure (cf. [Jovanovic 2003], [Pace 2012], [Auer 2004]).

A key objective of this work is to test the possibility of evaluating component condition by specifying the characteristic features of distinct recording signals.

Such an evaluation would not only create a basis for a condition-based maintenance planning, but would also permit the classification of individual routes within the network based on the state of individual components. The focus therefore lies not on the evaluation of individual recording signals *per se* (in their original form), but rather on a description of their features based on statistical indicators and distinct quality scores. Recording signals may be composed of various wavelengths; a first step is to describe the signal in terms of its absolute value and roughness. These two attributes can be summarized with the help of various statistical indicators such as the median and the standard deviation, whose evolution can then be described. Where these statistical indicators succeed in classifying different damage patterns with respect to the components, a description of the wear over time can be determined based on the evolution of the corresponding statistical indicators.

By contrast with many of the existing solutions, the following work does not aim just to visualize, but rather to classify and evaluate. In the case of track geometry, for example, according to the state of the art the standard deviation is used to compare the different regions. Calculating the standard deviation of the vertical alignment not only makes it possible to observe their evolution, but also enables signal features to be captured in a particular way in order to form conclusions. Firstly, the evolution, often neglected, makes it possible to assess when measures become necessary before specified thresholds are reached. Secondly, when calculating the standard deviation, the signal is considered as a whole, rather than divided into distinct frequency ranges. Such a division, however, may yield information about the exact pattern of damage.

The algorithm established here does not concentrate on verifying security-critical thresholds, but rather focuses on establishing a solid basis for decision-making leading to a sustainable asset strategy. When a security-critical threshold is crossed, an action will be triggered, thereby precluding any other options. A strategically sustainable action plan thus becomes obsolete, as only the effects of the actions can be discussed, and not their necessity.

The planning of the actual construction work is not done through the algorithm developed here, as neither the general parameters of the railway nor those related to construction are considered. The classification of the equipment condition gives those responsible for the infrastructure a basis to argue for particular measures and propose developments, although the decisions about the measures concerned, and therefore also the final responsibility, still lie with the infrastructure operator.

It is difficult to form an exact definition of the pattern of damage, since reactions to the various stresses vary according to the numerous different existing track components. It is therefore necessary to construct a rough definition, so that specific patterns of damage related to single recording signal features or feature combinations can subsequently be classified. Describing the condition of the rails and subgrade forms part of another thesis, whose findings are included within the GleisPROPHET research project and which will appear in parallel with or in advance of this one [Hansmann, Marschnig 2012].

Damage to the rails, starting with surface defects and continuing to rail wear, can be considered more or less independently of the overall system, since, with a few exceptions, rails can be replaced independently of the rest of the system. Only when the condition of the rail surface causes an increase in the forces exerted (e.g. due to corrugations) does it become necessary to consider this interaction in more detail [Hansmann, Marschnig & Veit 2011]. Due to this fact, recording signals relating to the rails will not be considered in this work.

Describing the state of the subgrade forms part of a thesis by Matthias Landgraf [Landgraf 2016] which will be published as part of the GleisPROPHET research project. Depending on the stresses, a non-negligible interaction can occur between the subgrade and the ballast bed. Parts of this thesis are therefore interdisciplinary and based on jointly-obtained results or evaluation techniques, and will be identified as such.

Various recording signals from the Austrian Federal Railway network form the basis for the evaluations carried out in this work (see Annex 1). Without loss of generality, the analysis

in Austria can therefore be restricted to the following typical damage patterns (cf. [Auer 2010], [Zhang, Murray & Ferreira 1999]):

Ballast Fouling	Subgrade Ballast deterioration Contamination introduced by transported goods
Loss of traction	Failure of rail mounting Wear of rail pads Deterioration of ribbed base plate Horizontal/vertical embedding of rail feet
Deterioration of sleepers	Crack Split

Table 1 Definition of damage patterns

Following this precise classification of the various damage patterns, the total track loads can be determined, statistical indicators can be defined and their evolution in response to growing loads analysed. Finally this combination leads to a classification of the asset. It is possible to validate this process using information regarding track renewals and mechanised maintenance within last 13 years, combined with detailed track in-situ inspection (track walks) related to more than 25 reinvestment projects. Working in cooperation with the ÖBB, these reinvestment projects have been examined in the context of the last three years.

Working closely with the ÖBB, specifically with the regional management for the West Region, it was possible to validate results from the GleisPROPHET project, within establishing a test region. In the context of this test region, it was possible to locally verify both the results of the recording signal evaluation and the inspections, in the context of the reinvestment projects.

2

Calculation of cumulative Load

2.1 Objective

The various forces to which the system is subjected lead to wear on individual track components and eventually to failure of the overall system. In order to describe the deterioration of individual components, it is necessary to record the progression of wear for each one separately. Starting with the assumption that component wear can be described by individual statistical indicators, this assumption may be inverted, resulting in the following objective: to describe how these statistical indicators evolve over the service life of the track.

Depicting just the development over time of particular statistical indicators enables only a limited version of such a description. Because such a comparison only permits partial correlation with the applied loads, meaning that the analysis of the statistical indicators is unavoidably subject to deviation. Two sets of components, where the track superstructure ages are the same, but the traffic loads differ, are subject to substantially different cumulative loads and their condition will therefore evolve differently, inasmuch as this is affected by the load.

Strongly divergent dynamic demands on the track system caused by differing vehicle-specific speeds and types of vehicle will not be taken into consideration. Individual vehicles with different operating characteristics will travel the same section of a route with different speeds, thereby resulting in a wide distribution of forces on the system. Due to both the

lack of information available for a description and the necessity of simplifying the problem, a different way of estimating or approximating this effect is required. Increasing system loads resulting from divergent curve radii are an exception, and can be approximately modelled. Independently of the aforementioned differences in curve geometry, the simplifying assumption is applied that the vehicles and their speeds over the studied track sections are evenly distributed, so that the gross tonnage is sufficient to describe the forces.

For example, it will be assumed that the distribution of the speeds at which straight track stretches are travelled is similar throughout Austria, independent of the geographical location of the route section and bounded only by the admissible speed of the section. Although subject to a certain amount of imprecision, this assumption makes it possible to consider the temporal evolution of the condition of the equipment merely in terms of statistical stresses.

The statistical stresses are composed of diverse longitudinal, lateral and vertical forces. The daily loads on the route provide the basis for modelling these forces. By considering different curves, it is possible to draw conclusions about the varying lateral forces, whereas the longitudinal forces are almost ignored. [Führer 1979]

Individual effects, such as the influence of weather conditions, can only be recorded with difficulty, and therefore will not be considered in the network-wide analyses.

2.2 Load Data

It is important to find a way to draw cross-section-specific conclusions about the cumulative load based on the available load data. The cumulative load approximates the forces applied to the system within a particular time period. Although this time period can be freely defined, in the context of this work it will be bounded by the year of sleeper installation and a selected reference point. Where track superstructure components have been reused, this assumption will lead to erroneous conclusions. In contrast to laying new track, track reuse does not incorporate new track materials, but reuses salvaged track materials. On the routes in the TUG network (see Annex 1) salvage materials are in the minority, meaning that this effect can be ignored.

2.2.1 Underlying Data

The available load data comprises various transport-related data collected over differing time periods and originating from disparate sources. This might initially seem unfavourable to an approximation of the cumulative load. The rest of this section will primarily provide an overview of the underlying data, identifying potential correlations and testing the plausibility and accuracy of the data. To this end, the load data analysis in this work distinguishes between section-specific (determined per section) and network-wide (determined across the network) load data.

Section-specific load data in total gross tonnes per day and per track is available for the years 1999-2002 and 2007-2013. The data for 1999-2002 specifies the daily track load for each numbered route section (DB776) of the existing network. These are determined based on a representative week and projected across the entire year. The track loads determined in this way are adapted to the structure of the TUG database and combined with the existing data.

For the years between 2007 and 2013, the loads were determined over the entire year by the caused track access charges. The mapping into the TUG database took place according to route cost centres, which further divide the network, thereby allowing for more precise information. Only the data from 2007 was included in the database. The loads during the year 2013 reflect the effects of the economic crisis and therefore do not by themselves constitute solid input data for a load model.

The load data contained in the database for 2010 is based on real, manually processed train figures for the entire year.

The **network-wide load data** comprises disparate traffic-specific figures and can be very generally divided into two groups based on the data source. The data from 1971 to 2001 is taken from the rail- and cableway statistics of the Austrian Republic [Bundesministerium für Wissenschaft und Verkehr 1971-2001]. Over this period, a few figures that generally pertain to the entire existing Austrian railway network, are missing just for the years 1992 and 1993.

After 2001, the ministry's responsibilities were partly taken on by Schienenkontrollgesellschaft GmbH (SCG), who continued to supply the statistics in a similar form. In parallel with this, the company reports of the Austrian Federal Railway [ÖBB-Holding AG 2013] provide additional, precise information; the figures from the SCG will always be compared to these. In so doing, it is nonetheless important to note that the data provided in the company reports only refers to the Austrian federal railway network, and in some areas to

parts of the corporation. However, it can be assumed that the reduction of the network length or the alteration of the reference network have a negligible effect on the evolution of the operational performance. This assumption is based on the fact that over the last few decades, the routes which have been decommissioned have naturally mostly been those with very low traffic volumes, and the share of private infrastructure operators in Austria is proportionally small (see Figure 1). Although it may be the case that there is a correlation between the operational performance of private infrastructure operators and the entire network, there will certainly be no significant influence on the evolution of the global operational performance.

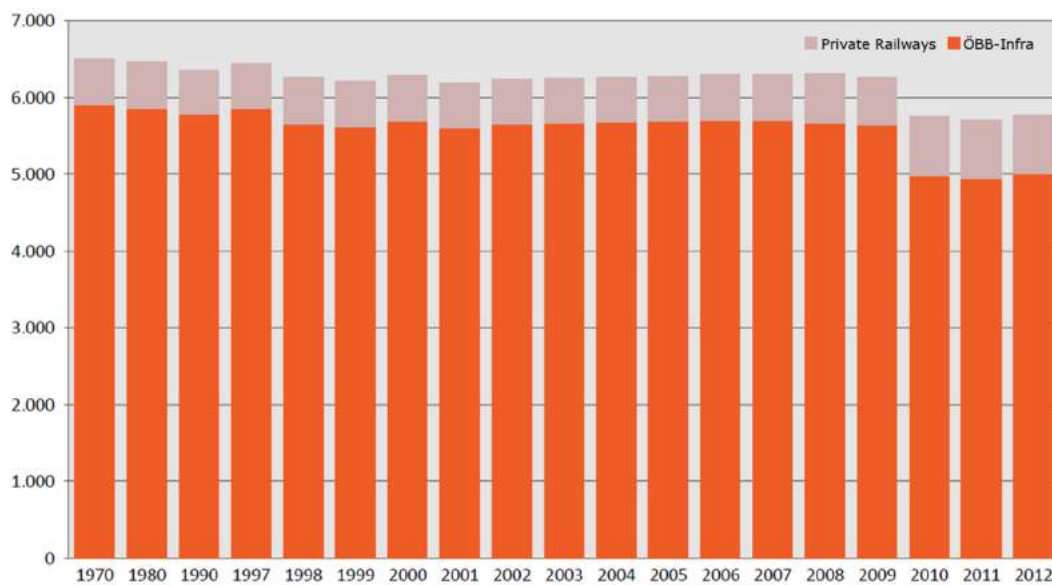


Figure 1 Evolution of the railway network in Austria (structural length in kilometres)
[Röhlsler 2013]

This correlation looks different, however, when the change in transported freight over the last 40 years is considered (see Figure 2). A detailed analysis shows a sudden increase in transported freight in 2009, which can be solely attributed to the acquisition of MAV Cargo. This example clearly demonstrates that specific attention must be paid to the data sources when interpreting individual values.

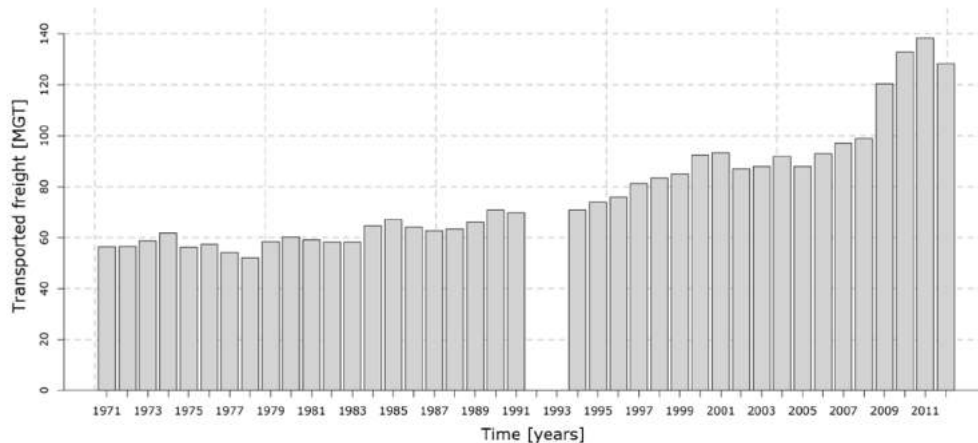


Figure 2 Temporal evolution of transported freight

For the initial analysis, the load data taken from control points on the TUG network in the years 1997, 1998, 1999, 2000, 2001, 2002, 2007 and 2010 serves a basis for calculating the cumulative load. It is important to consider the possibility of developing a load function from the available track-specific load data. This will permit the calculation of the cumulative load based, at a minimum, on the average service life of the equipment. The load function aims to make it possible to estimate the evolution of the load on the track through the course of its service life. Its function is not to accurately describe the evolution of the load in future years, nor to accurately model every development. To provide an overview of the available load data from individual control points, the temporal evolution of the average daily track load will be considered (see Figure 3).

2.2.2 The average section-specific Load as Indicator for the temporal Traffic Evolution

The temporal evolution of the average section specific load in the TUG network (see Figure 3) shows a clear increase in traffic loads up to 2007. The reduced track load in 2010 reflects the effects of the economic crisis, although the losses are smaller than expected. The simple fact that there are very few section-specific values makes it difficult to carry out a time series analysis of the evolution of the track load. The concentration of values in 2000 would strongly affect and partially distort any possible estimates of the load evolution resulting from a regression analysis. The values from 2010 should also be excluded from a time series analysis due to the fact that they do not reflect the historical load evolution over the service life of the track. The evolution of the section specific loads cannot be used for the calculation of the cumulative load, because firstly too few values are available and secondly because those which are available are highly compressed into particular time periods.

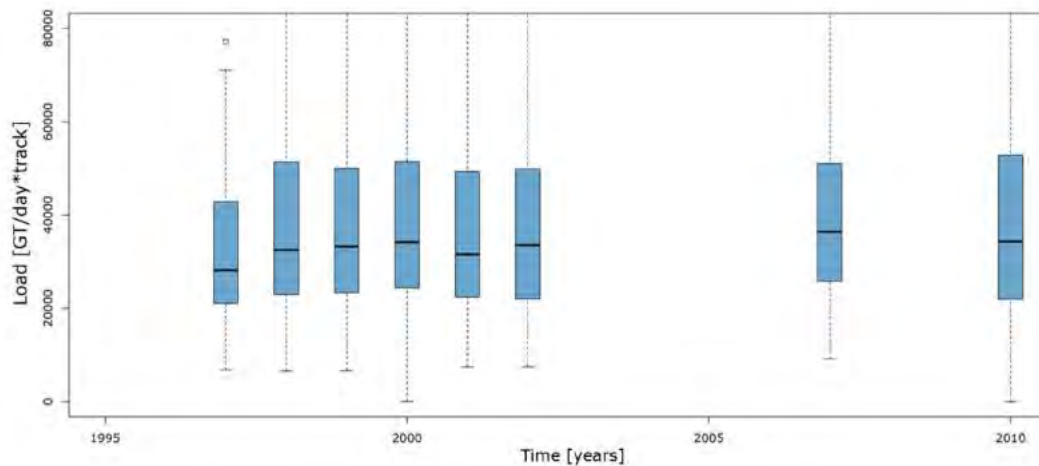


Figure 3 Evolution of the average track load in the TUG network

It is therefore necessary to find another way to obtain data on load evolution. The network-wide evolution of various indicators has a larger sample size, and thus permits a considerably more stable characterization of the load increase. The resulting regression function only describes the evolution of the load increase over the whole network. In the below work, it will be supposed that the average evolution can be projected onto individual routes. The network-wide load increase will therefore be converted to a route-specific evolution. The resulting loss of precision is acceptable, although this model cannot be used to model the apportioning of loads to newly created alternative routes or section-specific particularities. The load evolution per cross-section will be estimated over the evolution of the whole network, as it is impossible to determine it precisely.

Various indicators can be used to estimate the load evolution. Calculation of the cumulative load therefore requires an indicator which combines the weight of the train with the transport distance. The network-wide evolution of total gross tonne kilometres (gtkm) can therefore be used as the basis of the load model. The first stage is to collect various basic network-wide parameters from past years and compare them. This comparison will further act as a plausibility check between the data points and finally form the basis of the development of an estimation function. The estimation function will model the network-wide evolution of the selected indicators as far as possible, using a calculated regression model. The function therefore represents the network-wide development and should be used to calculate the load in each cross-section.

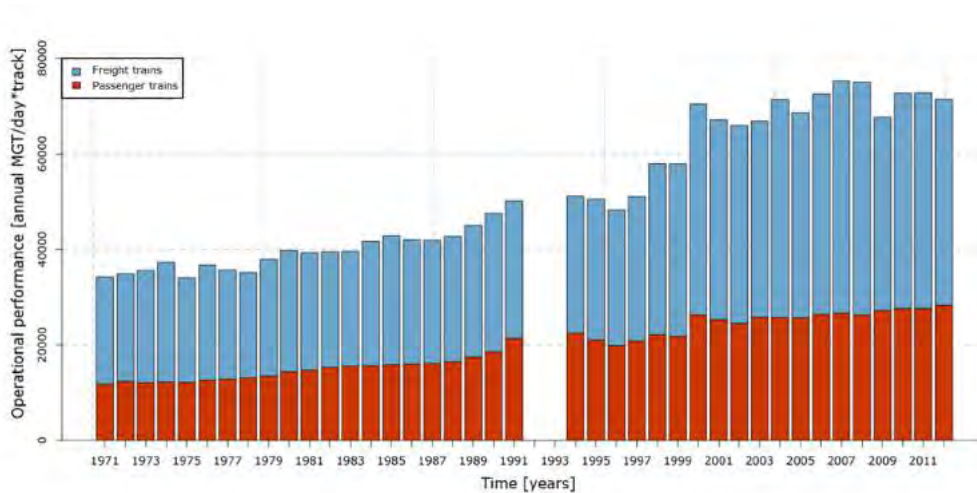


Figure 4 Network-wide evolution of gross tonne kilometres between 1971 and 2012

The increase in the transport volume carried on the Austrian railway network over recent decades can be clearly seen in the visualization of the operational performance in total gross tonnage (see Figure 4). The effects of individual economic crises, such as those in 1992 or 2007, are evident in the available data, as well as the significant influence of growth in the freight traffic data. Since information from 2001 is available both from the ÖBB company report (66,400 million tkm) and from the railway statistics, it is possible to confirm the influences of different underlying networks. A comparison shows that the two values only differ by around 1%, and therefore yield over 99% of the overall performance in the ÖBB network. This tiny divergence admittedly results in a very small statistical imprecision, but allows the difference between the reference networks to be subsequently ignored.

If the figures shown in Figure 2 are filtered to show only the Rail Cargo freight transport from 2001 onwards, the converted freight tonnages are as shown in Figure 5. Even though two distinct statistics are combined in this visualization, the rise in transport volume over recent years is readily apparent. However, care should be taken when interpreting these figures, since the difference between the numbers up to and including 2001 (when all transport through the Austrian railway network is taken into consideration) and after 2001 (when all Rail Cargo Austria's transport is taken into consideration) is greater than the operational performance suggests. Due to the elimination of kilometre information from the reference values, and the omission of private rail transport enterprise data, this difference amounts to almost 10% in 2001.

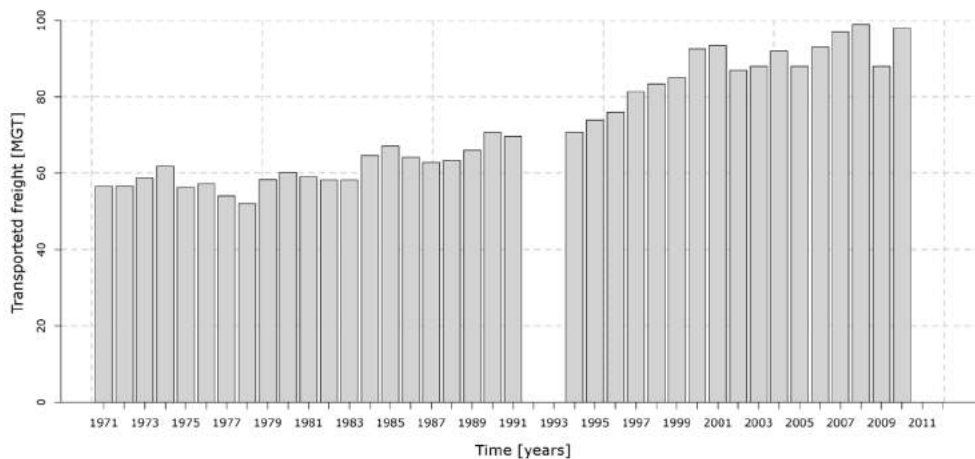


Figure 5 Volume of transported freight

Market liberalization particularly affected freight transport, resulting in a sharp increase in the contribution of private rail transport enterprises to the total traffic volume (see Figure 6).

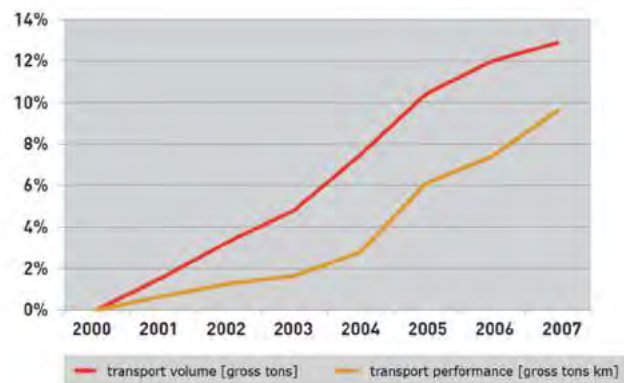


Figure 6 Market contribution of private rail transport enterprises to freight transport within the ÖBB network [Röhler 2013]

The equivalent rise can be seen reflected in the train-kilometre data, although it can be seen that passenger trains are the dominant factor in this case (see Figure 7). It is worth noting the abrupt increase in services following the introduction of the new Austrian schedule in 1991, and its withdrawal shortly after. Although scaling the assumptions may create the impression that freight traffic is subject to almost no increase, the increase is revealed by a closer look at the data.

The load increase within the network can best be modelled using the evolution of the total gross tonne kilometres over recent years. The previously-mentioned marginal influences of routes outside the ÖBB network and the variations in length of line operated will not be taken into consideration.

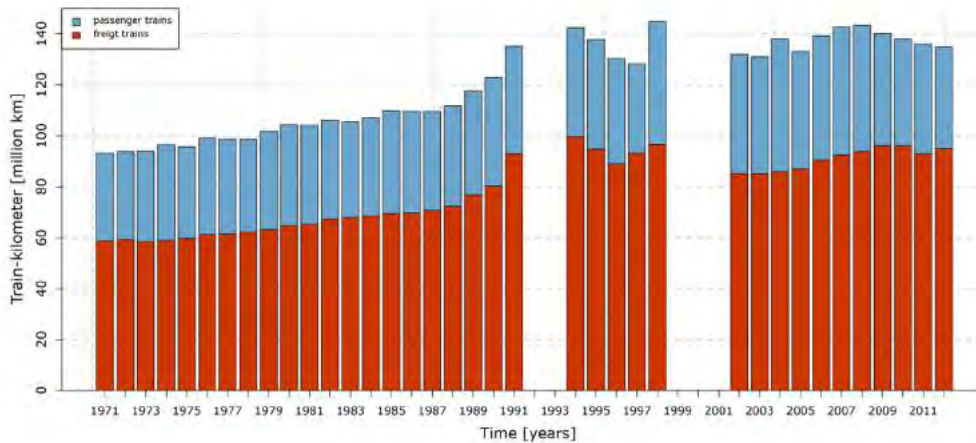


Figure 7 Evolution of train kilometres up to 2001 in the entire Austrian railway network and subsequently in the ÖBB network

2.3 The estimation Function

A regression analysis can be used to find the function which best matches the evolution of the operational performance. After the model has been constructed, it can be retrospectively applied to historical data. The values from 2008 to the present were initially excluded from the calculation. These values would cause the regression to be heavily influenced by the effects of the economic crisis, resulting in distortion of the model. Although the evolution of total gross tonne kilometres over the years clearly shows a non-linear approach, the following three models will be analysed more closely:

linear model: $y(x)=C_1*x+C_2$

exponential model: $y(x)=e^{C_1*x+C_2}$

quadratic model: $y(x)=C_1*x^2+C_2*x+C_3$

By calculating a linear regression model, it is possible to order these different models according to how well they fit the available data, or to exclude them completely if they do not fulfil specific conditions. [Backhaus 2011]

All three models exhibit corrected coefficients of determination of at least 90%, with the quadratic model displaying the highest value at 95.3%. Graphical verification of the results relating to autocorrelation, homogeneity of variance and the normal distribution shows that the quadratic model best describes the relationship. Plotting the results shows the differences between them in terms of their fit (Figure 8).

The evaluation also shows how the residuals of individual points are distributed and expressed in terms of their size (Figure 9). The assigned load values from 1985, 1996 and 2000 have the greatest deviation from the calculated regression curve. Since the residuals can be supposed to have a normal distribution, this observation is only relevant to the choice of data points.

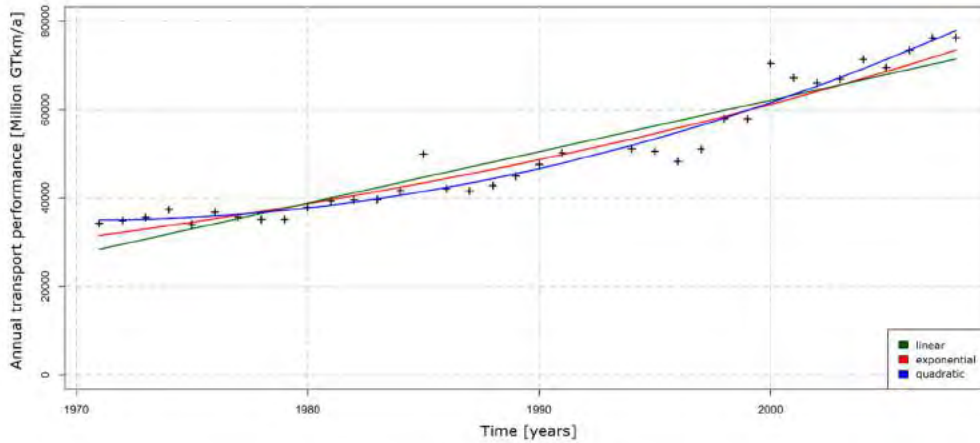


Figure 8 Overview of the results of the individual regression calculations

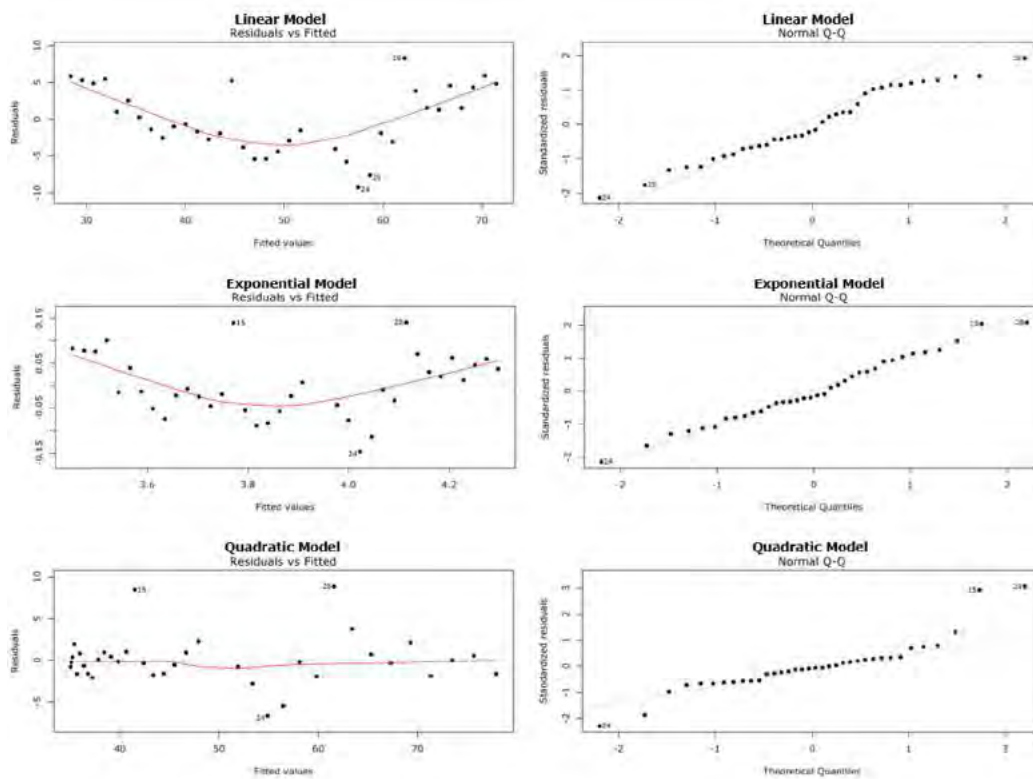


Figure 9 Graphical evaluation of the results of the regression models for the development of the operational performance in total gross tonne kilometres

Having established a method for describing the network-wide development of the operational performance, it is necessary to apply the trend to the individual cross-sections in the TUG network. In this way, it will be possible to approximate the load evolution for the route cross-section in recent years. In order to consider local load values in the process of the projection, it is necessary to identify a specific load value as a reference point for the approximation function. Starting from this reference point, time-shifted load values will be calculated sequentially, with relative differences according to the global load function. Assuming that the regression function yields a 20% increase in the total gross tonne kilometres between the calculated values for 2000 and 2007, the cross-section-specific load function would be determined using this relative value.

\overline{B}_n ... global load value given by the regression for year n

\overline{B}_0 ... global load value given by the regression for the reference year

b_0 ... section-specific load value drawn from the cross-section

\overline{b}_n ... calculated load value for the cross-section

$$\overline{b}_n = b_0 * \frac{\overline{B}_n}{\overline{B}_0}$$

With this approach, it is possible to apply the network-wide evolution to individual route cross-sections, even if the operational performance and the load on the route differ in terms of their base units. Under the assumption that a large part of the operational performance takes place within a stable network, the application of the operational performance to an average track load does not affect the results of the mapping process.

The selection of reference data points is of key significance. The load values for 2010 will by definition not be modelled by the approximation, and so can be excluded as potential reference points. This leaves only the load values from 2007 and the datapoints from 2000. As a first approximation, values from the years 1998-2002 will be summarized into a single value by calculating their median. The calculated median will then serve as the reference point for the estimation function and the hypothetical load value in 2000.

The median is particularly stable as a robust estimate with respect to possible outliers in the load values (Variant 1). The second variant will use the values from 2007 as potential reference points. This has the disadvantage that only one load value per cross-section will serve as a reference point (Variant 2). An example of the possible different results from the two variants is demonstrated in Figure 10 for one cross-section.

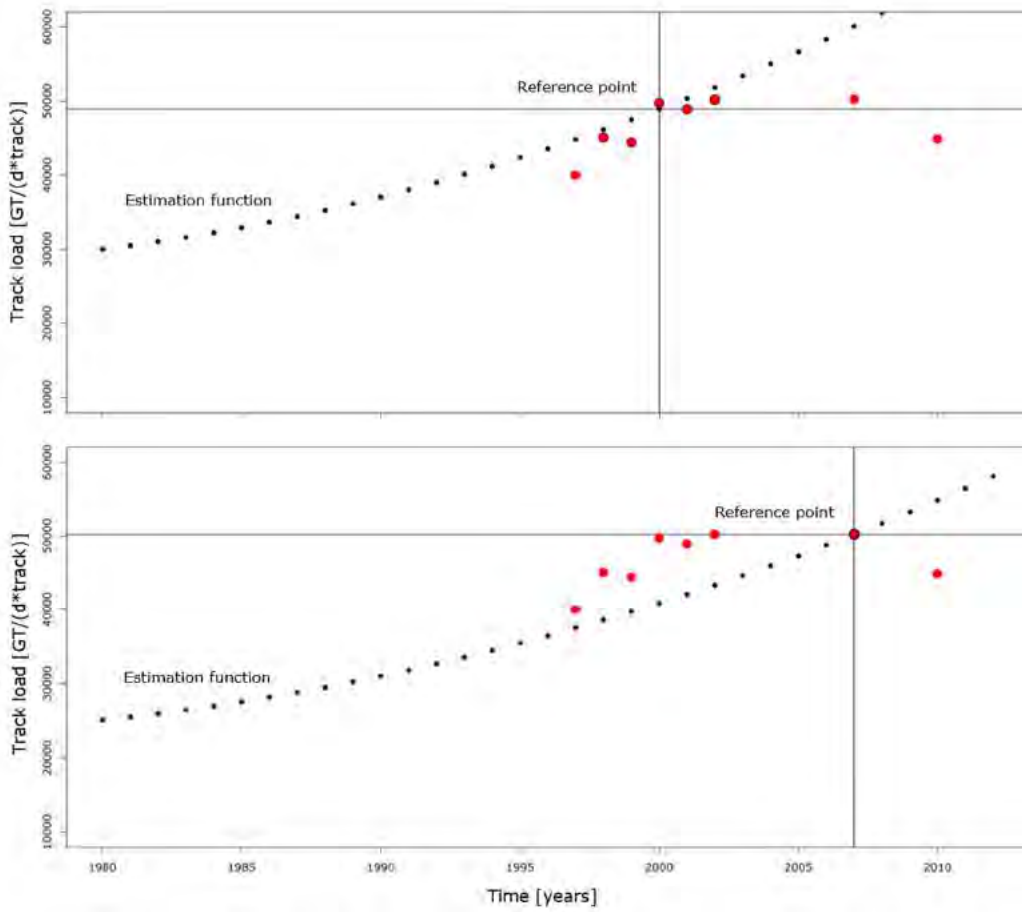


Figure 10 Calculation of the estimation functions on the same cross-section; above: Variant 1, below: Variant 2

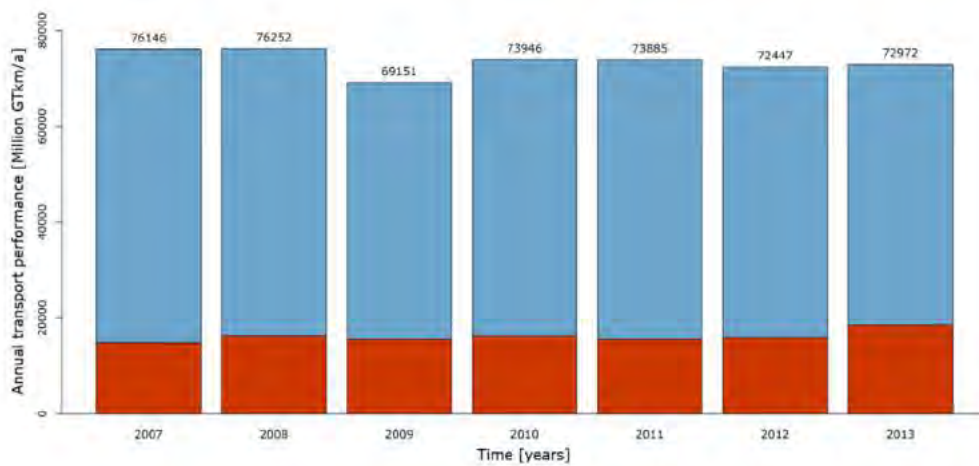


Figure 11 Proportion of the TUG network's (blue) operational performance within the entire network

These methods can be validated by calculating the operational performance in the TUG network according to the estimation function. Subsequently these values are compared with the values supplied in the statistical summary of the operational performance. However, since the TUG network does not include the entire ÖBB network, it is first necessary to determine the proportion of the TUG network's operational performance within the operational performance of the entire network, based on the load data from 2007 to 2013.

In order to carry out this calculation, the load data from individual route cost centres is associated with the route sections present in the TUG network. As shown in Figure 11, the proportion of the TUG network within the total operational performance proves to be between 75% and 80%. It is important to note that the mapping applied to the available load data is based on route sections. A track-specific classification of the load values is difficult, particularly around junctions, thus in the available database the load data for 2007 in these areas has been manually processed, or, in cases where a clear classification is unlikely, labelled as erroneous. Due to this partially impossible classification of track loads, the TUG network's proportion of the operational performance must be reduced further, now lying between 70% and 75%.

A comparison of the two variants through random sampling shows that at this point the load data available in the database only partially follows the proposed regression, or has a wider distribution (see Figure 10). An evaluation of the network will therefore clarify which reference points result in the best estimation. Figure 12 shows the already familiar progression of the operational performance over recent years.

The hatched area shows the 70%-75% and 75%-80% ranges. The margins show the proportion of the TUG network in terms of overall operational performance. The marked points represent operational performance calculated from the TUG database. By comparing them, it can be clearly seen that the calculated load values between 1997 and 1999 are too high on average. From this, it can be concluded that the calculation of the estimation function using Variant 1 tends to lead to inflated load values. Although the load values between 2000 and 2002 do fall between 75% and 80% of the operational performance, they nonetheless appear to represent a peak in the load progression, again leading to inflated load values.

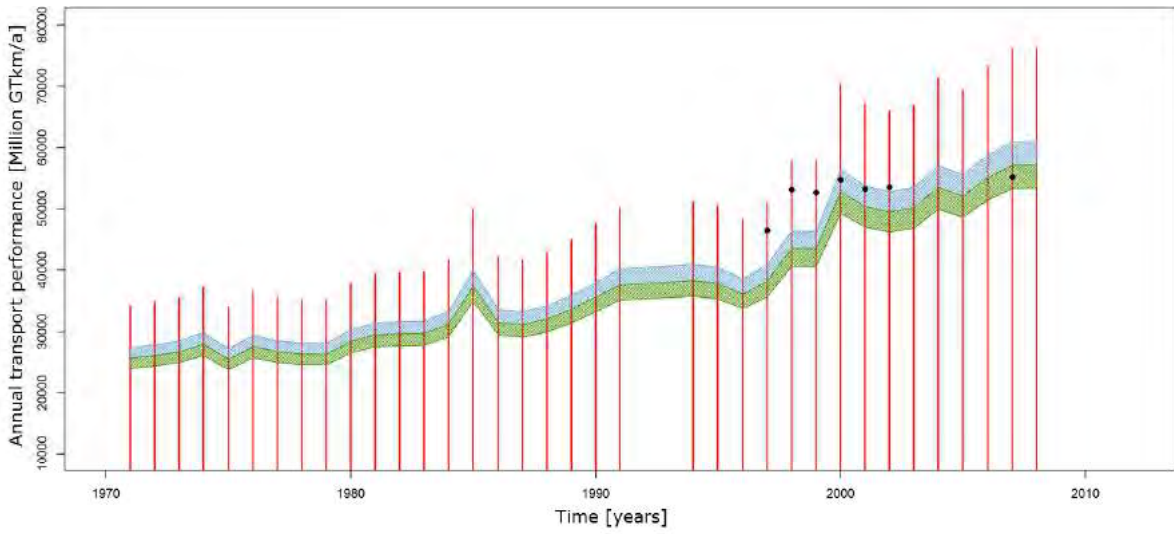


Figure 12 Proportion of the TUG network within the total operational performance of the route network

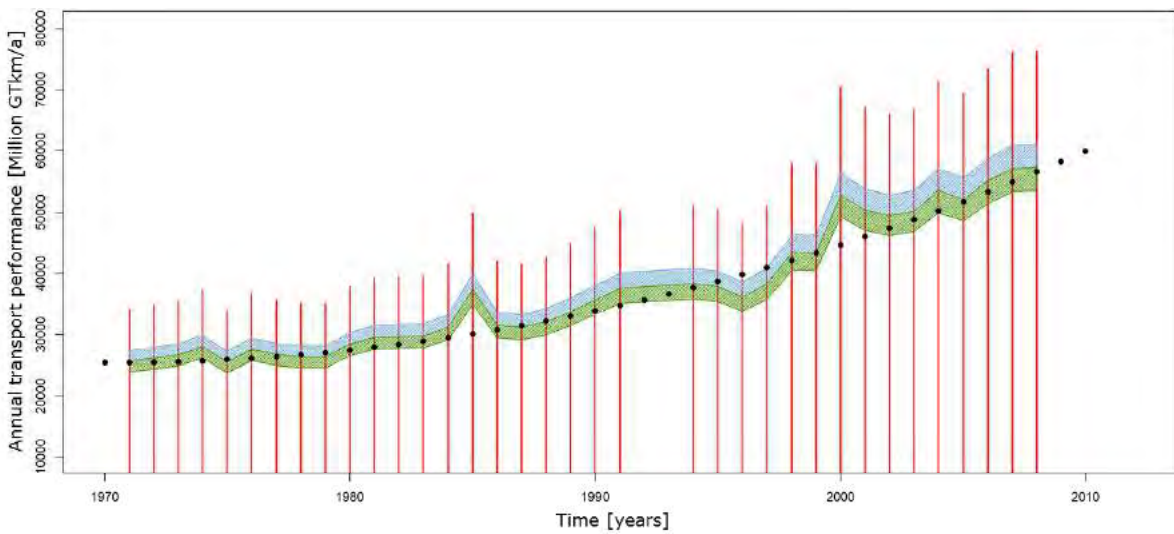
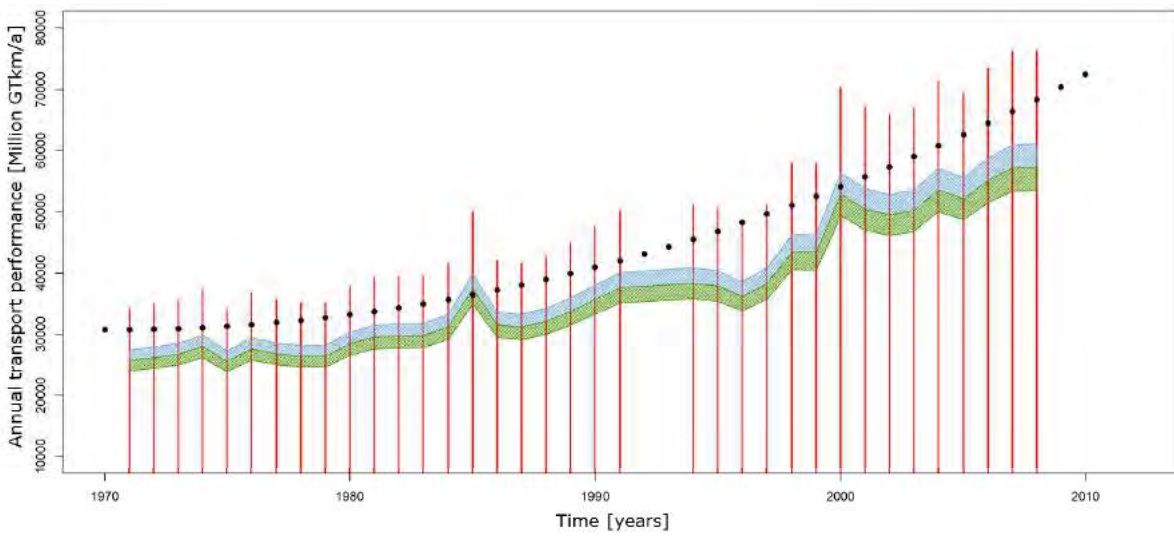


Figure 13 Comparison between the different estimation functions

Based on the estimated, cross-section-specific load evolution of the TUG database (providing that appropriate clear, error-free load values for the reference points are available), the operational performance of the TUG network can be calculated. The operational performance calculated in this way using Variant 1 exceeds the specified 80% of the operational performance.

The operational performance of Variant 2 reaches the predicted lower range of the estimation interval. The comparison between the distinct calculation variants demonstrates that the calculation of the applied loads using Variant 1 appears to lead to inflated loads and cannot, therefore, be considered acceptable. Consequently, for the remainder of this work, the cumulative loads will be calculated using Variant 2, using the load values for 2007 as reference points for the quadratic function.

2.4 Validation Process

The calculation of the estimation function using Variant 2 is based on the cross-section-specific load values from 2007. The above evaluation shows that the mean load values are a suitable basis for estimating the load evolution in the network, although some uncertainty arises from using single data points. In order to limit this uncertainty and thereby increase the model stability, it is necessary to carry out further verifications. The primary focus of these validations will be to verify the load data from 2007. A second step will evaluate the general traffic growth for a single cross-section. If a non-negligible difference between load data (e.g. diversions due to a track worksite) is apparent in the growth trend, this cross section can be disregarded in further observations.

The validation follows a three-step process, as shown in Figure 14. The first step is to calculate the relative deviation of the load data between 2007 and 2010. Despite the economic crisis, the operational performance proves to be approximately the same for each of the two years. Therefore it can be concluded that this trend will also be reflected in the cross-sectional load values. Providing the maximum deviation of the two values is $\pm 10\%$, the load value from 2007 will serve as the reference point for the estimation function. All cross-sections that do not meet this criterion will be compared successively with the median of the load values from 2000-2002. The operational performances from 2000 to 2002 are sufficiently close that it can be assumed that the track loads in these years also remain approximately constant. After this validation process the most suitable reference point is selected from the load data for the calculation of the estimation function.

The load data from 2010 lies outside the temporal application of the estimation function, but are nonetheless not solely used for validation. These data points may be partially used as reference points for the estimation function. In this context, the load data from 2007 will be replaced with the data from 2010, back-dated to 2007, since by definition the year 2007 remains an equally valid reference point for the calculation. In this case, the load data for 2010 will be multiplied by 1.03, to reflect the difference between the operational performances of the two years. The results of the validation process show that in 65% of cases the load data from 2007 serves as a basis, and only needs to be replaced with the data from 2010 in 20% of cases.

In just 15% of the cases it was impossible to determine, according to the selected criteria for the validation process, an estimation function which would calculate the cumulative load for individual cross-sections.

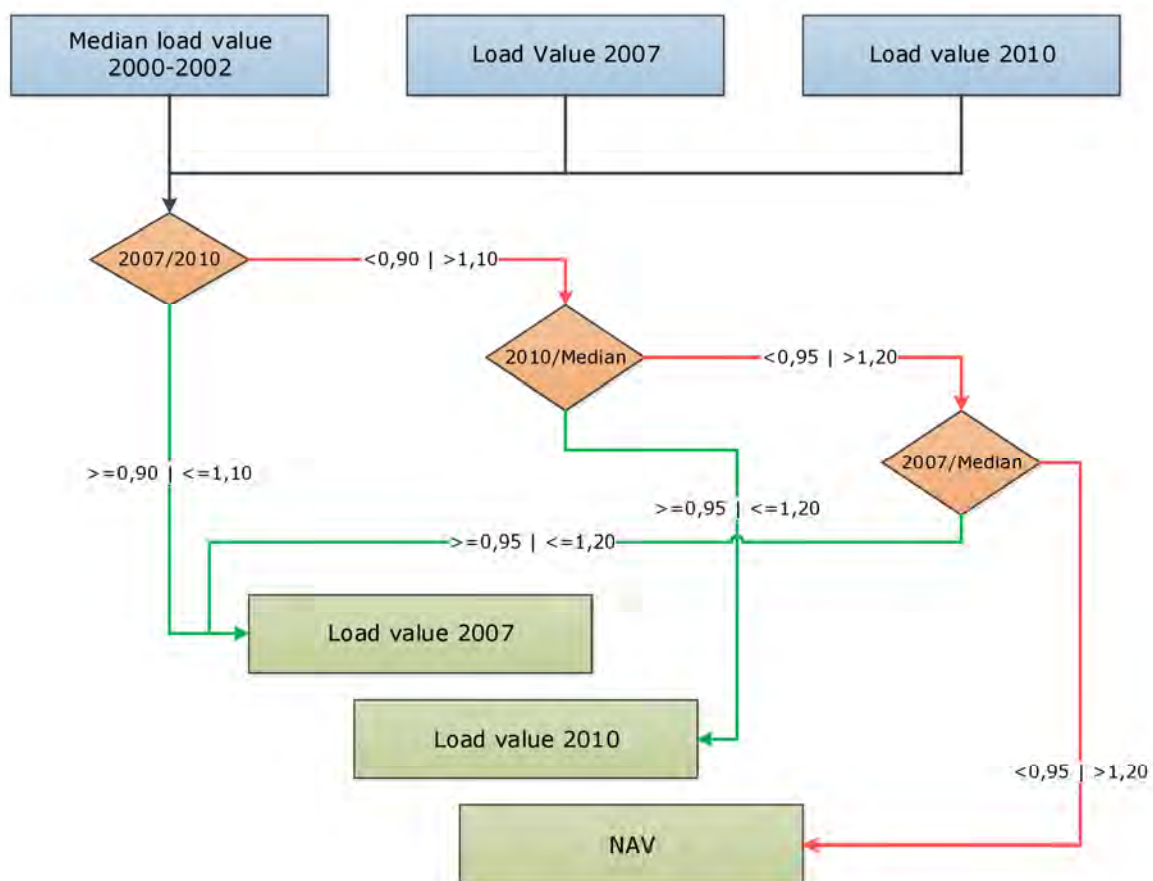


Figure 14 Flowchart for selecting a suitable reference point

The following example serves to illustrate the validation process in the context of a selected route cross-section. In 2007, this route cross-section exhibited a load of 43,531 gross tonnes/day. Comparing this with current data from 2010 (53,475 gross tonnes/day) yields a difference of almost 20%. The load value from 2007 is not valid since this difference between 2010 and 2007 exceeds the required 10%. The comparison between the load value from 2010 and the median load value from 2000 to 2002 (48,116 gross tonnes/day) yields a load increase of almost 11%, which is within the specified tolerance. Therefore, the load value from the year 2010 is applicable as a reference value for the estimation function in the following work. In this capacity, it will thus be increased by 3% and back-dated to the year 2007.

3

Track Geometry

The primary objective of this chapter is evaluate the track geometry of a track section in terms of its quality. This evaluation will enable the development of a sustainable maintenance strategy based on measurement-driven classifications which take diverse signals into account. A description of the effect which potential ballast contamination has on the track geometry is therefore central to the evaluation, along with the potential effects of subgrade without adequate load-bearing capacity. The following evaluations are based on various recording signals, quality signals and quality values. A precise definition in terms of the origins of these various signals is necessary in order to precisely distinguish the predictive powers and possibilities of individual evaluations.

Recording signals are signals recorded by track geometry cars, with a simple filter applied and locally adjusted before their use in further evaluations.

Quality signals are key indicators, either supplied directly by the track geometry car or calculated subsequently from the supplied data.

Quality values are values which result from a regression analysis of either recording or quality signals.

Possible points of discontinuity, such as railway crossings, switch areas or bridges, may influence the rate or manner of change of the track geometry. As the focus of this work is to describe the track in general, the data must be filtered before any analysis. Discontinuities would distort the data, rendering an evaluation of homogeneous sections almost impossible.

The analysis of track geometry in the TUG network will make it possible to ascertain details related to the following questions:

- I What is the correlation between the track geometry quality signals and the amount of tamping or new track?
- I Allowing for the different types of sleeper, how does the track geometry evolve over the service life of a component?
- I In the track renewal projects over the last five years, what were the average quality values relating to the track geometry, before and after the new track was laid?
- I Is it possible to obtain precise information about the origins of track geometry errors from the track geometry recording signal, and further to classify the origin as ballast or subgrade?

3.1 Introduction

The first stage will be to analyse the evolution of the track geometry in the TUG network (Annex 1) over recent years, outlining the possible effects of reduced or increased maintenance. This evaluation will refer to the following three distinct quality signals:

- I Standard deviation of the vertical alignment (SigmaH) (cf. [Auer 2004])
- I Standard deviation of the lateral alignment (SigmaR)
- I MDZ-a indicator (MDZ) (cf. [Rießberger 1997] [Hanreich 2004])

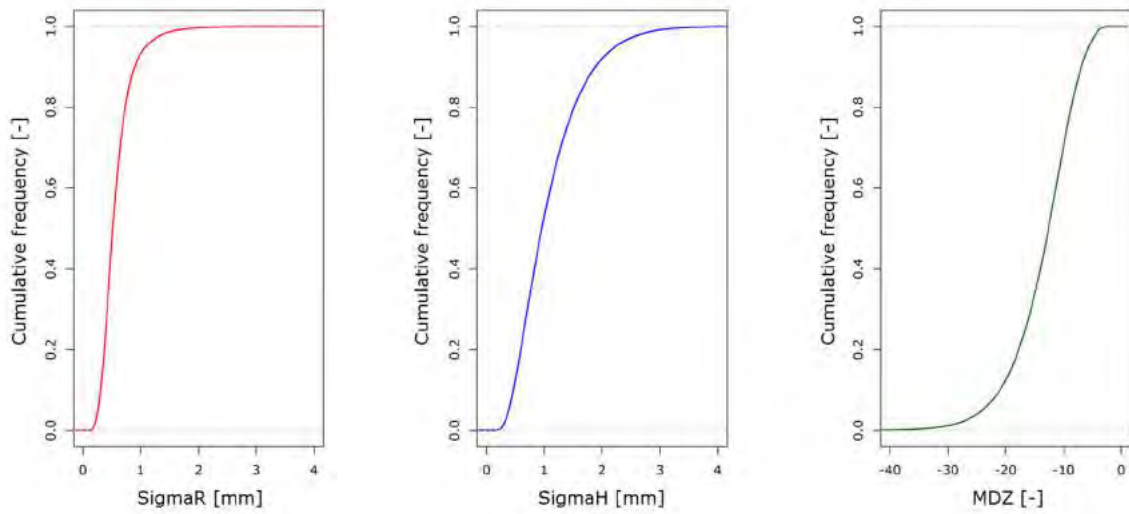


Figure 15 Frequency distributions of the quality signals from the first recording journey in 2012

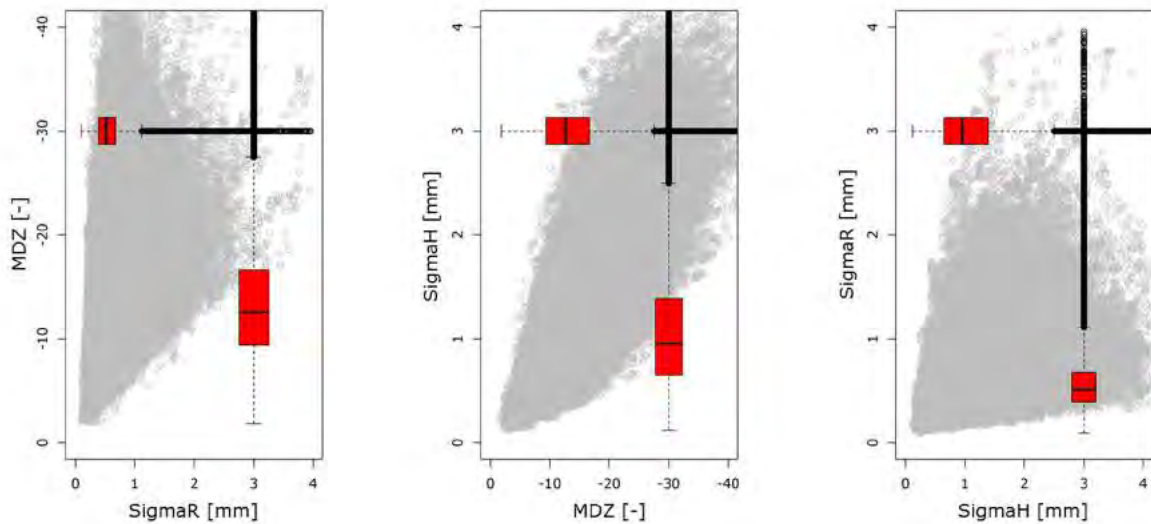


Figure 16 Comparison of the correlations between the three quality signals

The following models will present an overview of the individual quality signals, aiming primarily to outline a framework for the individual parameters. The models capture the structure of parameters such as the scattering range, without taking into account various correlations between the track superstructure and the signals. Considering the frequency distributions of the quality signals from 2012, the different distributions can be clearly seen. However, the values of SigmaR result in a much narrower distribution than those of SigmaH, as well as having noticeably different absolute values.

A review of the correlations between the different quality signals (from the first recording journey in 2012) reveals further insights on the value distribution and the correlations

between individual quality signals. While SigmaR has a median value of 0.5, the SigmaH values are almost double this. The calculated MDZ values are negative, meaning that smaller absolute values correspond to a better track geometry. The MDZ values have a median of -12.6, and exhibit the widest distribution. Although there appears to be an almost linear correlation between the MDZ values and the SigmaH values (see Figure 16 [centre]), a similar correlation cannot be seen in the other comparisons. The generally higher values of SigmaH also have a stronger influence on the resulting MDZ indicator. Track geometry errors in the vertical dimension appear larger on average than in the horizontal dimension. Should the calculation also take the effects of speed into account, it should then be borne in mind that alignment errors primarily arise in curves, which are of course travelled at lower speeds. Or to rephrase: when lateral alignment errors occur, they will have reduced effects on the MDZ calculation as a result of the lower speeds, as well as their generally lower absolute values. It is therefore clear that larger alignment errors will lead to larger MDZ values, conditional on the calculation. However, the reverse effect does not apply. There is a one-way, two to one dependence between vertical and horizontal alignment errors. Vertical alignment errors thus imply horizontal errors, but the reverse effect does not apply.

3.2 On the Relationship between the Track Geometry Quality and Tamping Measures

Corrections to the track geometry are carried out by implementing measures such as tamping or ballast bed cleaning. In order to preserve the components, the intervention is often applied before security-critical thresholds are reached. The correlation between the ballast bed and the resulting track geometry will be the focus of the following section. An analysis of cross-section-specific annual average values would not yield a meaningful result. When particular measures are implemented, there is a sudden change in quality during the year, so the annual mean would reflect neither the higher quality nor the quality before the measure was implemented. When considering the interpretations of results below, it is therefore necessary to estimate the quality either before or after maintenance takes place. However, this problem can be simplified. Making two assumptions, firstly, that a large part of the track improvement machinery is deployed between May and September and secondly, that it is deployed after the first recording journey has taken place, the following analysis will consider the first recording journey of each year to be cross-sectionally accurate, on the condition that it takes place during the first five months. In Figure 18 various

evolutions can be identified with the help of the grid and horizontal dark lines. The differences in individual annual values are often very small, making it vital to apply suitable scaling to the individual representations of the quality signal data.

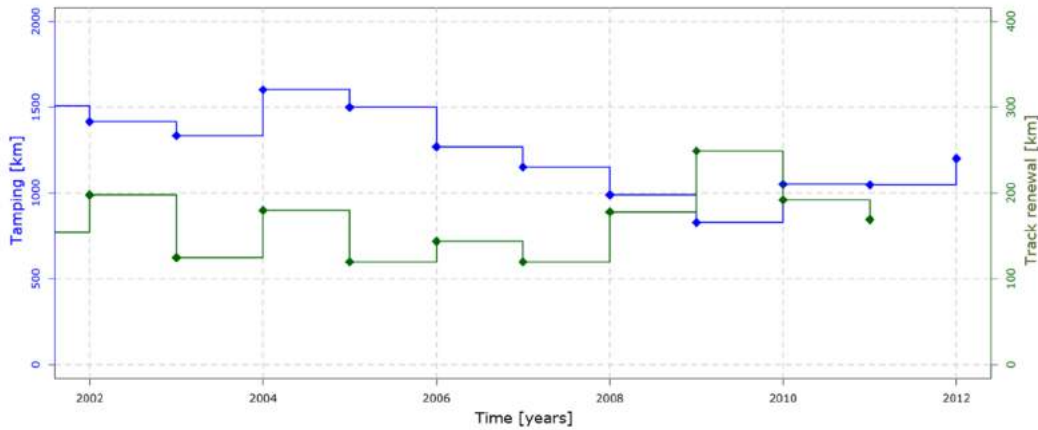


Figure 17 Change in the number of track renewal and tamping measures in recent years

Figure 17 shows the number of tamping measures (excluding tamping in the course of track replacement and single spots) and track renewal operations carried out in recent years over the entire ÖBB network. The number of track renewal operations in 2012 had not become available at the time this research was carried out and is therefore not considered in further analysis. Although the TUG network only models a part of the ÖBB network, it can be assumed that the measures implemented in the two networks will evolve in a comparable way. Ballast bed cleaning without the replacement of track panels is not a standard measure in the ÖBB, and is only carried out in specific circumstances. Around ten kilometres of the track bed is cleaned this way each year, resulting in significant improvements to the track geometry. In the two years 2003 and 2010, around 20 track kilometres of track bed were cleaned, almost twice as much as in any other year. Tamping measures were gradually reduced over the years up to 2010, reaching their lowest value of around 800 kilometres in 2009. In the same year, the reinvestment ratio rose disproportionately as a result of a temporary restructuring package. In general, it fluctuated between 120 and 190 kilometres over recent years with no discernible long-term trend.

3.2.1 Temporal Evolution of the Standard Deviation of the vertical Track Geometry

Figure 18 [right] shows the temporal evolution of the standard deviation over recent years, demonstrating that it has consistently deteriorated since 2005. The sudden improvement in 2005 can be attributed primarily to the short-term increase in track renewal and tamping measures in 2004 (see Figure 17). Due to the restrictions encountered, not every cross-section in the network is represented in this evaluation by a measurement value. In particular, there are significantly fewer measurement values from the years 2002 to 2004

than other years, meaning that the results from these years should be interpreted with caution; initially, the evaluations below will be restricted to the years following 2004.

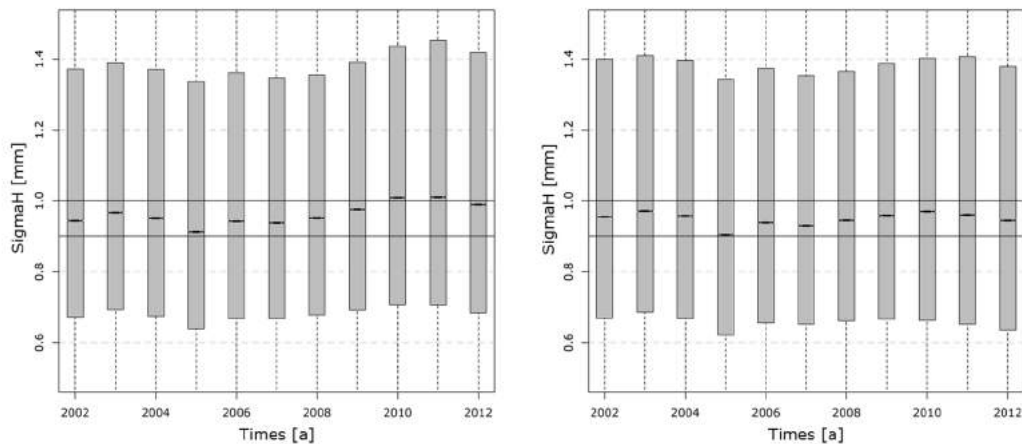


Figure 18 Temporal Evolution of the SigmaH between 2001 and 2012; left: without taking Track Renewal into account, right: taking Track Renewal into account

The comparison suggests that the continual reduction in tamping in relation to the scale of the track renewal has a negative effect on the network-wide track geometry. However, the correlation between the tamping measures and the resulting track geometry appears to be significantly smaller here than previously predicted. This arises partially because track renewal has also been taken into account. In order to quantify this effect to some extent, it is worth analysing the evolution of the track geometry without taking into account the direct track geometry improvements which result from laying new track. Figure 18 [left] shows this comparison, for each year excluding quality signals from any cross-section where track renewal has taken place within the previous five years. Various effects such as new materials, better installation quality or increased traffic loads cannot be directly quantified in this evaluation. Nonetheless, the tamping and track renewal measures can be clearly correlated with the track geometry. A continual reduction in tamping at a constant rate of reinvestment leads to an ongoing deterioration in the track geometry. However, the increase in tamping to over 1,000 kilometres in 2010 resulted in a reversal of the negative trend in the standard deviation. The future evolution of the track geometry will show whether a medium-term reduction in maintenance leads to a continual deterioration in track geometry that cannot be entirely reversed by individual measures.

3.2.2 Evolution of the Standard Deviation of the horizontal Track Geometry

SigmaR exhibits the opposite trend to the SigmaH. By contrast with the continual deterioration in values, a continual improvement can be observed in the alignment values over the past years. This improvement is visible to a lesser extent when track renewal projects (as in the previous consideration of SigmaH) are not considered (see Figure 19 [left]). An initial reason for the improvement in this value in recent years can be found in the installed track superstructure.

Looking at the proportions of different sleeper types used in the scope of annual reinvestment in the TUG network, shown in Figure 20, it can be clearly seen that in recent years new sleepers have principally been concrete, with or without under-sleeper pads (USP). This corresponds with the current strategy of the Austrian federal railway, which (in the TUG network routes) prescribes the installation of wooden sleepers only in curve radii of less than 250 metres and particular special cases (e.g. bridge construction) [ÖBB Infrastruktur AG 2009]. Furthermore, a closer look at the reinvestment projects within the TUG network over the last five years clearly reveals that over this period concrete sleepers, with or without USP, have essentially replaced wooden sleepers (see Figure 20). The network-wide increase in resistance to lateral displacement resulting from the installation of heavier types of sleeper may have contributed to the continual improvement relating to lateral errors and thus of the standard deviation, although other effects cannot be ruled out. The exact reason for the unusual deterioration in 2010 cannot be determined.

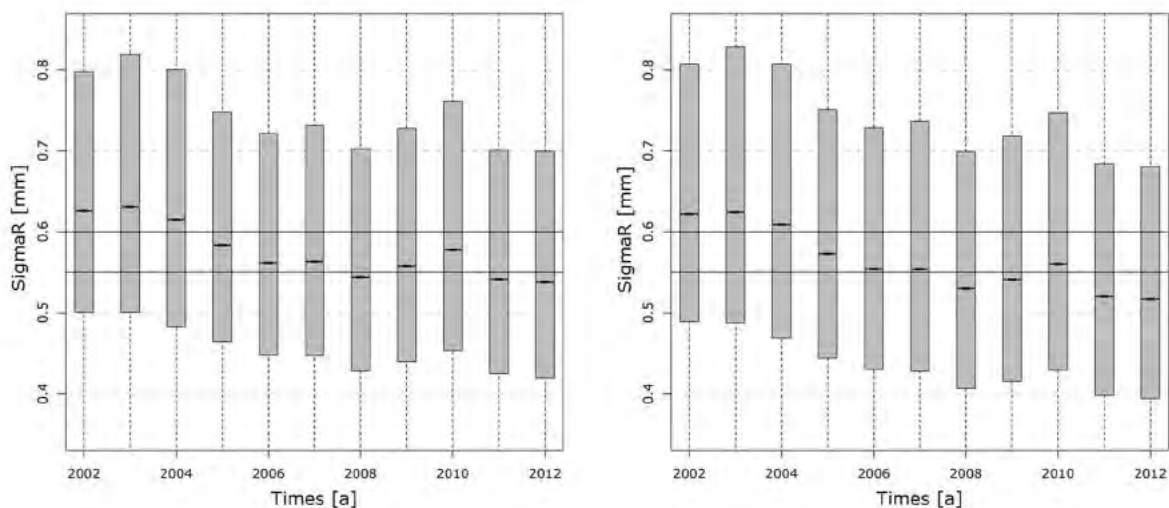


Figure 19 Temporal Evolution of the SigmaR between 2002 and 2012; left: without taking Track Renewal into account, right: taking Track Renewal into account

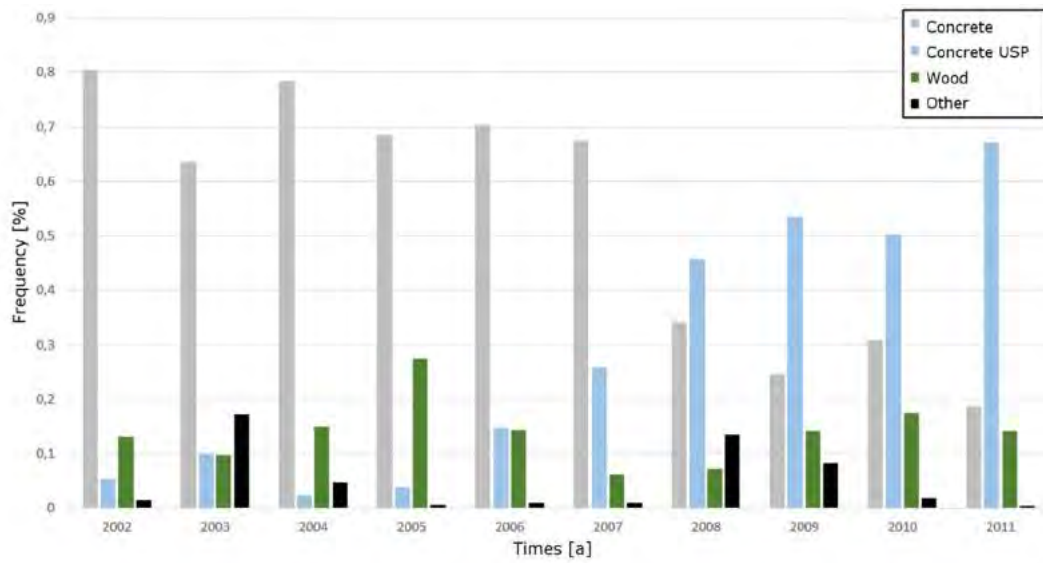


Figure 20 Proportions of the different Types of Sleeper installed in the context of Reinvestment Projects over recent Years in the TUG Network

3.2.3 Evolution of the MDZ-a Indicator

The MDZ-a indicator is calculated based on the interaction of a simplified train model with the track geometry. It combines the cross-section-specific speed and the resulting track geometry.

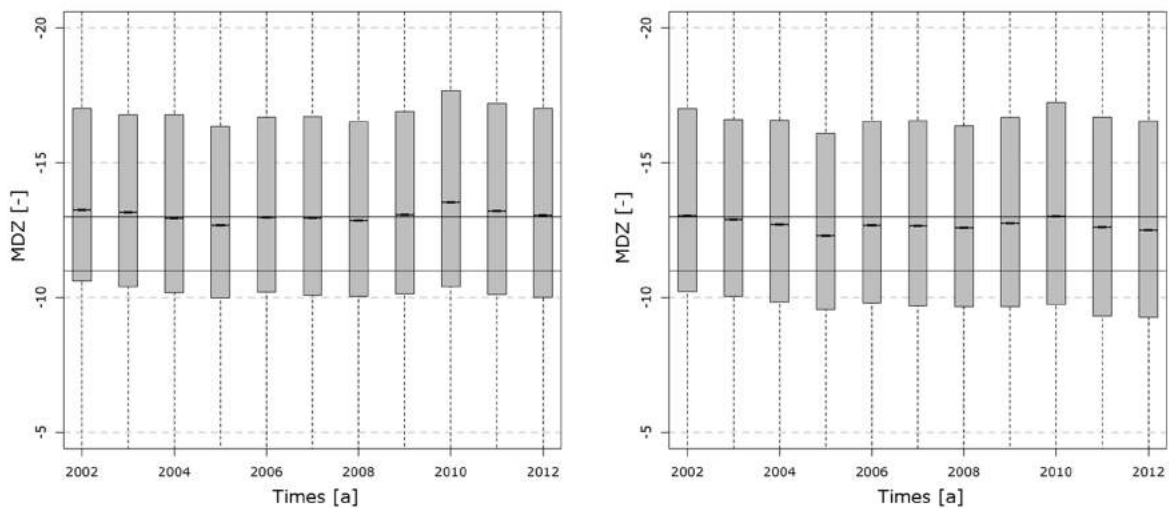


Figure 21 Evolution of the MDZ Indicator between 2002 and 2012; left: without taking Track Renewal into account, right: taking Track Renewal into account

The opposing evolutions of the two quality signals (SigmaH and SigmaR) thus overlap. However, the simultaneous increase in tamping and the amount of reinvestment in 2004 led to a significant improvement in the network-wide MDZ. Although the positive evolution of the standard deviation of the alignment reduces the extent of the negative evolution in quality resulting from reduced maintenance and reinvestment, the latter can nonetheless be clearly seen in the calculated MDZ-a figures up to 2010.

3.3 Installation Quality and Removal Quality

During the track's life cycle, the track geometry worsens due to the effects of loads and environmental conditions. The deterioration in track geometry leads to a deterioration in driving comfort, and eventually to a security-critical situation. With the help of various maintenance measures, such as tamping, it is possible to correct the track geometry. If, due to ballast fouling, it is no longer possible to improve the track geometry, replacement of the ballast bed can be carried out by ballast cleaning, in order to ensure travel operations can continue safely providing the admissible speeds are adhered to. The following section addresses this situation to explore the different installation qualities and qualities obtained shortly before the superstructure renewal. The reinvestment projects between 2008 and 2011 will act as the basis for this evaluation. The historical track superstructure data for these reinvestment projects is available, not only including the current track superstructure, but also indicating the materials which were installed before the track renewal project. This makes it possible to compare the installation and removal qualities of the reinvestment projects over a period of four years. When these projects are observed jointly in relation to their service life, the following picture emerges.

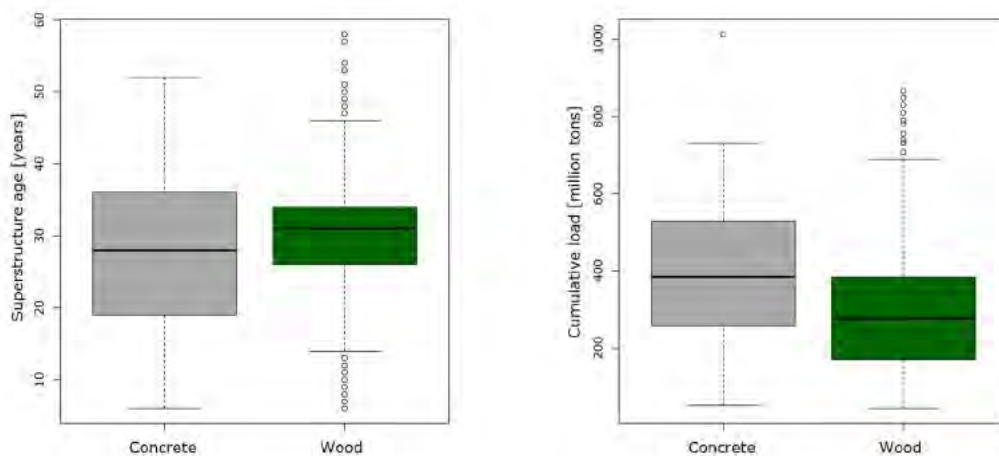


Figure 22 Service Lives achieved by the Reinvestment Projects between 2008 and 2011 in Years and cumulative Tonnage

A comparison between the achievable service lives of wooden and concrete sleepers is difficult. Prior studies [Veit 2013] show a clear relationship between the service life of railway tracks and various parameters, including for example curvature, rail profile, daily load. Assuming that these influencing parameters apply equally to the various sleeper types in the reinvestment projects, the comparison of the different service lives leads to fundamental insights. Considering the age of the track materials independently would give rise to the assumption that concrete sleepers are generally removed sooner than wooden sleepers.

Only if the cumulative load (as indicated by the load model) is taken into consideration, do concrete sleepers exhibit a longer service life than wooden sleepers. The vast majority of wooden sleepers achieve a service life of 31 years, independent of the load, while the service life of concrete sleepers is lower and has a much wider distribution. It therefore appears that wooden sleepers are removed after between 26 and 34 years in 50% of cases, regardless of their cumulative load. Concrete sleepers exhibit a longer service life with respect to tonnage, but are more sensitive to surrounding parameters, such as poor-quality subgrade, and thus display more scattering.

Without anticipating detailed statements about the evolution of the track geometry over the service life, the first question to arise concerns the quality of the track geometry when different types of sleeper are installed or removed. The quality signals and the data from the sleeper replacement will serve as a foundation for determining the different installation or removal qualities. Since track renewal, as per the ÖBB's standard construction methods, only takes place in combination with ballast cleaning, there must be a significant distinction between the two qualities. In order to eliminate possible outliers as far as possible, the track quality will be defined using groups of three recording runs, and in each case taking the mean of these. The number of recording runs considered will be kept low, in order to rule out the possible positive influence of tamping.

The exact process will be explained in more detail using the following example. If a sleeper replacement in 2009 is examined, the removal quality will be derived from three valid recording runs which took place on a date less than 2009.0, and the installation quality comprised of three valid recording runs greater than 2010.0. The time offset in the context of the calculation of the initial quality should deliberately exclude the initial settlement process (cf. [Lichtberger 2010]) from the rest of the calculation, so that the situation is only considered after consolidation has taken place.

The evaluation primarily follows the MDZ-a indicator, in order to be able to consider track sections with differing speeds.

Comparing the removal qualities, the box plots in Figure 23 only show a marginally better track geometry quality for wooden sleepers; a difference which hardly increases in significance when the straight route sections are considered independently. The picture for the installation quality proves to be the opposite. As well as the sleeper types already considered, this evaluation also considers sleepers with USP, which have been used increasingly in recent years (see Figure 20). Wooden sleepers are no longer standard for track superstructure in the TUG network routes, and are only considered for installation in special cases. These special cases are primarily characterized by particularly high demands, which are also reflected in the resulting installation quality. Concrete sleepers with USP are characterized by around a 25% better initial quality compared with ones without USP, thereby confirming the results of previous studies (cf. [Marschnig, Berghold 2011]).

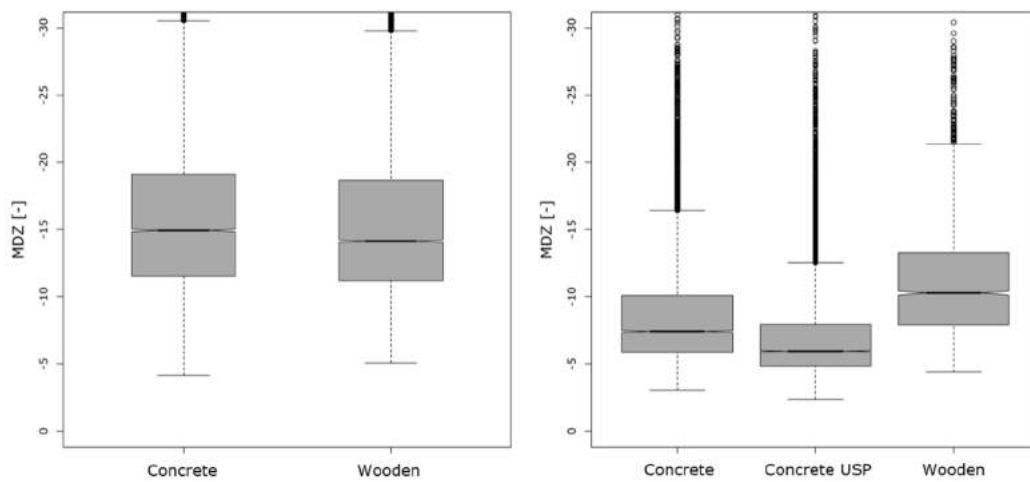


Figure 23 Comparison of the Track Geometry Quality (MDZ-a) of the Reinvestment Projects; left: Removal Quality, right: Installation Quality.

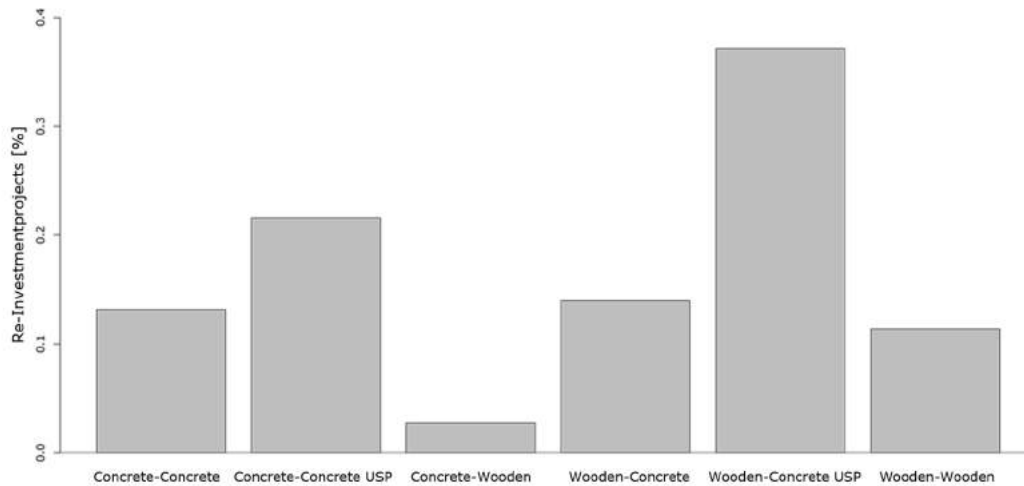


Figure 24 Overview of the Proportions of individual Track Superstructure Types from the Reinvestment Projects between 2008 and 2011; first named Track Material is the one being removed, second one the Material after the Replacement

If the evaluations are extended to additional quality signals, such as SigmaH (Figure 25) and SigmaR (Figure 28), it is then worth considering the influence of variations in speed. Differing speeds require different thresholds for tamping strategies and consequently influence the maintenance strategy and the acceptable track geometry (cf. [Österreichisches Normungsinstitut 2014]).

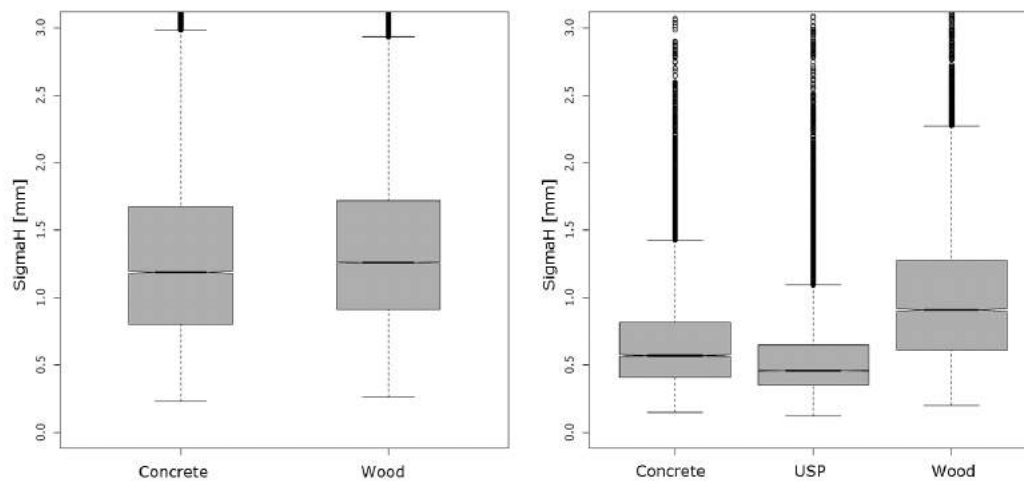


Figure 25 Comparison of the Standard Deviation of the vertical Alignment in the Reinvestment Projects; left: Removal Quality, right: Installation Quality

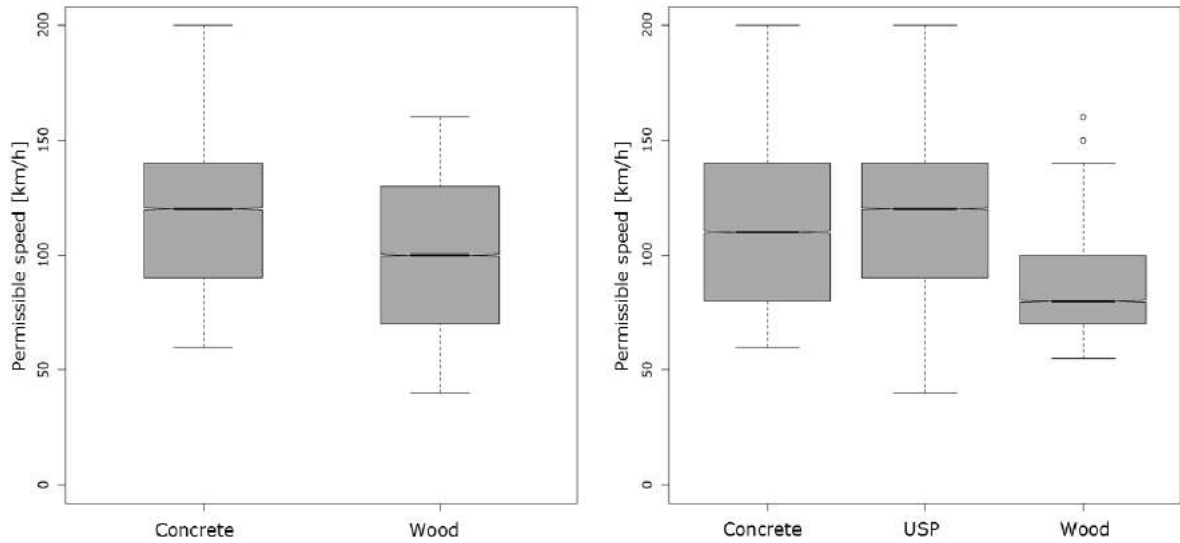


Figure 26 Speed Distribution across Track Superstructure Types; before [left] and after [right] Replacement

Considering the materials before track renewal, the permissible speeds are found to be almost 20km/h lower for wooden sleepers than for concrete sleepers (see Figure 26). The increased standard deviation of the vertical alignment is arguably due to increased thresholds and lower track requirements. In order to further investigate this effect, the evaluation of the SigmaH will be repeated, but now applied only to reinvestment projects with permissible speeds between 120km/h and 160km/h (see Figure 27). In this case, the removal qualities are better for wooden sleepers than for concrete sleepers. This filtering has a marginal effect on the track renewal quality, which can be primarily explained by the elimination of potential discontinuities; this will be detailed as part of the discussion on SigmaR.

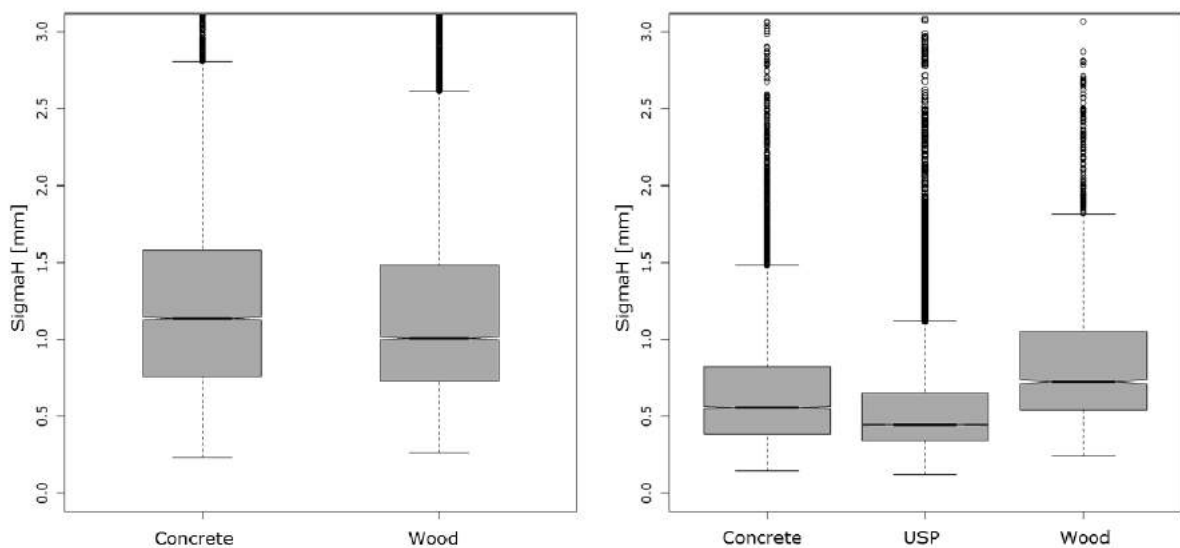


Figure 27 Comparison of the Standard Deviation of the vertical Alignment for Reinvestment Projects in Sections with Speeds from 120 km/h to 160 km/h; left: Removal Quality, right: Installation Quality

The median values of the removal qualities, for both wooden and concrete sleepers, are significantly better than the intervention level according to current standards (cf. [Österreichisches Normungsinstitut 2014] and [ÖBB Infrastruktur AG 2012]). This arises from the fact that reinvestment projects are only partially influenced by these levels, and not all projects are based exclusively on track geometry.

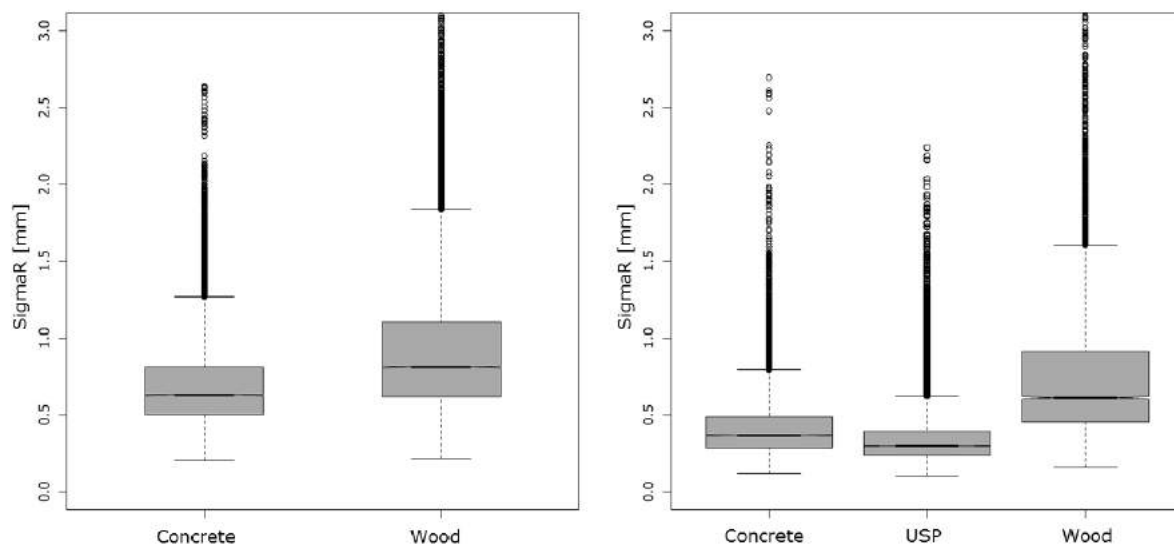


Figure 28 Comparison of the Standard Deviations of the lateral Alignment for the Reinvestment Projects; left: Removal Quality, right: Installation Quality

The evaluation of SigmaR results in a familiar picture. The values for wooden sleepers are noticeably higher than the values for concrete sleepers, which can be primarily attributed to their reduced resistance to lateral displacement [Iliev 2012].

When cross-sections with curve radii less than 600 metres are eliminated from the population, the absolute values are lower for both types of sleeper, but the difference between them remains. The median values do not become approximately equal (see Figure 29) until cross-sections with speeds higher than 100km/h are observed independently. In both cases, the values achieved are considerably below the thresholds defined as requiring attention by the current maintenance plan [ÖBB Infrastruktur AG 2012]. This suggests that, apart from special cases, maintenance is primarily driven by vertical track geometry errors. The fact that a perceptible reduction of the differences between the two sleeper types does not occur until lower speeds are excluded from consideration is explained by the observation that track sections with lower speeds but large curve radii occur in the intermediate straights following curves. In these straights, the vehicle passage and resulting forces are significantly affected by the preceding curves, putting higher demands on the ballast bed. Independent of the reason for this situation, a much stronger correlation develops between wooden sleepers and the resulting alignment than between concrete sleepers and the alignment, a fact that has already been recognized by prior studies (cf. [Lichtberger

2007]). An assessment of the standard deviation also clearly shows the advantages of concrete sleepers with USP over the traditional concrete sleepers due to their higher resistance to lateral displacement (cf. [Iliev 2012]).

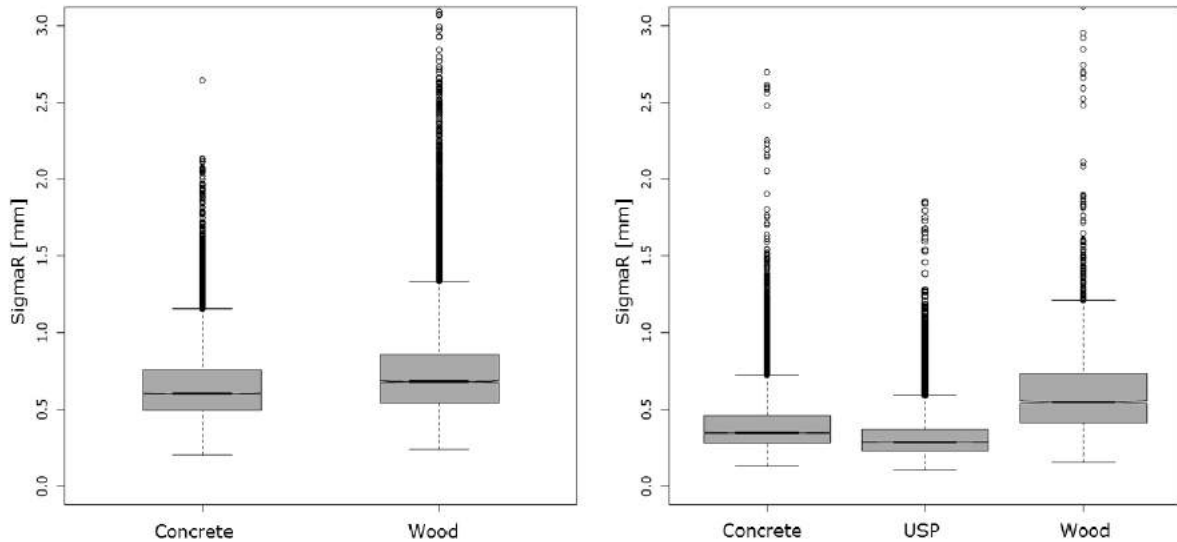


Figure 29 Comparison of the Standard Deviation of the lateral Alignment from the Reinvestment Projects with a Speed of more than 100 km/h; left: Removal Quality, right: Installation Quality

3.4 On the Relationship between the Track Geometry and cumulative Loads

The previous section primarily addressed network-wide evolutions and time-specific geometry qualities. However, the evolution of the track geometry over the service life is worth a more detailed investigation at this point. Quality signals provide a single piece of information about a particular instant in time. If the first recording run of the year is always used for the network-wide evaluations, then the time period between the quality recording and the most recent maintenance carried out is different for each cross-section. When considering the network-wide quality of the track geometry or the installation and removal qualities across the network, this factor only plays a minor role. However, in the context of a representation of the track geometry over the whole service life, it is essential to consider the quality signals independently of the time of year they were collected, and instead dependent on the time elapsed since the last maintenance measure. An exact description of the track geometry evolution over the service life can therefore be simplified using the quality values. A regression model is calculated individually for each cross-section in the TUG network based on quality signals (MDZ indicator and standard deviation). The calculated deterioration function between two maintenance measures reflects the different

quality values of the cross-sections (see 3.4.1). This calculation takes place for cross-sections at five metre intervals, making it possible to link superstructure information with machine deployments. More detailed information about the construction of the TUG database and the regression model can be found in the appendices (see Annex 1 or cf. [Hummitzsch 2009]).

3.4.1 Definition of Terms

With the regression model applied across the whole network, it is possible to analyse different parameters, which will be explicitly assigned to a period of time for the respective five-metre cross-section. Each period will then be delimited with real or imaginary machine deployments, also referred to as TUG-operations. TUG-operations thus precisely model unknown machine deployments, as well as inexplicable sudden alterations in the signal over time. In this way, consecutive periods for a cross-section describe the evolution of the track geometry over its service life, as well as the effects of individual tamping operations on the resulting quality signal. Beginning with the replacement of the track superstructure and the cleaning of the ballast, it is possible to enumerate the consecutive periods up to the end of the service life. In the course of this evaluation, however, only individual periods or consecutive pairs of periods will be considered. Where sequences are discussed, it will thus be sufficient to refer to period one and period two. A sequence therefore clearly defines starting qualities Q_1 and Q_2 as well as the associated deterioration ratios b_1 and b_2 .

T1_1	Start time of 1st period
T1_2	End time of 1st period
T2_1	Start time of 2nd period
in which:	$T1_2 \equiv T2_1$
T2_2	End time of 2nd period
ME[T]	Machine deployment at time T
Q1_ult period	Track geometry quality at time T1_2 - quality at the end of the period
Q2_ult	Track geometry quality at time T2_2 - quality at the end of the period
DeltaSchnitt	Quality of the regression model
Qb	Quality at a specific point of time within the period

The load data described in chapter 0 and the attributes from the generated load function are applied to each cross-section. The particular integration of the load functions enables the cross-section-specific calculation of the cumulative load for the TUG network, under the conditions specified in chapter 0. The lower bound of the integration is therefore specified by the installation year of the sleeper, while initially the time at the centre of the first period will be used as the upper bound of the interval.

The construction of a network-wide regression model gives rise to certain describable or indescribable uncertainties or distributions. In addition to fundamental uncertainty in the data, which can be partially resolved, the regression model serves to describe the evolution of the global track geometry, and is consequently influenced by a wide range of factors. The exponential approach will therefore be used as a basis for the deterioration of the track geometry between two machine deployments, and it is valuable to investigate the evolution of the track geometry over the total service life of the system. A discussion of which approach has the best fit is not the goal of this work, and has already been covered in detail by other research work ([Hummitzsch 2009], [Guler, Jovanovic & Evren 2011], [Audley, Andrews 2013], [Rießberger 1997], [Rohim Boy Berawi 2013]). An exponential regression admittedly makes interpretation of the results more complex, but it permits a wide fit of functions representing different deteriorations, without needing to change the mathematical formulae.

3.4.2 The Relationship between Q_n , b_n and Q_{ult}

The end quality of the period represents a purely calculated value based on the quality at the beginning, the rate of deterioration and the specified tamping cycle. The exponential relationship makes it more difficult to quantify how the start quality and the rate of deterioration individually affect the calculated end quality. Therefore it is necessary to establish how the individual parameters affect the end quality. This leads to a goal of describing these influences, quantifying how the resulting end quality is affected by the start quality or the rate of deterioration. Figure 30 shows three different temporal evolutions of track geometry. Case 1 is the "reference" case ($Q_n = -8$ und $b_n = 0,1$). In case 2 the start quality from the first case is reduced by 50%, while in case 3 the same reduction is applied to the rate of deterioration. It can be clearly seen that, up until the fourth year, the effects of the lowered start quality predominate. With of a threshold of -15, this difference would entail extending the tamping intervals to one year.

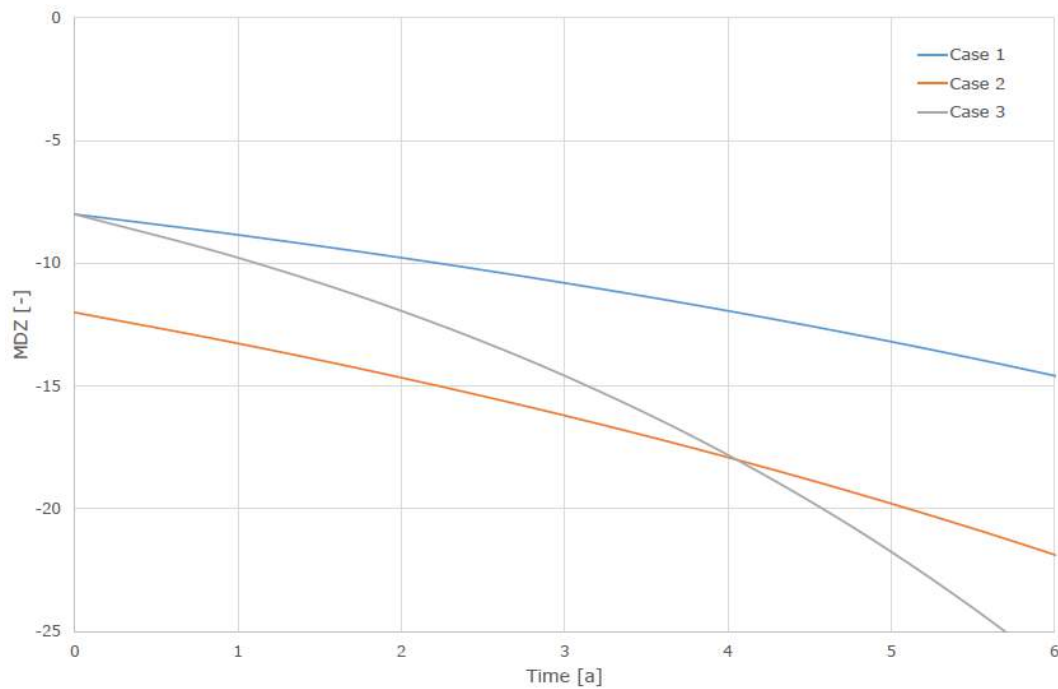


Figure 30 Influence of the Start Quality and the Rate of Deterioration on the End Quality

The following mathematical comparison helps explain how changing the start quality or the rate of deterioration by the same factor ξ affects the calculated end quality. The aim is to find the intersection between the two curves, which is the point where the two variants achieve the same end quality.

$$Q_n * e^{\xi * b_n * t} = \xi * Q_n * e^{b_n * t}$$

$$e^{\xi * b_n * t} = \xi * e^{b_n * t}$$

$$\xi * b * t = \ln(\xi) + b * t$$

$$t = \frac{\ln(\xi)}{b(\xi - 1)}$$

It can be clearly seen that the effect of the relative change on the end quality remains constant for different start qualities, while the influence of the rate of deterioration is proportional to its value. Figure 31 aims to depict this relationship, clearly showing that if the rate of deterioration is around 0.1, the start quality is proportional to the absolute value of the end quality. The higher the rate of deterioration leads to a smaller influence of the start quality. This is conditional on the start quality being above possible thresholds, meaning that a deterioration process is actually able to begin.

Independent of this, the end quality is dependent on all the parameters mentioned. Hence it is not part of the stated goal to focus maintenance purely on either the start quality or

the rate of deterioration. Consequently, this section will not focus on any particular parameter, but rather demonstrate the mutual dependency of the parameters within the end quality calculation.

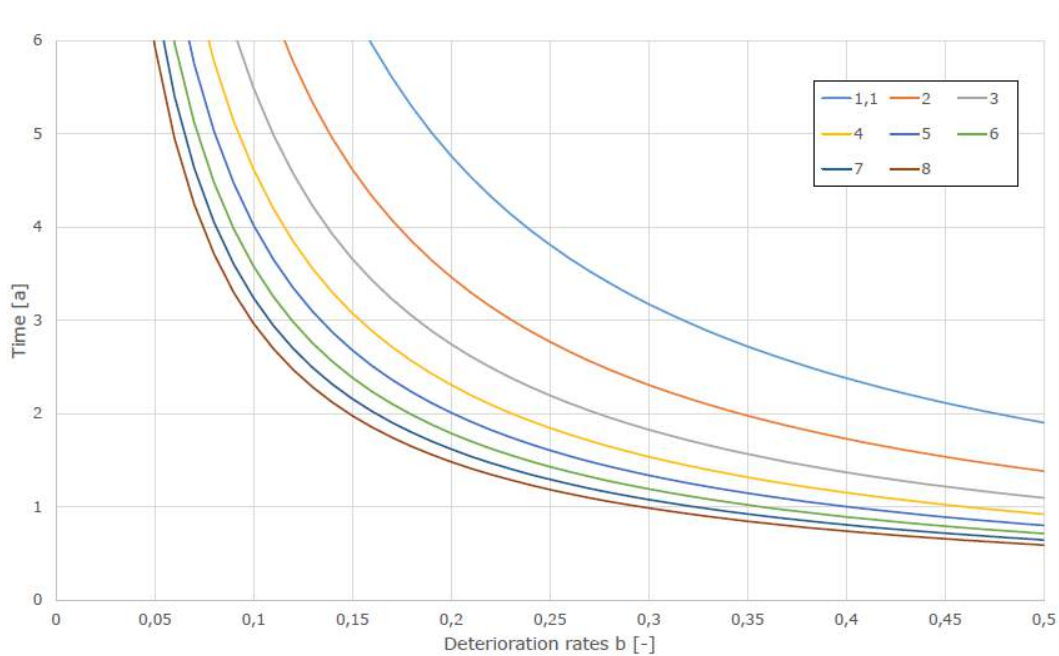


Figure 31 Graphical Representation of the Relationship between the Rate of Deterioration, the Tamping Cycle and the ξ Factors .

3.4.3 Different Parameter Sets

By filtering for various environmental parameters, such as sleeper type, switch areas, etc., it is possible to homogenise the otherwise heterogeneous population, and create detailed queries with specific parameters. The parameters include known data concerning track superstructure, as well as load data and other details concerning the quality values or machine deployments. The challenge is to formulate queries which are at once as general as possible and as detailed as necessary. If the population is too greatly restricted, both the value distribution and the range of the evaluation are reduced, leading to the risk of not only making specific statements about the selected track sections, but of defining them as global trends. The focus of this work is the uninterrupted global evolution of the track geometry throughout its service life. When evaluating the evolution, it is therefore necessary to select a large population, and only subsequently to identify possible outliers. For this, a kind of sensitivity analysis will be carried out by comparing the results of two evaluations with different filtering criteria. This section will use queries based on an analysis of the MDZ-a indicator, which makes it possible to compare different-speed cross-sections with respect to the track geometry. Furthermore, the MDZ-a indicator makes it possible to

consider the lateral and vertical alignment errors together, showing their effects on a virtual vehicle [Rießberger 1997]. Although it is possible to carry out speed-independent evaluations, and subsequently model the speed with the resulting MDZ-a indicators, the main evaluations used here (queries V1 and V2) will restrict the speed to the range between 80km/h and 160km/h. The restriction concerning higher speeds is due to the increasing dynamic loads on the tracks, which lead to different demands and thus to deterioration of the track geometry. The necessary increased quality and lower thresholds of these tracks are reflected in the ÖBB's current maintenance plan (cf. [ÖBB Infrastruktur AG 2012]). By only considering speeds greater than or equal to 80km/h, it is possible to exclude short intermediate straights, where the requirements are strongly affected by the preceding curves, leading them to exhibit divergent behaviour. The possible influence of lateral errors can be ignored in the straights. The network analyses in section 3.2 also show no correlation between the lateral signal and the amount of tamping, which may lead to the conclusion that only a few of the tamping measures in the TUG network are initiated as a result of lateral errors. Tracks built later than 2010 will be excluded from the evaluations, since it can be assumed that the load model will not be valid for such tracks.

Query V1

The quality values can be restricted to periods following tamping operations (MDZ) and will not be bounded by TUG operations at the end of the period. In the first year following track replacement, the periods up until the fourth tamping operation will be excluded from consideration, as will periods which do not have a continually describable condition. The period will therefore begin after the year the sleepers were installed, thereby preventing the situation from being classified with the wrong track superstructure. The quality signal's average deviation from the function may not be more than 0.75 MDZ points. All the observed quality values meet the valid length criteria (see Annex 3 or 4.2.1).

Query V2

The restrictions concerning the second machine deployment will be lifted. In this way, the query may include TUG operations as machine deployments delimiting the end of the period.

Query V3

By removing the valid length criterion, this query also enables discontinuities to be taken into consideration, or a combination of the discontinuity and the uninterrupted track section. However, the possibility of using a TUG operation as a delimiting machine deployment will be removed. This is based on the fact that quality periods which evolve discontinuously

give distorted quality values, and thus distort the evolution of the track geometry over the service life.

Query V4

This is the most-general query formulation. No restrictions will be applied before the first machine deployment. The first machine deployment must be an MDZ operation.

	ME1	ME2	Valid length	Delta Schnitt	permissible Speed	Required values	Year of construction
V1	MDZ	<>TUG	TRUE	≤0,75	80-160	400	>100 & <2010
V2	MDZ	n.r.	TRUE	≤0,75	80-160	800	>100 & <2010
V3	MDZ	<>TUG	n.r.	≤0,75	80-160	800	>100 & <2010
V4	MDZ	n.r.	n.r.	≤0,75	80-160	800	>100 & <2010

kE ... no restriction

100 ... Error value for sleepers where the year of installation is unknown

Table 2 Overview of individual Filter Criteria

The cumulative load is as far as possible (see 2.3) calculated uniquely over the estimation function and used as an aggregate value (in groups of 25 million tonnes), in order to show the evolution of the quality values over the service life. The daily load used is that calculated by the estimation function for the year 2007.

3.4.4 Evolution of the Track Geometry in straight Sections (R>600m)

The selected criteria for query V1 reduce the population considerably. From the 126,382 output quality values, concrete sleepers dominate in the portrayal of the evolution of the global track condition (see Figure 32). In the case of concrete sleepers, it is possible to identify a reduction in quality associated with the increase in cumulative load. The interpretation of the resulting period start qualities for wooden sleepers is difficult due to the small number of cross-sections. Load groups which comprise fewer than 400 values (see Table 2) will not be considered in the context of this evaluation. It can be supposed that groups with such a small number of cross-sections are not representative of the global condition, hence their exclusion.

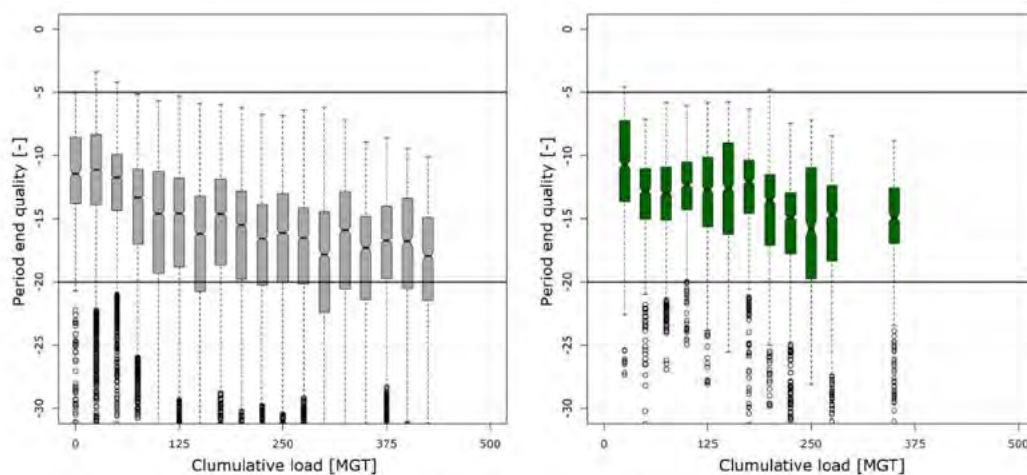


Figure 32 Evolution of the Period Start Quality over cumulative Loads (Query V1); left: Concrete Sleepers, right: Wooden Sleepers

The limits of the service lives are strikingly different, bounded by the last box plot shown (see Figure 32). Although the absolute values require detailed examination, it is noticeable that wooden sleepers have a 25% lower service life. Wooden sleepers exhibit a similar trend to that shown by concrete sleepers. The box plots for 25 million and 40 million tonnes strongly distort the picture, and the possible regression analysis does not give encouraging results for wooden sleepers. The comparison of the two evolutions follows a logarithmic progression over the cumulative loads, which is particularly evident for concrete sleepers (see Figure 32). Only the period start qualities shortly after replacement and at 325 million tonnes diverge from the global trend for concrete sleepers; while a logarithmic deterioration with a coefficient of determination of barely 80% is determined for wooden sleepers.

In the course of the evaluations, three distinct model approaches to describing the evolution and the period end quality were tested (see Figure 33).

A linear model does not suffice to describe the relationship between the cumulative tonnage and the resulting track geometry quality in either case, while the quadratic and logarithmic model both exhibit good results.

The logarithmic model not only has a marginally better fit (both in terms of the coefficient of determination and the distribution of the residuals), but also harbours operational advantages. An improvement of the track geometry over the course of the service life can be excluded with the logarithmic approach, while by contrast it is at least mathematically possible with the quadratic approach.

Track Geometry

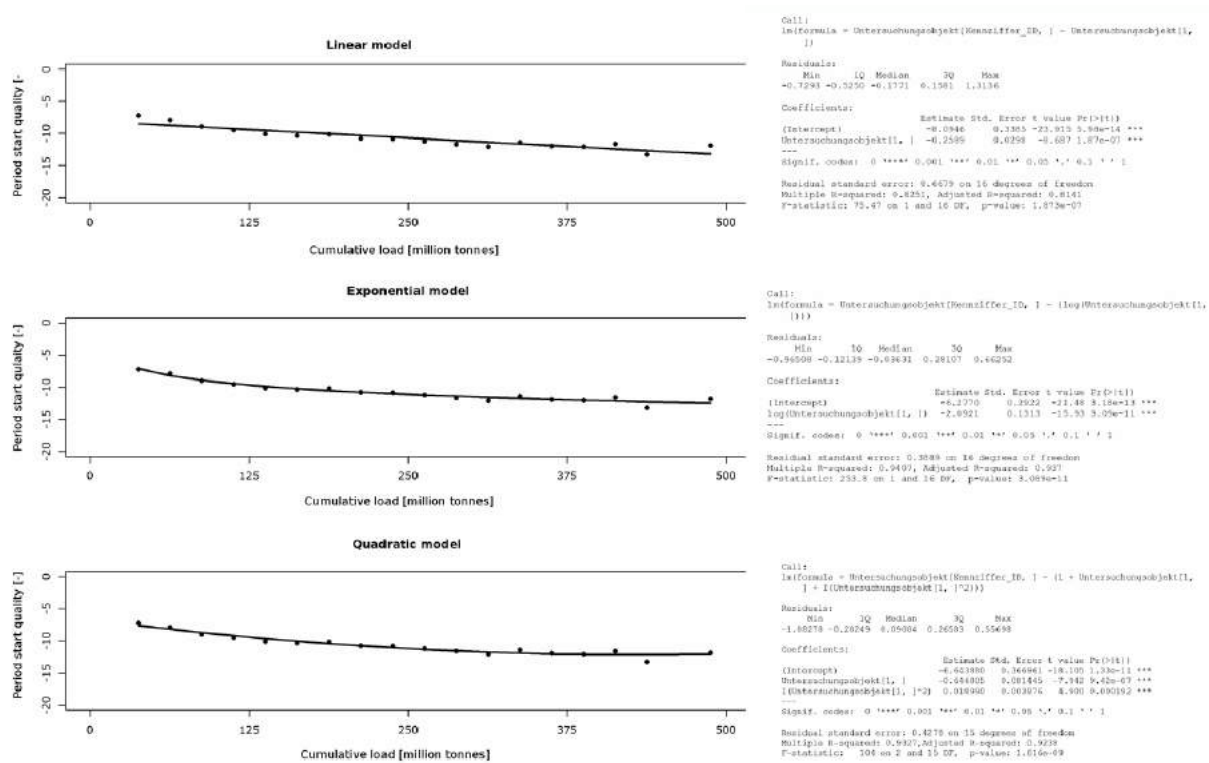


Figure 33 Evaluation Methodology for Regression Qualities using the Median Value for the Period Start Quality for Concrete Sleepers as an Example

As a result, the logarithmic approach is more stable than the quadratic approach with respect to outliers. A method for handling the mathematical uncertainty in the logarithmic function at the null point should also be discussed. The goal of the function is to describe the evolution of the track geometry over its service life, hence the evolution between the starting settlement level and 2 million tonnes will not be considered to be within the valid range. The lower bound of the function is therefore bounded to settlement levels starting at 0.5 million tonnes, which means that the logarithmic function remains continuously determinable. This may appear to be a purely mathematical trick, but in fact it has key significance for the software implementation of the classification algorithm. As a result of the influence of the deterioration rate and the resulting additional distribution, the regression qualities are typically lower for period end qualities than period start qualities. However, they can be considered sufficiently accurate.

Looking at the deterioration rate, at the beginning of the service life significantly mutually high values are exhibited (see Figure 34). The deterioration rate for concrete sleepers appears not only to result in a larger distribution, but also in larger values than for wooden sleepers. There is no identifiable trend, and furthermore, there are dramatic differences between the load groups.

By contrast with the deterioration rate for concrete sleepers, the deterioration rate for wooden sleepers grows continuously after the first 100 million tonnes, approaching the same level as the concrete sleepers.

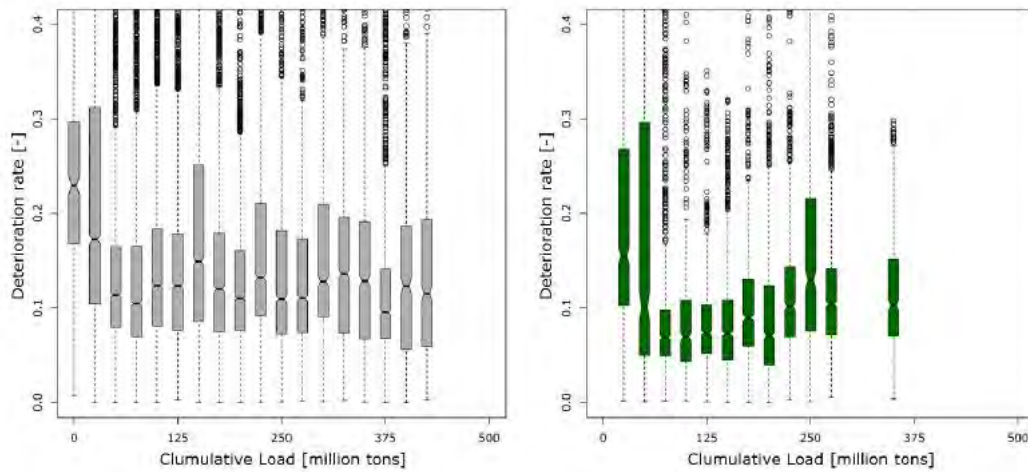


Figure 34 Evolution of the Deteriorate Rate over cumulative Loads; left: Concrete Sleepers, right: Wooden Sleepers

The period start qualities and the associated deterioration rates yield the period end qualities; that is, the qualities which trigger maintenance measure or emerge shortly before the measure. Despite some sudden changes in deterioration rates, the period end qualities exhibit a logarithmic progression, as do the period start qualities.

The evolution of the period end qualities is dependent on the type of sleeper installed, exhibiting a generally higher level for wooden sleepers. This implies that wooden sleepers are maintained at a higher quality level than concrete sleepers.

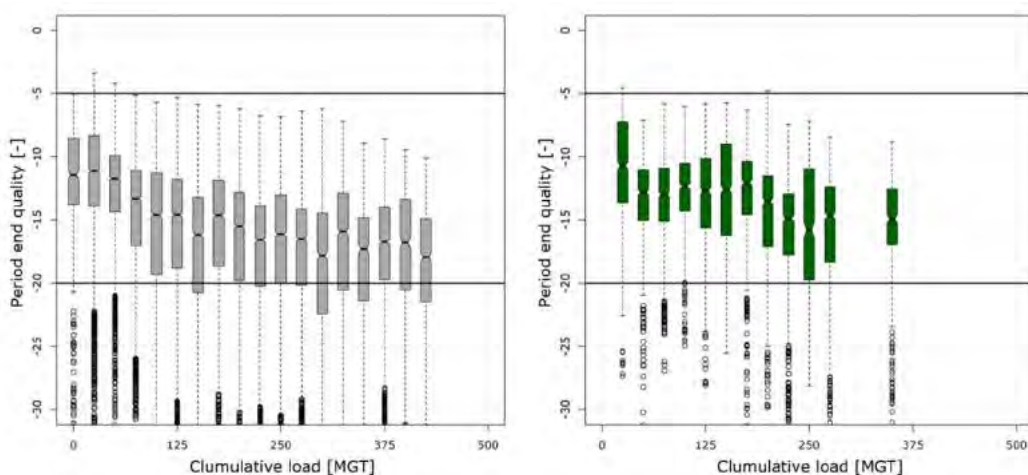


Figure 35 Evolution of the period end qualities over the cumulative tonnage; left: concrete sleepers, right: wooden sleepers

The insights thus far have been based on evaluating the basic query V1 and should be compared with the results of other queries, initially with the results of query V2. Particular attention should be paid to investigating the rate of deterioration and the evolution of period start qualities related to wooden sleepers. Query V2 relaxes the restrictions from the original questions, thus admitting additional quality values (see Table 2). In this way, the sample population is increased by 50% for concrete sleepers, and by as much as 100% for wooden sleepers. Using the evaluation method previously applied to V1, it becomes possible to observe the evolution of the period start qualities over the cumulative tonnage, and to compare the regression of the median value and the quartile values from each variant (see Figure 36).

The representation above makes it possible to compare queries V1 and V2 with respect to the different evolutions of the start period qualities over the cumulative tonnage. It shows the evolution of the interquartile range and the median. This makes it possible to directly compare concrete and wooden sleepers.

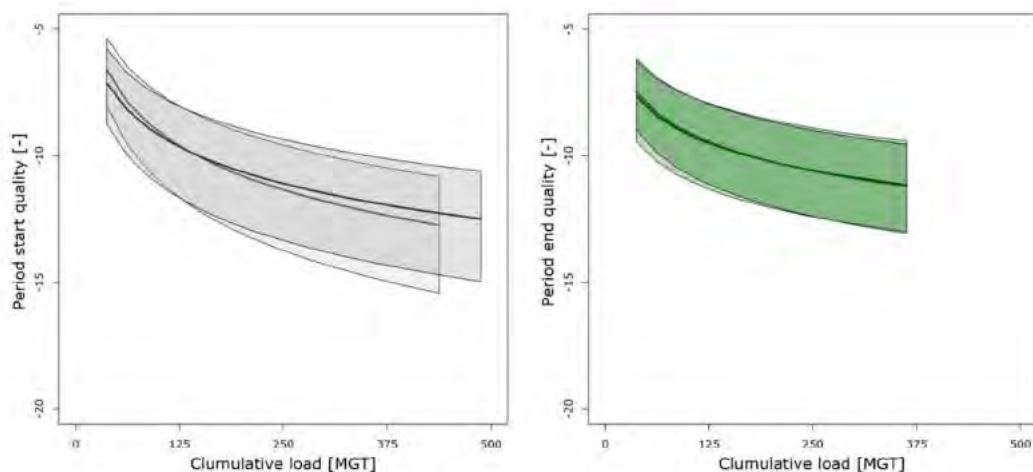


Figure 36 Comparison of the evolution of the period start quality between the queries V1 [grey median value] and V2

Despite the smaller population, the additional cross-sections do not lead to noticeable changes in the approximated condition for wooden sleepers, although they do increase the coefficient of determination for the regression. A similar picture emerges for concrete sleepers, although in this case it is possible to identify a slight displacement of the regression curve. Even if the change in the curve is marginal and can be ignored, it does show the particular sensitivity to environmental parameters exhibited by concrete sleepers.

This understanding, combined with the fact that hardly any change to the evolution of the deterioration rate is evident in Figure 37, makes it possible to carry out the further evaluations based on the data points from query V2. The further evaluations will be primarily

based on a closer examination of concrete sleepers. The larger sample size permits a more detailed examination, as well as enabling a division into distinct groups, which would run the risk of not leading to representative results when including wooden sleepers.

Considering the MDZ-a indicator as the basis for the evaluation, it is largely possible to separate it from the consideration of different speed ranges. In Austria and therefore in the TUG network, the planning of measures to correct the track geometry is based on the use of EN13848-6, and therefore primarily on the observed standard deviation of the longitudinal elevation. Although a modified form of the standard deviation with a different constraint length is used in Austria, the thresholds defined are nonetheless dependent on the speed [Auer 2004].

The MDZ-a indicator is by definition used in a speed-independent manner. Nonetheless, a correlation between the evolution over the service life and the speed-dependent thresholds cannot be ruled out. Therefore, it is worth exploring the extent to which possible differences in speed affect the evolution of the quality over the service life, or rather, what effects are implied by speed-dependent thresholds. In Query V2, two distinct intervals can be distinguished in terms of the stipulated maintenance thresholds. [Österreichisches Normungsinstitut 2014]

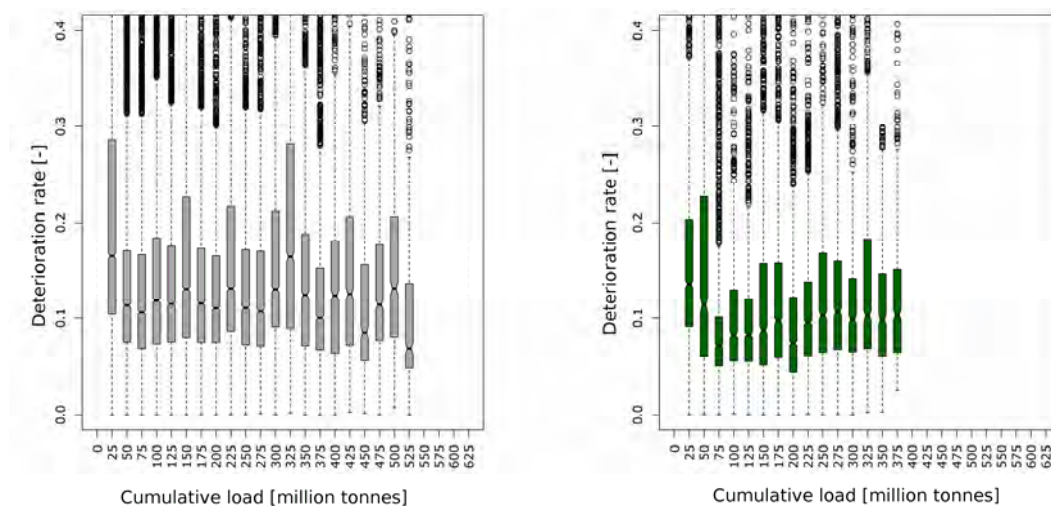


Figure 37 Evolution of the Deterioration Rates over the cumulative Load; left: Concrete Sleepers, right: Wooden Sleepers

Interval A describes the speed range from 80km/h to 120km/h, while speeds from 120km/h to 160km/h fall into interval B. Both evolutions can be described by the logarithmic approach, which reveals differences between them. Both the regression function for interval A and that for interval B approach -12, with the difference between the two intervals reducing as this limit is approached (see Figure 38).

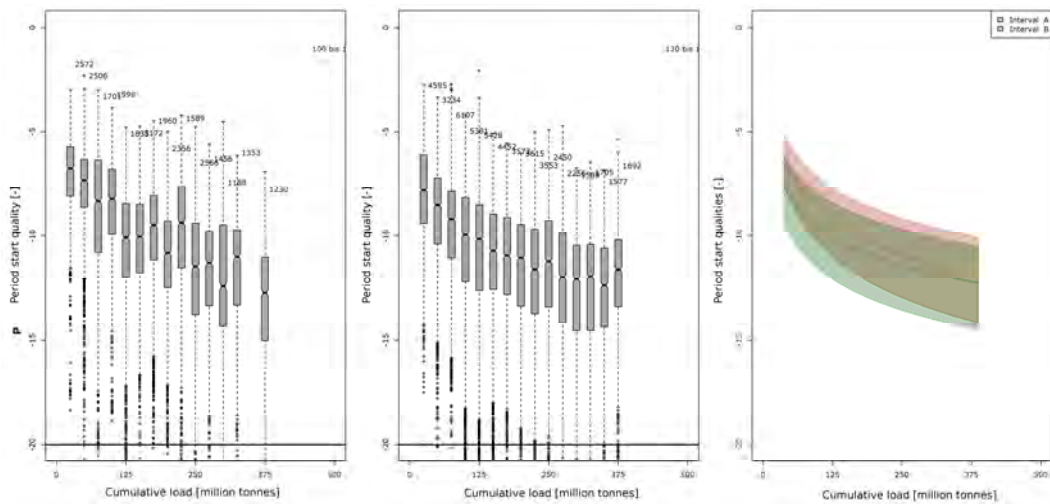


Figure 38 Evolution of the Period Start Quality in distinct Speed Intervals

A comparison of the period end qualities shows that both evolutions have a similar progression, but with displaced absolute values (see Figure 39). Therefore, route sections with lower speeds tend to exhibit better track geometry quality than cross-sections with speeds in interval B. However, the goal of the present standardization process is to define the higher requirements for the track geometry quality which are associated with increasing speed. In order to make more detailed statements about the precise origins of these distinctions, it is necessary to quantify the correlation between the speed and the resulting rate of deterioration. No clear pattern is apparent when looking at the rate of deterioration in individual intervals, which suggests that the value of the deterioration rate is mainly affected by other parameters and only marginally by the admissible speed. The difference in the period end quality is thus attributable primarily to diverse speed-dependent maintenance strategies. It could be speculated that the thresholds decided for track sections with low speeds tend to be too high. When the evolution of the period end quality over the standard deviation of the vertical alignment is considered, an inverse progression appears. Route sections with lower speeds exhibit worse track geometry quality. Bringing these observations together, it is possible to establish that the different speeds in the observed intervals have only a marginal influence on the resulting period start qualities (in MDZ-a). The period end qualities reflect the maintenance strategy.

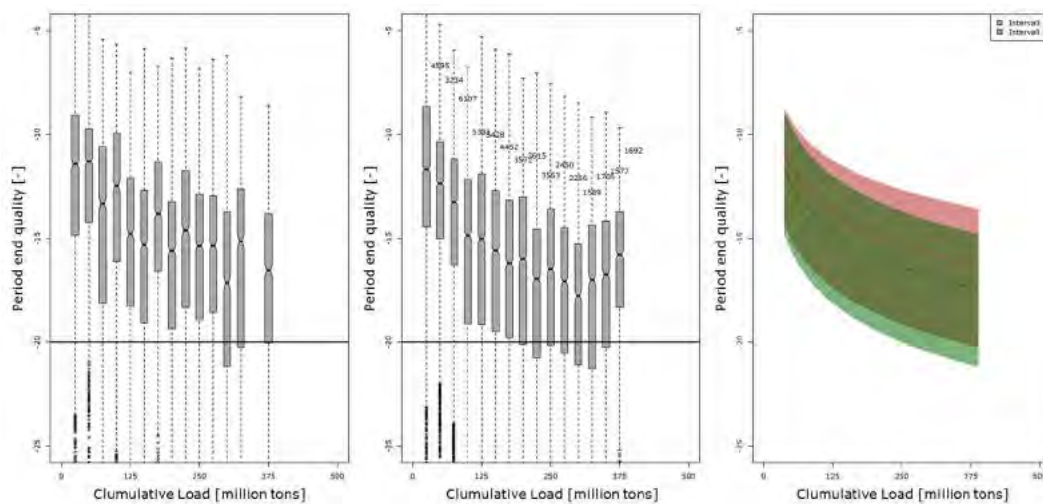


Figure 39 Evolution of the Period End Quality in distinct Speed Intervals

The different speeds thus do not affect the actual evolution of the track geometry quality, but just result in different levels. Assuming that the MDZ indicator theory is correct, this enables a speed-independent classification of the track, since it already takes the speed into account in the calculation. Based on this, it is possible to talk about a uniform value for the track geometry, making it possible to specify individual thresholds network-wide independent of speeds.

The observation of the cumulative load results in a combination of the track superstructure age with the daily load, thereby establishing a common grouping criterion. The new "cumulative load" parameter makes it possible to significantly increase the sample size, making direct observation of the daily load redundant. It is nonetheless worth first clarifying the influence of the different daily loads on the evolution of the track geometry over its service life. It appears (see Figure 40) that there is no relationship between the different daily loads and the evolution of the track geometry over the cumulative load. The recognizable differences between the quality progressions for individual daily loads result mainly from the general distribution of concrete sleepers, and cannot be attributed to the different daily loads. For the load category >70,000 tonnes per day and per track, there are not enough values to provide a representative picture over the service life.

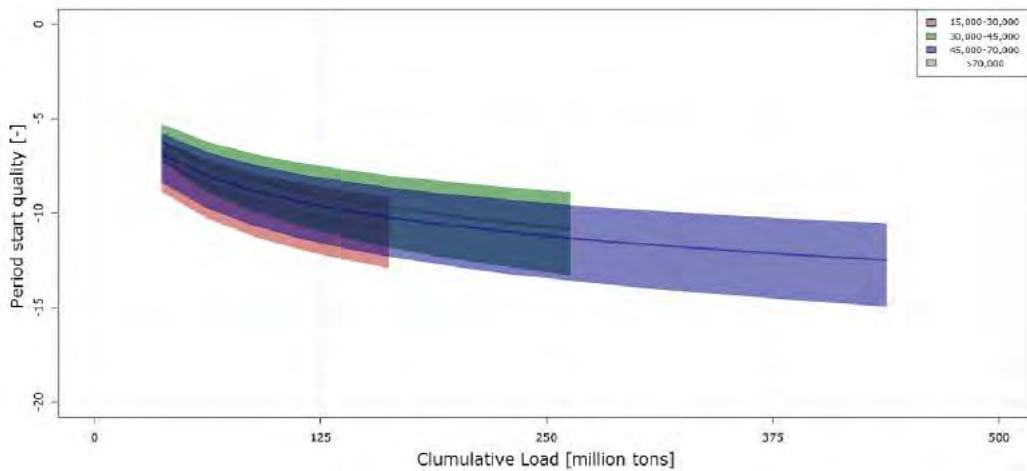


Figure 40 Evolution of the Period End Qualities for different daily Loads, in the Case of Concrete Sleepers

By contrast with the evolution of the period end qualities, a clear relationship can be seen between the daily load and the evolution of the deterioration rate over the service life (see Figure 41). In every load category examined, the first 25 million tonnes exhibit particularly high deterioration rates compared to the rest of the life span, reducing over time to level out at distinct levels at ca. 125 million tonnes.

In the 30,000-45,000 tonnes per day and track load category, the difference between the initial deterioration rate and the final stable level increases noticeably. In the third load category considered, 45,000-70,000, the deterioration rate exhibits noticeably higher values across the whole range, with particularly high initial deterioration rates. The difficulty in analysing the deterioration rate lies in separating the various effects from each other. Both the rail profile and the daily load influence the rate of deterioration. In general, smaller rail profiles are installed in areas where the load on the route is lower, and thus are subject to different stresses. This scenario has been studied in detail by Robert Hummitzsch [Hummitzsch 2009] and will not be considered further in this work.

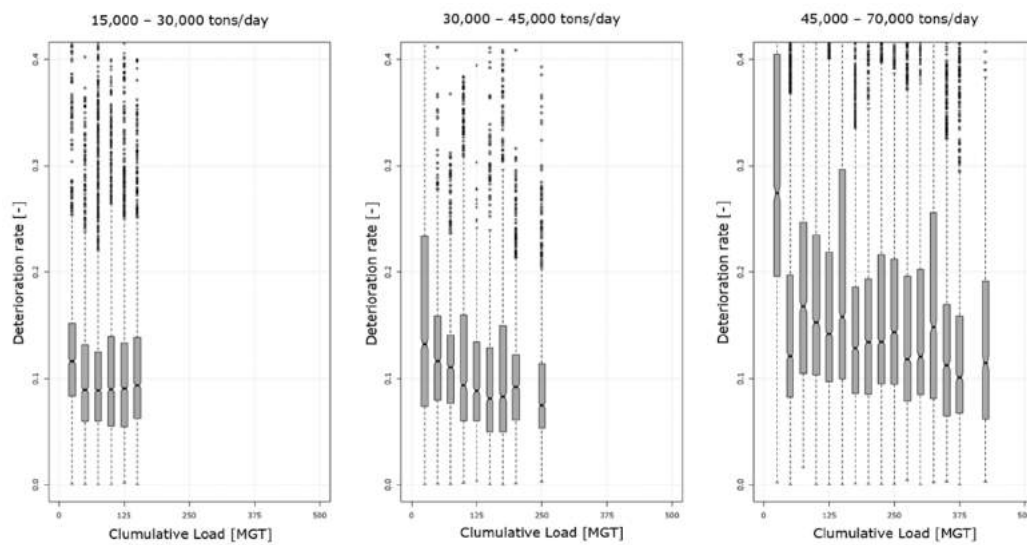


Figure 41 Evolution of the Deterioration Rate over the cumulative Load depending on the individual Load Group, for Concrete Sleepers

The expression of this effect in wooden sleepers is not apparent in the same way, although it is difficult to obtain clear evidence due to the smaller population. As a result of the smaller sample sizes and the proven dependency between daily loads and deterioration rate, it is difficult to establish the difference between concrete and wooden sleepers. In general, wooden sleepers exhibit a deterioration rate around 30% lower than that of concrete sleepers. The rise previously established in the deterioration rate for wooden sleepers over the cumulative load can initially be attributed to the characteristic distribution of the cross-sections in the individual load groups.

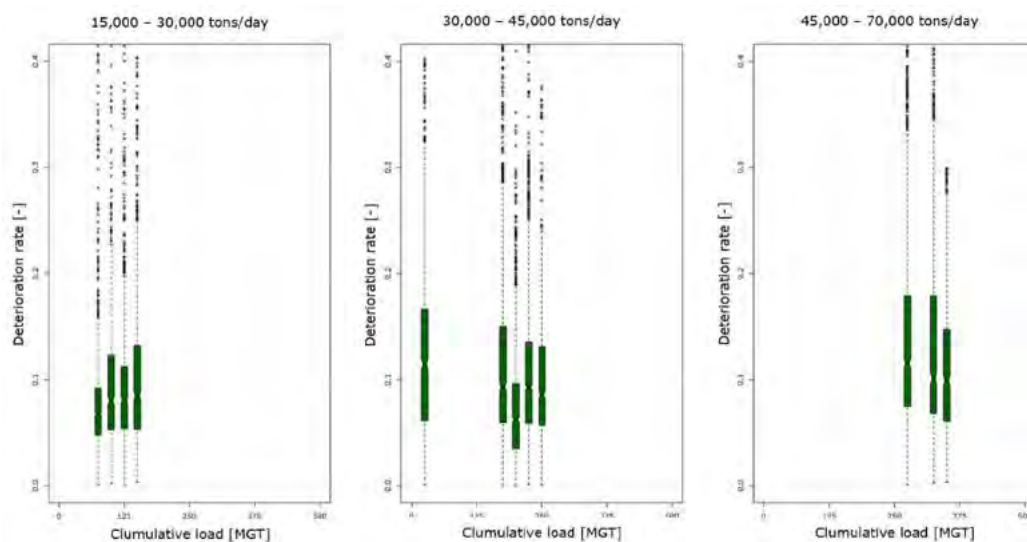


Figure 42 Evolution of the Deterioration Rate over the cumulative Load depending on the individual Load Group, for Wooden Sleepers.

Precise determination of the evolution of the deterioration rate over the service life is limited or simply not possible. The distance between the boundaries of the first and third quartiles is almost a factor of two in some areas. The wide distribution of deterioration rates thus makes it difficult to establish a clear classification. Parameters such as different subgrade characteristics, vehicle structure, performance qualities, etc., appear to have a greater influence on the rate of deterioration than the evolution of the period start qualities ([Landgraf et al. 2014]). The daily loads reflect the above evaluation in terms of the values of the deterioration rate. Towards the goal of classifying the condition of the track geometry, the standardization of the deterioration rates (cf. [Hummitzsch 2009]) will be dispensed with, only distinguishing between very high and very low deteriorations, dependent on the daily load. The first classification criterion will be the period start quality or end quality, while the deterioration rate will only be used for the secondary classification.

If the work is to be objective, however, it is important to consider how different deterioration rates affect the resulting absolute (i.e. period start quality) track geometry. The deterioration rates will be divided into three categories according to their distribution, using the first and third quartiles as the boundaries. This division does not lead to any discernible alteration in the evolution of the period start quality (see Figure 43). Therefore, it would appear that there is no relationship between the deterioration rate and the period start quality in the same period.

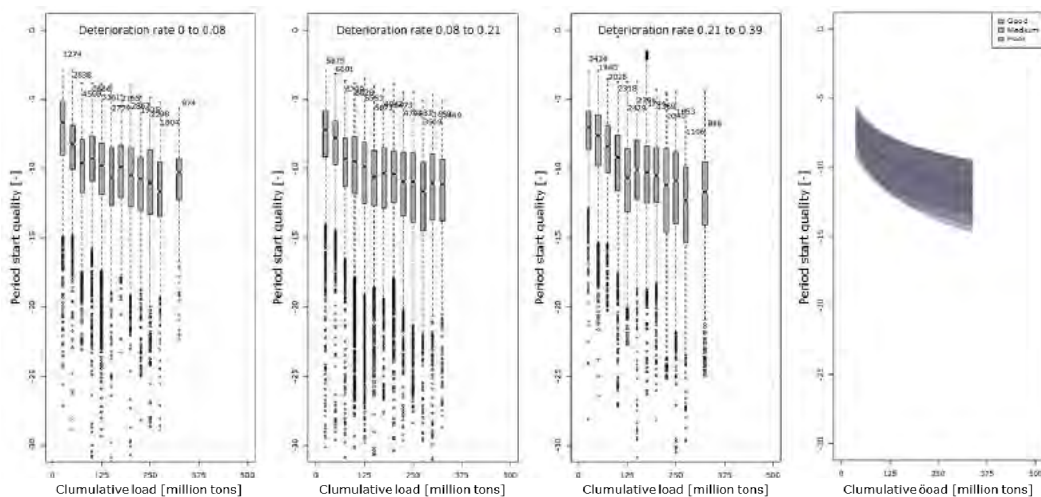


Figure 43 Effect of different Deterioration Rates on the Period Start Quality

The grouping of the deterioration rates has a contrasting effect on the period end quality, as shown in Figure 44, resulting in a significant change to the results. The boundaries for the groups result from the division of the deterioration rates and correspond to the 25% and 75% quartile values. The corresponding boundaries for individual categories are shown in the figure. As the deterioration rate increases, higher period end qualities are exhibited.

This relationship follows logically from the calculation of the period end quality. Furthermore, it follows that maintenance measures on tracks with a higher deterioration rate exhibit a worse absolute value for the track geometry than on tracks with better deterioration rates.

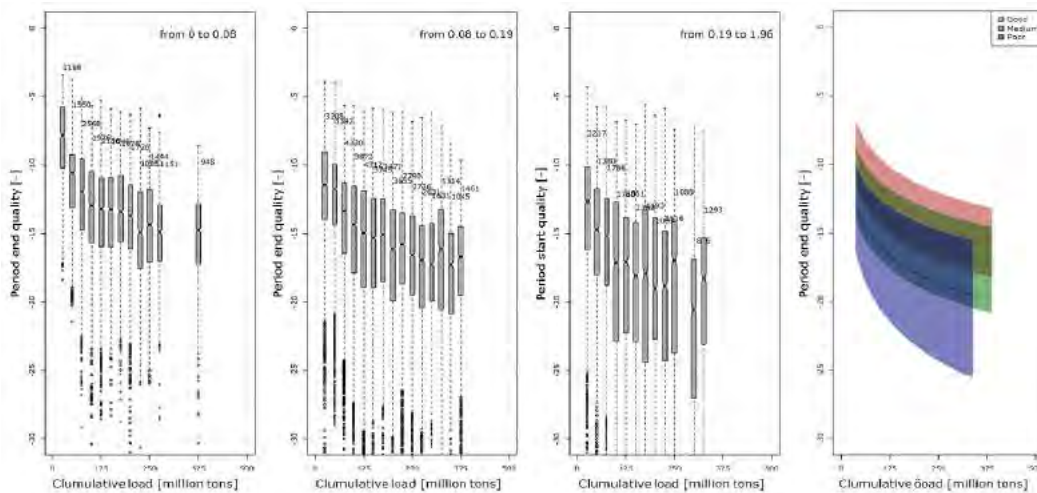


Figure 44 Effect of different Deterioration Rates on the Period End Quality

Therefore, it is worth clarifying why tracks with a smaller deterioration rate are tamped at a higher quality level. There are two different reasons for this apparent paradox:

1. The planning of tamping measures is more or less independent of the track geometry, taking place based solely on time intervals.
2. Individual track sections are combined into a large average area. This means that the machine deployments can be maximized for minimum costs. Therefore, some of the areas which are tamped will exhibit a much higher quality level.

In order to address this problem, it is necessary to examine the qualities exhibited before the tamping measure more closely. The difficulty with this approach is that it is no longer sufficient to consider the cross-section or the period quality parameters individually. It is also necessary to consider the tamping measure with respect to the associated section qualities. This information, however, is only indirectly available from the database, because although the tamping measures are recorded by cross-section, their association with a track section is lost. In order to re-establish this correlation, tamping measures which have the same operation load, and which occurred within the same route and track during the period, must be associated with a section, and the corresponding quality information then assigned to them. The association with individual cross-sections follows on the basis of the restrictions defined in V3. In the evaluations, tamping measures will only be considered which comprise a length of no less than 100 metres and no more than 9000 metres. These

limits will be applied partly to explicitly exclude particularly short tamping measures (correction of single failures) from the evaluation, and partly to exclude potential erroneous data. Machine deployments will consequently be indicated as erroneous entries if the operation length is longer than the maximum output for a single operation. If the route sections with better and worse track geometry are combined, in order to model longer average stretches, then the different individual sections affect the resulting route section quality. Route section quality refers to the period end quality which proves decisive in triggering the maintenance measure.

The statistical values associated with the section are therefore of key significance. The simplest option consists of modelling, over the section, the mean value of all the quality values for the cross-section whose end time matches the time of the tamping operation. However, mean values are significantly influenced by outliers, which can distort the results in sections with wide distributions. Quantile values are much more stable robust estimators in relation to outliers, and therefore meet the requirements established for the evaluation. A tamping measure will be uniquely identified in these queries by a start kilometre and end kilometre. Providing the section meets the criteria described considering the length, it will be possible to determine the period end quality before the tamping measure from the uniquely associated cross-section values.

In order to assign a unique value to the section from the collection of period end qualities, the calculated median will be used. Each tamping measure is thus associated with a median value which uniquely describes the quality of the route section shortly before the tamping measure (section quality). Each tamping measure can similarly be assigned a specific cumulative load or load group. The tamping measure qualities are naturally somewhat distributed, but very clearly exhibit the logarithmic trend over cumulative loads which has already been identified (see Figure 45). Regarding the distribution of values in the individual load clusters with respect to the aforementioned trend, it is possible to determine what percentage of the tamping measures verifiable by the regression models take place over the track geometry.

Consideration of the section qualities shows that they are naturally scattered to some degree. Similarly to the approach used in the above sections, the box plot of associated section qualities is determined for individual load clusters, providing at least 20 tamping measures are available in the associated load cluster. Here, once again, it is worth identifying possible outliers among these measures, which will subsequently be excluded from consideration. In this evaluation, the period qualities clearly exhibit the typical logarithmic progression. For the remainder of this work, the logarithmic regression of the medians will serve as the basis of the comparison with the previous investigations.

When interpreting Figure 45, it should be recalled that tracks with unfavourable boundary conditions tend to require reinvestment before they achieve higher cumulative traffic loads. By contrast, tracks with high cumulative traffic loads often exhibit extremely favourable characteristics. This results in such tracks often exceeding the trend described above.

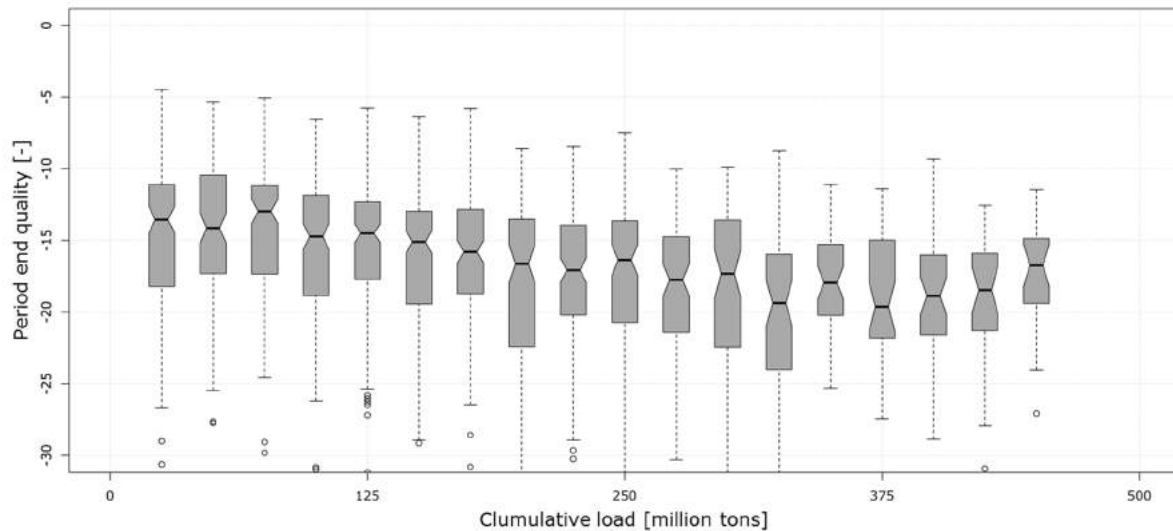


Figure 45 Evolution of the 50% Section Quality over the cumulative Tonnage

When considering Qult in the context of query V3 it is worth taking into account the fact that in this query, the demands on the cross-section have been reduced. The restriction on the evaluation to cross-sections with the valid length criteria was removed in order to increase the sample size. Accordingly, the period end qualities can be considerably larger than in the previous queries, since individual discontinuities are no longer excluded from consideration. The condition of the components at these discontinuities can be significantly different from that of the base population. By comparing the queries, it can be seen that this divergence is particularly evident in the case of wooden sleepers.

The regression of the evolution of the median of different section qualities is clearly reflected in the different resulting progressions. The 25% section quality lies well outside the quartile range of the general evolution of concrete sleepers.

Particularly as a result of the reduced daily load, but also as a result of the different components conditions, wooden sleepers not only exhibit better start qualities, but correspondingly also better end qualities (see Figure 46). This difference indicates that wooden sleepers are typically tamped with a higher quality level than concrete sleepers. The majority of wooden sleepers are nowadays only installed in route sections with lower loads or particularly tight bends, but nonetheless exhibit a better period end quality. From a technical

point of view, the current standard does not distinguish between different track superstructure types when defining thresholds, but rather defines them only dependent on the speed. An evaluation of the installed track superstructures with respect to the associated speeds clearly shows that wooden sleepers are typically installed in tracks which are travelled at lower speeds (see Figure 26). This is the foundation of the distinction between concrete and wooden sleepers over the aforementioned speed difference, and the resulting different thresholds in the maintenance strategy. However, the difference between the period end qualities for wooden and concrete sleepers has only peripheral effects on the classification of the track geometry. For this classification, various period end qualities will act as boundary values, making it possible to distinguish the track geometry in distinct quality groups. The track superstructure will therefore be of secondary significance to the track geometry.

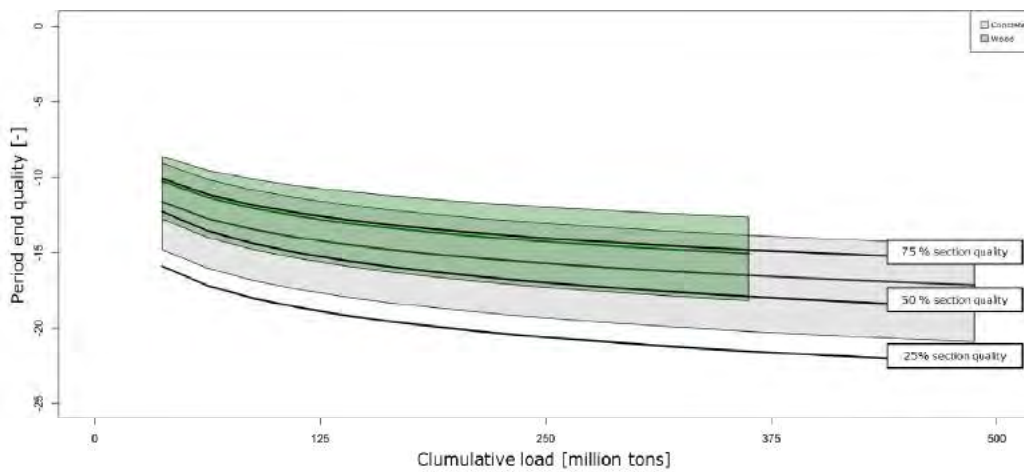


Figure 46 Comparing Route Section Qualities with the Evolution of the Period End Quality for different Sleeper Types

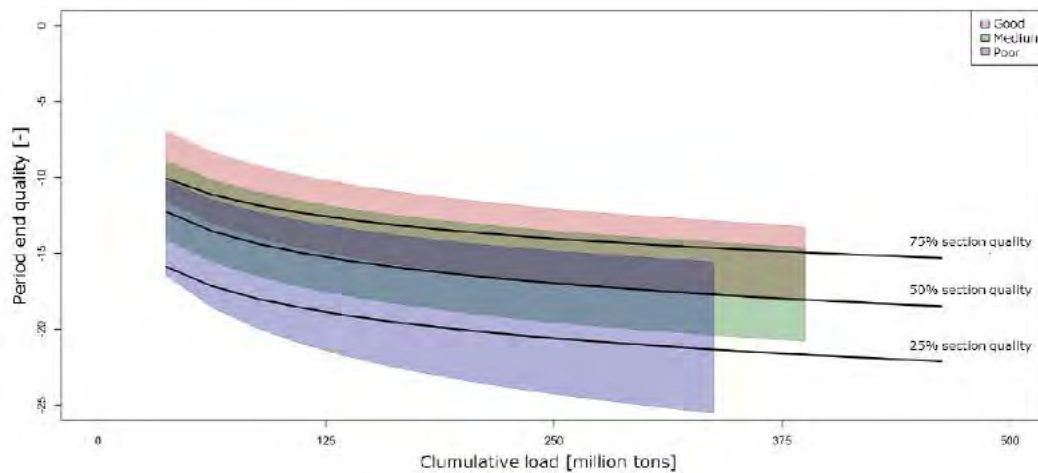


Figure 47 Comparing various Route Section Qualities for Concrete Sleepers with the Evolution of the Period End Quality over the cumulative Load, taking into account the current Deterioration Rate

When considering the section qualities, it is crucial to bear in mind the fact that different deterioration rates lead to different period end qualities. In other words, a worse track geometry quality appears to be tolerated for high rates of deterioration than for lower rates.

If the calculated section quality is associated with the different evolutions for period end qualities, then the comparison shown in Figure 47 emerges. The section quality lies significantly below the 50% quality of the general progression of the period end quality. This scenario can be explained as a result of the elimination of restricting parameters such as the length criterion. Due to this elimination, discontinuities with particularly poor track geometry have additional influence on the median value, bringing it down. Despite these additional influences, the period end qualities exhibit the same logarithmic progression identified by the previous queries.

In more than half of the tamping operations, the operation is significantly impacted by individual poor sections, which make up over half of the route section. It can therefore be concluded that the distribution of track geometry errors is not random, but rather based on the system's exposure to stresses and its resistance. Through this non-random value distribution, it can be established that the majority of tamping measures in the TUG network take place on the basis of the track quality. It is clear that tamping measures occur at least partially in sections with particularly poor track geometry, which are aggregated with sections of better track geometry quality. A plan based exclusively on the condition of the component is, however, not available.

In some areas, the plan is apparently based on a time-dependent or load-dependent maintenance plan. In order to further substantiate this result, it is worth examining the current tamping intervals.

This examination aims to capture the difference in tamping intervals for diverging deterioration rates, to which end particular attention will be paid to keeping the other known environmental parameters as constant as possible. It is thus worth testing the assumption that cross-sections with strongly deteriorating track geometry are tamped more often than cross-sections with lower deterioration rates. This verification will also be extended, in reverse, to the period start quality. Thus, only cross-sections with concrete sleepers, a daily load between 45,000 tonnes/day/track and 70,000 tonnes/day/track and the rail profile 60E1 will be considered. A clear difference in the average tamping intervals over the service life emerges. Accordingly, cross-sections with higher rates of deterioration will be tamped more often than those with lower rates of deterioration (see Figure 48). This evi-

dence again confirms the prior supposition that in the majority of cross-sections maintenance is dependent on the component condition and merely aggregated into larger sections.

There is no significant correlation evident between the period start quality and the tamping cycle (see Figure 49). As has already been shown by the evolution of the period end quality, the maintenance regime is based on a threshold which evolves over the service life (accordingly, a compliant threshold). Newer tracks are tamped at better track geometry qualities than older tracks. Given this, it can be supposed that a worse quality is tolerated for older tracks.

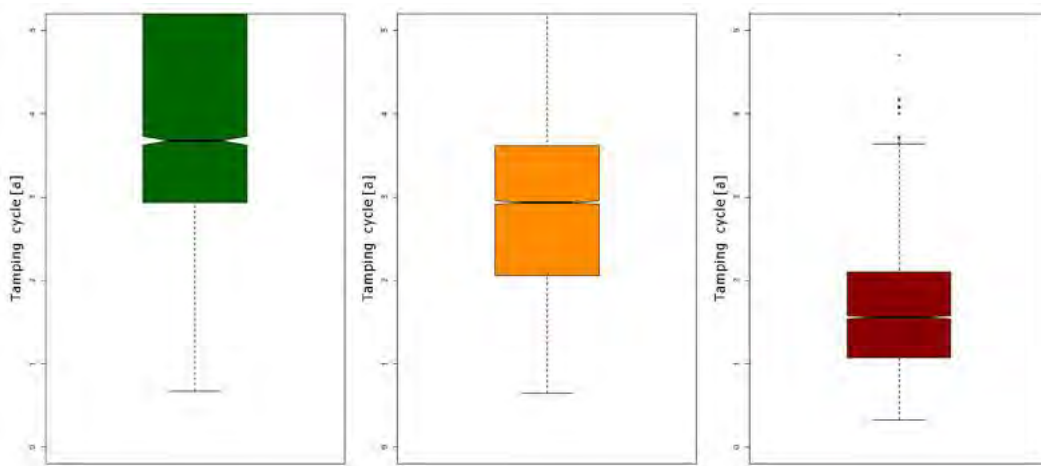


Figure 48 Average Tamping Cycles grouped according to lower to higher Deterioration Rates from left to right

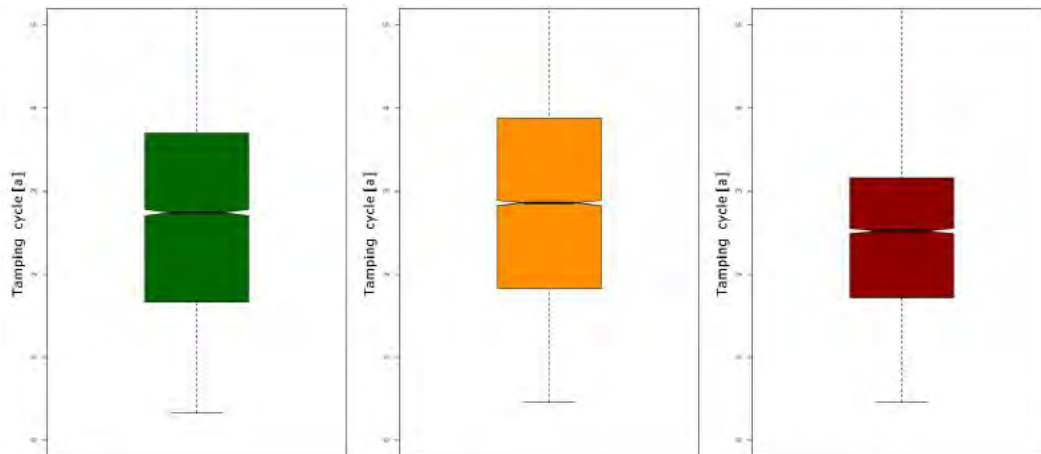


Figure 49 Average Tamping Interval Group according to good/medium/poor Start Qualities from left to right

3.4.5 The Relationship between consecutive Maintenance Periods

A detailed evaluation of the relationship between two consecutive periods generates additional information to help describe the track geometry over the service life. In connection with this, one of the questions which arises is the effect of poor period end qualities on the period start quality of the subsequent period. For example, whether it is possible to achieve the same subsequent period start quality for a significantly worse period end quality as for a much higher starting level. It is further worth clarifying the effects of different deterioration rates on the period start quality of the subsequent period. The basis of this evaluation is a modification of the quality value output based on query V3, which does not only take two consecutive periods into account, but furthermore returns their associated qualities. In general, query V3 results in much wider distributions than the queries so far considered; however, this must be accepted in order to achieve the required sample population size for the following evaluation. Independent of the reason for the different thresholds for different deterioration rates, the question arises of whether these affect the resulting period start quality after the tamping operation.

Figure 50, by contrast with Figure 43, a small but distinct relationship can be identified between the period start quality Q_2 and the deterioration rate b_1 . By contrast, only particularly poor Q_1 values influence the deterioration rate of the subsequent period. However, if the period start quality of the subsequent period is only affected by a small part of the absolute value of the deterioration rate b_1 , then the question arises of what effect the threshold value Q_{1_ult} has on the subsequent quality.

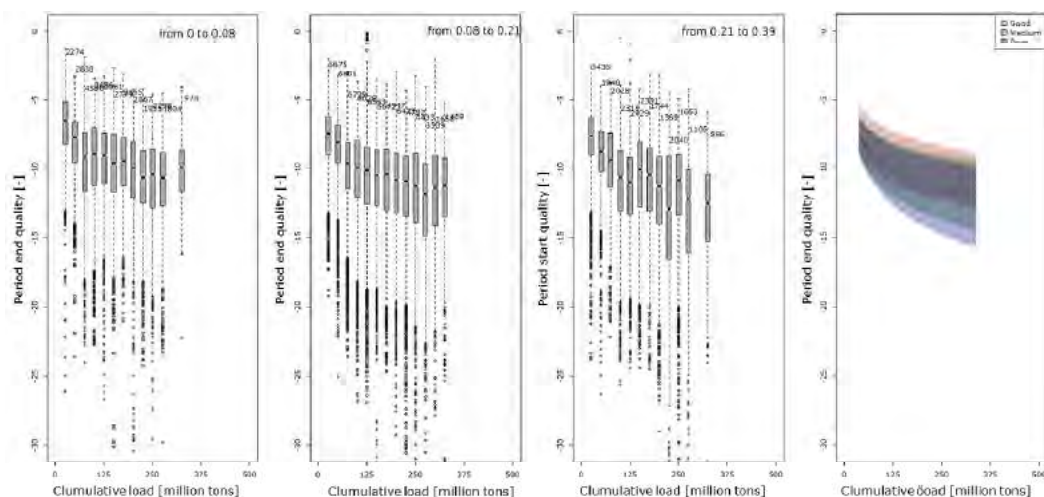


Figure 50 Evolution of the Period Start Quality Q_2 over the cumulative Load Group according to b_1

The period start quality Q_1 significantly affects the period start quality of the subsequent period, although the extent of this relationship varies over the service life. There is certainly

always a correlation between Q_1 and Q_2 , however, whether this is of a positive or a negative nature depends strongly on Q_1 and the previously achieved service life of the track. Good period start qualities tend to worsen significantly following a tamping operation at the beginning of the service life ($Q_2 > Q_1$), while cross-sections which have poor period start qualities act in the opposite way. This situation has already been the subject of detailed study [Hansmann 2011] and will not be further investigated here. Independent of the value, the clear relationship between the consecutive period start qualities can nonetheless be seen. Given that Q_2 is clearly dependent on the two parameters Q_1 and b_1 , the described dependence can also be seen between the calculated end qualities. At this point, further evidence will not be provided. The expression of a logarithmic evolution is thus a valid characteristic for the period start and end qualities.

Observing two consecutive periods also makes it possible to estimate the possible increase in quality following a maintenance measure, as well as the change in the deterioration rate. This observation has been studied in more detail in previous research [Hansmann 2011] and can be considered in a highly simplified form in the classification.

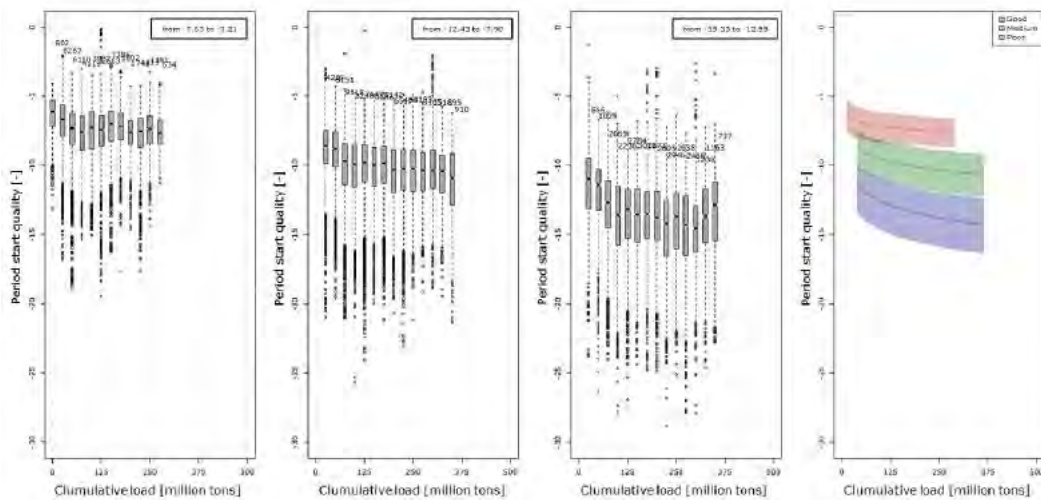


Figure 51 Evolution of the Period Start Quality Q_2 over the cumulative Load, grouped according to Q_2

3.4.6 Sensitivity Analysis

The track geometry analysis used will serve as a solid basis for the development of an evaluation standard, allowing different routes to be classified in terms of the condition of their track geometry. Route cross-sections within curves have been excluded from the evaluations discussed so far. In curved sections, the track panels result in different stress characteristics than in straights, due to the curving passage of the vehicle and the geometrical requirements. Due to the resulting forces, tracks in curves are typically more likely to suffer lateral alignment errors. The occurrence of potential distortion of the track errors will be discussed separately. This situation has been clearly illustrated by the evaluation of the standard deviation of the alignment. On the one hand, the greater manifestation of errors prevails over the smaller error values in terms of the MDZ indicator on the other, which are due to the reduced speeds. Despite the particular requirements, the effects of the speed-dependent maintenance strategy and the smaller sample size, it is worth comparing the results with the results discussed above. This comparison will act as a kind of sensitivity analysis, although the results of the curve evaluation should be interpreted with caution. The evaluations are therefore principally based on the query requirements for V3 and V4, and thus already lead to wide scattering.

The goal of the sensitivity analysis is to superimpose the evaluations of queries V1 to V3, in order to better understand the robustness of the results. In this comparison, the logarithmic regression of the median value will be considered to be exclusively representative of the entire sample population. The resulting curves for period end quality and period start quality thus identify each area where the track geometry quality lies below 50% of cases.

In principle, all the results (see Figure 52) exhibit similar progressions, thus confirming the reproducibility of the evaluation. Individual deviations, such as the period end quality for query V3 for wooden sleepers, correspond to specific contexts, and appear randomly; they can thus be ignored. In general, concrete sleeper tracks generally result in more scattering, which is particularly apparent when looking at their deterioration rates. The more generally the queries are formulated, the sooner route sections whose conditions exhibit abnormalities that do not correspond to the global condition of track geometry will be considered. Nonetheless, an unusually high stability can be identified, especially in the period start quality. The distribution of the period end qualities with the MDZ-a point has a tolerable uncertainty.

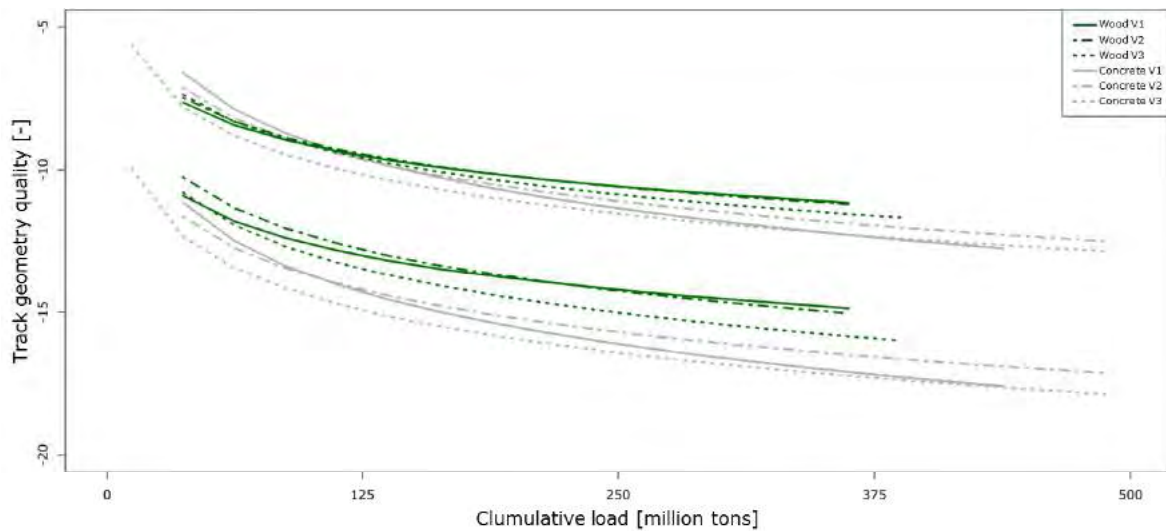


Figure 52 Envelopes resulting from Queries V1 to V3

When the evaluation is extended to take into account curved sections with concrete sleepers, a new picture emerges. In this case, cross-sections which exhibit a radius of between 300 metres and 600 metres are taken into account. A comparison of the evaluation of the radius query V3 with straight sections yields a significantly higher standard deviation of the vertical alignment (σ_H), and correspondingly worse values. When the MDZ indicator is evaluated, however, both the period start quality and the period end quality have visibly better levels, depending on the speed. This phenomenon can already be seen when considering different speed-dependent maintenance intervals, and can be attributed to the selected maintenance levels being too high for routes with low speeds. In the case of curve sections, distortion of the track errors often trigger a tamping operation long before the observed quality signals reach critical values. Query "Radius V4" appears to compensate for this effect due to larger values for track geometry errors, with qualities which reach approximately the same levels as in previous evaluations. The stability of the results means that the evolution of the track geometry over the cumulative load can be used as the foundation of a quality-based categorization for an asset. The spread of results from a single query about an MDZ point only needs to be taken into consideration when deciding the breadth of individual quality categories.

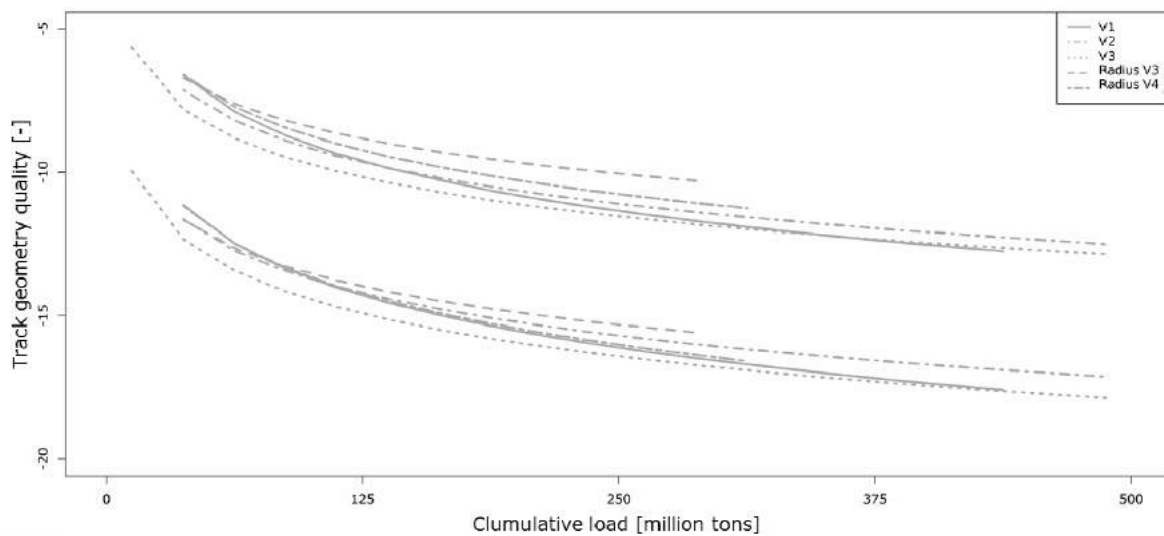


Figure 53 Comparison of the Results from the different Queries V1 to V4, for Period Start and End Qualities, with Concrete Sleepers

3.5 Summary of the Classification Algorithm

3.5.1 Model Construction

In the previous evaluations discussed in this work, it was assumed that the deterioration of period start and end qualities followed a logarithmic trend. In order to compare individual queries in terms of their different progressions, and to test for a significant difference, this assumption proves sufficiently accurate. However, for the following classification, a more detailed investigation is necessary.

The classification of track geometry makes it possible to compare the prior track geometry quality of a section with average evolution of the track geometry over its service life. Consequently, the evolution of the period end quality is particularly significant, as it represents the quality which determines the triggering of a measure. Period end qualities are affected not only by the period start quality, but also significantly by the deterioration rate and the tamping cycle, resulting a wider distribution for their evolution. The wider distribution of the individual median values leads to smaller coefficients of determination in the examined regression model, which reach between 80% and 90%. In this context, quadratic, linear and logarithmic regression models were investigated.

Above a load of 250 million tonnes, the period end quality appears to remain constant, and can still only partially be described by the logarithmic approach. The fact that the period end quality levels off after a particular point in time represents a significant divergence from the evolution of the period start quality, and is an effect which neither the logarithmic nor the quadratic approaches are able to model precisely. In order to take this situation

into account in the classification, the classification boundaries will be kept constant above a load of 250 million tonnes. Subsequent evaluations demonstrate the extent to which this alteration affects the results. The classification algorithm consists of two separate steps: the primary classification and the secondary classification, which will be described in more detail in the section below.

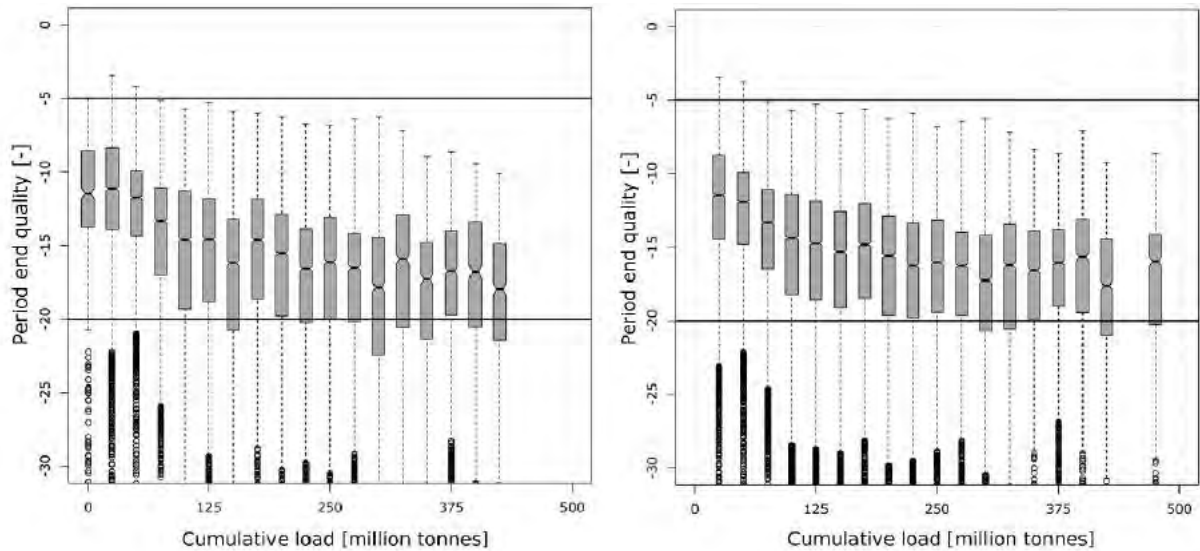


Figure 54 Evolution of the Period End Quality, with Concrete Sleepers; left: V1, right: V2

3.5.2 Primary Classification

The primary classification evaluates the track geometry quality of a cross-section at a selected point in time. The point in time can essentially be chosen randomly, with the condition, which a valid regression model exists for this point in time. The quality calculated by the regression model (Q_b) is compared with the selected classification boundaries. These classification boundaries take different values of the period end quality over the cumulative load into account and thus reflect the evolution of the track geometry over the service life of an asset (see Figure 55). If a cumulative load is available, these boundaries evolve as a function of the cumulative load.

The following boundaries are thus generated considering different deterioration rates:

Class 1: > upper quartile of the medium deterioration rate

Class 2: Median - upper quartile of the medium deterioration rate

Class 3: Median - lower quartile of the medium deterioration rate

Class 4: Lower quartile of the medium deterioration rate - lower quartile of the poor deterioration rate

Class 5: Lower quartile of the poor deterioration rate

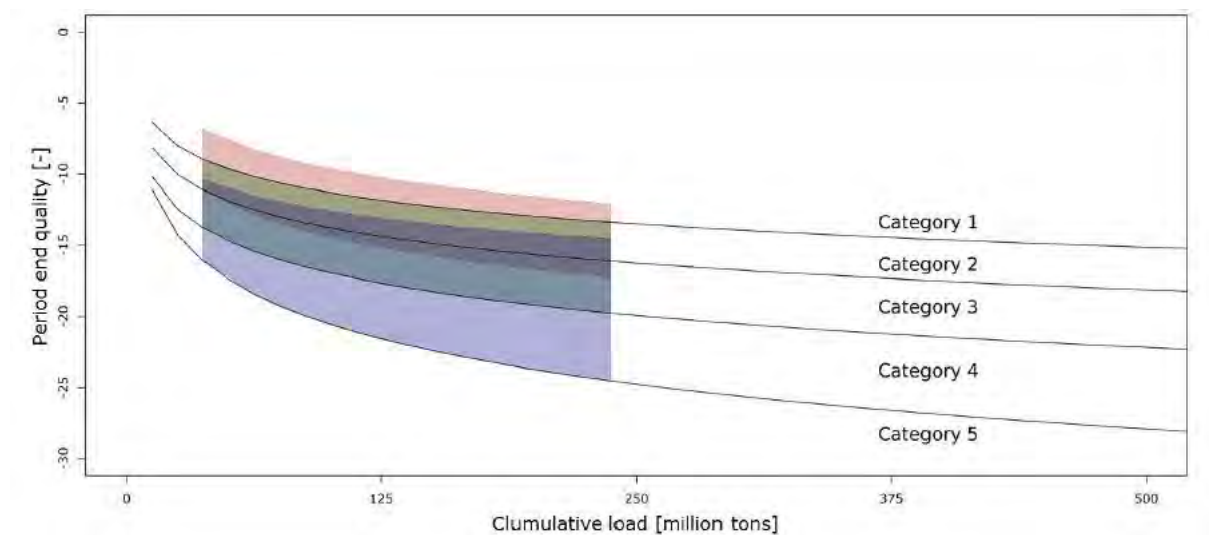


Figure 55 Class Division of the Period End Quality

If classification is to be possible, the cumulative load must be calculated correctly. The classification is therefore dependent on the existence of a valid load model, as well as a known year of construction. In order to find a way to classify the 25% of the TUG network where at least one of these conditions is not met, the cross-sections will be assigned a standard load of 250 million tonnes.

3.5.3 Secondary Classification

The secondary classification exclusively evaluates the prior deterioration rate. It is generally also possible to establish this evaluation in a load-independent manner, although deterioration rates over the service life result in far higher distributions than the period start qualities. The deterioration rate results in hardly any alteration over the service life, or rather, no alteration can be clearly associated with the increase in cumulative load. The secondary classification thus aims just to identify cross-sections with particularly high deterioration rates. A daily-load dependent classification will not be undertaken and a distinction between high and low deterioration rates will only be applied globally.

Cross-sections with a high deterioration rate will then automatically be downgraded to the next quality class. The secondary classification thus serves as an estimator for the temporal stability of the classification, and may be taken into account in the overall algorithm, or can be left out of consideration. In addition to the classification, the deterioration rate also makes it possible to estimate how much time can elapse without implementing any measures, before the next class is reached.

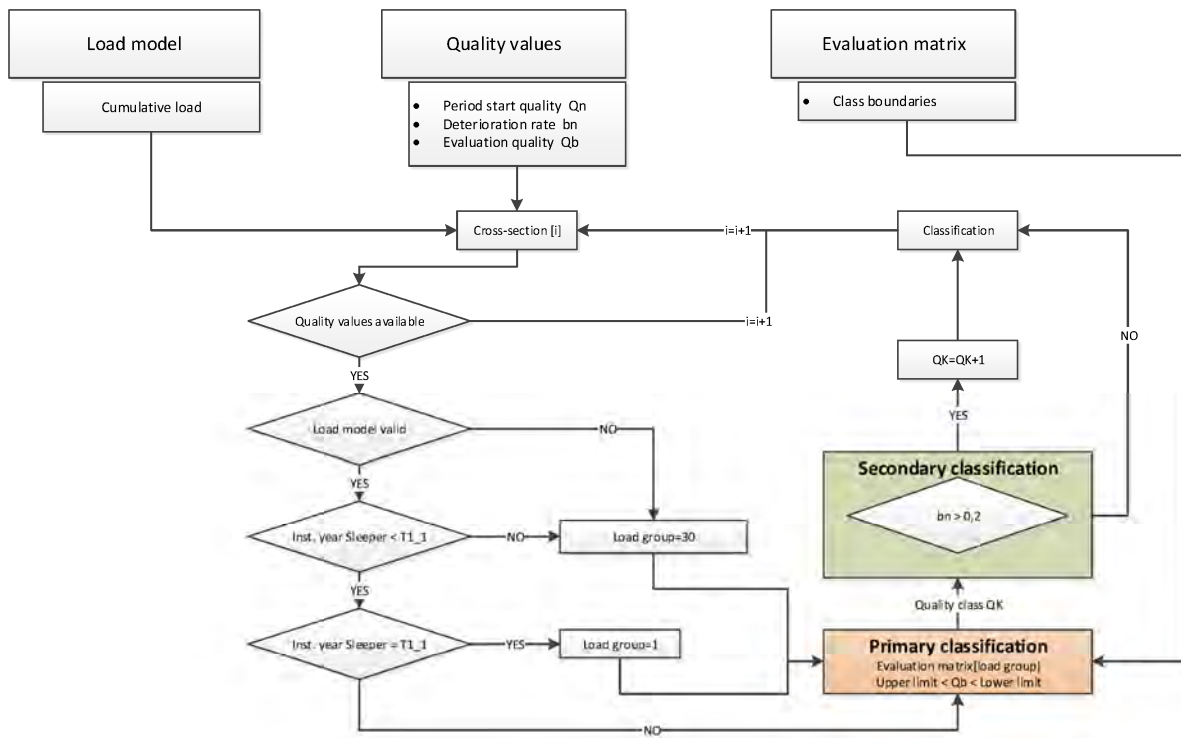


Figure 56 Schematic Representation of the Classification Process for Quality Values

3.5.4 Comparison between fully and partially logarithmic evaluations

Section 3.5.1 addressed the challenge of correctly constructing a model for selecting classification boundaries. By evaluating the quality values from 2011, it is possible to carry out random comparisons of the results of the two different approaches. In this comparison, the results of the logarithmic approach will be compared with those of the partially logarithmic approach (see Figure 57).

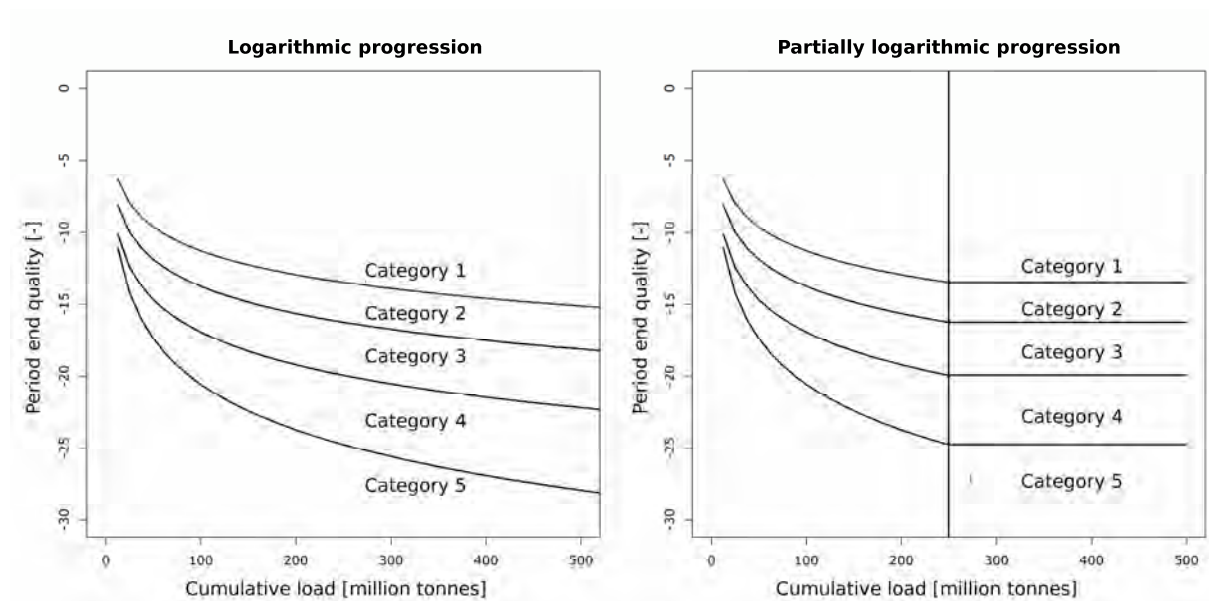


Figure 57 Evolution of the different Class Boundaries with the logarithmic [left] and partially logarithmic [right] Approaches

As expected, the partially-logarithmic classification results in a tendency to more severe evaluation of the track geometry, since the class boundaries after 250 million tonnes remain constant rather than continuing to increase. This constant progression of class boundaries has a stronger effect on the higher classes, since the changes in boundaries after 250 million tonnes are much more likely to be wrong for higher classes than for the lower ones.

However, the difference between the two queries appears to be smaller than originally supposed (see Figure 58). This marginal difference presents one possible index for the high stability of the results, and it could certainly be suggested that it is due to the concentrated value distribution in the individual track geometry classes (see Figure 59). Below, the partially-logarithmic approach will be used for the definition of individual boundaries.

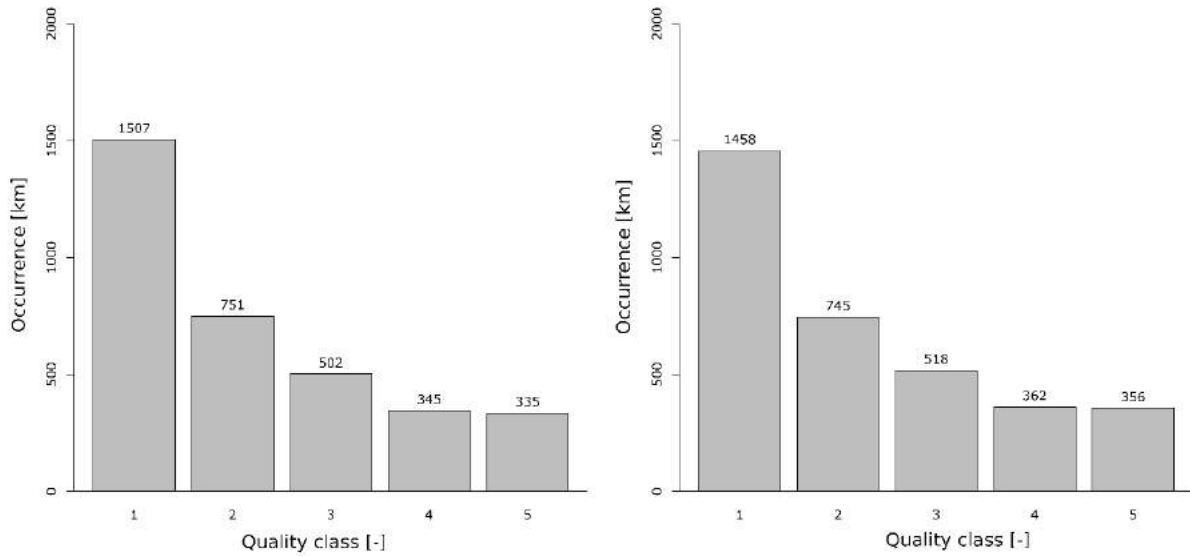


Figure 58 Evolution of Class Divisions with the logarithmic [left] and partially logarithmic [right] Approaches

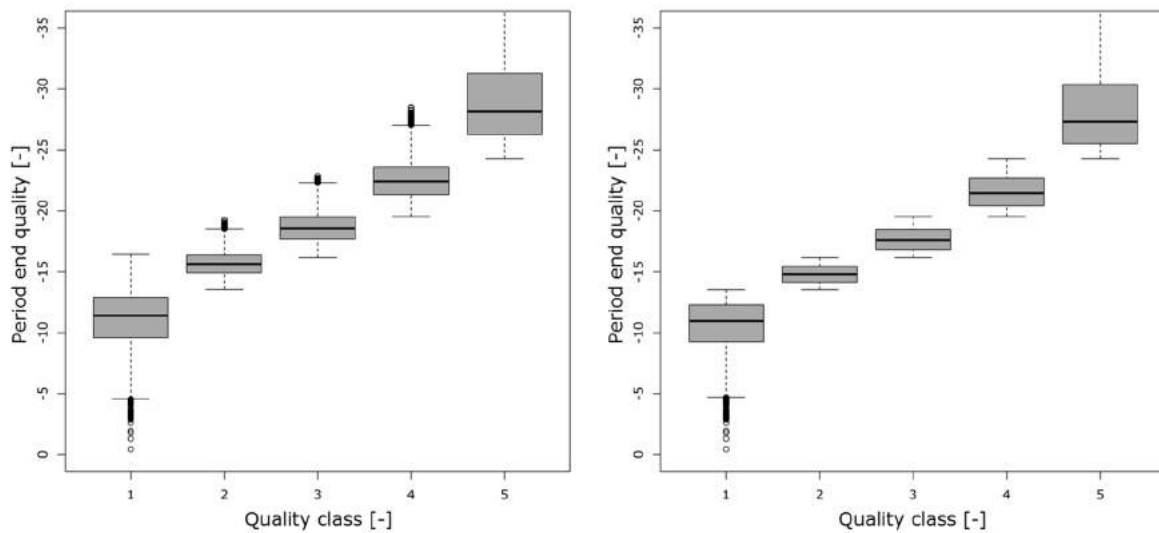


Figure 59 Distribution of the Value Qualities within the Quality Classes with a logarithmic Approach [left] and a partially constant Approach [right] before the secondary Classification

3.5.5 Implementation of the Classification in the TUG Network

The preceding sections aimed to describe in detail the evolution of the track geometry over the service life or over the applied cumulative load. The sensitivity analysis demonstrated the stability of the evolution when various parameter values are taken into account. If these results are to be applied to the complete TUG network, this stability becomes a particular challenge. It is possible to apply the classification to quality values as well as to quality signals, without a secondary classification. Each option has advantages and disadvantages. The existence of a regression and the regression qualities in individual cross-

sections essentially define how meaningful the classification is. While the regression qualities can be positively influenced by the selection of various criteria (see Table 2) as the algorithm is built, a similar restriction would strongly restrict a network-wide application of the classification. By comparison, the observation of quality signals turns out not to be particularly robust with respect to possible measurement outliers, meaning that it proves to be difficult to classify maintenance measures which have been carried out. Taking these advantages and disadvantages into account, the classification algorithm will be applied network-wide to the quality values from the years 2005 to 2012. The classes then can be defined as follows:

- Class 1: The track geometry qualities are at a very good level for the cumulative load on the track.
- Class 2: The track geometry qualities are at a good level for the cumulative load on the track.
- Class 3: The track geometry qualities are at a comfortable level for the cumulative load on the track.
- Class 4: The track geometry qualities are at a satisfactory level for the cumulative load on the track, a measure to improve the track geometry is recommended.
- Class 5: The track geometry qualities are not at a satisfactory level for the cumulative load on the track, a measure to improve the track geometry is necessary.

The dynamic evaluation of the condition over the service life is important for the classification. The evaluation takes into account the fact that the condition of the track leads to a particular deterioration, and establishes an average behaviour as a reference. The boundaries established between the quality levels do not remain constant over the service life, but evolve dynamically along with it.

A track geometry of -12 MDZ points can be assigned within the classes 1 to 3, depending on the applied loads and independently of the secondary classification. This evaluation takes into account the significantly higher thresholds for planning tamping measures at the beginning of the service life than at the end.

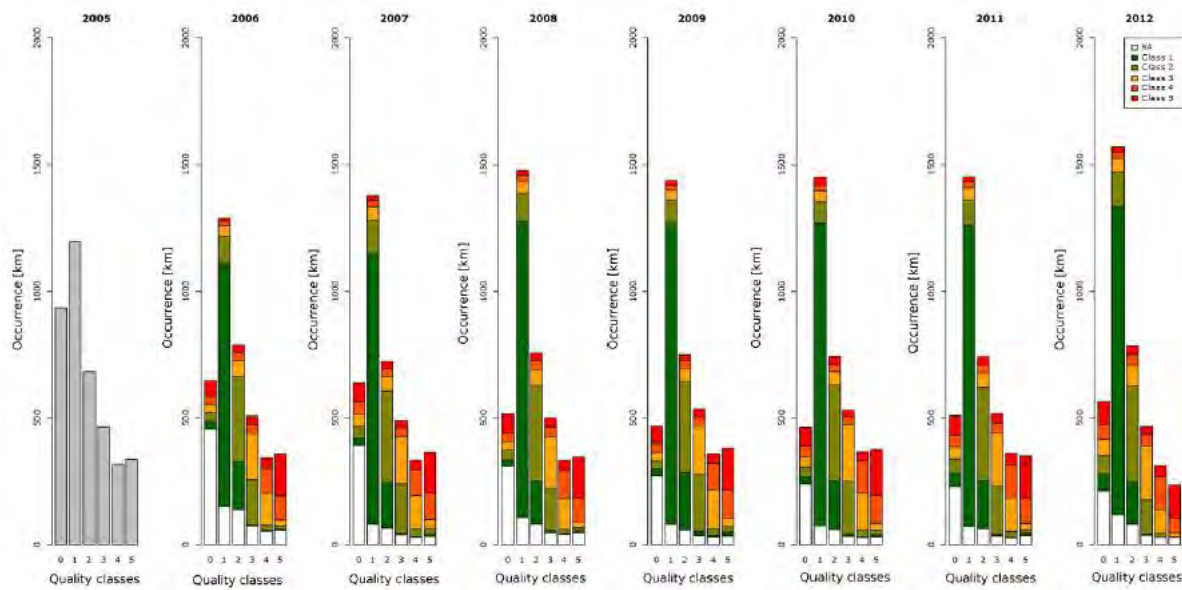


Figure 60 Evolution of the Classification from 2005 to 2012 in absolute Figures

The evolution of the classification previously discussed is shown in Figure 60 for the years 2005 to 2012. The coloured bars provide information about the classification of the cross-section in the previous year. This colour-coding clearly shows how the different cross-sections behave over the years within the individual classes. It can be seen that once assigned to a particular class, the majority of cross-sections will remain in this class, or alternate with the neighbouring classes. It is, however, significantly rarer that a cross-section will move by more than one class within a year. This regularity is reduced beyond class 3, since tracks in this quality class are maintained more often than tracks in higher quality classes. In the years between 2005 and 2007, there was an increase in the number of cross-sections where no valid regression model could be assigned. Consequently, the results of the classification in these years should be interpreted conservatively.

If these results are excluded from the wider consideration, a steady reduction in class 1 can be identified between 2008 and 2011. The number of cross-sections in classes 4 and 5 exhibits an equivalent increase. These classes are identified as critical classes, since they often trigger measures. The increase in reinvestment ratios is only reflected in the classification of the track geometry from 2012, at which point the number of cross-sections in class 1 increases substantially.

In the next stage, the results of the route classification will be compared with the tamping operations carried out in recent years. The route numbers make it possible to compare the tamping and the route class, although a geographical classification of the results is deliberately not possible. This comparison will show whether it is possible to establish a corre-

lation between the amount of tamping and the quality classification. To this end, two horizontal lines indicate the 70% and 50% marks, which are intended to make the interpretation of results easier. If the cross-sections in the fourth and fifth classes are aggregated, a significant difference between the individual route qualities becomes evident. While routes 9 to 13 have a particularly low expression in these classes, some individual tracks considerably exceed the 70% boundary.

A historical view of these results makes it possible to evaluate the stability of the results of the classification algorithm, taking maintenance and reinvestment quotas into account. Individual results which exceed the boundary values can be primarily attributed to the uncertainty in the cross-section-related regression model. As with the network-wide evaluation of the classification, particular attention should be paid to the number of invalid results. This situation is particularly evident in the analysis of the results for route 18. In years where there were fewer invalid results, the number of critical classifications increased substantially.

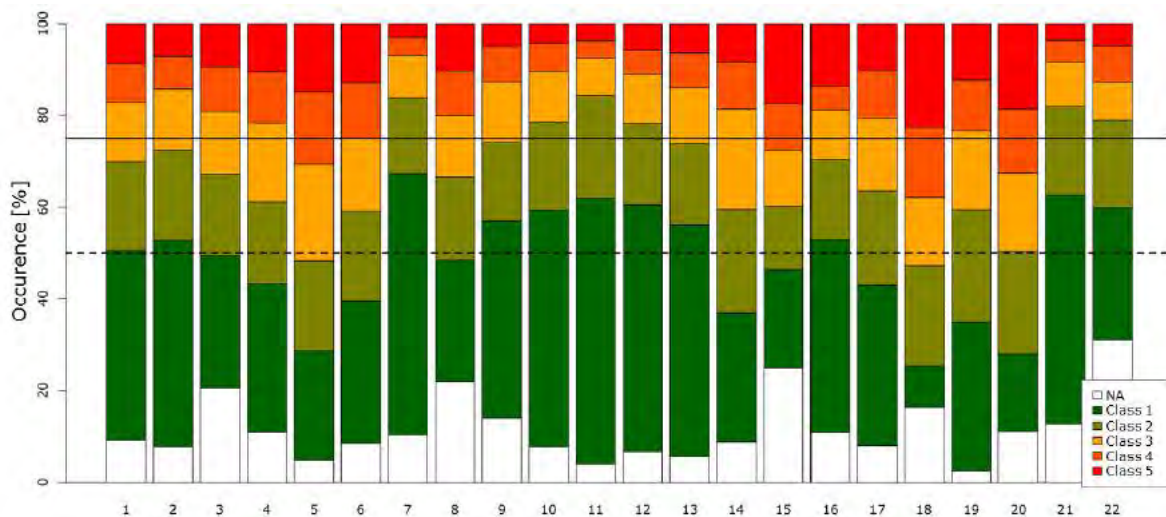


Figure 61 Apportioning of Quality Classes to individual Routes in 2009

	1	2	3	4	5	6	7	8	9	10	11	12	13	14	15	16	17	18	19	20	21	22
2012	12%	10%	22%	15%	29%	15%	5%	26%	15%	11%	8%	7%	9%	24%	20%	5%	19%	30%	27%	17%	6%	17%
2011	16%	12%	23%	20%	34%	22%	6%	26%	25%	13%	10%	13%	12%	26%	19%	5%	21%	19%	27%	20%	8%	11%
2010	18%	12%	23%	18%	32%	20%	7%	24%	19%	13%	10%	11%	13%	22%	21%	9%	19%	7%	25%	43%	9%	21%
2009	17%	14%	19%	22%	31%	25%	7%	20%	13%	10%	8%	11%	14%	19%	28%	19%	21%	38%	23%	33%	8%	13%
2008	16%	14%	15%	18%	26%	24%	6%	23%	15%	13%	8%	18%	14%	21%	29%	11%	16%	10%	18%	26%	10%	4%
2007	16%	16%	15%	17%	27%	24%	7%	24%	14%	12%	9%	11%	12%	19%	23%	11%	19%	44%	20%	23%	11%	10%
2006	18%	20%	22%	21%	30%	21%	7%	22%	12%	12%	16%	10%	12%	18%	23%	14%	16%	12%	25%	22%	8%	4%

Tamping length since 2006	22%	20%	25%	13%	9%	27%	13%	26%	18%	23%	11%	15%	4%	13%	28%	29%	26%	22%	21%	19%	22%	26%
Tamping length since 2008	23%	18%	24%	12%	8%	26%	12%	25%	18%	21%	8%	17%	4%	13%	27%	29%	23%	23%	17%	22%	23%	25%
Track laid since 2006	17%	17%	33%	10%	5%	25%	17%	26%	17%	20%	1%	37%	2%	0%	29%	41%	31%	22%	9%	9%	28%	13%
Track laid since 2008	12%	12%	28%	10%	4%	17%	11%	21%	16%	14%	1%	33%	1%	0%	22%	33%	18%	22%	3%	8%	27%	6%

Figure 62 Temporal Evolution of the route-specific Classification by Comparison with the Length of tamped and relaid Track in Proportion to the Route Length.

Throughout the classification, figures highlighted in red will indicate years when more than 20% of the routes were assigned to critical classes. In the same way, in routes with tamped or relaid stretches, those which exhibit the 10 highest values will be identified.

With the exception of a number of routes, it can be seen that routes with a consistently high proportion of critical classes are tamped more often than routes with a lower proportion (see Figure 62). However, routes do exist that appear to be in poor condition with respect to their classification, but whose poor condition does not seem to be due to the amount of tamping. Route 5 exhibits this behaviour particularly clearly.

The opposite effect can also be seen. There are some routes where a large proportion of the route has been reinvested or tamped, but the route does not exhibit particularly remarkable track geometry. In conclusion, it can be stated that the classification of the routes identifies those parts of the network with which large numbers of maintenance measures are associated.

3.5.6 Summary and Discussion of Results

Maintaining the track geometry is a central part of the responsibilities assumed by railway infrastructure operators. Driven by the need to maintain safe railway structures, a central goal has become sustainable use of the infrastructure.

The medium-term reduction in MDZ operations between 2004 and 2009 to about 60% of their original scope did not lead to a proportionally large decrease in track geometry quality within the TUG network. However, it can be noted that the track geometry in the TUG network worsened by almost 10% between 2002 and 2010. The increase in maintenance measures and track renewal projects in the years 2010 and 2012 halted this negative development. It is not currently possible to judge the long-term effects or non-effects of the measures. The track replacement carried out mitigated the deterioration of the track geometry in particular areas, but did not reverse the trend.

The increased installation of sleepers with USP over recent years has led to a continual improvement in the standard deviation of the lateral alignment. This effect remains almost unaffected by the reduced maintenance, or compensates for the negative effects of it on the whole system. When the MDZ indicators are considered, the two effects are superimposed, although the negative effects of reduced maintenance can be clearly seen. A comparison of the installation and removal qualities of different track superstructure types confirms the advantages of concrete sleepers with USP compared to the other sleeper types. An improvement in vertical track geometry of around 20% for concrete sleepers with USP as compared to the equivalent without USP has already been demonstrated in

previous studies, and is confirmed by the evaluations here (cf. [Marschnig, Berghold 2011]). The track geometry of a railway asset deteriorates according to the cumulative load applied to the system, following a logarithmic trend in the case of the data studied here. A detailed analysis of the evolution of the period start qualities enables these to be divided into three separate ranges, which are noticeably distinct with respect to their condition. The boundaries established for these sectors are 125 million and 250 million tonnes (see Figure 63). A similar situation has also been established in prior studies (cf. [Chrismer, Selig 1993]). In terms of the evolution of the deterioration rate, the absolute values of this variable are correlated with the daily track load, although it is not possible to identify any specific trend based on its evolution over the cumulative load. Wooden sleepers not only have a significantly lower deterioration rate by comparison with concrete sleepers, but also exhibit a significantly slower deterioration of period start qualities. Both types of sleeper have higher deterioration rates at the beginning of their service life, which level out to a constant value during the first 100 million tonnes. In the case of concrete sleepers, the deterioration rates are widely distributed around this level; in particular, they exhibit considerable sensitivity to the quality of the existing subgrade.

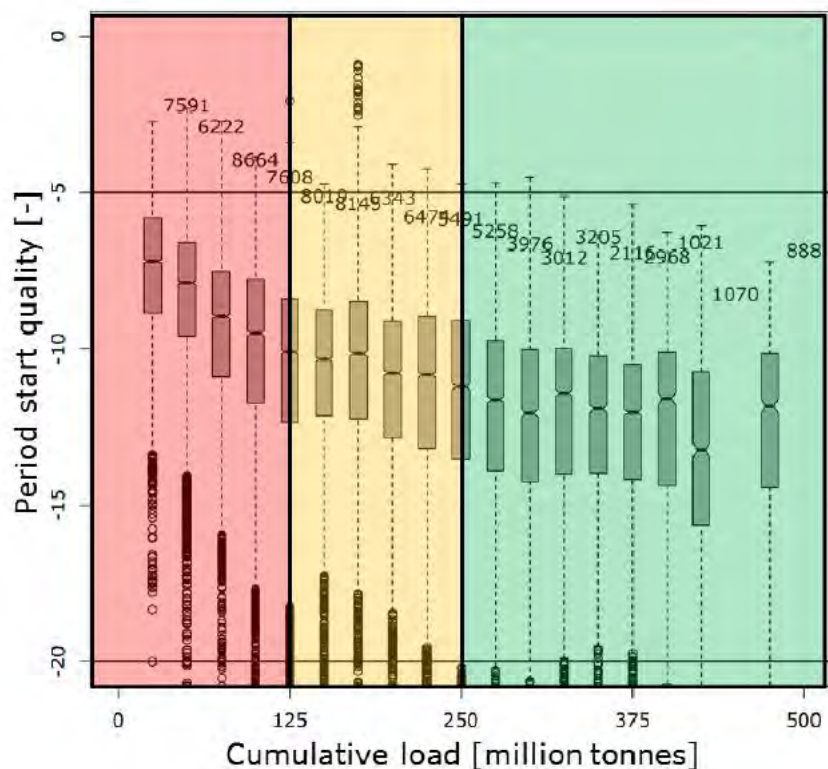


Figure 63 Evolution of the Period Start Quality for Concrete Sleepers based on Query V2

3.6 The Connection between Wavelengths and Damage Characteristics

The following section arises from work completed in close association with Dip.-Ing. Matthias Landgraf and comprises results and parts of text passages which have already been published. Identical text passages will be identified as such.

The emphasis in the previous section was on the observation of different quality signals or rather, their temporal evolution in the form of a regression model and the resulting quality values. Both the standard deviation and the MDZ indicator represent calculated values which reflect just one specific characteristic of either the lateral or vertical alignment signal, depending on the calculation method. Different wavelengths affect the expression of the quality signals in strongly diverse ways. Researches [Auer 2003] show the frequency ranges which have the strongest influence on the expression of the MDZ and SigmaH quality signals (see Table 3) Wavelengths which are shorter than 5 metres affect the MDZ indicator considerably more than the standard deviation of the vertical alignment, which, by contrast, is predominantly affected by wavelengths greater than 10 metres. This is primarily due to the fact that wavelengths between 5 and 20 metres tend towards particularly large amplitudes. Should the mean value of the observed recording signal tend to fluctuate around the null value (see [Auer 2004]), then the formula for the standard deviation can be reduced to the evaluation of the quadratic mean. High amplitudes are thus reinforced more than small ones. The MDZ indicator takes into account the acceleration differences on an imaginary model vehicle, and is more strongly influenced by smaller wavelengths.

	SigmaH	MDZ
<5m	4%	51%
5-10m	35.9%	27.5%
10-20m	38.6%	15.5%
>20m	21.4%	5.9%

Table 3 Influence of different Wavelengths on the SigmaH and MDZ Quality Signals [Auer 2003]

Quality values describe the average track geometry in specific areas and form a basis for planning which measures will be implemented and when.

When the recording signals are observed more closely, they are found to be quite distinct in terms of wavelength and amplitude. By filtering, it is possible to isolate the signals in terms of different wavelength ranges and then to consider specific wavelength ranges. The applicable standard EN13848-6 proposes the following three ranges:

D1: 3m to 25m

D2: 25m to 70m

D3: 70m to 150m in the case of vertical alignment

70m to 200m in the case of alignment

(cf. [Österreichisches Normungsinstitut 2014])

The investigation into track geometry signals in terms of the interaction between the amplitude and the associated wavelengths has already been addressed in various studies. This problem was originally approached from a mechanical engineering point of view, in order to better describe vehicle reactions and thus the journey comfort (cf. [Frederich 1984] und [Rießberger 1997]) Later on attempts were made to find potential correlations between the power density spectrum and resulting damage mechanisms [Schöpp 2011], as well as to define new demands for high speed routes. [Kipper, Gerber & Schmeister 2013]

In previous sections, the evolution of the track geometry has been discussed in detail; however, the different causes of deterioration have not been addressed. The evaluations in section 3.4 clearly indicate the average relationship between the loads applied to the system and the deteriorating track geometry. The significant influence that the subgrade quality and the ballast have on the speed of this deterioration is indisputable. Only by a precise alignment of the different track layers, from the track panels over the ballast and down to the subgrade, can it optimally withstand the applied loads. Discontinuities in this alignment lead to errors in the track geometry, requiring a corrective measure to be carried out. The intrusion of fine particles from the subgrade, a lack of drainage, or the installation of low-quality ballast result in track geometry errors forming more rapidly, maintenance intervals becoming closer together and the service life of the track being significantly reduced. Reactive measures treat the effects of errors rather than their causes.

The question arises of whether it is possible to draw more specific conclusions about the reasons for deterioration based on the error characteristics of the track geometry. In addition to the evolution of the track geometry over the service life, this analysis will present

an opportunity to confirm the precise causes of errors and thus to make a correction which is appropriate to the cause rather than merely battling the symptoms. In particular, in Austria, the service life of the ballast is limited by ballast contamination resulting from the applied loads or the intrusion of fine particles from the subgrade. Furthermore, the lack of drainage or inadequate drainage installation considerably accelerates the deterioration of the track geometry.

The power density spectrum makes it possible to separate the recording signal into its constituent periods [Rießberger 1997] and associate these with the calculated power densities. To put it more simply, the power density spectrum makes it possible to determine the composition of the signal in terms of its different wavelengths and amplitudes. The power density spectrum thus provides a sound basis for detailed analysis, although a network-wide application appears somewhat pointless. Individual researches have investigated the various ways in which the large quantities of information provided by a power density spectrum can be used. Frederich [Frederich 1984] approximates the progression of the power density spectrum using a cubic parabola, and associates the parabola parameters with different quality levels. Based on this approximation, it is possible to adequately describe the signal characteristics and then reduce the information to the essentials. Further attempts to compare different frequency ranges [Schöpp 2011], in order to identify potential unsupported sleepers, have also been successful on random samples.

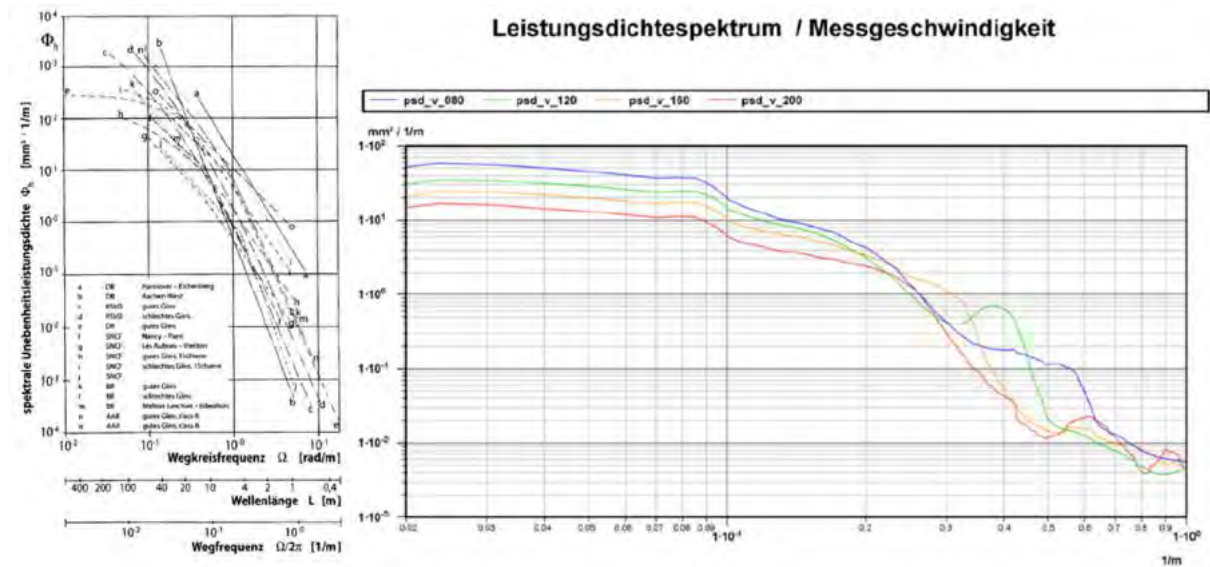


Figure 64 Different Applications of the Power Density Spectrum; left: Research on different Tracks in terms of their Signal Characteristics [Frederich 1984] right: Signal Characteristics for Tracks with different Speeds [Schöpp 2011]

Despite the appreciable success, the frequency-dependent track geometry analysis it did not find a place in the current standards until 2014 [Österreichisches Normungsinstitut 2014]. The standards currently only mention the power density spectrum as a possibility, omitting any results from further analysis techniques or threshold values. The previous examples have demonstrated that implementation of a network-wide application for the frequency-dependent track geometry analysis requires a simplification of the evaluation method. Only then a network-wide application can be possible or reasonable.

Therefore, the simplification of the frequency-dependent track geometry analysis is the focus of the next section. It is important to make an evaluation of the characteristics of a recording signal possible.

Using classical geometry, it is not possible to describe the characteristic of a recording signal. Benoit B. Mandelbrot developed a way [Mandelbrot 1977] to measure the roughness of objects whose description had not previously been describable [Mandelbrot 1983]. The fractal dimension of an object is expressed in various ways, dependent on this roughness, and is thus also suitable to describe the roughness of the track geometry. Hyslip [Hyslip 2002a] recognized the potential of fractal analysis to determine the roughness of the track geometry, and applied it for the first time in the context of an evaluation of the Northeast corridor of the National Railroad Passenger Corporation (Amtrak).

Fractal analysis aims to test the possibility of obtaining more detailed information about the condition of the railway track from the track geometry analysis or signal characteristics.

3.6.1 Historical Development of Fractal Analysis

[Hansmann, Landgraf 2013]

In order to illustrate the fractal analysis approach, the example defined by Mandelbrot himself is ideal. Mandelbrot addresses the question of the length of Great Britain's coastline in order to present a detailed illustration of fractal analysis. Although this problem appears simple at a first glance, Great Britain's rugged coastline exhibits numerous irregularities, making it almost impossible to establish the structure of the coast, never mind determining its length. This makes it a perfect example for the application of fractal analysis.

Fractal analysis is based on the fact that it is possible to linearize non-linear geometric curves by dividing them into continually smaller segments, finally using the tangents of individual points to describe the curve (see Figure 65).

In general, classical geometrical figures can be explained by means of whole-number dimensions. [Mandelbrot, Blumen 1989] Thus, curves have a single dimension, while surfaces can be described in two dimensions. Mandelbrot took as a starting point the fact that curves, as a result of their roughness, may lie between these integers, and he described the resulting new dimensions as fractal dimensions.



Figure 65 Describing the Length of Great Britain's Coastline with the help of the Modified Divider Length Method [Hyslip 2002a]

Various methods, such as the Divider Length Method or the Box Method then make it possible to calculate the fractal dimension of a curve. This can subsequently be assigned a value between one and two, depending on its complexity. In the process of the Modified Divider Length Method, the curve will be divided into segments of equal length λ and eventually, the length of the resulting polygonal chain $L(\lambda)$ is calculated. In the next step of the calculation, the lengths of the segments are reduced, and the polygonal chain recalculated. As the iteration progresses, the polygonal chain comes to fit the curve increasingly well, until it finally describes it precisely.

Mandelbrot proved that the following relationship holds between the real lengths of the curve, the number of segments and their lengths:

$$L(\lambda) = N * \lambda^{1-D_r}$$

where:

L(λ): length of the polygonal chain as a function of λ,

λ: length of the segments

N: number of segments

D_r: fractal dimension.

This equation yields:

$$\log L(\lambda) = (1 - D_r) \log \lambda + \log n$$

The increase in the length of the polygonal chain as the number of segments increases thus follows an associated regression and can be described by its slope. If the calculated polygonal lengths are plotted in relation to their segment lengths using a logarithmic representation (Richardson Plot), the fractal dimension of the curve becomes

$$D_r = 1 - m$$

where:

m: slope of the approximated lines.

The fractal dimension is thus described as the slope of each straight section, which is most suitably depicted on a log-log projection. Curves with just one fractal dimension are referred to as self-similar curves. The self-similarity of a curve can be considered to correspond to recurring signal characteristics at different scales (see Figure 66). If a single straight line no longer adequately describes the progression in the Richardson Plot, then the curves investigated generally exhibit different self-similarities (see Figure 67). As the self-similarity of track geometry data is not a central component of this work, further details will be omitted. The reader is referred to the prior work. [Hyslip 2002b]

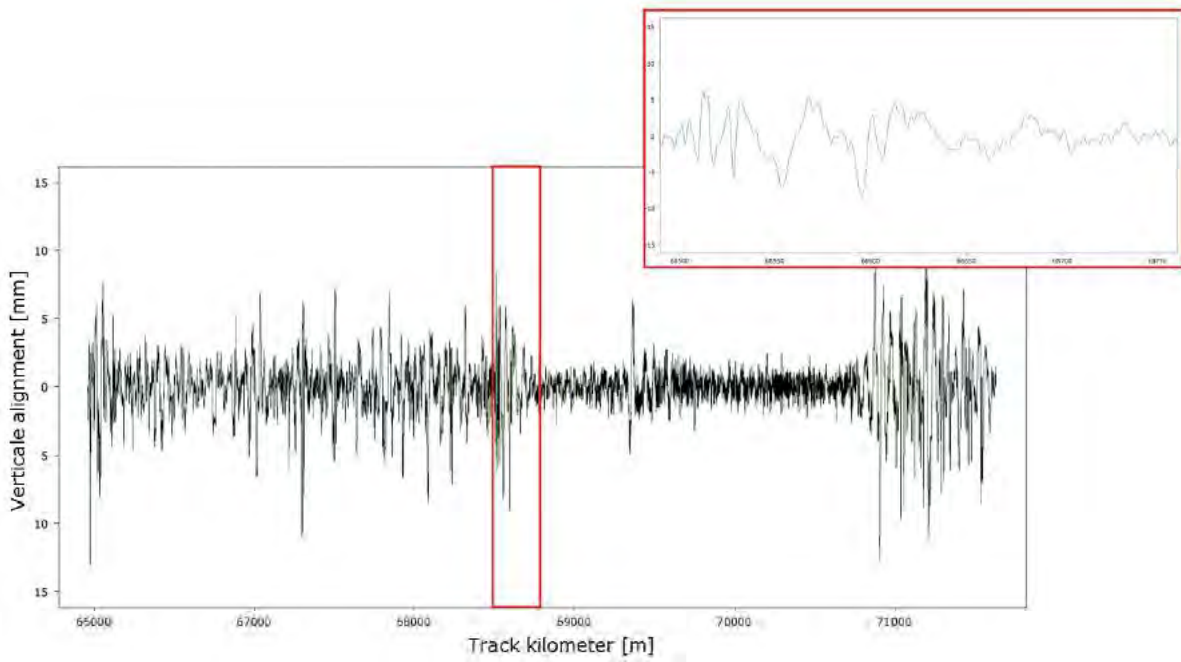


Figure 66 Plot of the Track Geometry at different Scales, emphasizing the Lack of Self-similarity

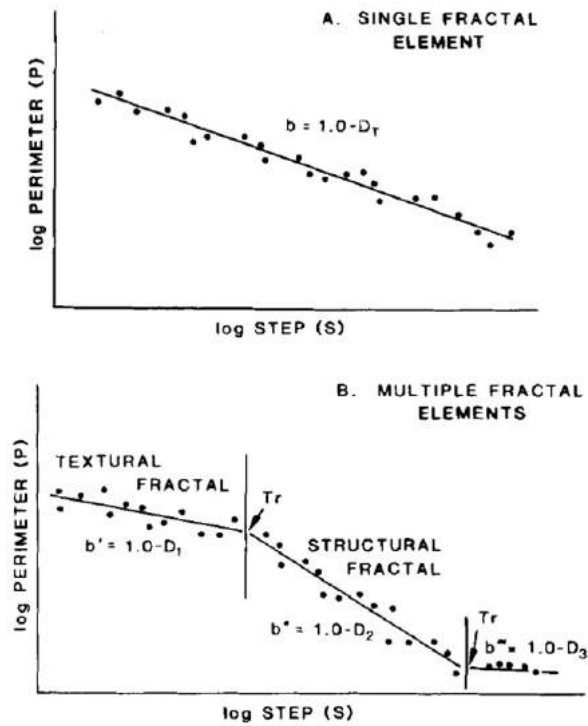


Figure 67 Emergence of a single Fractal Element (above) or of multiple Fractal Elements (below) [Orford, Whalley 1983]

3.6.2 Application of Fractal Analysis to the Track Geometry in the TUG Network

[Hansmann, Landgraf 2013]

In the following discussion, the Modified Divider Method calculation will be applied to the track geometry in the TUG network. Fundamentally, fractal analysis makes it possible to compare sections with different extents, since the fractal dimensional analysis of the section is independent of this decision. A network-wide sliding-window application of fractal analysis nonetheless does require a particular window length to be established, in order to obtain reproducible results over time for the same section. The fractal dimensions will be determined for the vertical track geometry recording signal of the left and right rails (sample rate=0.25m), filtered between 1m and 70m.

The choice of window length combines two considerations: on the one hand, the maximum occurring wavelength in the signal affects the choice of the window length. The Modified Divider Length Method requires at least two base points (see Figure 71) to precisely describe a wavelength. If the maximum occurring wavelengths are thus taken into account, then a minimum window length of 140m should be aimed for. On the other hand, if the selected window length is too large, then errors or unknown values arising in the large sections may mean that no statement can be made. It is also the case that if the signal is filtered at a wavelength of 70m, larger window lengths do not add any value. Taking the window lengths of other quality signals into account, the window length for the fractal analysis was set at 150m.

The measurement values from both rails were entered into the algorithm and checked for erroneous values or missing values. All 601 individual measurements must have valid values for the fractal analysis of the particular section to be possible. An inexact window length is required to ensure the individual localization of the values to a track cross-section. Consequently, the window lengths yielded are not precisely 150m, but rather 150.25m. At the end of the calculation, the values from the fractal analysis will be associated with the route kilometre at the centre of the data segment. The data segment is iteratively divided into continuously smaller subsections λ (see Figure 68), where each subdivided point is associated with a unique point on the recording signal. In order to obtain a continuously determinable recording signal, the progression between two measurement ticks is linearly interpolated. The length of the resulting polygonal chain is determined using Pythagoras' theorem and associated with the length of subsection λ :

$$L_i = \sum_1^N L_i = \sum_1^N \sqrt{(Y_{i-1} + Y_i)^2 + \left(\frac{EL}{N}\right)^2}$$

where:

Y_n : value of the signal at point n , N : number of subsections

i : index variable EL : length of the data segment.

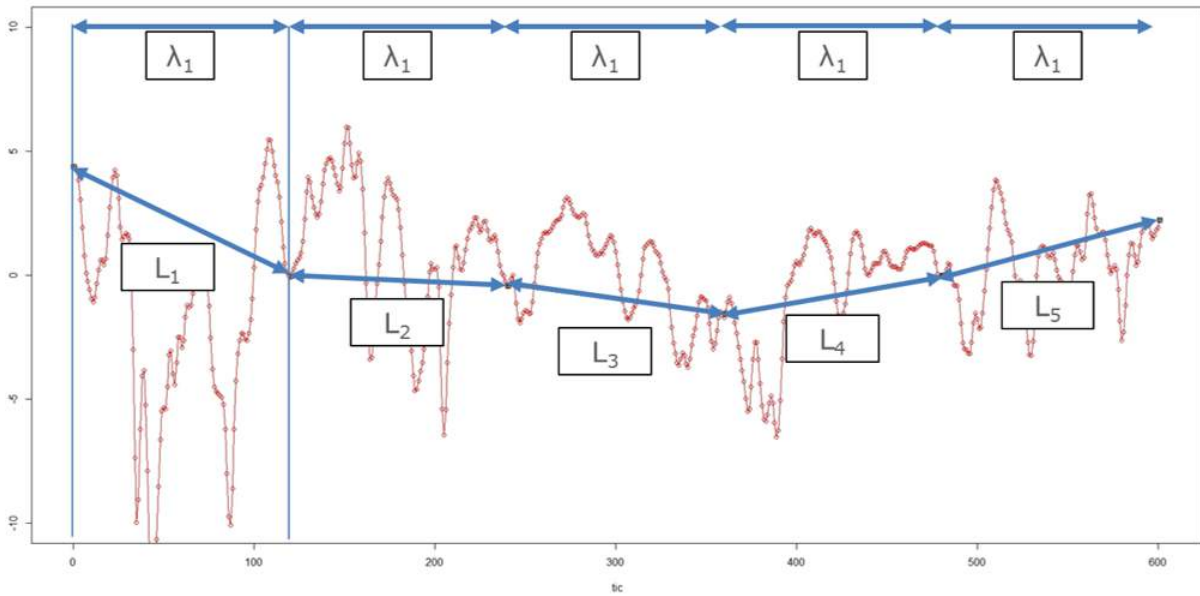


Figure 68 Example Interpolation of a Recording Signal with 600 Measurement Ticks (=150m) following the Division into 5 equal Segments of Length λ

A log-log comparison of the length of the polygonal chain and the length of the subsegments exhibits the characteristic picture shown in Figure 69 and makes it possible to determine the fractal dimensions. The "1-70m" track geometry appears to comprise three fractal dimensions. Earlier evaluations, applied to Amtrak's Northeast corridor, assign more fractal dimensions in order to achieve a sufficiently accurate description. Hyslip [Hyslip 2002a] only specifies two sectors in his researches, but does not take wavelengths less than 3m into account.

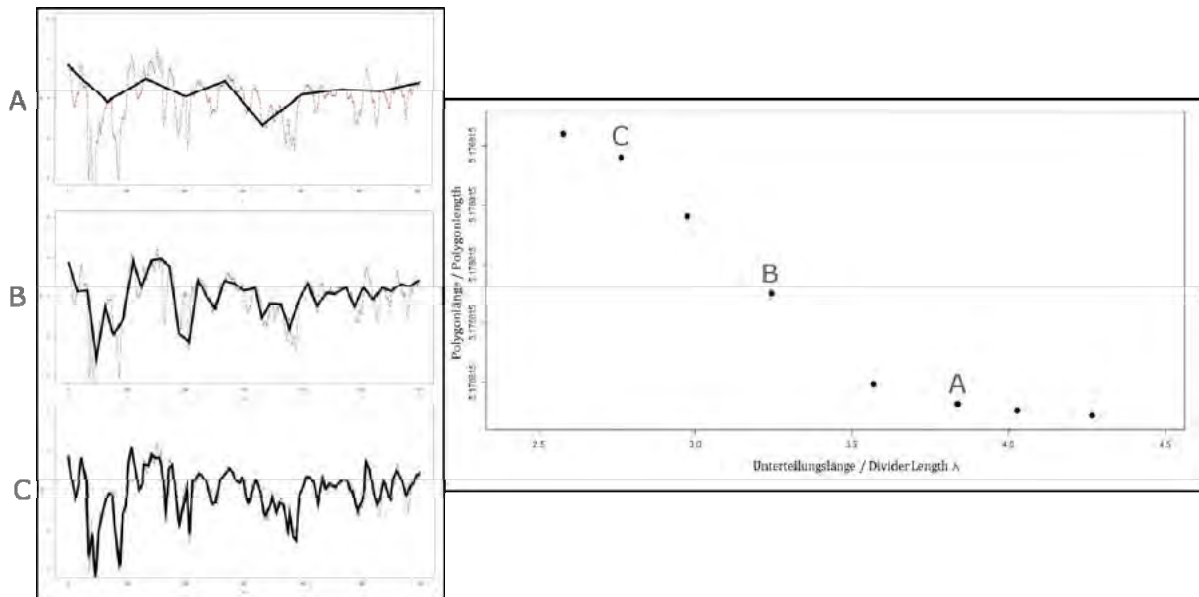


Figure 69 Characteristic Progression of the polygonal Length in Relation to the Subsection Length λ

Before it is possible to focus on the network-wide analysis of the fractal dimensions, it is necessary to evaluate their predictive power. What is the correlation between the occurring wavelengths and the fractal dimensions? Initially, the analysis appears to follow by means of a simple sine wave, whose wavelength is progressively modified (see Figure 70).

Calibrating the fractal analysis makes it possible to compare different expressions of individual dimensions for wavelengths of 20m (case A) and 100m (case B), as well as their superposition (case C). The result is the displacement of the maximum slope of the specified regression line from left to right in the Richardson Plot. In the case of a 20m wavelength, the slope of the middle section increases noticeably, while a wavelength of 100m only leads to an increase in the slope of the right section.

The slope of the first section is only marginally affected by the different wavelengths. A relationship is visible between the lengths of the subsections, the fit of the recording signal and the occurring wavelengths. The greatest increase in the fit of the polygonal chain to a waveform results when the wavelength of a curve is twice or four times as large as the subsection lengths, depending on the location (see Figure 71). A precise determination of the occurring wavelengths in a signal – as for the application of the power density spectrum – is not possible using fractal analysis.

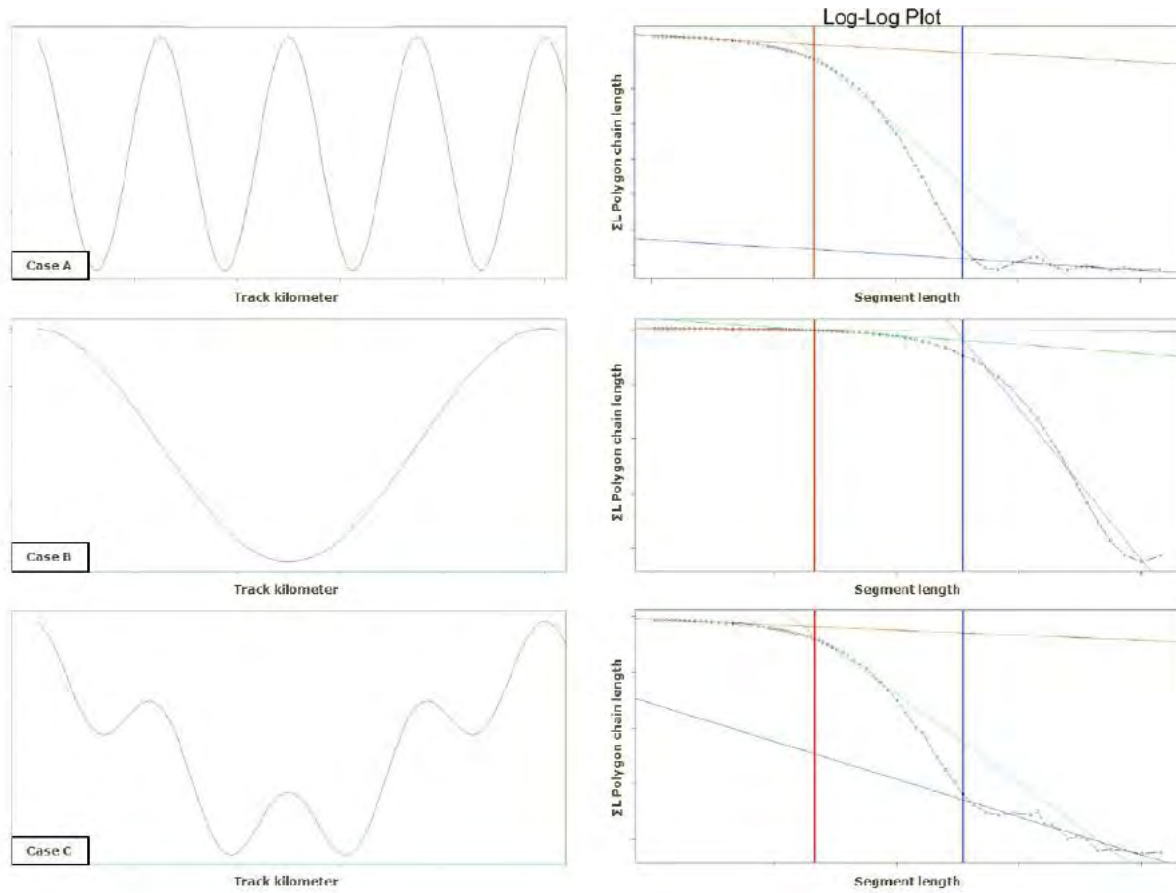


Figure 70 Effects of different Wavelengths on the Fractal Dimensions

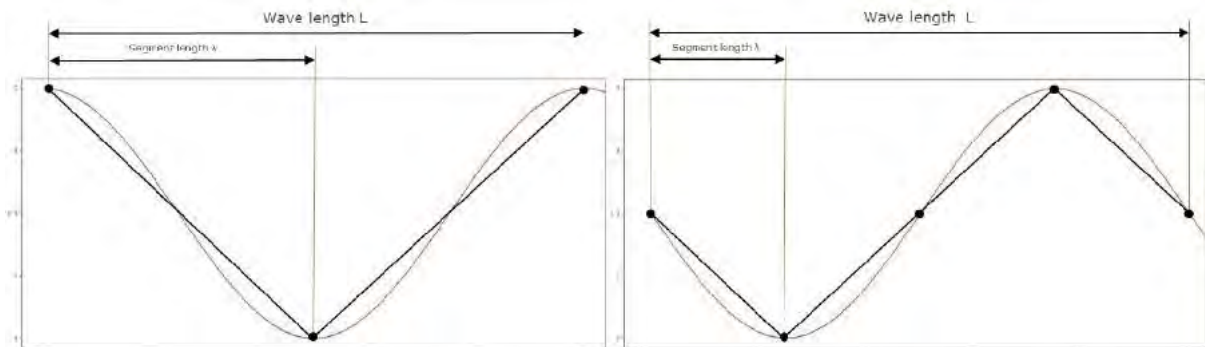


Figure 71 Correlation between the Subsection Lengths and the Wavelengths of the available Signals.

By contrast, specific frequency ranges can be described with the dimension of the signal. The individual sectors are separated from each other. While the first limit occurs at 2-5m, the second is placed between wavelengths of 10-20m. The selection of limits is based on various considerations, some of which are empirical. The first limit mainly serves to free the second sector (medium-wave sector) from the influence of very small wavelengths.

The second limit separates the second and third (long-wave) sectors, thereby becoming a deciding factor for the standard deviation.

The slopes of the tangents are calculated within these sectors using linear regression models. In the short-wave (Slope1) and medium-wave (Slope3) sectors the calculation begins at the left-hand side of the sector and is carried out point by point to the sector boundary. By contrast, in the long-wave sector the calculation begins at the right-hand side. With the point-by-point progression, the coefficient of determination for the modelled line also changes. As a result, it can be used not only as a quality criterion, but also as a decision-making basis for the final regression model. From the point-by-point regression model thus calculated, a model for each sector will be selected which exhibits the highest coefficient of determination and is based on at least five values.

The fractal analysis aims primarily to describe the frequency ranges which cannot already be modelled by the current track geometry analysis, which focuses on the standard deviation of the vertical alignment. Ballast fouling causes the continual deterioration of the track geometry and thus the end of the service life for the track ballast. Ballast brake down and subgrade problems are the main reasons for ballast fouling. Consequently the question arises if these damage causes are manifested by different signal characteristics or not. The differentiation between short, medium and long wavelengths is thus based on a theory supported by previous research ([Hyslip 2002b], [Schöpp 2011], [Holtzendorff 2003], [Rohim Boy Berawi 2013]). According to this research, it can be concluded that most ballast contamination occurs in short-wave and medium-wave ranges, while subgrade problems are primarily exhibited in the long-wave range. This theory is consistent with the characteristic relationship in the Richardson Plot and will be further investigated in the next section. Following the calculation of the different slopes in the individual sectors, the values will be smoothed over a length of 100m and finally output into every five-metre cross-section. This makes it possible to then investigate the temporal evolution of the values, significantly reducing the necessary computing power and time. A time series analysis without this averaging process would otherwise lead to wide distributions.

3.6.3 Network Analysis

In the context of network-wide analyses, it is first important to note that the restriction of the fractal analysis exclusively to valid measurement values has a significant effect on the population in the network. The fractal analysis was carried out in the complete TUG network from the year 2005. For the network wide evaluations, only annual values will be used, unless otherwise stated. As with previous analyses, only the first recording journey of the year will be used, subject to the condition that this was carried out during the first five

months. These requirements result in 62% of the network having valid dimensional values for the fractal analysis (see Figure 72). This is a sufficient sample size to establish statements about the value distribution and correlations. Evaluations which only study one aspect, such as the influence of the rails, will be carried out representatively for the year 2011, as the sample size is greatest for this year.

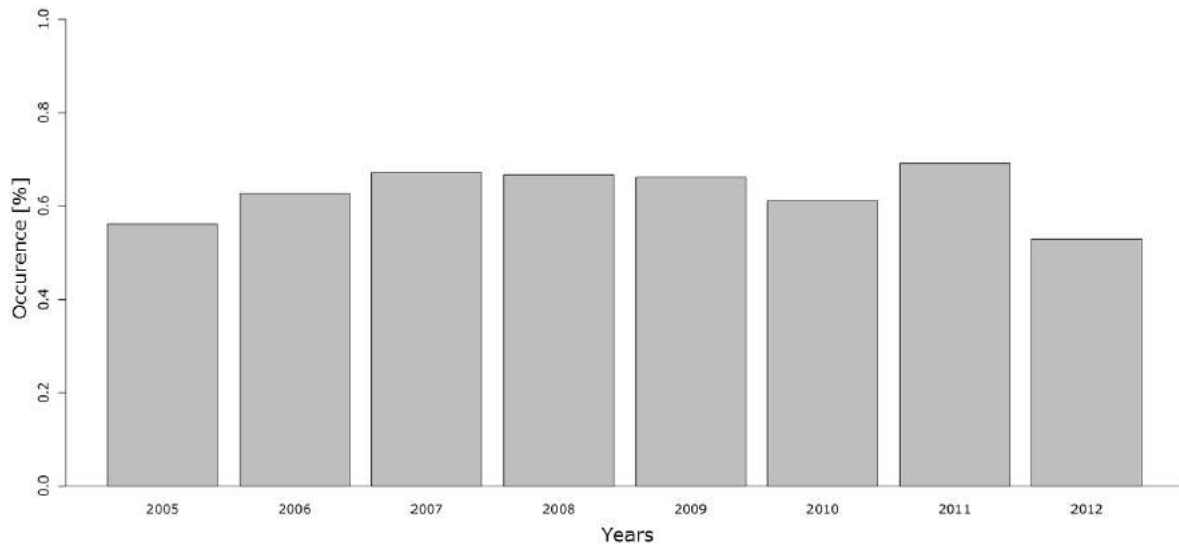


Figure 72 Relative Proportion of valid annual Values in the entire Network.

The measurement of track geometry gives different values for the left and right rails. The extent to which this difference affects the results of the fractal analysis will be explained in the following section.

In the frequency distribution, the left and right rails appear to follow approximately the same progression (see Figure 73). The different slopes have very small values, and they are multiplied by a factor of $10 \cdot e^7$ for all the evaluations to render their expression more clearly. When this factor is taken into consideration, the values of Slope1 and Slope2 are approximately equal. The marginally stronger expression of Slope1 can be ignored at this point. The strongest slope is seen in the middle sector, as already identified in the typical Richardson Plot. Even when the frequency distributions have the same function for the left and right rails, the difference between the two cannot currently be precisely explained.

In order to carry out a detailed investigation of the difference between the two rails, it is necessary to consider the differences between the fractal analysis values of each single recording car run. This evaluation is thus not based on the annual values, but compares the measurement results with each other. For each cross-section, the 10% and 90% quantiles of the dimensions will be calculated for the observed differences between the left and

right rails considering all runs within the database. The 10% and 90% quantile values are distributed as shown in the box plots in Figure 74.

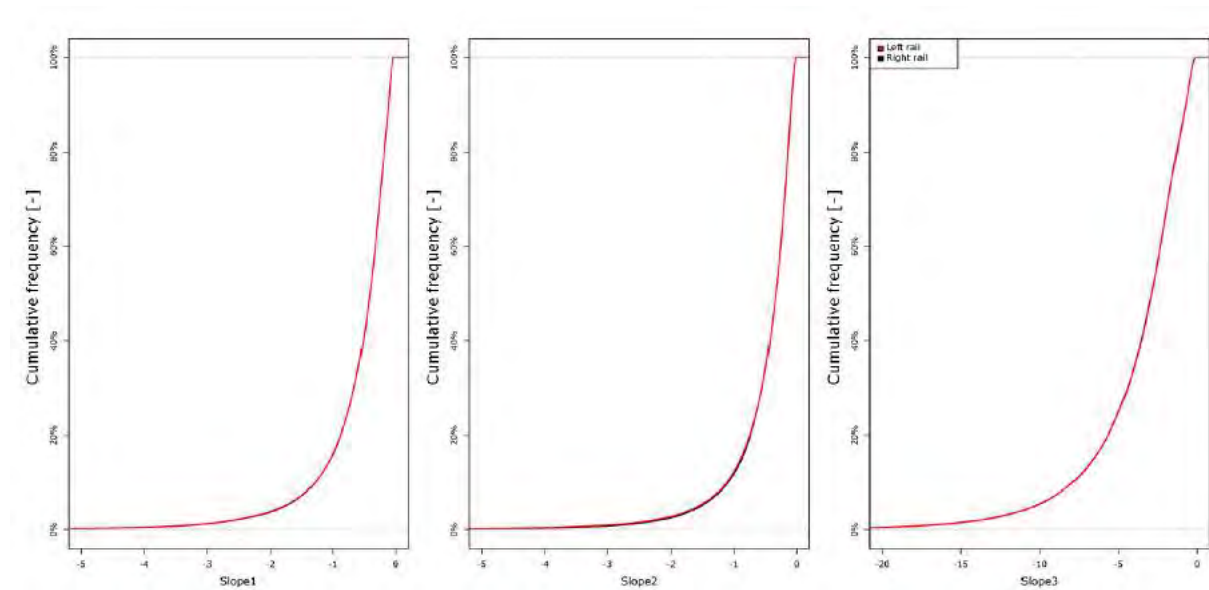


Figure 73 Frequency Distribution of Slope1 to Slope3 divided into the individual Rails, drawn from the Year 2011.

In all three dimensions, the deviation between the rails varies significantly below 1. In the short-wave range, the distinction between the two rails is the smallest, although it must be taken into account that the absolute values cannot be compared with any of the medium-wave dimensions (see Figure 73). The difference between the left and right rails should thus be considered differently in each of the different dimensions. However, since the focus of consideration is not to compare values, but to examine their expression, the values will not be standardized. Nonetheless, the difference between the two rails for particularly small dimensional values may reach a non-negligible size (see Figure 74). The extent to which this difference affects the evaluation of the component's condition is shown in the following analyses.

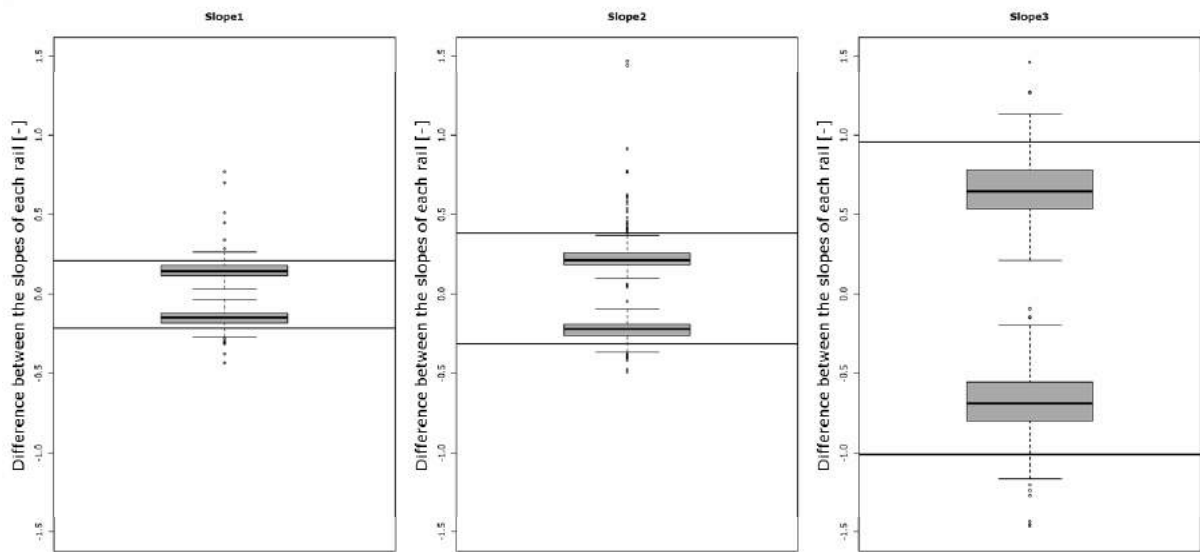


Figure 74 Box Plots showing the Distribution of the 10% (above) and 90% (below) Quantiles of the Differences between the Slope Values for each Rail

The fractal analysis does not aim to replace the traditional track geometry analysis (see 3.1), but is rather intended as an additional information source. To this end, it is important to consider possible correlations between the individual dimensions and the traditional methods, in order to maximize the information thus extracted. Figure 75 compares the dimensional values from 2011 with the associated values of the standard deviation of the vertical alignment. The box plots include the values of the fractal analysis dimensions and are aggregated into groups over the standard deviation of track geometry, rounded to one decimal place. The scale of the representation is adapted to the value distribution, comprising values between -20 and 0 in the medium-wave sector, and values between -5 and 0 in the other sectors. With larger slope values, the standard deviation of the vertical alignment also increases in all dimensions.

This relationship is logically founded in the mathematical calculation of the standard deviation over sum of square errors. The correlation is more evident in the medium-wave and long-wave sectors than in the short-wave sector. This can be explained by the influence of different frequencies on the standard deviation (see Table 3).

The progressions of the available correlations are only marginally different from each other. The long-wave correlation grows more slowly with small values of the standard deviation than for values greater than 1. This relationship is inverted for the short-wave and medium-wave correlations. The values of the two dimensions grow strongly as the standard deviation increases, finally levelling out almost to a constant for large values. This effect is particularly noticeable for Slope1.

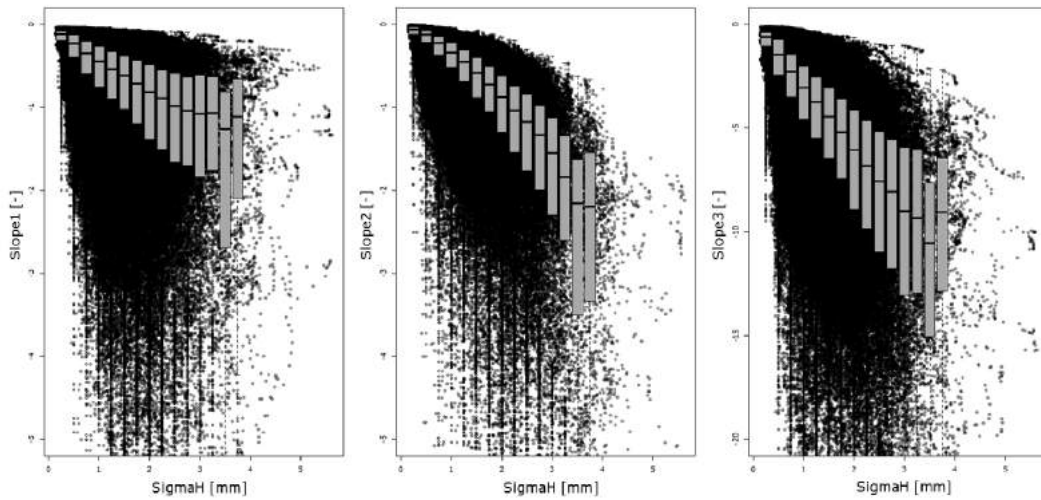


Figure 75 Comparison of the individual Dimensions and associated Values for the Standard Deviation

The relationship shown in Figure 75 is expressed somewhat differently for the long-wave dimension in the original application – described above – of the network-wide fractal analysis (see Figure 76 [left]). The first comparisons show a much stronger correlation between the long-wave range and the standard deviation than originally expected.

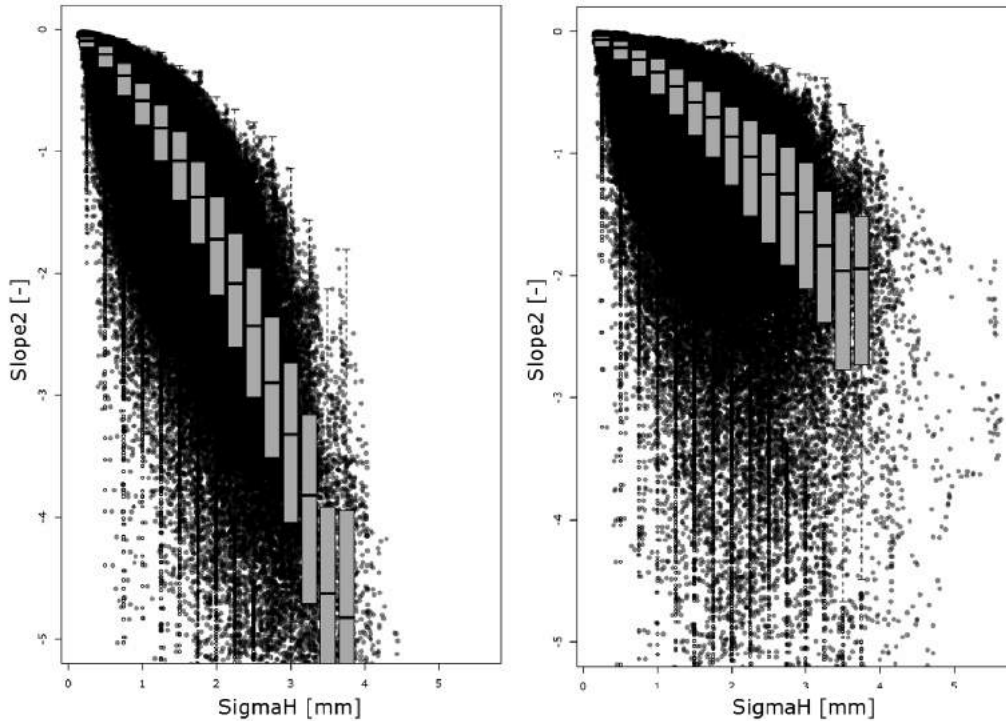


Figure 76 Comparison of the long-wave Dimensions with the associated Values for SigmaH in the old (left) and new (right) Calculations.

The long-wave dimension exhibits very small increases, and thus also very small differences between the individual points in the Richardson Plot. In the old calculation method, these small differences often lead to the slopes of the lines being dominated by points near the edge of the medium-wave sector (see Figure 76).

The search for an optimal fit to the available points, i.e. with the highest coefficient of determination cannot change this fact, conditional on the small deviations. With a relationship of this sort, there is a risk of describing similar effects with different quality values. In order to exclude this possibility from the following work, or at least reduce the effects, the limit of the long-wave sector will be moved so that it only includes wave-lengths over 25m.

The interaction established by the original fractal analysis between the standard deviation and Slope2 is reflected in the comparison of Slope1 and Slope3 (see Figure 77 [left]). This relationship is a necessary result of the fractal analysis method and arises from the fact that errors in different wavelengths never occur completely independently. This also explains the much smaller effect between Slope2 and Slope3.

The analyses in the prior work concentrate on ballast breakdown and its distribution in the fractal analysis. Evaluations of the long-wave dimension are restricted to merely network-wide evaluations in order to observe the database structure and possible correlations more closely. A selected example, however, will demonstrate the possibilities of fractal analysis as an evaluation tool for possible subgrade problems.

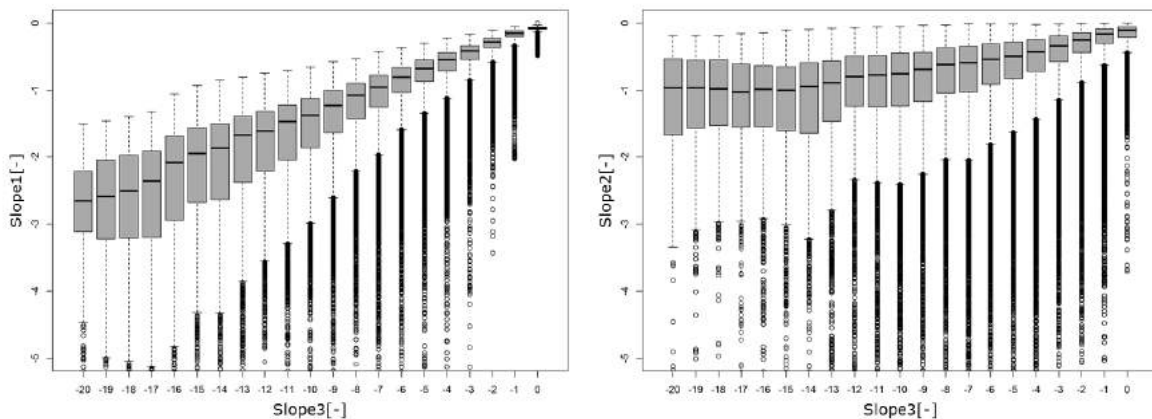


Figure 77 How the Fractal Analysis Dimensions affect each other

3.6.4 Effects of ballast bed breakdown from a fractal analysis viewpoint

In order to test whether fractal analysis presents real possibilities for determining the condition of the ballast, it is necessary to further validate the results. A first step is to compare the results of the fractal analysis before and after ballast cleaning. A cleaning of the ballast bed without changing the track panels is not a standard measure for the ÖBB and therefore only occurs if there is a particular necessity and technical foundation. The fact that ballast cleaning, unlike track renewal, is driven exclusively by the condition of the ballast, aids the investigation. Given the necessary relationship between the signal and ballast breakdown, it must be possible to uniquely describe the ballast condition using the signal characteristics.

A comparison of the resulting fractal dimensions clearly shows that ballast decontamination has an identifiable effect on the values in the medium-wave and short-wave ranges. Naturally, a ballast bed cleaning also affects the standard deviation of the vertical track alignment and the MDZ indicator, although this effect is less evident.

The ballast bed cleaning significantly improves the expression of Slope3 as well as Slope1. This situation corroborates the original assumption that it is possible to obtain more detailed information about the ballast condition from the slopes of the fractal analysis. If the long-wave range is to actually act as an indicator for possible subgrade problems, the values of Slope2 must remain almost unchanged by a ballast bed cleaning. This effect can be clearly seen in Figure 79.

It is now possible to correctly evaluate the results of the observations from both rails in their dimensions. The expression of the dimensions in the scales presented here shows the difference between the two rails for the distribution of the ballast condition to be negligibly small. However, for the purposes of this study, the question of whether the information about the difference between the two rails varies between additional evaluations was not considered further, and thus cannot be excluded.

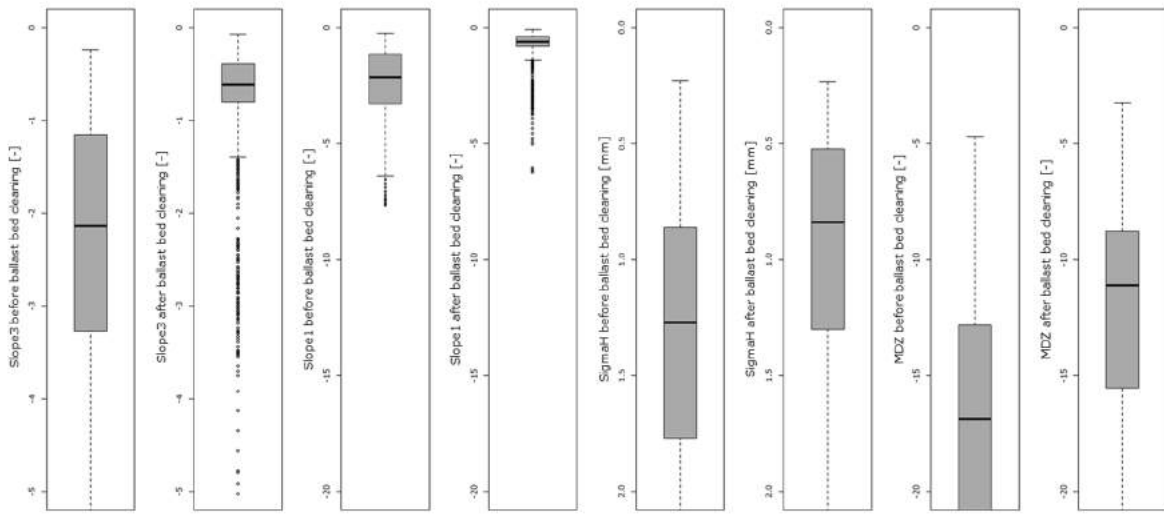


Figure 78 Effects of the Ballast Cleaning on individual Quality Signals

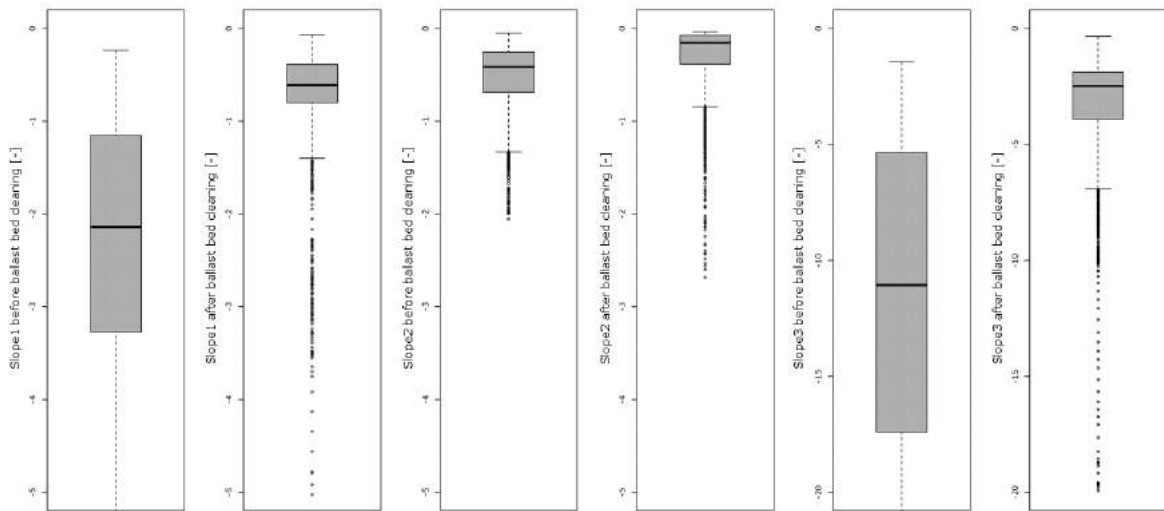


Figure 79 Effects of a Ballast Cleaning Operation on the individual Fractal Analysis Dimensions; left: before the Cleaning; right: after

If Slope3 and SigmaH are presented on a scatterplot, an interesting anomaly is revealed (see Figure 80). This anomaly is not reflected in the relationship between the two scales, but rather exhibited in their "non-relationship" (the orange points). Although this anomaly did appear in previous years, it cannot be depicted with the currently available possibilities. The cross-sections do not meet the specified parameters for the current observation of the annual first run with recording car.

In these cross-sections, the track geometry is significantly dominated by medium wavelengths, but hardly exhibit any anomalies in terms of usual track geometry analyses. Precisely these cross-sections represent a section of the TUG network which must be decontaminated due to advanced ballast fouling. A similar phenomenon can be seen between SigmaH and Slope1, although by contrast, the values in Slope2 remain almost untouched.

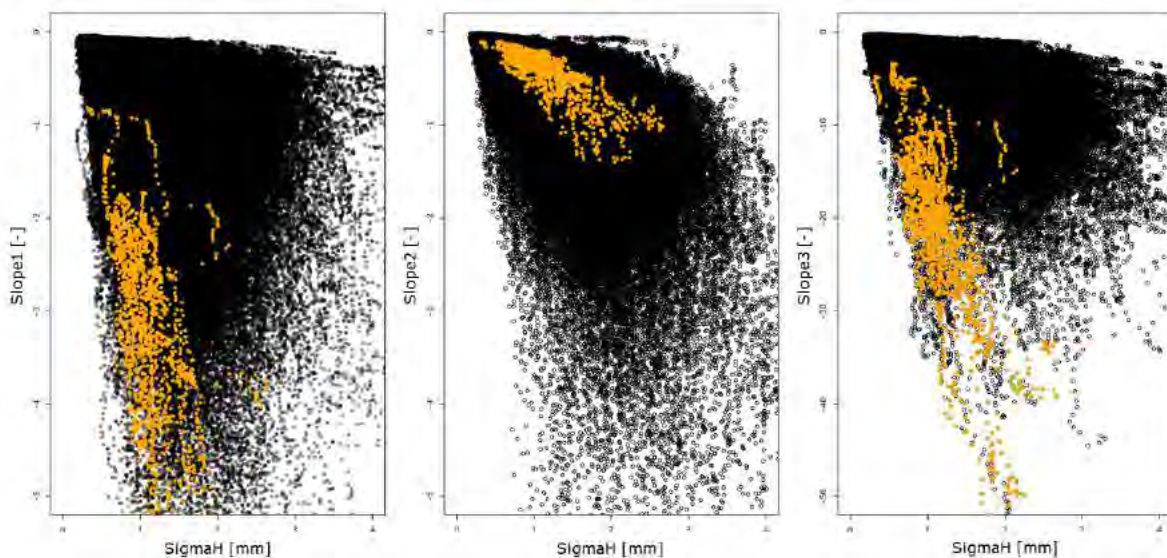


Figure 80 Anomaly in the Relationship between SigmaH and Slope3

3.6.5 From Theory to Practice – visual Track Inspection

In the second stage, the obtained results will be used to select areas of the TUG network which exhibit particularly high fractal values. The visual track inspections carried out on these route sections capture the local condition of the track, and thereby serve as sample validations of the fractal analysis. A total of seven areas were selected for the analysis exemplified in case study A. The detailed evaluation of other case studies is omitted from this section. However, in order to obtain an overview of the individual case studies, key information about the individual sections is shown in table form. Included therein is common information such as the calculated cumulative load and the average tamping interval since 2005.

The results tables give an idea of the distribution of quality signals, standard deviation of the track geometry, Slope1, Slope2 and Slope3. The values specified represent the mean value of each section from the year 2005. The 75% quartile is also supplied in brackets. Using these values, it is possible to arrive at an estimated classification of the sections in terms of their track geometry evolution, making a sample-based validation possible in combination with the picture presented by a track inspection.

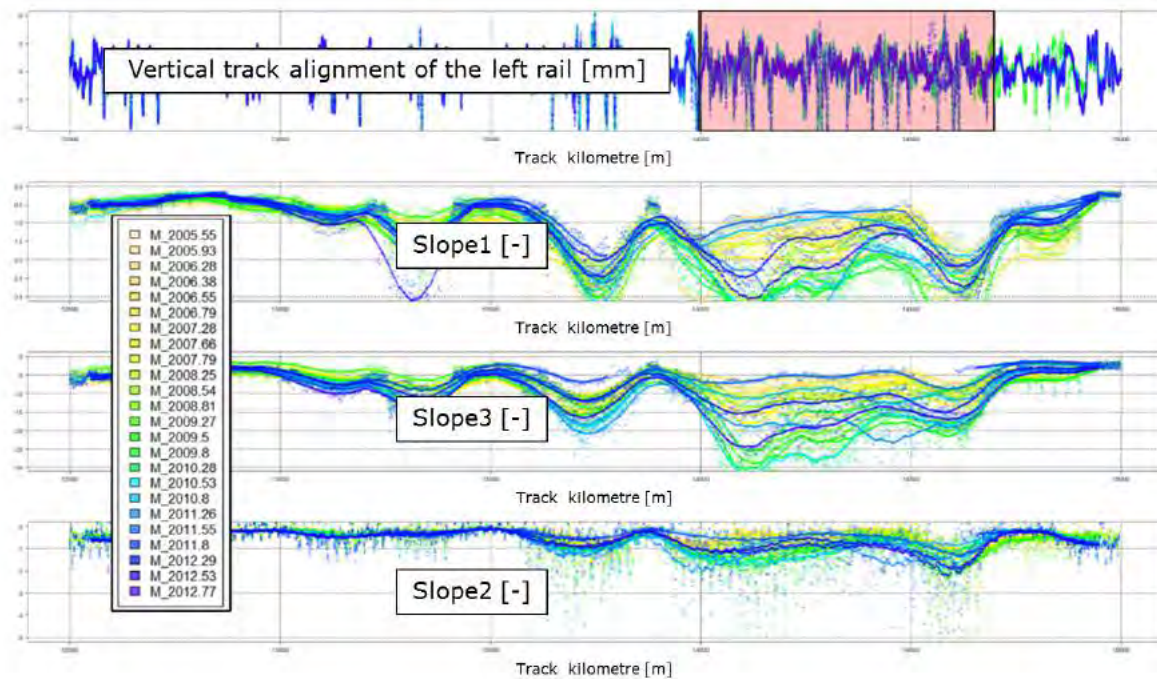


Figure 81 Detailed Fractal Analysis for the left Rail in Case Study A

Figure 81 provides a rail-specific overview of the calculated values from the fractal analysis for a 2500m-long section. In this concrete example, particularly high values can be seen in some areas (the red area) between kilometres 14.000 and 14.700 in the short- and medium-wave ranges. When these areas were inspected, the ballast showed significant signs of wear, generally referred to as "white spots", which exemplify advanced ballast breakdown. The area under investigation (case study A) is within a station area and exhibited the aforementioned wear pattern at regular intervals. Given the relatively low cumulative load of 193 million tonnes, it is possible to conclude that in this case the advanced ballast wear can be attributed to the unfavourable conditions in the station and is only peripherally related to the forces applied.

While case study B (Table 5) also shows increased values for Slope3, it nonetheless serves as a textbook example for the occurrence of a long-wave error and its basis in reality [Hansmann, Landgraf 2013]. As with case study A, this route section also has a small cumulative load. Despite the small cumulative load and the wooden sleepers installed, a tamping measure takes place in this section every two years. The occurrence of individual white spots indicates already advanced wear in the ballast bed. The high values in the long-wave region of the fractal analysis, the special rack layout and the vegetation in the ballast bed (see Table 5) suggest that in this section the upper part of the track is no longer adequately drained. Both ballast bed cleaning and replacement of the drainage system come within the responsibility of the regional authorities.


Case A			
Tamping interval: 3 a Cum. load: 193 MGT Inspection date: 16-07-2013 Track KM: 14.000-14.700		Left rail	Right rail
	SigmaH	1.14 mm (1.43 mm)	
	Slope1	-1.9 (-2.5)	-1.9 (-2.4)
	Slope2	-0.9 (-1.2)	-0.8 (-1.0)
	Slope3	-13.1 (-17.3)	-13.4 (-18.3)
			

Table 4 Case Study A


Case B			
Tamping Interval: 2 a Cum. load: 121 MGT Inspection date: 17-07-2013 Track KM: 134.000-134.300		Left rail	Right rail
	SigmaH	1.13 mm (1.43 mm)	
	Slope1	-1.0 (-1.1)	-1.1 (-1.2)
	Slope2	-2.1 (-2.7)	-1.9 (-2.51)
	Slope3	-6.1 (-8.1)	-6.7 (-8.9)
			

Table 5 Case Study B

Case study C (Table 6) is within a switch area with a load of just 400 million tonnes per line. The high values from the fractal analysis are reflected in a local examination of the condition of the track. Here, not only the ballast, but also individual sleepers exhibit signs of advanced wear. Along with other parts of the track, the sleeper fasteners are affected, showing signs of corrosion which indicate the high dynamic requirements of the entire system.


Case C			
Tamping Interval: 3 a Cum. load: 385 MGT Inspection date: 14-10-2013 Track KM: 71.200-72.000		Left rail	Right rail
	SigmaH	1.18 mm (1.51 mm)	
	Slope1	-2.3 (2.8)	-2.3 (-2.8)
	Slope2	-0.5 (-0.8)	-0.5 (-0.6)
	Slope3	-16.1 (-19.8)	15.8 (-18.4)
			

Table 6 Case Study C


Case D			
Tamping Interval: 2 a Cum. load: 579 MGT Inspection date: 15-10-2013 Track KM: 38.900-39.100		Left rail	Right rail
	SigmaH	1.13 mm (1.47 mm)	
	Slope1	-1.6 (-1.9)	-1.6 (-2.0)
	Slope2	-0.7 (-0.8)	-0.8 (-0.9)
	Slope3	-13.3 (-16.5)	-14.3 (-17.9)
			

Table 7 Case Study D

Although Case studies D (Table 7) and E (Table 8) do not cover a unified area, it is nonetheless helpful to consider them together. They both occur in the same route section, but on different tracks, and they have almost identical cumulative loads. The familiar white spots in the ballast are visible on the surface. After the rail pad was lifted, severe damage was identifiable at the bottom edge of the sleeper (abrasion), and a large proportion of small particles could be identified, particularly in the upper part of the ballasted track. The complete section underwent a ballast bed cleaning in 2013 after the local inspection.

Case E revealed a surprisingly intact ballast bed. This was due to a ballast bed cleaning, which had been carried out two months previously, and thus was not yet taken into account by the recording signal analysis. The old ballast could still be photographed and observed more closely (see Table 8).

Case E			
Tamping Interval: 2 a Cum. load: 578 MGT Inspection date: 15-10-2013 Track KM: 38.100-39.100		Left rail	Right rail
	SigmaH	1.14 mm (1.47 mm)	
	Slope1	-1.5 (-1.8)	-1.5 (-1.8)
	Slope2	-0.6 (-0.8)	-0.6 (-0.8)
	Slope3	-13.3 (-16.4)	-13.3 (-16.4)






Table 8 Case Study E

Case Study F highlights the dangers that can result from advanced ballast fouling. The ballast breakdown reduces the elasticity of the entire system, resulting in the sleepers being subjected to increasing loads. These loads ultimately lead to malfunction of the system and the sleepers or rails breaking. The pictures come from an area where the values

for the short-wave and medium-wave dimensions considerably exceed the average for the entire section (164.150km) and can only be considered as examples for the emergence of an extreme case. A conspicuous feature of this region is the rapid deterioration of Slope3 throughout the section.

Case F			
Tamping Interval: 3 a Cum. load: 218 MGT Inspection date: 15-10-2013 Track KM: 163.700-164.500		Left rail	Right rail
	SigmaH	1.12 mm (1.53 mm)	
	Slope1	-1.4 (-1.74)	-1.4 (-1.7)
	Slope2	-0.4 (-0.5)	-0.5 (-0.6)
	Slope3	-8.0 (-9.9)	-7.9 (-9.8)
			

Table 9 Case Study F

For the final example, a region was deliberately chosen in which, although the fractal values are raised, their value is nonetheless smaller than in the previous regions. In the area presently under investigation, uniquely delimited white parts are already visible in the ballast. The ballast beneath the sleepers exhibits a significantly increased proportion of fine particles (see Table 10). In the medium term it will become necessary to reinvest in this section, or replace the ballast bed. Nonetheless, the ballast damage has not yet reached the same level as the previous examples. This fact is reflected in the values for the individual dimensions. For the first time in the results discussed here, the left rail exhibits noticeably higher values for the medium-wave dimension than the right rail. Since the previous evaluations confirm that this case does not follow the general rule, further analysis will be omitted at this point. Whether the reason for this difference lies in the section curve geometry will be left to future research.

Case G			
Tamping Interval: 5 a Cum. load: 439 MGT Inspection date: 17-07-2013 Track KM: 3.900-4.300		Left rail	Right rail
	SigmaH	1.18 mm (1.46 mm)	
	Slope1	-1.0 (-1.1)	-0.7 (-0.8)
	Slope2	-0.3 (-0.4)	-0.3 (-0.3)
	Slope3	-5.0 (-6.0)	-3.6 (-4.3)






Table 10 Case Study G

Both the analysis of the ballast bed cleaning operations over the last five years, and the random sample validation of the results through track inspections, confirm the relationship between the ballast bed deterioration and the values of Slope1 and Slope3. Since the short-wave dimension is subject to the risk of being additionally affected by surface errors to the rails and noise in the measurement system, the analyses which follow concentrate on the analysis of the medium-wave region, although without entirely disregarding the values from the short-wave dimension.

3.6.6 Construction of a Regression Model and its Possibilities

Following the investigation of the effects of the ballast bed cleaning on the fractal analysis, the question arises of how the fractal values respond to a tamping measure. In order to answer this question, it is necessary to describe the temporal progression of the dimensional values, and detect potential incremental improvements. To this end, an answer can be found by comparing the detected improvements with the actual tamping operations carried out. As an example, this approach was applied to two routes in the TUG network. The aim is to compare 250 track kilometres which have been both tamped and partially cleaned in recent years. An observation of the cross-section time series also makes it possible to validate the reproducibility of the results, while a detailed functional description of the condition is only a secondary aim. Given that the function fit is not a primary goal of this work, a linear model will be assumed adequate to describe the temporal evolution.

The time series analysis is the result of an algorithm named ProgMod which will be described here in more detail. ProgMod's goal is the identification of sudden changes in the temporal progression of a statistical indicator, as well as the identification and elimination

of outliers. For the fractal analysis, the algorithm uses a simple threshold of 4 and compares this with the differences determined by two consecutive recording journeys. This threshold results firstly from observing random samples of individual time series, and secondly is adapted to the values of the standard deviation over time. Figure 82 clearly shows that distributions up to 3 generally accord with the rule for time series. Selecting a too-small limit would thus appear pointless, and also run a risk that the time series may be classified without maintenance measures, depending on the natural distribution. If the calculated regression model subsequently leads to erroneous statements, the threshold will be lowered further and the effects on the results more closely examined. Should a measurement point exceed the threshold in terms of its difference from previous and subsequent values, then it will be marked as an outlier and excluded from further consideration. If the difference only exceeds the threshold on one side, then a measure will be implemented between the two recording journeys, and the regression restarted for the next recording journey.

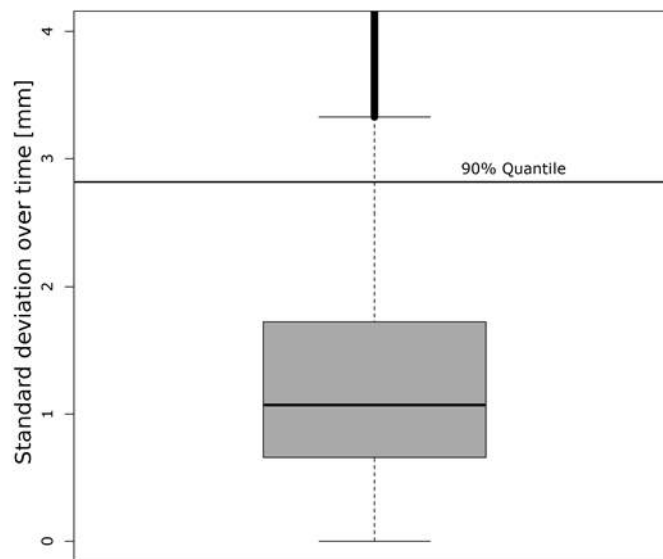


Figure 82 Standard Deviation over Time for Slope3 calculated according to Cross-sections

The effects of "normal" deterioration can only be determined under consideration of a regression model. Until the effects of maintenance measures on the fractal analysis values have been understood in more detail, a comparison of the temporal coefficients of variation for existing quality signals would hardly be a meaningful proof of their reproducibility.

The first stage is to demonstrate the validity of the regression model. Given the repeatedly confirmed assumption that Slope3 is correlated with the immediate ballast condition, the regression model should generally result in a negative slope for the relevant tracks. The emphasis on an effect occurring the majority of the time may appear strange at first glance, but it is based on the fact that in this analysis no distinction is made between the free

section of track and any potential discontinuities. Discontinuities often exhibit not only particular maintenance measures, but also tend towards complex situations whose description is not in the scope of this work. In fact, the slope of the regression lines, as shown by the examples of routes 3 and 4, has a negative value 75% of the time, thus following the expected progression. The regression model, safeguarded by the structure of the 90% quantile, makes it possible to achieve the required description of the deterioration of the medium-wave dimension (see Figure 84).

Despite the decision to formulate a very simple model, the absolute mean deviations from the calculated regression model yield very small values, as do the variations between the left and right rails (see Figure 74). If these deviations are considered in relation to the previous analyses, the existing deviations can be considered small enough to ignore.

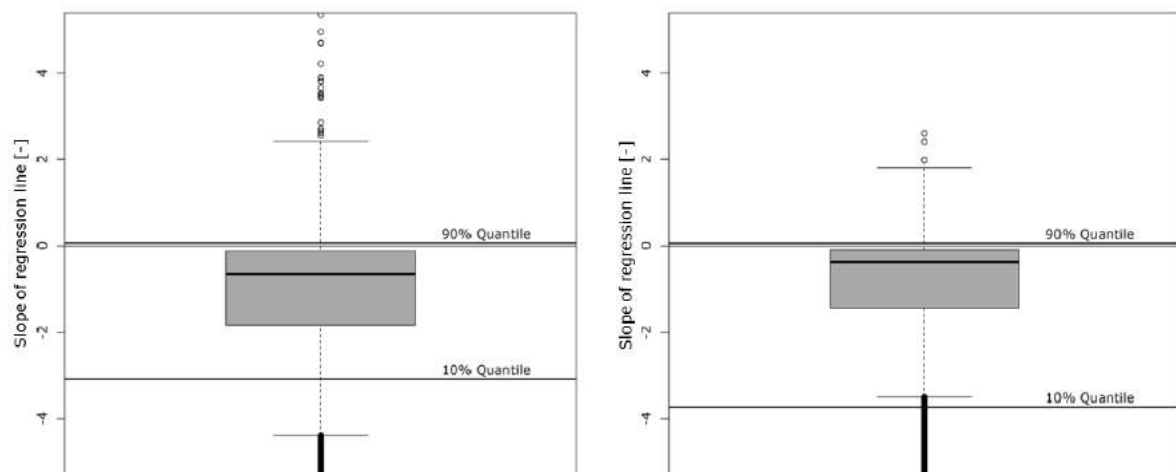


Figure 83 Comparison of the calculated Regression Lines for an Estimation of the Evolution over Time of Slope3 in the Cross-section. left: Track 4, right: Track 3

Having confirmed the reliability of the regression model with the above analysis, the model can be used as a basis for verifying the effects of tamping measures on the medium-wave sector. The ProgMod algorithm makes it possible to identify sudden alterations in the state of a quality signal, without assigning them a concrete cause. The existence of a relationship between these sudden changes and a tamping operation taking place can be confirmed by a graphical random sampling test, or equally by a cross-section-specific comparison between the actual number of tamping operations and the operations determined by the algorithm. There is a significant difference between the two values determined. In general, too few tamping operations are identified by considering sudden changes in the condition, while ballast bed cleaning noticeably affects the evolution.

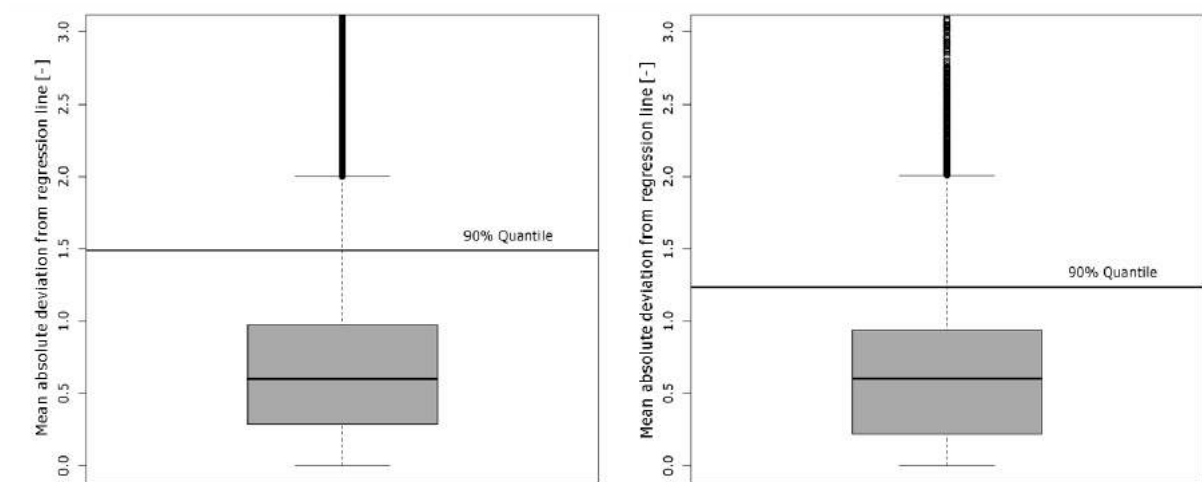


Figure 84 Distribution of absolute Mean Deviations from the Regression Lines, for the medium-wave Sector of the left Rail; left: Track 4, right: Track 3

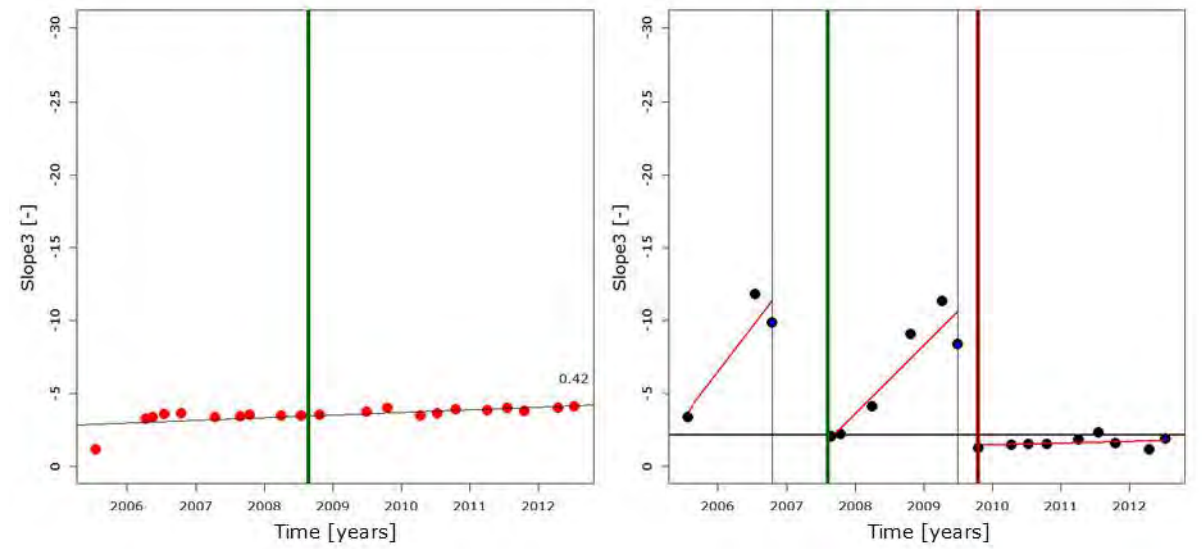


Figure 85 Results of the ProgMod Algorithm;
 left: no Improvement in the Slope Value through a Tamping Operation (green)
 right: Improvement in the Slope Value through a Tamping Operation (green) and Ballast Cleaning (red)

At this point, it should also be mentioned that the algorithm is only able to detect the measures if corresponding measurement run data is available before and after the operation. If the measurement runs are so far apart that deterioration leads to the track geometry returning to a similar level between the journeys, then the algorithm will not be able to identify an operation. In order to take this fact into account, routes were selected which featured a long interval between tamping operations. Random sampling tests of the algorithm show that an improvement in Slope3 through a tamping operation primarily occurs with very large slopes. No precise reason for the partial improvement of the fractal dimensions can be determined. Whether the improvements are due to the particular type of

tamping operation (e.g. affected by the amount of new ballast included), or indicate the quality of the operation itself, will be left for future research.

The comparatively small effects from tamping operations on Slope3 make it possible to observe the evolution of the values over the service life, without restricting the evaluation to quality values (see Figure 86). Such an evaluation is not expedient for conventional track geometry analysis: there would too often be sudden changes in the quality signals due to the maintenance carried out. The figure shows the median values calculated over the year, thereby increasing the sample compared to the originally used first measurements of the year. Almost 75% of the network is described by these evaluations.

An almost linear, uninterrupted deterioration in the values with increasing load is discernible. Wooden sleepers and track replacements after 2011 were not considered in this representation. Furthermore, in order to prevent the box plot from being distorted by local specificities, the number of values necessary for their inclusion on the plot was set at 2000 per cumulative load group.

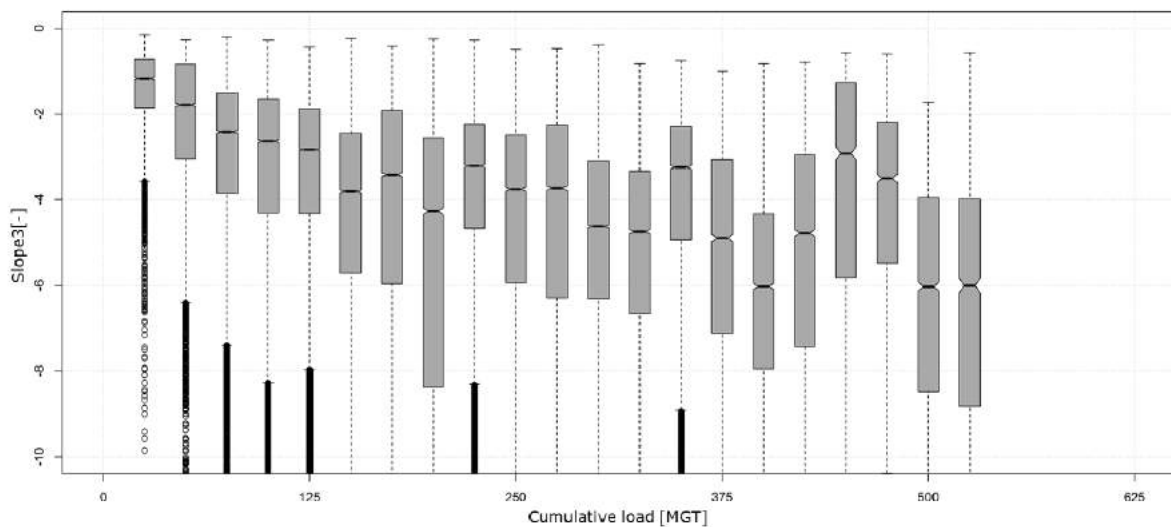


Figure 86 Evolution of Slope3 (annual Median Values) over the cumulative Load, with Concrete Sleepers

Three of the box plots noticeably exceed the identifiable trend. A closer look at their value structure shows that they are significantly affected by just one related route section of a TUG network. The reason for their unusual behaviour cannot be definitely established, but both the above fact and their clear unilateral geographic associations identify them as outliers. On average, concrete sleepers achieve a slope value of -6 shortly before their renewed; however, 25% of them reach -8.

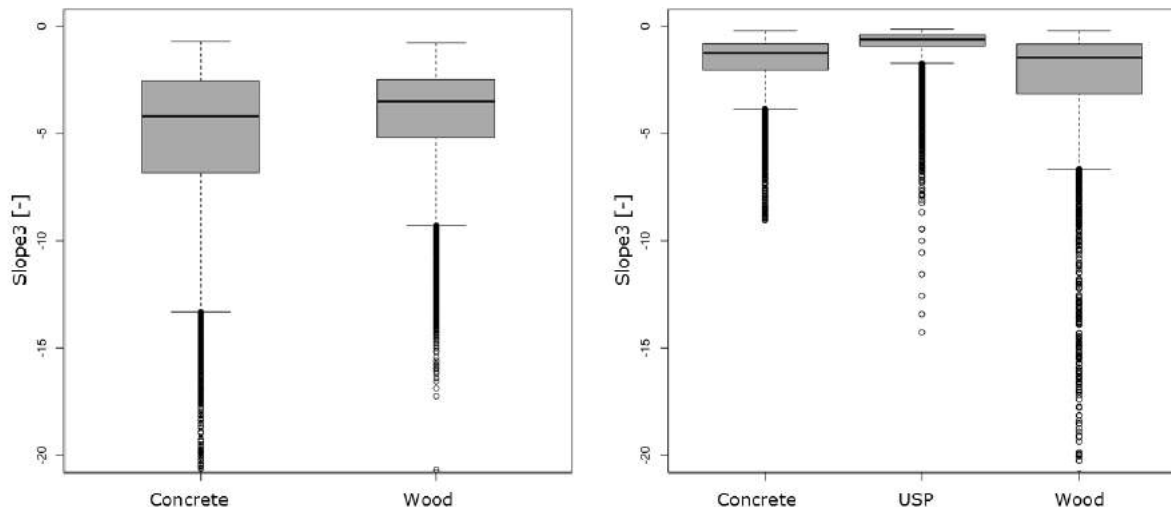


Figure 87 Expression of the Medium-wave Dimension in the Case of different Sleeper Types before [left] and after [right] a Track Renewal.

Comparing an observation of reinvestment projects and their removal quality with the previous track geometry evaluations, a contradictory picture emerges. In the basic evaluation of the standard deviation (see Figure 25), wooden sleepers exhibit worse track geometry than concrete sleepers, both before and after track renewal. Investigations show that this effect disappears when specific speed intervals are filtered for. In the comparison of slope values (see Figure 87) before and after the replacement, wooden sleepers exhibit better levels before the replacement even without filtering. This leads to the conclusion that in the TUG network the replacement of railway tracks with wooden sleepers is not generally due to advanced ballast break down. There must, therefore, be another reason behind the reinvestment of these. The values for concrete sleepers result in a similar picture, although these values are noticeably more distributed. Regardless of the track geometry quality signals considered, the positive attributes of sleepers with USP remain evident.

Primarily, the slope values appear to be more or less stable over the years, with a small number of exceptions (see Figure 88). The effects of the cleaning operation on route 4 can be seen in the evolution of individual values. However, a clear difference emerges between the routes. While certain routes have median values below the the network-wide median – identified by the black line – others exhibit significantly higher values. In some cases, even the 75% quartile lies above the network-wide median. It is not possible to judge from this analysis whether this difference can be attributed to the higher or lower cumulative loads, or whether the ballast quality still varies despite standardized requirements. It is, however, possible, based on the evaluation, to clearly identify regional focus points for future measures such as ballast bed cleaning or reinvestment.

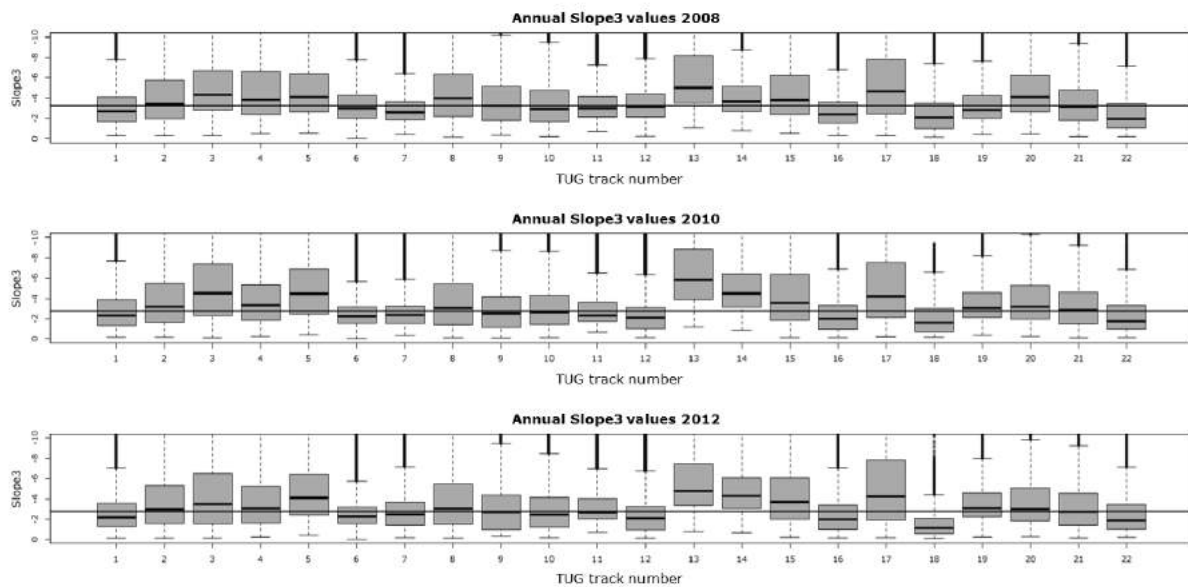


Figure 88 Route-specific Evolution of the Dimensional Values (Slope3) in 2008, 2010 and 2012

The evaluation of the ProgMod algorithm on route 4 offers a brief glimpse into the potential of a detailed time series analysis. In addition to information about the current ballast condition, it is possible to make predictions about its evolution by extrapolating from the regression line. The prediction thus establishes an evaluation of the ballast condition. When considering Figure 89 it is worth noting that possible track replacements since the reference year 2012 have not been taken into account. When the ballast in a system is changed or cleaned, a new lifecycle begins, which is no longer represented in this study. Depicting selections from the total range of results up until year 95 can in no way be considered to determine achievable service life. This direct portrayal of the results rather indicates that ballast damage is not the central cause for track replacement. As has already been shown by other evaluations, other components apparently have a significant effect on the service life of the track in these regions. Assuming the prediction to be accurate, an estimate of the measures for the next 10 to 20 years would hardly be expedient, in particular because the effects of tamping measures cannot yet be fully evaluated. This results in the characteristic image for route 4, the route currently under consideration. Other routes may exhibit other values, depending on the age of the current tracks and the sleeper types.

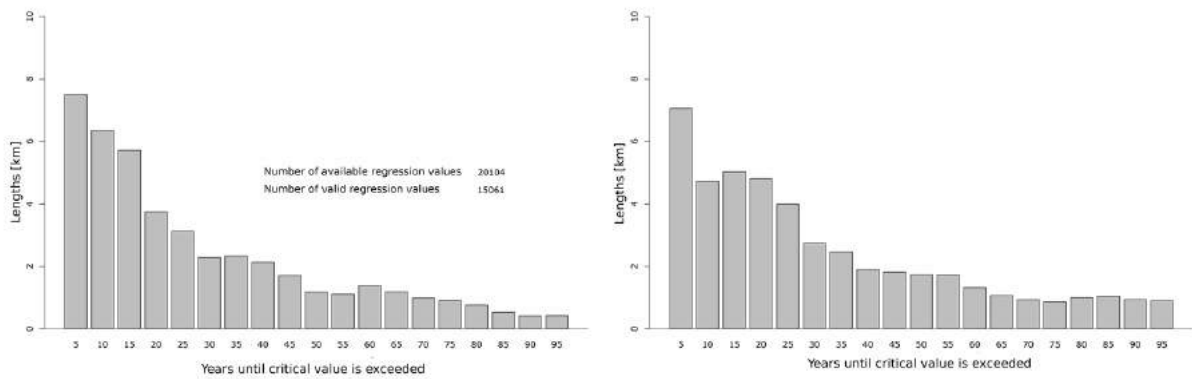


Figure 89 Applying the Prediction Model to estimate the remaining Service Life of the Ballast; left: Critical Value=-8, right: Critical Value=-10

As there is no network-wide predictive model, it is necessary to evaluate the ballast damage in the context of the fractal analysis of the quality signals. A detailed division into quality categories, as carried out using the classical track geometry analysis framework, is not envisaged for this purpose. However, in order to establish the condition of the remaining network, the median values over the year will be used for the evaluation. These median values should prevent the evaluation from being distorted by individual measurement outliers. The influence of possible maintenance measures carried out during the year will be deliberately ignored in this approach. The year 2012 will be taken as a reference year.

Should the annual median values exceed the critical value -8, it will be indicated that a measure is recommended in the cross-section in the following year.

3.6.7 Summary and Future Developments

A central element of this section outlining the application of fractal analysis is the validation of a system associating characteristic track geometry signal features with specific damage patterns. Fractal analysis makes it possible to determine track geometry signal features in a reproducible manner and output them on a network-wide basis. Tests of the potential these values have to describe ballast damage give consistently good results. Evaluations of ballast bed cleaning and reinvestment projects in recent years verify the information provided by track inspections and confirm Hyslip's hypothesis that there is a correlation between ballast damage and the values in the medium-wave fractal analysis dimension.

Fractal analysis does not replace the standard track geometry analysis, but is rather an addition to it. The short-wave and long-wave sectors were only briefly touched on in this work, requiring further analysis before they can definitely be included in asset strategies based on recording data.

Although the evolution of Slope3 over the cumulative load already gives stable results, questions remain regarding the different influences of tamping operations. The prediction model makes it possible to determine the remaining matter in the ballast bed, inasmuch as this is limited by ballast damage resulting from the applied loads. In so doing, a basis is created for planning medium-term operations, thus creating a possible foundation for planning resource allocation.

There is potential for future research to extend the fractal analysis, e.g. to the alignment geometry, as well as to answer a number of open questions. For example:

- I How can the differing effects of individual tamping operations on the fractal analysis be explained?
- I What information can be obtained from the short-wave dimension?
- I Can information about the stability of embankments be obtained from the alignment geometry?
- I Do additional parameters in the Richardson Plot offer possibilities for a more detailed description of the ballast condition?
- I What additional value is offered by analysing the difference between the two rails?

4

Sleeper Condition Monitoring

Evaluations of track geometry showed that the track geometry itself is not always the reason for reinvestment. Wooden sleepers exhibit significantly lower service life than concrete sleepers (in cumulative tonnage), although they appear far better in terms of their track geometry condition. Assuming that the track geometry reflects the condition of the ballast and subgrade, the reason for upgrading wooden sleepers must thus be found in a different component.

Rail wear or the emergence of errors on the rail surface certainly leads to the rails – inner and/or outer – being exchanged sooner or later; however, this is rarely a reason for reinvestment of the track. A reinvestment of the track is thus only necessary when other components besides the rails also exhibit signs of advanced wear, so that the remaining service life of the entire track is limited. Rail replacement is expedient in the context of a sustainable asset strategy based on life cycle costs only if the remaining service life of the other components is sufficient that the annual costs of the track will be returned to the level before the rails were exchanged. Or, to express it differently: a rail replacement is only expedient for the system if the remaining components could acquire sufficient service life that an exchange of the entire system would cost more than the rail replacement. A rail replacement can thus lead to the reinvestment of a system, but only triggers it indirectly.

As part of the track superstructure, the sleepers primarily serve to create and sustain the track, secure the rails and distribute the load (cf. [Lichtberger 2010]). They are subject to high demands and, due to the high costs of a single sleeper exchange, significantly limit the service life of the entire system.

Due to the waterproofing possibilities for wooden sleepers, which are still acceptable, biological damage plays only a minor role, although if cracks can do appear they may lead to the end of the effective service life. Wooden sleepers exhibit a tendency to no longer be able to guarantee the necessary traction, due to the expansion of mounting holes or cracks in the sleeper and the deterioration of the ribbed base plate. [Schultheiß, Schulz 1985]

Concrete sleepers exhibit much higher resistance to the applied loads; however, they transmit the loads to the ballast over a smaller contact zone than wooden sleepers. The result is more dramatic ballast damage, which is additionally accelerated by the increased weight of concrete sleepers and their reduced elasticity.

Although concrete sleepers exhibit high resistances, earlier sleeper types particularly tend to develop cracks as a result of inadequate pretensioning. This eventually results in replacement of the concrete sleepers becoming necessary [Auer 2010]. These damage patterns rarely occur in the sleeper types that are currently installed as standard in Austria, providing rail pads are exchanged appropriately in order to prevent on-going damage to the rail bed.

4.1 Introduction

The following chapter focuses on the continuous description of the interaction between sleepers and rails and consequently the sleeper condition. Starting from the current approaches to this subject, various possibly ways of determining component condition can be identified.

Firstly, research work shows that automatic analysis of high-resolution images [Yella, Dougherty & Gupta 2009] makes it possible to precisely identify cracks in wooden sleepers and individual defects in concrete sleeper fastenings [Terashima et al. 2011]. However, with this evaluation technique, it is not possible to form any conclusions about the wear of the rail pad. The work so far has focused on generating as much information as possible about the current condition of the track and its evolution based on the recording signal. These methods have not presently been applied network-wide in Austria. Thus this possibility for determining components condition will not be elaborated further.

Secondly, an evaluation of the current rail inclination and its temporal evolution leads to informative results. This analysis makes it possible to estimate when it is necessary to exchange the rail pad or the ribbed base plate in case of wooden sleepers. The measurement of rail inclination is directly coupled with rail profile measurements, and thus makes it possible to determine the current rail-specific inclination of the profile. These results

indicate that an exterior rail pad thickness of 2mm is the optimal time to exchange it. When this value is transposed to the rail profiles installed, this means in general that it is necessary to exchange the rail pad when zero is exceeded. (cf. [Auer 2005])

Restdicke Zwischenlagenrand in Abhängigkeit der gemessenen Schienenneigung													
Profil	Fußbreite	Schienenhöhe	1/40	1/80	1/160	0	- 1/160	- 1/80	- 1/40	- 1/20	- 1/10	Tangens	Schienenneigung
60 E1	150 mm	172 mm	6	4.1	3.2	2.3	1.3	0.4	-1.5	-5.3	-12.8	mm	Restdicke Zw
54 E2	125 mm	151 mm	6	4.4	3.7	2.9	2.1	1.3	-0.3	-3.4	-9.6	mm	Restdicke Zw
49 E1	125 mm	149 mm	6	4.4	3.7	2.9	2.1	1.3	-0.3	-3.4	-9.6	mm	Restdicke Zw

Figure 90 Effective Rail Pad Layer Thickness for the Exterior in Relation to the Rail Inclination [Auer 2010]

However, where it is not possible to identify the profile from the rail profile measurement, it is also impossible to measure its inclination. In order to obtain information about its condition in this situation, and to further confirm the information regarding to the rail inclination, it is useful to extend the evaluation. Furthermore, the rail inclination measurements exhibit some weaknesses, particularly in their reproducibility, and the results are noticeably scattered. By extending the evaluation, it should be possible to support existing results, without establishing new measurement systems.

It has been ascertained that the loads applied result in wear on the components. On both the straights and the curves, the system yields beneath the load, then eventually returns to its initial position. With the increasing cumulative load, the movement within the system is increased, and the initial condition continually worsens. Depending on the demands on the system, it becomes more or less impossible for it to return to the original position. Random sample evaluations make it clear that this motion is reflected in the short-wave noise in the track signal. Network-wide evaluations should therefore show whether it is possible to generate information about the condition of the components based on the roughness in the track gauge signal.

As a result of wear on the rail profile, the deterioration of rail pad, base plate and the horizontal displacement of the rail foot, the track gauge tends to widen in curve sections. The recording car measured the track gauge for a damaged profile, 14mm below the rail level. [Österreichisches Normungsinstitut 2009] While rail replacement would generally reduce the gauge widening, it does not result in a return to the original condition, as the widening is influenced by various parameters. The track gauge's strong dependency on various influences means that an automatic evaluation is almost impossible. It does not make sense to just exchange the rail pads resulting from gauge widening, without also looking at the rail profile. The focus of the following observations is not on the gauge widening itself, but rather on the evolution of signal noise.

In the course of this investigation, it will be valuable to answer the following questions:

- I Is it possible to obtain information about the condition of the sleeper components or the traction, based on the gauge signal roughness?
- I Is there way to continuously capture the roughness and then describe its evolution over the service life?
- I Does the roughness in the gauge signal depend on the particular track superstructure as well as the age of the system?
- I What are the subsequent effects of rail grinding on the parameters here determined?
- I Is it possible to identify traction improvement measures from these parameters?

4.2 Roughness of the track gauge

In the available recording signal, the actual gauge of the track is not supplied, but rather its deviation from the standard track gauge of 1435mm. The majority of new lines or reinvested tracks in Austria over the last few years have been built with a standard track gauge of 1437mm (cf. [ÖBB Infrastruktur AG 2009], [ÖBB Infrastruktur AG 2012]). New route sections therefore exhibit an installed gauge widening in the TUG network. In order to simplify the nomenclature, the following work will refer to the "gauge" statistical indicators, although the indicators are actually referring to the deviation from the normal track gauge and not to the absolute track gauge.

The simplest way to determine the noise (roughness) of a signal is through sliding window calculation of the standard deviation. This is the same approach as currently used for the track geometry analysis (cf. Chapter 0), and has been standard practice for several years. When observing the gauge recording signal (see Figure 91 [first row]), it is possible to divide the signal into two separate signal characteristics; in curve sections, the gauge tends to large values over the entire region (gauge widening), while in straights, the deviations are distributed around zero. Consequently, a calculation of the standard deviation of the gauge (see Figure 91 [second row]) would be significantly influenced by the long-wave gauge widening in the region of curves. Calculating the standard deviation from the original signal shows this effect clearly. The calculated values increase significantly, primarily in the transition curve, i.e. exactly in the area where rapid changes in values occur. In the

actual curve, the values then decrease, before increasing again in the following transition curve. The extension of the recording signal evaluation is not, however, focused on the long-wave noise in curve sections, but rather aimed at capturing the short-wave and medium-wave noise in the gauge signal. It is expected that the interaction between the rails and the sleepers will be quantifiable using a description of the noise. Furthermore, the motion arising from effects such as wear in the rail pad or the deterioration of the base plate should also be reflected in this range.

In order to capture the roughness of the gauge signal, a simple filter on the original signal can be used. In the context of this signal filtering, a first step will be to calculate the sliding mean using a window length of 25m (see Figure 92 [above]). The sliding mean acts as a low-pass filter for the description of elements of the track with a minimum element length of 25m. This mean value will then be subtracted from the original recording signal, thus making it possible to filter the effects of the gauge widening in curve sections from the signal. The shorter wavelengths remain. The formerly strongly fluctuating mean value of the gauge takes the value zero (see Figure 92 [below]). It is now possible to quantify the roughness of the signal using the standard deviation calculation on the thus modified recording signal (see Figure 91 [third row]).

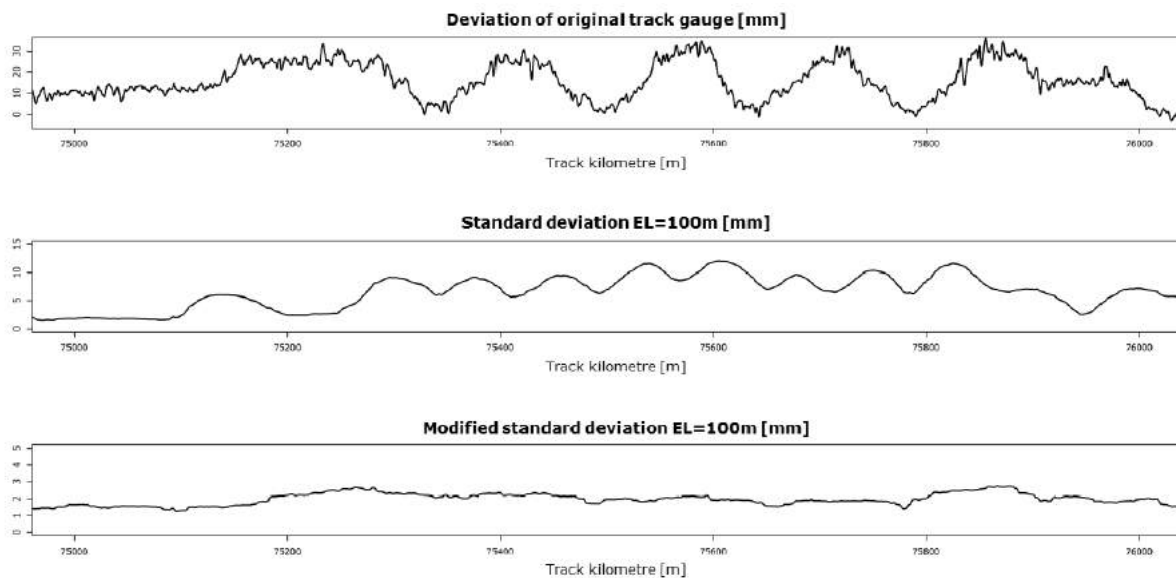


Figure 91 Example Evaluation of the Standard Deviation of the Gauge and its normalized Equivalent

As well as the aforementioned minimum element length, this algorithm also requires the increase in gauge widening to be linear rather than sudden. Sudden gauge widening only occurs in switch areas or indicates particular system failures. The extent of such sudden changes in the gauge is significantly below 25m, and is thus hardly affected by the filtering.

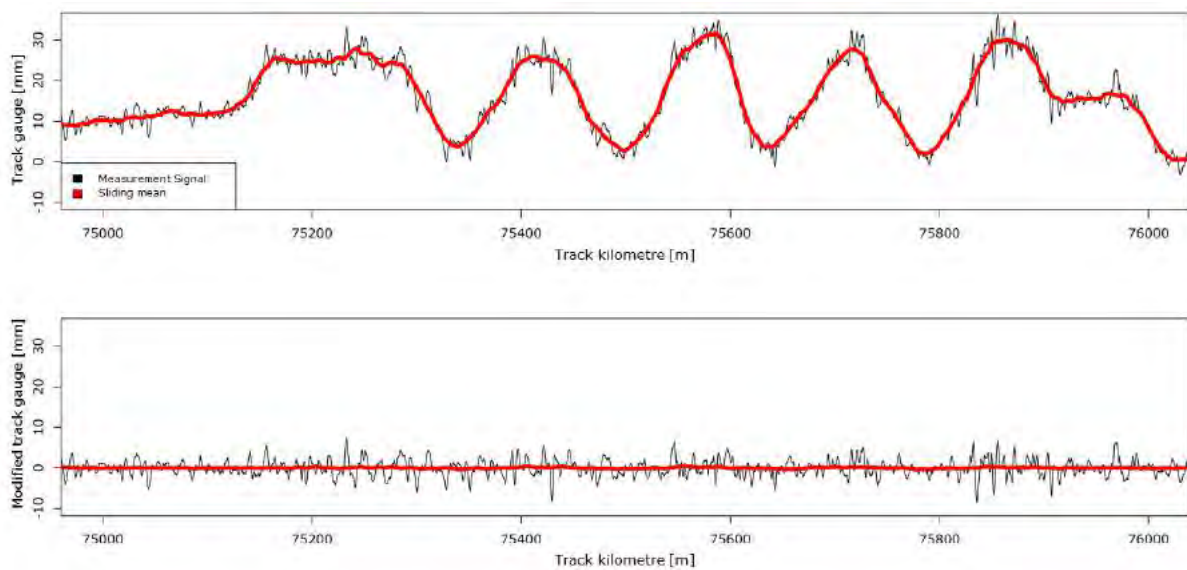


Figure 92 Normalisation Process for the Gauge;
above: original Signal with the Sliding Mean, below: modified Signal

4.2.1 The Discontinuity Algorithm

Before the modified standard deviation of the gauge can be applied to the entire TUG network, it is necessary, as for the track geometry analysis, to apply certain restrictions to the population. Without these restrictions, the evaluations would result in too large a distribution, and furthermore lead to the risk of depicting surreal conditions. While standard deviations in transition regions between concrete and wooden sleepers admittedly represent correctly calculated values, they do not depict the condition of either the one system or the other. Moreover, as this work focuses by definition on a description of the state of continuous tracks, the evaluations must be filtered accordingly.

During the track geometry analysis, this effect was excluded from consideration by the "valid length" attribute. The valid lengths take into account not only the beginning and end of machine deployments, but also the radius, the load category, the rail profile, the sleeper type, station areas, switches, bridges, intersections and tunnel sections (cf. Annex 1 and Table 11). The gauge signal analysis requires these restrictions to be revised, as they are too strict in places and too broad in others. A "discontinuity algorithm" aims to identify the individual pieces of information which are associated with cross-sections in the TUG network in terms of their variability in a pre-defined area, making it possible for them to act as identifiers of possible erratic or discontinuous features.

Taking machine deployments into account appears to have little point in the context of the current analysis. The TUG database takes only large machine deployments into account, whose effects on the gauge signal (other than track renewal) are not mechanically justifiable. The only exception to this may be grinding operations. At present, it cannot be excluded that wear on the rails also has effects on the standard deviation of the gauge, since a relationship has been determined between the absolute expression of the latter and the wear geometry. A comparison of the standard deviation of the rails before and after a grinding operation clearly shows that the evolution of the quality signal is independent of this operation. This independence is not surprising, given the short wavelengths of track surface errors and their amplitudes, but nonetheless should be investigated before the analysis continues. The model presented below provides an example of such a comparison.

In this model, only curves with a radius $< 250\text{m}$ were considered. In these curves it can be assumed that a grinding operation will entail reprofiling of the rail itself. In principle, an effect on the gauge can therefore be taken for granted. The mean values before and after the grinding operation are significantly different, while the standard deviation does not exhibit this significance. Equivalent evaluations for the remaining radius categories yield no difference in the mean value, nor in the standard deviation.

Finally, as the evaluation is noticeably more sensitive to measurement outliers than when quality values were being considered, the revision of the valid lengths aims at increasing the sample population size and thereby minimizing the risks associated with sensitivity to outliers.

Installations such as switches, bridges, intersections and tunnels will be treated by the discontinuity algorithm in the same way as previously explained for the determination of the valid lengths. Station areas will not be separately excluded as such (see Table 11). The discontinuity algorithm tests the homogeneity of a section. The section length can be adopted considering the evaluation length statistical indicators. Combined with the standard deviation of the gauge using a window length of 25m , the discontinuity algorithm will only return values for sections whose parameters do not alter, or only do so within the specified tolerances.

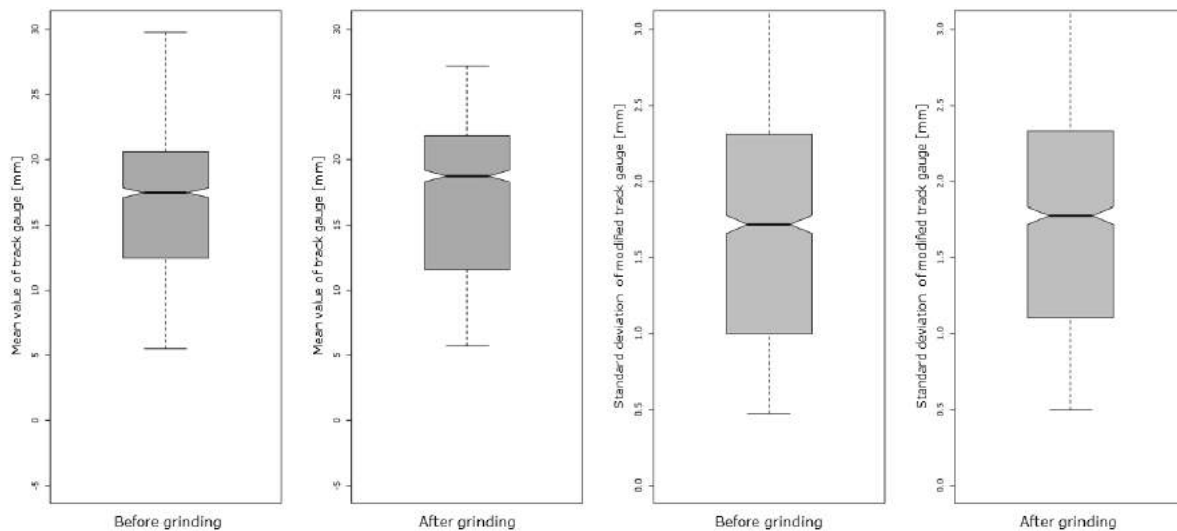


Figure 93 Evolution of the Gauge Quality Signal before and after a Grinding Operation.

The discontinuity algorithm determines the difference between the curvatures of consecutive route cross-sections on a network-wide basis. This difference makes it possible to identify transitional curves. Only after setting a constant radius $<600\text{m}$ can cross-sections be identified for a possible curve evaluation where window lengths are not taken into account.

The consideration of different sleeper forms or rail profiles continues in an equivalent manner, with the window length now being taken into account. In the case of a rail profile exchange, the values within the scope of half a window length remain unconsidered both before and after the exchange. It is difficult to resolve the question of the extent to which differing installation ages can be taken into account or ignored. The discontinuity algorithm treats installation dates which differ by five years or less as equivalent; any differences greater than that are identified and output by the algorithm, dependent on the selected window length. The installation year of the rails is not available in a rail-specific manner, meaning that the effects of exchanging rails on just one side cannot be taken into account by the discontinuity algorithm.

Sudden changes in the load do not lead to a restriction on the cross-sections, since the different circumstances are not modelled on the track superstructure age, but rather on the load model developed and the resulting cumulative load. Only 25% of the TUG network fulfils all the valid length conditions. This small sample clearly represents the somewhat conservative assumptions. By contrast, the discontinuity algorithm identifies definite discontinuities in around 40% of the network. This value can be reduced by 50% when only transition curves with a radius $<600\text{m}$ are excluded.

Information about the different fastening systems, rail pad or work associated with the different components or their exchange is currently not available in the TUG network. Statements about the signal deterioration can only take into account a combination of rail profile and sleeper type.

	Valid length	Discontinuity algorithm
Machine deployments	Yes	No
Discontinuities (intersections, switches, bridges)	Yes	Yes
Tunnels	Yes	Yes
Station areas	Yes	No
Sleeper type	Yes	Yes
Rail profile	Yes	Yes
Installation year of the sleepers	No	Yes
Installation year of the rails	No	Yes
Load category	Yes	No
Routing	Yes	Yes

Table 11 Comparison of Input Parameters for determining the valid Lengths and for the Discontinuity Algorithm

4.2.2 Value Distribution

After normalization, the values follow the sliding-window calculation of the standard deviation of the gauge with two different window lengths over the entire TUG network. This calculation is carried out by the SlidingWindow algorithm, as it makes it possible to perform a sliding calculation of different statistical indicators over the entire network. It is then possible for the user to freely select the required indicators (median, mean, standard deviation or MAD) and to define the window length. Subsequent evaluations concentrate on capturing the gauge roughness, while the remaining statistical indicators, other than the mean, will not be considered in this work. The algorithm tolerates a maximum error value or number of erroneous values of 10% within the evaluation length in either the original or the normalized recording signal; failing this, an error value will be assigned to the current cross-section.

The rail inclination and the track gauge differ with regard to the recording system sampling frequency. While the rail inclination is output every 2.5m, the track gauge values are output every 25cm. This makes it possible to produce an exact evaluation. The sliding windows selected for the calculation were 25m and 100m. The 100m window length represents a continuous window length, familiar from the track geometry analysis. A smaller window

length makes it possible to capture the occurring errors more precisely in terms of their position and scope.

For a 100m window, describing the condition becomes particularly difficult in short curved areas. At decreasing window lengths, the algorithm becomes more susceptible to outliers, in particular when applied with values which are not robust, such as the standard deviation and the mean. For this reason, a time series analysis should generally be carried out with large window lengths. The window length of the discontinuity algorithm reflects the choice of window length for the statistical indicator.

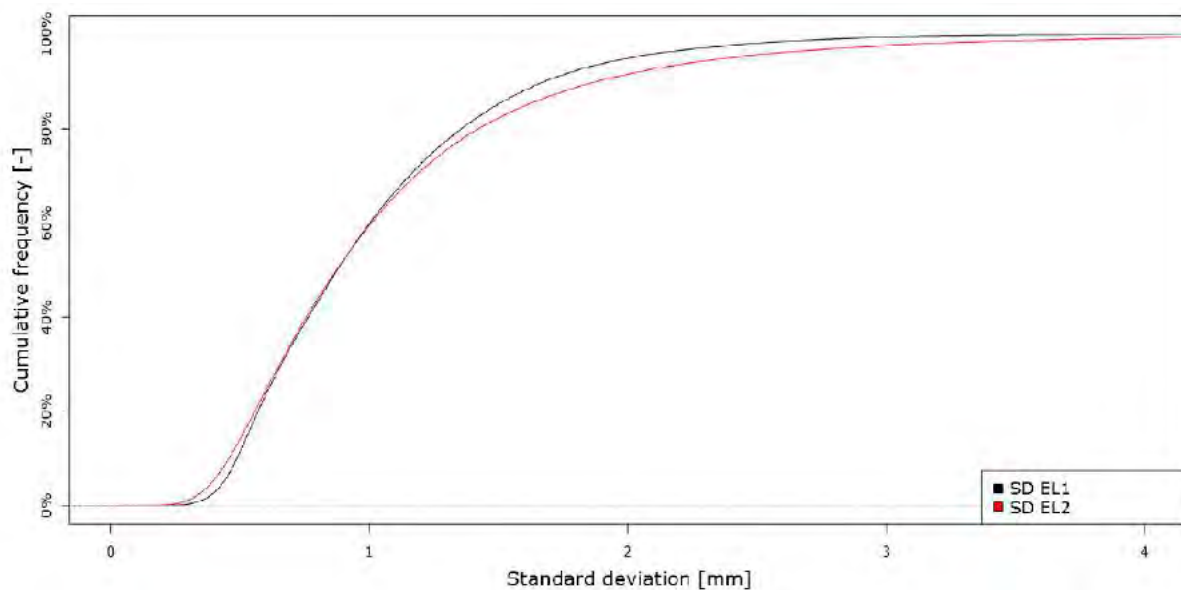


Figure 94 Comparison of the Frequency of different Window Lengths for the Standard Deviation of the Gauge in the Reference Year 2011

Both window lengths yield almost the same median value. The smaller window length, however, has a larger distribution, which is indicated by the flatter progression of the cumulative frequency distributions. This situation can be explained by the greater detail given by smaller window lengths. By contrast with large window lengths, high values for the standard deviation are concentrated locally around the discontinuity, while this information is reflected throughout the entire region in the case of large window lengths. Nonetheless, the interquartile range exhibits a small difference between the two window lengths.

The calculation of cross-section-specific annual values over the mean of the 2011 recording journeys makes it possible to determine the current value distribution of the statistical indicators. To what extent different maintenance works distort this value will not be discussed at this point. This evaluation focuses primarily on clarifying the effects of reducing the calculation to discontinuity-free cross-sections. Potential differences in the age structure of the various discontinuities are not taken into account.

Irrespective of these different simplifications, a clear distinction emerges between the discontinuities and the clear track (see Figure 95). In order to prevent the overlap of individual discontinuities, this evaluation only represents cross-sections with a single occurring discontinuity type. That is, only one kind of discontinuity may be detected in the cross-section and act as an input to the evaluation. The transitions between either different rail profiles or different sleeper types result in an increased standard deviation of the gauge. It is known that discontinuities often develop in the transition areas between sleepers or rail profiles, and this is reflected in maintenance expenditure.

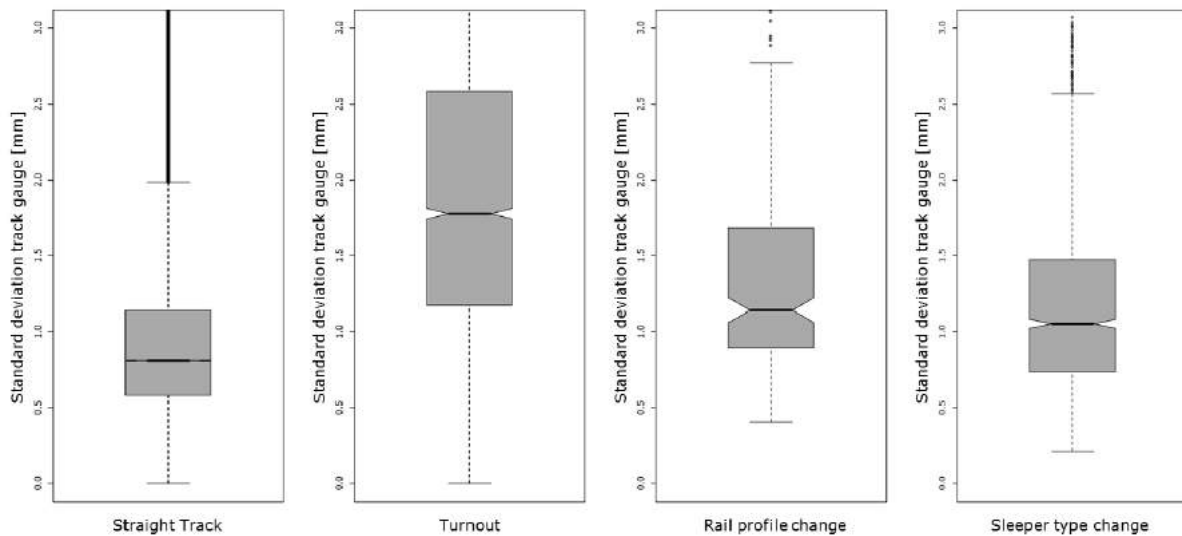


Figure 95 Size of the Standard Deviation for different Discontinuities within Track

Determining the rail inclination makes it possible to draw conclusions about the current condition of the rail pad or the wooden sleepers. However, the lack of certainty and reproducibility for the measurement makes it difficult to ascertain the temporal evolution for this parameter. Comparing the coefficients of variation subsequently leads to conclusions concerning the possibility of determining these parameters reproducibly from the standard deviation of the track.

Figure 96 assigns a significantly higher reproducible precision to the temporal measurement of the standard deviation of the gauge in 2011. Figure 97 makes it possible to apply the familiar results from the rail inclination to the standard deviation of the gauge, using the recognizable correlation. A higher value for this standard deviation indicates, for concrete sleepers, that the rail pad should be exchanged.

Based on a critical range for rail pad exchange of between 0 and -0.5 (cf. [Auer 2010]), it is possible to project this value onto the standard deviation of the gauge. In this range, 75% of the values reach the 1.1 dimension. As a first approximation, when this value is

reached a potential rail pad exchange should be considered. However, it is not possible to apply this more specifically to different types of rail pads or fastening systems.

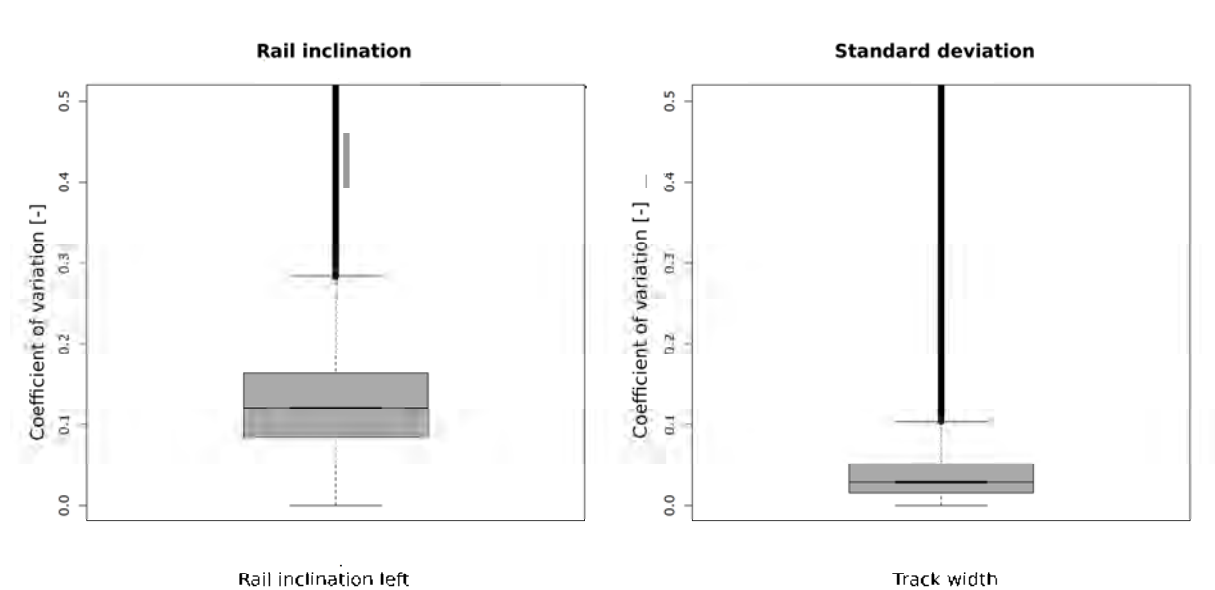


Figure 96 Coefficients of Variation of the Means of the Rail Inclination for the left Rail [left] and the Standard Deviation of the Track [right] based on the Recording Car Runs in 2011

4.2.3 Installation Quality and Removal Quality

If the installation and removal qualities are considered (see section 3.3) track geometry for more detailed information about the calculation), wooden sleepers exhibit higher values after renewal than concrete sleepers. This situation can be straightforwardly explained by the different component upgrades. While for concrete sleepers, only the rail pad provides elasticity between the sleeper and the rail, a wooden sleeper system is in general more elastic.

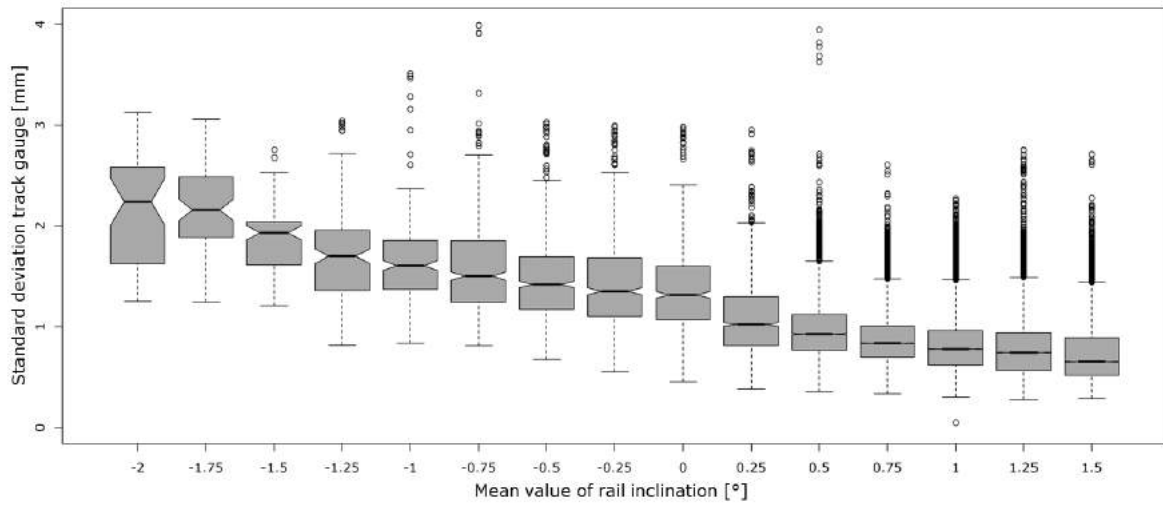


Figure 97 Correlation between the available Mean of the Rail Inclination and the Standard Deviation of the Gauge in straight Railway Lines with Concrete Sleepers and no Discontinuities

In curve sections <600m, the vehicle puts increased demands on the system due to the increased forces applied (cf. forces [Führer 1979]). The increased demands are reflected in more advanced wear, which can also be seen in the resulting removal quality. The median removal quality for concrete sleepers is significantly higher than the specified critical value of 1.5, and is almost 2.5 for wooden sleepers. The difference between the sleeper types is particularly evident in curve sections, which can be primarily attributed to the deliberate installation of wooden sleepers in tight curves (R<250m). The installation quality of wooden sleepers is almost twice as high as that of concrete sleepers, while the difference between sleepers with and without USP is vanishingly small.

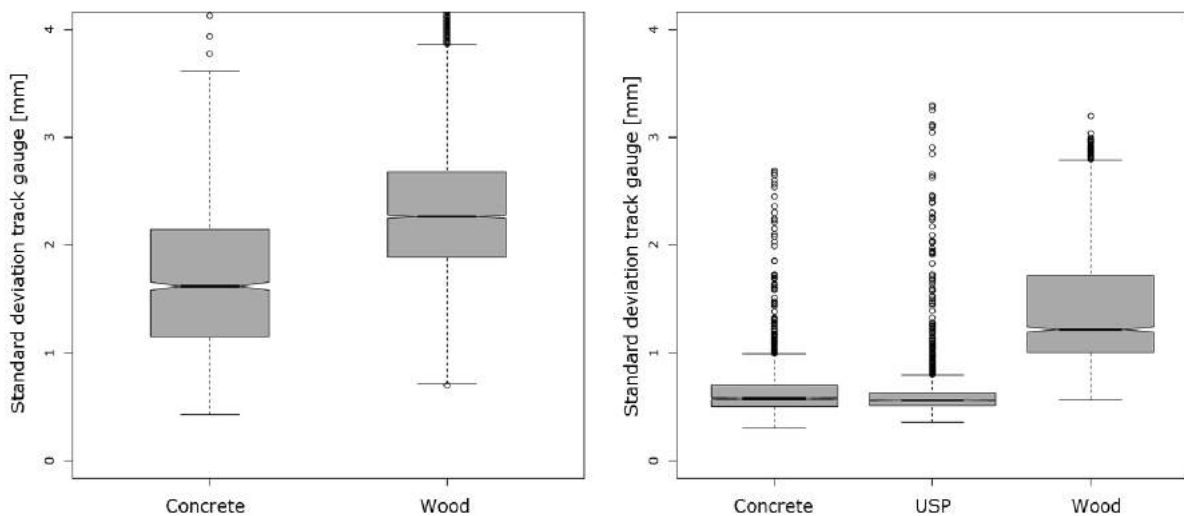


Figure 98 Average Standard Deviation Track Gauge before [left] and after [right] a Reinvestment in the System, in Curve Sections with a Radius less than 600m.

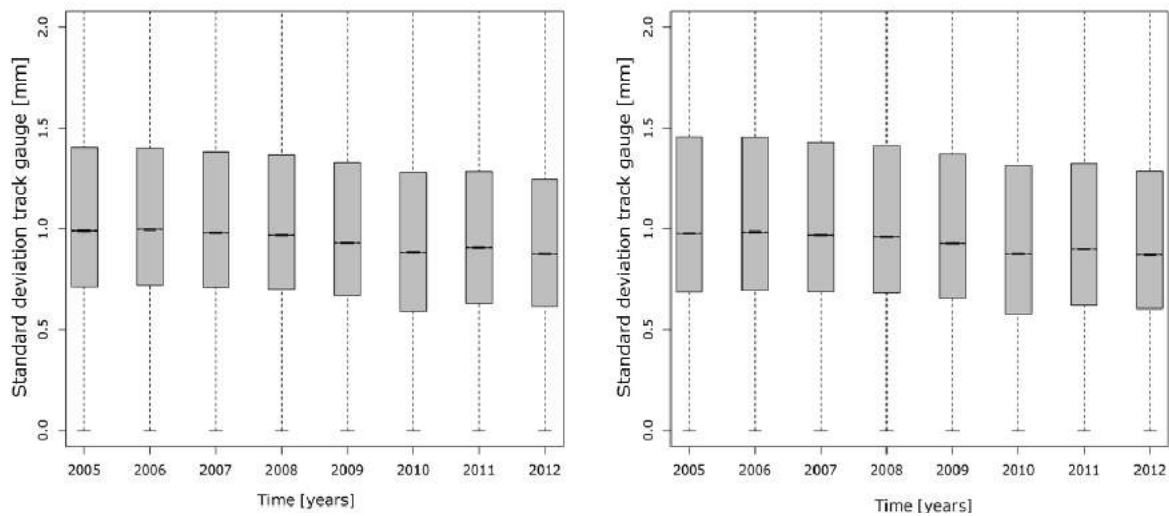


Figure 99 Evolution of the annual Values for the Standard Deviation of the Track since 2005; left: Window Length 25m, right: Window Length 100m

Whether the reason for this difference is the application of wooden sleepers in regions with particular requirements, as has already been seen in the track geometry analysis, will be shown in further evaluations. The widespread removal of wooden sleepers in the ÖBB network and the replacement of the majority of these with concrete sleepers with USP is also reflected in the positive evolution of these indicators over the last five years (see Figure 99). No difference between the 25m and 100m window lengths can be identified in this network-wide evaluation of annual values.

Before the temporal evolution of the standard deviation over the cumulative load is observed more closely, it is worth investigating in more detail the effects of any maintenance work on this evolution. Information relating to the carrying out or timing of measures such as rail pad exchange, fastening system repairs or adjustment of track fastenings is not available in the database at present. Therefore, an attempt must be made to estimate the frequency of such measures, or rather, to determine their effects by random sample testing of individual operations.

4.3 ProgMod Prediction Model

The ProgMod algorithm will also be applied during the fractal analysis. It is a simple, structure-checking algorithm which, in the context of this work, is revised and calibrated by means of various statistical indicators.

4.3.1 Construction of the Algorithm

The algorithm tests the difference between two temporally consecutive statistical indicators in a cross-section, and compares it with an empirically determined threshold. The application of the algorithm for different indicators varies in terms of the selection and number of thresholds. Although in the cases of fractal analysis and the analysis of the standard deviation of the gauge, the calculated difference could be compared with a single constant threshold, this approach is not appropriate for the mean value of the gauge. The mean value of the gauge has the particularity that an improvement in the system condition could equally result in positive or negative difference values. Consequently, a one-sided comparison of these differences would lead to a false conclusion. In order to take this fact into account, when the mean value is under consideration the comparison will be based on the absolute value of the difference. Evaluations with a single threshold reveal a further challenge: in straight sections, the system before the replacement often exhibits a narrowed gauge, while in curved radii, gauge widening is more typical. The relative improvement of the statistical indicators following a measure proves to be different in the two cases. In order to model this fact, the threshold adapts to the MAD of the cross-section calculated over time.

In statistics, MAD refers to the median absolute deviation, that is, the median deviation of individual temporal values from their own median. The MAD is a robust equivalent to the standard deviation, which can also be used to identify outliers (cf. [Lehmann 2012]).

The difference value will be determined twice consecutively. It will then be associated with the first of the two recording runs. In this way, each measurement point, with the exception of the last in the time series, will be associated with a unique difference value. Although the first pass of the ProgMod algorithm will always compare absolute values, the second pass will take into account either absolute values or real difference values depending on the indicator.

The first pass serves to determine outliers in the time series, in order to improve the quality of the resulting regression model. If two consecutive difference values exceed the specified threshold, then the algorithm identifies the second as an outlier and the results in this cross-section for the associated measurement run are excluded from further consideration.

Figure 100 shows an example of the described time series analysis. The vertical lines in the left image identify the values which are above the specified threshold (0.5 for the standard deviation of the gauge). The right image displays the values of the time series analysis after the automatic outlier identification.

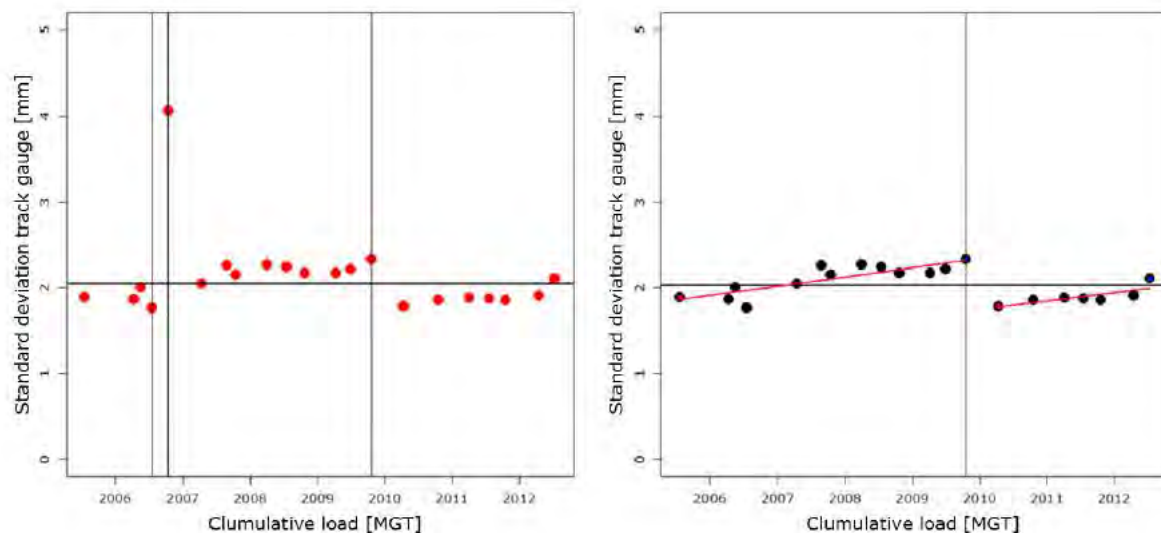


Figure 100 Determination of Outliers and Calculation of the Regression using the Prog-Mod Algorithm, for the Example of the Standard Deviation of the Gauge

The results of the ProgMod algorithm are consistent for both the standard deviation and the mean of the gauge, using the previously-discussed window length of 100m. Track 1 of TUG route 4 will be used as a basis for discussion of the results, the same track as for the fractal analysis.

4.3.2 Results of the Regression Model

The regression model described was applied to 136 track kilometres, permitting initial conclusions from the quality signal regarding condition of the components. The selected route 4 is notable for its mixture of curve sections and straight sections, resulting in a wide load spectrum. The lack of information concerning individual maintenance measures makes it difficult to validate the calculated regression model.

Where the standard deviation makes it possible to model the condition of the sleepers or the interaction between rails, fastenings and sleepers, a significant difference emerges between installation and removal quality, as previously shown in section 4.2.3. It is worth verifying whether this difference is also identified by the ProgMod algorithm. In order to perform this verification, two regions of track renewal were selected which were reinvested between 2005 and 2012. While the one section is exclusively straight, the other largely consists of a 350m curve.

In both cases, the algorithm clearly indicated the region of track renewal. While in the straight stretch (see Figure 101 [left]) the replacement was almost fully detected by the algorithm, in the second stretch the results are less conclusive. In the replaced region (47.200km to 47.500km) the algorithm determined several sudden changes in condition. A closer observation of the time series clarified that various unidentified measures had already taken place in this area prior to the renewal, resulting in an improvement of the quality signal.

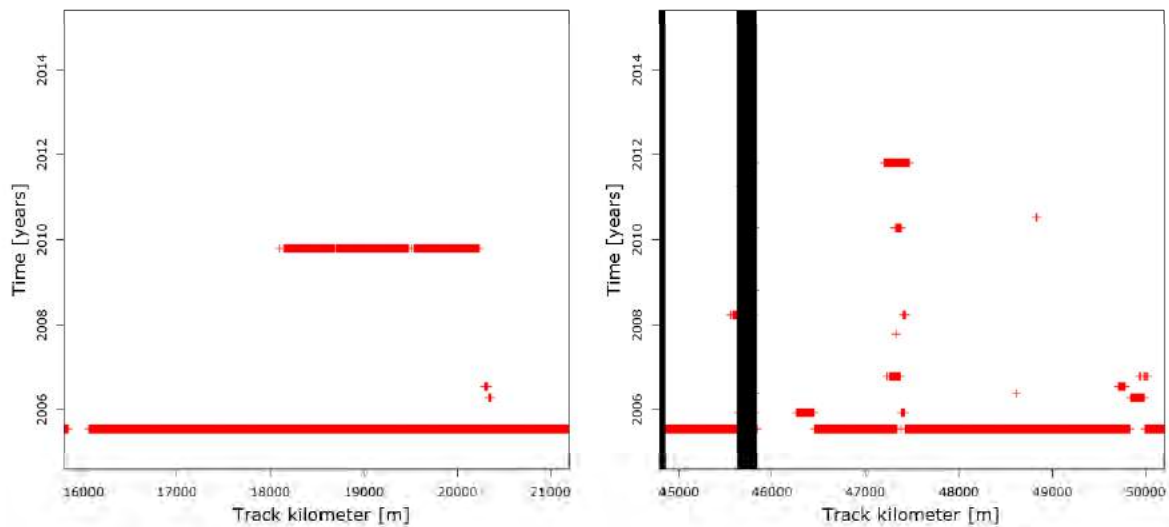


Figure 101 Determining Track Renewals with the ProgMod Algorithm

Sudden changes in the time series limited to a few metres often indicate measurement outliers. In regions of discontinuity, as in indicated by the black bars in the right-hand image, temporal evolutions typically follow other regularities. The two examples demonstrate the applicability of the algorithm, but also clarify the challenges that arise when determining implemented measures from recording signals.

As a second stage, it is valuable to verify the validity of the regression model over the specified parameters. In doing so, the slopes for the mean value of the gauge in the curve section are of particular interest, by comparison with those in the straights. A significant difference emerges between the two slopes (see Figure 102). As expected due to the applied loads, the applied forces in curve areas lead to a positive increasing slope and thus a tendency towards gauge widening. By contrast, the gauge typically narrows in the straights. This can be attributed to the off-centre impact of the loads and the inward-rotating moment (cf. [Liu 2012]).

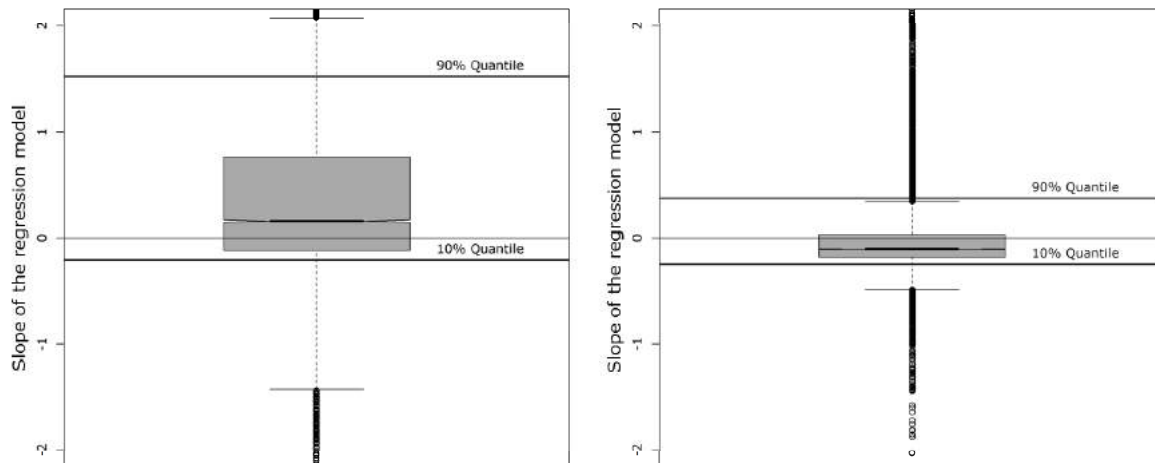


Figure 102 Calculated Regression Lines for the Mean Value of the Gauge; left: for Curves, right: for straight Track Sections

The regression calculation of the standard deviation track gauge allocates a negative slope to both curves and straights in 75% of cases. The value of the slope is greater in curve areas than in straights.

The position of the 10% quantile clearly indicates that the standard deviation of the gauge deteriorates with increasing cumulative load and thus perfectly models a deterioration process.

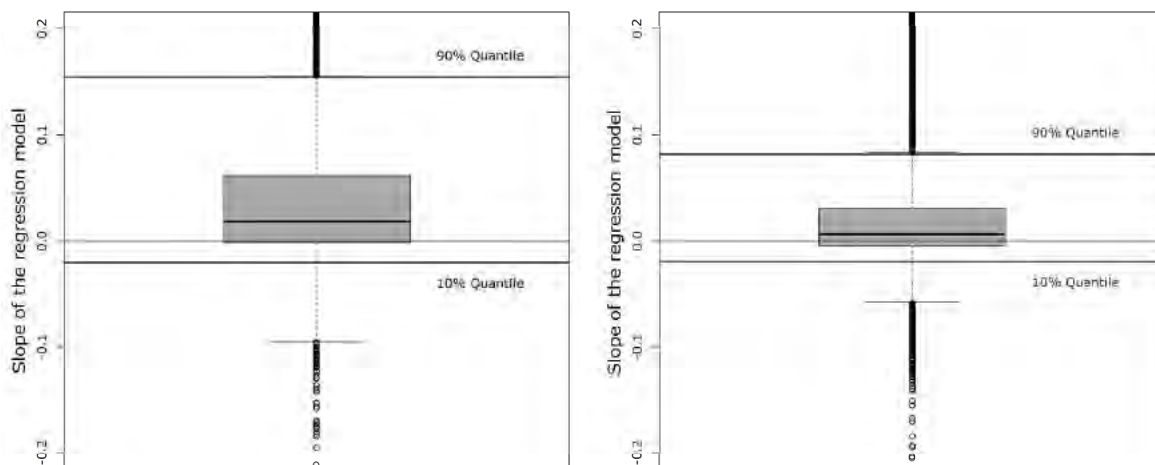


Figure 103 Calculated Regression Lines for the Standard Deviation Track Gauge; left: for Curves, right: for straight Route Sections

The mean deviations from the regression lines for the mean value and the standard deviation differ in size (see Figure 104). The small deviations between individual recording journeys can be deduced from this distribution, meaning that the model assumptions can be considered sufficiently accurate for this route.

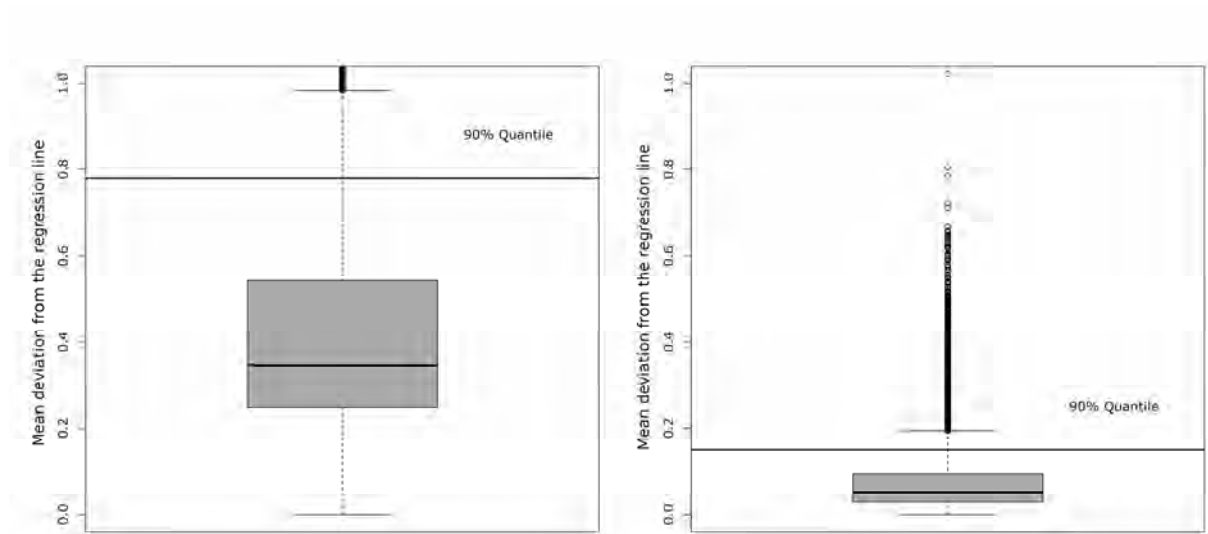


Figure 104 Mean Deviation from the Regression Lines; left: Mean Value, right: Standard Deviation

In summary, it can be established that the available regression model exhibits the required precision to describe the evolution of the standard deviation and the mean of the gauge. Missing information concerning maintenance measures which have been carried out can be estimated in terms of the times of the measures.

In some cases, no relationship between sudden changes in the mean and sudden changes in the standard deviation could be established. A sudden change in the standard deviation was detected in almost 18% of the cross-sections, only a quarter of these occurring on curve radii. The majority of improvements in the quality signal can be explained by track renewals.

Additional information concerning maintenance work would improve the results and permit more detailed analysis. The small number of sudden changes detected makes it possible to consider the quality signal over the cumulative load without further restriction. Nonetheless, the effects of known maintenance work should first be verified.

4.4 Effects of Maintenance Actions and different Superstructure on the Quality Signal

The lack of information concerning the measures implemented (rail pad exchange, adjustment of track fastenings, etc) makes it impossible to carry out a network-wide evaluation of their effects on the quality signal. A random sample analysis of areas where it is known that a measure has been implemented can demonstrate the possibilities of the standard deviation of the gauge. To this end, the annual values and their means before and after a measure will be compared. As previously in the fractal analysis context, the values in brackets refer to the 75% quartile and the value outside them to the mean quality in the region under investigation.


Case H		
Superstructure: Wood 54E2 Cum. Load: 409 MGT	Inspection date: 16-07-2013 Track KM: 60.050-60.200	
	Before action:	After action:
Standard deviation [mm]	1.4 (1.6)	2.1 (2.3)
Mean [mm]	13.9 (17.8)	8.5 (10.8)
		

Table 12 Case Study H

In case study H (see Table 12) a sudden change in the quality signal of the gauge is noticeable. Even before the measure, the wooden sleepers in the section exhibit a standard deviation of 1.4, a high value which corresponds to their age and the curve shape. The installation of tie plates in 2012 resulted in a reduction in the gauge widening, while the standard deviation of the gauge increased significantly. A local assessment of the condition indicated corrugations and in places badly worn sleepers. Since track renewal in this area is not possible due to operating conditions, fastening system repairs will be considered within the coming years.

Case studies I and J illustrate the effects of such a fastening system repair on the gauge quality signal. The standard deviation of the gauge is clearly improved, although it is not possible to judge the effects of this measure on the medium-term evolution of the sleeper

condition. The number of values available following the fastening system repair is too limited to predict the future evolution of the condition.

Case study I is distinguished from the other examples with wooden sleepers by its a much larger curve radius ($R=1500\text{m}$). Since, in the context of fastening system repairs, individual sleepers will be exchanged where necessary, it is difficult to establish a general evaluation of this effect. Nonetheless, the effect of the action is clearly shown in the standard deviation of the gauge.

While the analysis so far has focused solely on wooden sleepers, the next example investigates more closely the effects of a rail pad exchange for concrete sleepers (case study K, Table 15). The rail pad was replaced in the route section as part of an action in 2012. The measure covered 500m of a curve with a radius of 550m. The rails themselves were not exchanged. The improvement achieved in the track is clearly shown by a reduction in standard deviation of the quality signal to just 0.5. The rail pad exchange was carried out on both tracks and led to comparable results, although the improvement is more strongly expressed on track 1. In the context of this work the results for track 1 were concretely examined. These results showed a particularly high value of the standard deviation of the spur at kilometre 4.100. A close investigation of this region showed that shortly after installation the rail pad was already exhibiting visible signs of wear (see inspection images, Table 15).


Case I		
Superstructure: Wood 54E2 Cum. Load: 409 MGT	Inspection date: 04-10-2012 Track KM: 23.200-23.700	
	Before action:	After action:
Standard deviation [mm]	1.8 (2.1)	0.8 (0.8)
Mean [mm]	1.6 (3.0)	0.3 (0.8)
		

Table 13 Case Study I

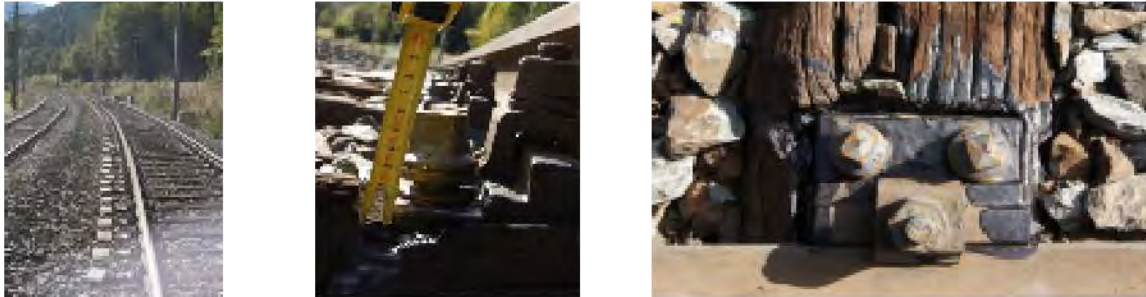
Case J		
Superstructure: Wood 49E1 Cum. Load: 482 MGT	Inspection date: 04-10-2010 Track KM: 60.050-60.200	
	Before action:	After action:
Standard deviation [mm]	1.4 (2.1)	0.9 (0.9)
Mean [mm]	7.4 (13.0)	3.3 (3.4)
		

Table 14 Case Study J


Case K		
Superstructure: Concrete 60E1 Cum. Load: 546 MGT	Inspection date: 15-10-2013 Track KM: 3.800-4.300	
	Before action:	After action:
Standard deviation [mm]	1.4 (1.7)	1.0 (1.2)
Mean [mm]	5.3 (7.0)	0.6 (2.0)
		

Table 15 Case Study K

Case study L is notable for its relatively small cumulative load. It refers to track laid in 2006. This newly laid section had an estimated load of 150 million gross tonnes in the following seven years, exhibiting clear signs of wear. A comparison of the average annual values shows a clear increase in the quality signal. In this section, the breakage of individual SKL fastenings, the cracks in individual tension fastenings and the visible wear in the rail pad across the whole section make the implementation of a measure urgently necessary.


Case L		
Superstructure: Concrete 60E1 Cum. Load: 151 MGT	Inspection date: 14-10-2013 Track KM: 90.400-90.700	
	Before action:	After action:
Standard deviation [mm]	0.6 (0.6)	0.9 (1.0)
Mean [mm]	7.3 (8.7)	12.0 (14.7)
		

Table 16 Case Study L

This section will be rounded off with an example that demonstrates the effects of neglecting to replace the rail pad in terms of the quality values. In a straight section the standard deviation of the gauge increased from 1.6 to 2.0 over recent years. On a local inspection of the rail feet, advanced damage to the sleeper fastening was already visible (see Table 17, left-hand image), while the applied forces applied resulted in some cases in cracks in the concrete sleepers (see Table 17, right-hand image).


Case M		
Superstructure: Concrete 54E2 Cum. Load: 385 MGT	Inspection date: 15-10-2013 Track KM: 71.500-71.600	
	2008	2013
Standard deviation [mm]	1.6 (1.6)	2.0 (2.0)
Mean [mm]	-1.0	-1.4
		

Table 17 Case Study M

In summary, a rail pad exchange is recommended for concrete sleepers with a standard deviation of 1.0 to 1.5. This is not only shown by the evaluation of the case studies, but also by the correlation with the rail inclination.

Standard deviations that are significantly higher than this indicate a partial system failure, necessitating other measures such as the exchange of individual sleepers. Fastening system repairs should be carried out for wooden sleepers with a standard deviation of 1.5 to 2.0. Although at the present time the medium-term evolution of the sleeper condition cannot yet be estimated, this measure indicates clear success. The effects of adjusting the track fastenings could not be further investigated in this work due to a lack of information.

4.5 Evolution of the standard deviation over the cumulative load

The findings in the previous chapter demonstrate that additional information about the condition can be determined from the standard deviation of the gauge.

In the case of concrete sleepers, the standard deviation of the gauge makes it possible to determine the condition of the rail pad and the fastening system. In places, statements can even be made about the condition of the sleeper itself.

For wooden sleepers, higher values for the gauge indicate possible traction problems and thus describe associated bottlenecks on the sleeper itself.

The values for the standard deviation are dependent on the installed sleeper type at various levels. Wooden sleepers naturally exhibit higher standard deviations for the gauge. To explain this difference, a closer examination of the evolution of the standard deviation over the cumulative load is required. An additional question arises concerning the effects of different rail profiles on the calculated value. Previous research (cf. [Liu 2013]) demonstrates increased rail foot tension in cases of different rail profiles (60E1 and 54E3). This tension mismatch must be reflected to some extent in the evolution of the standard deviation of the gauge.

In order to illustrate such a difference, it is necessary to depict the evolution of the statistical indicators over the cumulative load. To investigate the load-dependent evolution, it is necessary to differentiate between individual track superstructure combinations (rail profile and sleeper type), without, however, limiting the sample population too stringently. If the sample population size is too small, the results of observing the evolution will be widely distributed, making interpretation difficult.

Given that around 80% of the TUG network lies in straight route sections ($R > 600\text{m}$), the evaluation of different track superstructure combinations will focus entirely on these. An overview of the frequency distribution for the installed track superstructure yields three major combinations. Based on these, the following evaluation investigates the differences

between track superstructure combinations 54E2 and 60E1 for concrete sleepers and 45E2 for wooden sleepers, in terms of the evolution of the standard deviation of the track gauge. Potential cross-sections with a cumulative load greater than 500 million tonnes are not considered in this analysis.

Previous evaluations have already indicated a general difference in the absolute expression of the standard deviation of the track gauge between wooden and concrete sleepers. Irrespective of the type of rail profile, a similar difference is discernible over the entire evolution. Concrete sleepers begin their evolution at a value of 0.5, independent of the installed rail profile, while wooden sleepers start off with a value almost double that. The deterioration rate of wooden sleepers reduces over time, while for concrete sleepers it exhibits an approximately linear progression.

Despite the distribution of the results, some conclusions can be drawn from this evolution. A 54E2 rail profile leads to a greater increase in the standard deviation of the gauge than the 60E1 rail profile for concrete sleepers. The emergence of corrugations in the wooden sleepers results in a rapid increase in the standard deviation over the first 125 million tonnes. Eventually, the increase is equivalent to that of concrete sleepers. By contrast, wooden sleepers result in much wider scattering, which can be attributed to the wide variety of different fastenings.

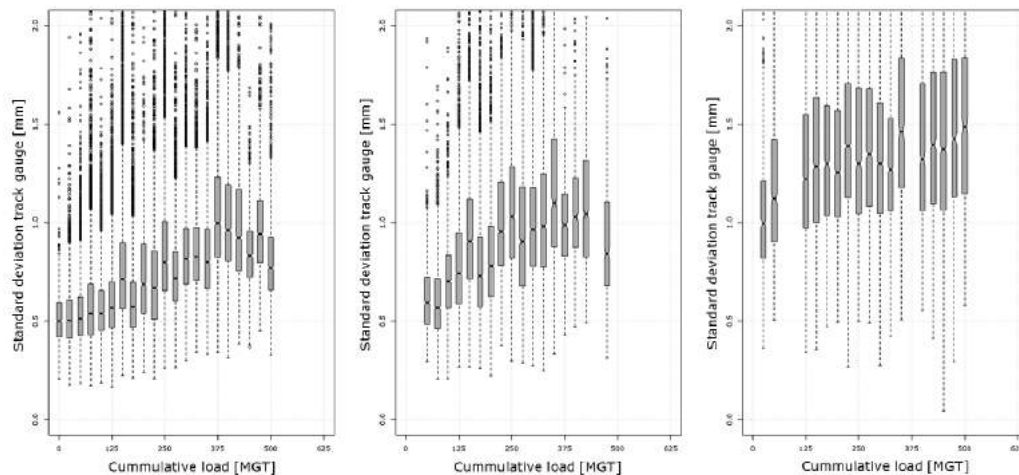


Figure 105 Evolution of the Standard Deviation Track Gauge for a Window Length of 25m, for different Combinations of Track Superstructure Types; left: 60E1 Concrete Sleepers, middle: 54E2 Concrete Sleepers; right: 54E2 Wooden Sleepers

Applying a filter to the rail profile would result in too small a population to visualize the effects of routing elements on the evolution of the standard deviation. Despite the above insights regarding the different track superstructure types, the difference between individual rail profiles will be considered acceptable for the purposes of the following evaluation. In order to reduce the extent of scattering, a linear regression will be calculated from the

means of individual load groups and categories, and their parameters compared. However, the difference between the individual sleeper types for wood and concrete cannot be neglected, as the difference between their standard deviations is too great. These and the radius categories: $R > 600$ (R1), $400 < R < 600$ (R2) and $250 < R < 400$ (R3) will form the parameters considered in the following evaluation.

The specified thresholds are based on the previous results. The evaluations of the installation and removal quality and the correlation between gauge and rail inclination will be taken into account, as will the local inspections. These will be treated as guidelines, although further investigation is necessary to demonstrate their stability.

The evolution of the standard deviation of the gauge for concrete sleepers has a uniform start value of 0.5 for all the radius categories under consideration, and results in a larger increase for smaller radii. As such, it reflects the increased stresses in curves which affect rails, fastenings and sleepers. A similar picture emerges for wooden sleepers, although these initially exhibit higher values in straight stretches than curve areas. This difference may be due to the fact that wooden sleepers are nowadays only installed in straight stretches where particular circumstances require them. In most cases, these special circumstances lead to increased demands, and thus to increased wear. Despite this, the difference can be ignored.

Interestingly, wooden sleepers in different radius categories exhibit different cumulative loads at removal, but the same value for the standard deviation of the gauge. An equivalent phenomenon is not observed, or rather inversely observed, for concrete sleepers. However, this would further imply that if a component is removed at a uniformly determined quality, when the component reaches this quality then it has reached the end of its service life. Accordingly, it follows that wooden sleeper tracks are removed due to the condition of the sleepers.

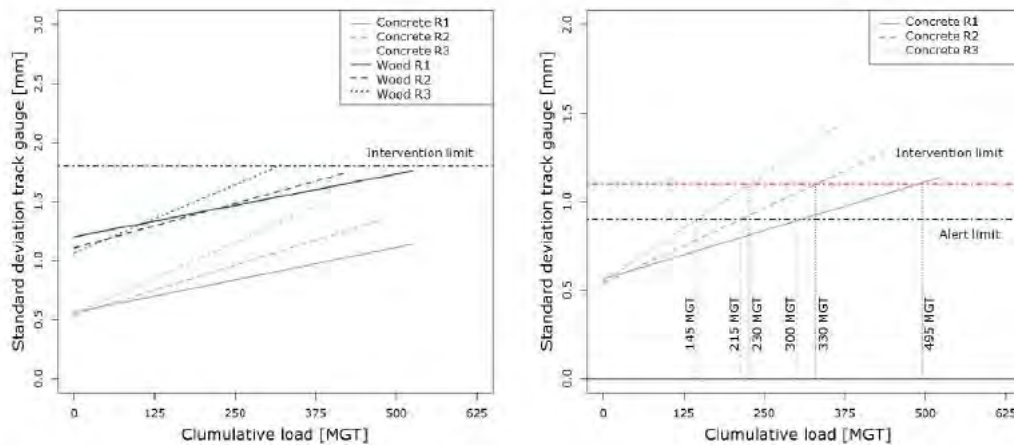


Figure 106 Evolution over the cumulative Load of the Standard Deviation of the Gauge with a Window Length of 25m, filtered by Radii Classes and Sleeper Form

However, in all concrete sleeper radius categories, it is the rail pad replacement which emerges as the dominant factor. By projecting the points of intersection with the threshold lines (marking points where it is necessary to consider an exchange of the rail pad, or urgent exchange of the rail pad against the increasing standard deviation of the gauge, for concrete sleepers, it is possible to identify the suggested cumulative load for component exchange. For the attention threshold (consider an exchange), these suggestions take marginally higher load values than have been identified in currently published works (cf. [Auer 2005]).

The glancing intersection with the straights has a marginal alteration in threshold value, which leads to a massive increase in the cumulative load threshold. If the threshold for immediate exchange is altered, the effect on the resulting number of rail pad exchanges must be clarified by a sensitivity analysis. The load value for this threshold is clearly approximately 100 million tonnes higher (see Figure 106).

Nonetheless, the marginal deviation from existing values (see Figure 107) indicates the feasibility of this result, despite the different approaches.

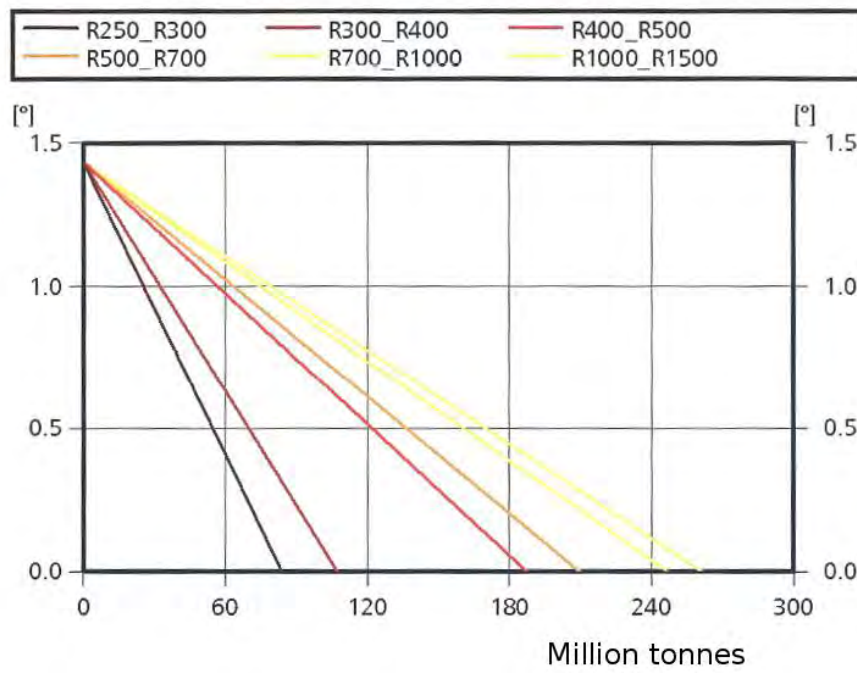


Figure 107 Change in the Rail Inclination (60E1, Rail Pad K2a Concrete Sleepers) [Auer 2005]

4.6 Network-wide Evaluation

Wooden sleepers are installed in only 25% of the TUG network, and their numbers continue to decrease. Concrete sleepers are installed in 65% of the network, 10% of them with USP. In the remaining part of the network, sleepers are installed which have not been considered in the evaluations due to their small sample sizes or which have not been clearly assigned due to a lack of information.

Discontinuities are generally excluded from the evaluation; these include switches, intersections, bridges and tunnels. Transition regions between rail profiles and sleeper types have, however, been taken into account. If the rail pad exchange for concrete sleepers is taken as an initial focus for the evaluation, then, after the discontinuity algorithm restrictions have been applied, the length of track evaluated should be either 2.052km (for a window length of 100m) or 1.597 (for a window length of 25m). The standard deviation track gauge with a window length of 100m exceeds the alert limit on 400km of track. This value appears sensible given the selection of the threshold, which was chosen with a conservative certainty of 0.9. If this value is increased to 1.1, and the calculation then repeated, the algorithm only indicates 200km. Without further investigation towards confirming the thresholds, there is no way to reduce the variation in results. Nonetheless, providing this uncertainty is taken into account, the standard deviation track gauge makes it possible to estimate whether a rail pad replacement is necessary.

According to the evaluation, the standard deviation of around 14 km of concrete sleepers and 73 km of wooden sleepers, considering a sliding window length of 100m, exceeds the assumed threshold for the critical sleeper condition. This clearly shows the difference arising from the choice of window length. This results from the fact that these values are principally exceeded in short sections, and the shorter window length will thus result in the high value being more strongly represented.

4.7 Summary

The evolved parameter describing the standard deviation track gauge makes it possible, based on the above findings, to describe the interaction between the rails, fastenings and sleepers. For concrete sleepers, it is then possible to draw conclusions about the condition of the rail pad, as well as the partial failure of individual components (broken sleepers). When describing wooden sleepers, the standard deviation of the gauge primarily aims to determine the traction, thus making it possible to indirectly generate information about the condition of the sleeper.

Time series analysis of both the mean and the standard deviation of the gauge leads to reproducible results which fulfil the original expectations. While the mean of the specified gauge tends to widen in curved sections as a result of the applied forces and the unequal use of the rail profile, in straights, the gauge tends to narrow. A positive increase in the standard deviation of the gauge is evident for both areas, but considerably more so in curve sections than in straights. The lack of information concerning measures to improve the condition makes it difficult to determine the condition of the sleepers or the interaction between rail, fasteners and sleepers. Local inspections combined with observations of track renewal projects over recent years make it possible to formulate suggested threshold values. Comparing the annual standard deviation values with the specified thresholds results in an estimation of the necessary rail pad exchange and enables a description of the sleeper condition.

The topic of component distribution still presents many questions for future work. The subject of medium-term effects of fastening system repairs or adjustment of track fastenings has only been touched on in examples at this point. An extension of the analyses to additional signals would improve the precision of the description of the track condition and thus has future potential.

5

Epilogue

The work presented here outlines a method for determining the condition of the different track components based on the analysis of recording data, in order to construct a sustainable asset strategy. The analysis of existing recording data makes it possible for infrastructure managers to evaluate the current component-specific condition of the individual components as well as to predict their temporal evolution, thereby enabling long-term strategic maintenance and investment planning.

The condition evaluation takes place for various components, beginning from the individual cross-section leading to a network-wide evaluation. The network-wide evaluation of the asset condition provides a way to plan medium-term, goal-oriented budgets. It is, however, difficult to make detailed statements about future machine deployments from the available analyses. Since operational parameters are major factors, simple analysis of measurement signals does not make reliable action planning possible. The measurement signal analysis aids the planning, provides arguments for necessary measures, and facilitates strategic planning, but does not replace strategic planning. In addition, planning of measures and strategic planning are subject to economic considerations.

The observation of the track geometry in the context of this work is based on two different approaches:

Regression model analyses establish a **track geometry quality evaluation** dependent on the cumulative loads applied to the system. The assignment of individual cross-sections

to different quality categories makes it possible to plan the focus of maintenance operations and reinvestment projects in medium term.

By contrast, fractal analysis thresholds do not support the allocation to individual category classes but give you detailed information if the track geometry is influenced by weak sub-soil or ballast brake down. The temporal evolution of dimensional values for the cross-section makes it possible to estimate the remaining service life, thus facilitating a **long-term prediction about the evolution of the track ballast**.

The standard deviation of the gauge presents a quality signal which makes it possible to determine the interaction between the rails, sleepers and fastenings, based on the existing recording signals. By representing this interaction, it is possible to make long-term plans for rail pad exchanges based on a regression model, and for wooden sleepers, to **determine the condition of the sleeper** itself.

In a final step, the findings are combined. Application of the resulting combined algorithm to 42 planned reinvestment projects in the TUG network aims to demonstrate the possibilities of determining the condition of the components based on recording data. A combination of the individual indicators into a single combined indicator has not been proposed, as this would reduce the predictive power of the individual evaluations.

Forty-two reinvestment projects of varying length were examined as part of a multi-year project with the ÖBB, with attention being paid both to the technical aspects and to their economic sustainability. All of these reinvestment projects will be carried out by the ÖBB within the next few years. The height of the bars in Figure 108 indicates how many cross-sections are included in the calculation. The height of the bars for track superstructure information indicates the length of the project. This is used because, unlike the observed quality signals and values, there are no missing values. In order to simplify the interpretation of the figure, only the critical classes have been visualized. The critical classes are defined as follows:

- I Track geometry class 3 to class 5
- I Fractal analysis from a value < -7 (values for Slope3)
- I Standard deviation track gauge > 1.8

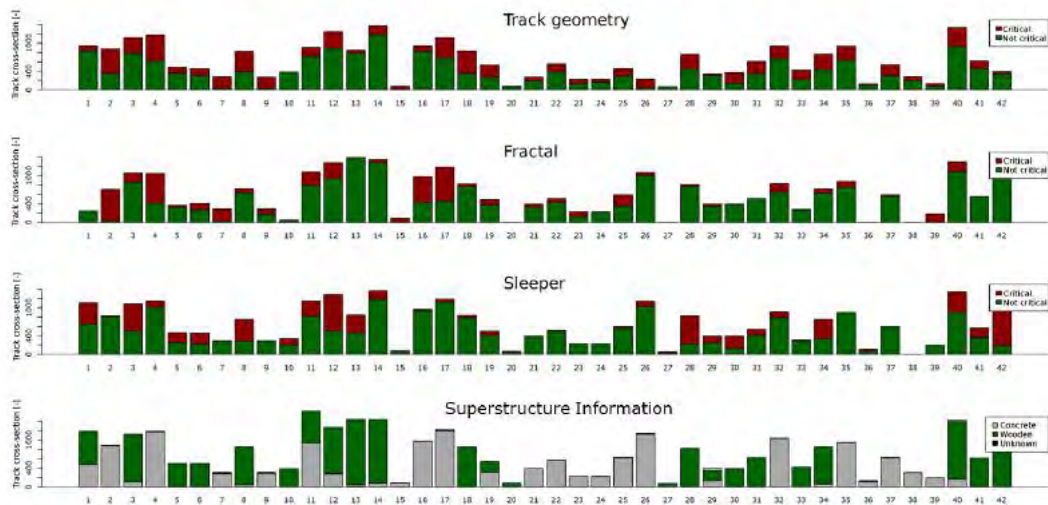


Figure 108 Algorithm to determine the Condition of Track Components based on Recording Data is applied to 42 Reinvestment Projects planned for the next three Years.

However, despite the existing definitions, it became necessary to extend the classes (to decrease limits) in order to account for temporal deterioration. This reduction aims to take into account the fact that there are at least three years between the project assessment and its realization. This will result in an estimate, since a network-wide regression model is not available for all assessments and therefore the temporal evolution of the parts can only be approximated. More than 90% of the reinvestment projects exhibit a clear proportion within the critical class for at least one of the three areas (track geometry, fractal, sleepers), thereby presenting technical grounds for reinvestment in part of the track. The only exceptions are project 14 and certain projects which have a project length of less than 400m.

The algorithm developed here for determining the condition of the track based on recording data provides a basis for reasoning about necessary measures, therefore making goal-oriented resource allocation possible. The question of economic sustainability for individual projects cannot be generally answered by this analysis, as the example of project 14 clearly shows. However, this was not the stated goal of the work. By contrast, within individual reinvestment projects, technical weaknesses in the track can be clearly identified, thus making it possible to classify the component condition.

Measure everything that can be measured.

And everything that cannot be measured, make it measurable.

Archimedes 287-212 BC

Bibliography

- Audley, M. & Andrews, J.D. 2013, "The effects of tamping on railway track geometry degradation", *Proceedings of the Institution of Mechanical Engineers, Part F: Journal of Rail and Rapid Transit*, no. 4, pp. 376-391.
- Auer, F. 2013, "Internationaler Trend in Richtung Multifunktions-Messfahrzeug", *Eisenbahntechnische Rundschau*, no. 12, pp. 26-30.
- Auer, F. 2010, *Zur Verschleißreduktion von Gleisen in engen Bögen*, Graz University of Technology.
- Auer, F. 2005, "Optimierter Zwischenlagenwechsel bei den ÖBB", *ZEV Glaser Annals*, no. 10, pp. 440-443.
- Auer, F. 2004, "Gleislagequalitätsanalyse zur Instandhaltungsoptimierung", *Eisenbahntechnische Rundschau*, no. 4, pp. 838-844.
- Auer, F. 2003, *Theoretische Untersuchung des Gleislagequalitätsparameters MDZ nach ADA II im Oberbaumesswagen EM250 der Österreichischen Bundesbahnen*, Research paper of the Austrian federal railways, Vienna.
- Auer, F., Zuzic, M., Schilder, R. & Breymann, H. 2007, "13 Jahre Erfahrung mit gleisgebundener Untergrundsanierung im Netz der ÖBB", *Eisenbahntechnische Rundschau*, no. 12, pp. 817-827.
- Backhaus, K. 2011, *Multivariate Analysemethoden: eine anwendungsorientierte Einführung*, Springer, Berlin.
- Bocciolone, M., Caprioli, A., Cigada, A. & Collina, A. 2007, "A measurement system for quick rail inspection and effective track maintenance strategy", *Mechanical Systems and Signal Processing*, no. 3, pp. 1242-1254.
- Bundesministerium für Wissenschaft und Verkehr 1971-2001, *Eisenbahn- und Seilbahnstatistik*, Republik Österreich, Vienna.
- Bundesministerium für Wissenschaft und Verkehr 01.01.2013, "Rahmenplan 2014-2019", [Online].
- Chrismer, S. & Selig, E. 1993, "Computer model for ballast maintenance planning", *Proceedings of 5th International Heavy Haul Railway Conference, Beijing, China*.
- Enzi, M. 2011, *Optimaler Re-Investitionszeitpunkt für den Oberbau von Streckenabschnitten*, Graz University of Technology.
- Faiz, R.B. & Singh, S. 2009, "Information analysis of rail track for predictive maintenance", *WSEAS Transactions on Computer*, pp. 1123-1133.
- Frederich, F. 1984, "Die Gleislage – aus fahrzeugtechnischer Sicht", *Zeitschrift für Eisenbahnwesen und Verkehrstechnik – Glaser Annals*, no. 12, pp. 355-362.
- Führer, G. 1979, *Oberbauberechnung*, Verlag für Verkehrswesen, Berlin.

- Guler, H., Jovanovic, S. & Evren, G. 2011, "Modelling railway track geometry deterioration", *Proceedings of the ICE-Transport*, no. 2, pp. 65-75.
- Hanreich, W. 2004, "Modern Fahrweginspektion mit dem oberbautechnischen Messwagen EM 250", *ZEV Rail Zeitschrift für das gesamte System Bahn*, no. 9, pp. 18-27.
- Hanreich, W., Wogowitsch, M. & Datler, M. 2008, "Umsetzung des Instandhaltungsplanes bei ÖBB Infrastruktur nach internationalen Normen", *Eisenbahntechnische Rundschau*, no. 9, pp. 548-551.
- Hansmann, F. 2011, *Entwicklung eines Prognosemodells zur Planung von Stopfeinsätzen*, Institute for railway engineering and transport economics, Graz University of Technology.
- Hansmann, F. & Landgraf, M. 2013, "Wie fraktal ist die Eisenbahn?", *ZEV Rail Zeitschrift für das gesamte System Bahn*, no. 11-12, pp. 462-470.
- Hansmann, F., Marschnig, S. & Veit, P. 2011, *Eisenbahnwesen 1, Integrierte Instandsetzung- Versuch der Darstellung ihrer Auswirkung auf die Gleislage*, Institute for railway engineering and transport economics, Graz University of Technology.
- Hansmann, F. & Marschnig, S. 2012, "Der GleisPROPHET - ein Impuls zur Nachhaltigkeit", *ZEV Rail Zeitschrift für das gesamte System Bahn*, no. 9, pp. 350-357.
- Hempe, T. 2014, "Oberbau im Instandhaltungs- und Anlagenmanagement", *Eisenbahningenieur*, no. 9, pp. 112-116.
- Holtzendorff, K. 2003, *Untersuchung des Setzungsverhaltens von Bahnschotter und der Hohllagenentwicklung auf Schotterfahrbahnen*, Berlin University of Technology.
- Holzfeind, J. 2009, *Zur Prognostizierbarkeit des Qualitätsverhaltens von Gleisen- Analyse des Qualitätsverhaltens am Einzelquerschnitt*, Graz University of Technology.
- Hummitzsch, R. 2009, *Zur Prognostizierbarkeit des Qualitätsverhaltens von Gleisen- Statistische Analyse des Gleisverhaltens zur Erstellung eines Prognosemodells*, Graz University of Technology.
- Hyslip, J.P. 2002a, "Fractal analysis of track geometry data", *Transportation Research Record: Journal of the Transportation Research Board*, no. 1, pp. 50-57.
- Hyslip, J.P. 2002b, *Fractal Analysis of Geometry Data for Railway Track Condition Assessment*, University of Massachusetts Amherst.
- Iliev, D. 2012, *Die horizontale Gleislagestabilität des Schotteroberbaus mit konventionellen und elastisch beschlten Schwellen*, Chair and Institute of Road, Railway and Airfield Construction, Technical University of Munich.
- Jovanovic, S. 2003, "Kostenreduktion bei der Oberbauinstandhaltung durch ECOTRACK", *Eisenbahningenieur*, no. 5, pp. 30-34.
- Kipper, R., Gerber, U. & Schmeister, J. 2013, "Bestimmung langweiliger Gleisverformungen und deren Bewertung", *ZEV Rail Zeitschrift für das gesamte System Bahn*, no. 2, pp. 11-16.

- Landgraf, M. 2016, *Zustandsbeschreibung des Fahrwegs der Eisenbahn - Von der Messdatenanalyse zum Anlagenmanagement*, Thesis, Graz University of Technology.
- Landgraf, M., Hansmann, F., Marschnig, S. & Veit, P. 2014, "Track Geometry and Substructure - a Provable Correlation?", *ACTGEORAIL 14*, ed. Librairie Ifsttar.
- Lehmann, R. 2012, *Der Einfluss statistischer Ausreißer auf die Schätzung der natürlichen Variabilität in Daten zu Biota*, Rheinisch-Westfälische Technische Hochschule Aachen.
- Lichtberger, B. 2010, *Handbuch Gleis*, 3. edn, DVV Media Group, Hamburg.
- Lichtberger, B. 2007, "Der Querverschiebewiderstand der Gleise", *EIK Eisenbahningenieurkalender*, pp. 61-76.
- Liu, J. 2013, *Einfluss der Schienenbefestigungskomponenten auf das laterale Verformungs- und Lastverteilungsverhalten der Schiene*, Technical University of Munich.
- Mandelbrot, B.B. 1983, *The fractal geometry of nature*, Macmillan.
- Mandelbrot, B.B. 1977, *Fractals: form, chance and dimension*, 1st edn, Freeman, San Francisco.
- Mandelbrot, B.B. 1967, "How long is the coast of Britain", *Science*, no. 3775, pp. 636-638.
- Mandelbrot, B.B. & Blumen, A. 1989, "Fractal Geometry: What is it, and What Does it do? [and Discussion]", *Proceedings of the Royal Society of London A: Mathematical and Physical Sciences*, no. 1864, pp. 3-16.
- Marschnig, S. & Berghold, A. 2011, "Besohlte Schwellen im netzweiten Einsatz", *Eisenbahntechnische Rundschau*, no. 5, pp. 10.
- Matsuda, H., Takikwan, M., Ogiso, K. & Yazawa, E. 2011, "Study of Condition Monitoring for Track Irregularity and Track Materials using Commercial Test Car", ed. World Congress on Railway Research.
- ÖBB Infrastruktur AG 2012, *Instandhaltungsplan- Oberbauanlagen DB IS 2 Teil 1*, Interne Richtlinie, Vienna.
- ÖBB Infrastruktur AG 2009, *B50- Teil 1 Oberbauformen*, Interne Richtlinie, ÖBB Infrastruktur AG, Vienna.
- ÖBB-Holding AG 2013, "Geschäftsbericht 2007-2012", [Online].
- Oberlechner, G., Metzger, B. & Zywiel, J. 2001, "GPS-unterstütztes Standortsynchronisation", *Eisenbahntechnische Rundschau*, no. 1/2, pp. 53-55.
- Orford, J. & Whalley, W. 1983, "The use of the fractal dimension to quantify the morphology of irregular-shaped particles", *Sedimentology*, no. 5, pp. 655-668.
- Österreichisches Normungsinstitut 2009, *ÖNORM EN 13848-1*, Richtlinie, Österreichisches Normungsinstitut, Vienna.

- Österreichisches Normungsinstitut 2014, *ÖNORM EN 13848-6*, Richtlinie, Österreichisches Normungsinstitut, Vienna.
- Pace, P. 2012, "Time to eliminate the data graveyards", *Railway Gazette International*, no. 12.
- Plasser & Theurer 2013, *Track Recording Cars*, Plasser & Theurer Export von Bahnbau-maschinen Gesellschaft m.b.H., Vienna.
- Rießberger, K. 1997, "Gleisgeometrie und Wirtschaftlichkeit- oder: wie gut muss ein Gleis sein?", *Österreichische Verkehrs Gesellschaft- Spezial*, pp. 64-94.
- Rohim Boy Berawi, A. 2013, *Improving Railway Track Maintenance Using Power Spectral Density*, University of Porto.
- Röhlsler, M. 2013, "Jahresbericht 2005-2013", [Online].
- Schöpp, A. 2011, *Gleislagequalität – Hohllagen bei Betonschwellengleisen*, Leopold-Franzens University, Innsbruck.
- Schultheiß, H. & Schulz, G. 1985, "Schwellen für die Deutsche Bundesbahn", *Eisenbahn-technische Rundschau*, no. 10, pp. 723-728.
- Selig, E., Cardillo, G., Stephens, E. & Smith, A. 2008, "Analysing and forecasting railway data using linear data analysis", *Proceedings of the 11th International Conference on Computer System Design and Operation in Railways and other Transit Systems*.
- Terashima, R., Matsuda, H., Takikawa, M. & Kozeki, M. 2011, "Study of Condition Monitoring for Track Irregularity and Track Materials using Commercial Test Car", World Congress on Railway Research.
- UIC 2010, *Guidelines for the Application of Asset Management in Railway Infrastructure Organisations*, 2nd edn, International Union of Railways, Paris.
- Veit, P. 2013, "Instandhaltung und Anlagenmanagement des Fahrwegs", *Handbuch Eisenbahninfrastruktur*, pp. 1009-1054.
- Woodhouse, J. 2014, "Briefing: Standards in asset management: PAS 55 to ISO 55000",
- Yella, S., Dougherty, M. & Gupta, N.K. 2009, "Condition monitoring of wooden railway sleepers", *Transportation research part C: emerging technologies*, no. 1, pp. 38-55.
- Zhang, Y., Murray, M. & Ferreira, L. 1999, "An integrated model for track degradation prediction", *World Transport Research: Selected Proceedings of the 8th World Conference on Transport Research*.

Annex 1 Glimpses into the TUG database

The TUG database was created in the Institute for Railway Engineering and Transport Economy at the Graz University of Technology in 2009, and has been gradually extended over recent years. The database combines information about the railway from a variety of data sources, allowing both network-wide and cross-section-specific evaluation of the data. Individual publications (cf. [Hummitzsch 2009], [Holzfeind 2009] and [Enzi 2011]) have already given detailed attention to explaining the precise construction of the database, thus only the main features will be outlined here.

Information is not assigned continuously in the TUG network, but discretely every five metres for route cross-sections. This means that data is available at five metre intervals, with no data in between. This system reduces the amount of data stored, and paradoxically rules out a loss of essential information, since more detailed data output would not be supported by the input accuracy. Even when the recording signals exhibit a smaller sampling rate than the distance between two route cross-sections, the calculated quality signals will simply be associated with the particular cross-section.

Annex 2 Construction of the TUG database

In order to use the information from varied data sources, it is necessary to convert it into a suitable datastructure. The foundation for the projection is based on aggregating individual ÖBB routes into larger connected sections with increasing lengths (see Figure 109). The resulting sections are then labelled as TUG routes.

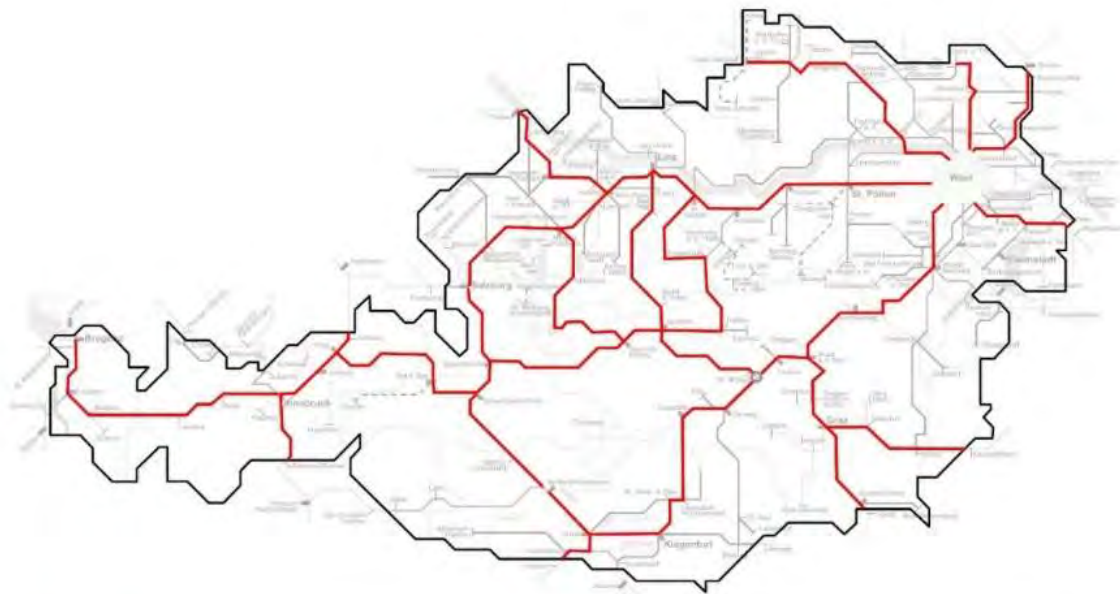


Figure 109 Visualization of the Austrian railway network [grey] and the TUG network routes [red]

The three levels of categorization, "TUG route", "track number" and "track kilometre" make it possible to form a primary key to individually identify every route cross-section in the TUG network. Using this system, the complete TUG network is divided into 22 TUG routes which covered around 3,000 kilometres of track at the time of writing. This makes it possible to represent a large part of the main ÖBB network in the TUG network.

Structures	Bridges Tunnels Stations Intersections Turnouts Station names	Measurement signal	Track gauge Distance between rail feet Rail inclination Rolling lap Track geometry filtered 1-70 m Track geometry filtered 3-25 m
Layout	Curvature Radius Cant Speed restriction	Quality signal	SigmaH SigmaR MDZ-a Standard deviation track gauge Mean value of track gauge
Machine information	Operation type Operation time	Quality value	Period start quality Deterioration rate DeltaSchnitt
Superstructure	Rail profile Rail grade Rail installation year Sleeper type Sleeper installation year	Load Data	1997 1998 1999 2000 2001 2002 2007 2010

Figure 110 Overview of the information assigned to each route cross-section.

Annex 3 Recording signals, quality signals and quality values

An ÖBB recording car captures the condition of the track at regular intervals, in the form of measurements or quality signals. These data are validated and added to the TUG network annually. The database does not currently aim to represent short-term developments or to determine the precise temporal condition of the assets, but rather to provide a database for various researches.

In principle, the current database contains the details of all valid recording journeys between 2001 and the end of 2013, as well as additional information (see Figure 110). In order to use a consistent database for the evaluations in this work, only the journeys before 2001 and the end of 2012 were consulted. In this way, potential subsequent changes in the data could not affect the results developed here. The number of annual recording journeys increased significantly over the years up to 2005. As a result, the main evaluations, providing they do not take a regression model into account, refer to the period between 2005 and 2012. Before 2005, due to the smaller number of values it was not possible to achieve adequate network coverage. Certain quantities would be too small, since for part of the network few or no values would be available to provide information about the track. With a regression model, it is possible to ignore this fact, since the temporal evolution of the values can still be interpolated over the resulting trend even when there are few measurements.

Previous researches (cf. [Hummitzsch 2009]) have established a network-wide regression model for individual quality signals (MDZ-a and SigmaH). Through this regression model, it is possible to describe the deterioration of the track geometry between two machine deployments (real or imaginary) with an exponential approach. A sudden improvement in the track geometry level when a machine deployment is not known to have taken place will be identified as an imaginary machine deployment, or "TUG operation". This operation is not only able to represent machine deployments which have not been input, but also identifies possible outliers in the time series. Whether imaginary or real, both types of machine deployment divide the observed time series in a route cross-section into individual time periods. Within these time periods, the evolution of the track geometry is described by a regression model, in which an exponential relationship is assumed (cf. [Rießberger 1997]).

The exponential approach arises from the claim that a good track deteriorates slowly, while a poor one deteriorates faster. This fact can be described mathematically with a differential equation, which can be solved to give the following form for the deterioration:

$$Q(t) = Q_n * e^{b_n * t}$$

in which Q_n represents the period start quality of the n th period after the ballast installation year. The period start quality represents the quality in the regression model taken at time zero within the n th period. For example, in the route cross-section shown in Figure 111 it is possible to identify five distinct periods. The vertical lines symbolize different types of machine deployments, where the TUG database distinguishes the following types of operation:

- Subsoil rehabilitation
- Ballast cleaning
- Track renewal
- Tamping and stabilization of tracks
- Turnout tamping
- Grinding

Other than grinding operations, all the operations mark an individual quality period. In each period, the period start quality, deterioration rate and the quality criterion "DeltaSchnitt" can be uniquely assigned. DeltaSchnitt is the absolute value of the deviation of individual measurements from the calculated regression and thus enables statements about the fit quality of the regression curve.

Potential discontinuities or transition regions affect the formation of individual quality signals and thus make precise interpretations of the results more difficult. Evaluations without these influences take into account the "valid length" criterion for the track geometry (cf. section 4.2.1). The valid length criterion detects homogeneous regions and only considers route cross-sections where the track radius, load, acceptable speed, rails, sleepers and machine deployments do not change. Structures such as stations, switches, bridges, intersections or tunnels cannot occur in valid length regions. The valid length criterion is a way to create a homogeneous sample population where the effects can be assessed free of known discontinuities.

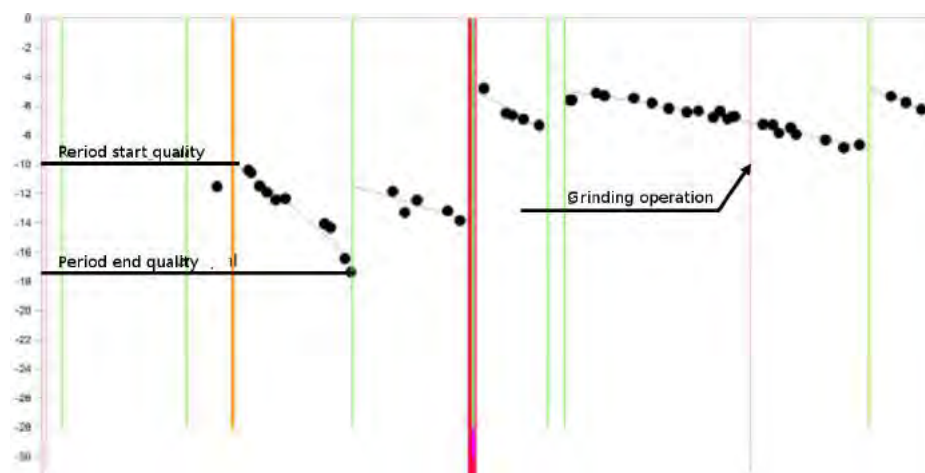


Figure 111 Typical progression of a route cross-section

Using various queries, it is possible to filter data from the database population according to specified criteria. This filtering can be cross-section specific or period-specific as required. In this way, it is possible to precisely determine the average value of a quality signal before a track renewal, or the average deviation from the standard track gauge for wooden sleepers in 2008. Using unique associations between data there is virtually no limit to the possible analyses.

Annex 4 The origins of recording signals – track geometry cars

Recording signal analysis forms a central component of this work. Therefore, without loss of generality, the measurement possibilities of a track geometry car will be described in more detail in the following section. For this description, the focus of attention will be on the recording system used to provide the signals for this evaluation. To this end, the ÖBB EM-250 recording cars (Figure 112) and the new recording car group from Plasser & Theurer will be primarily described.

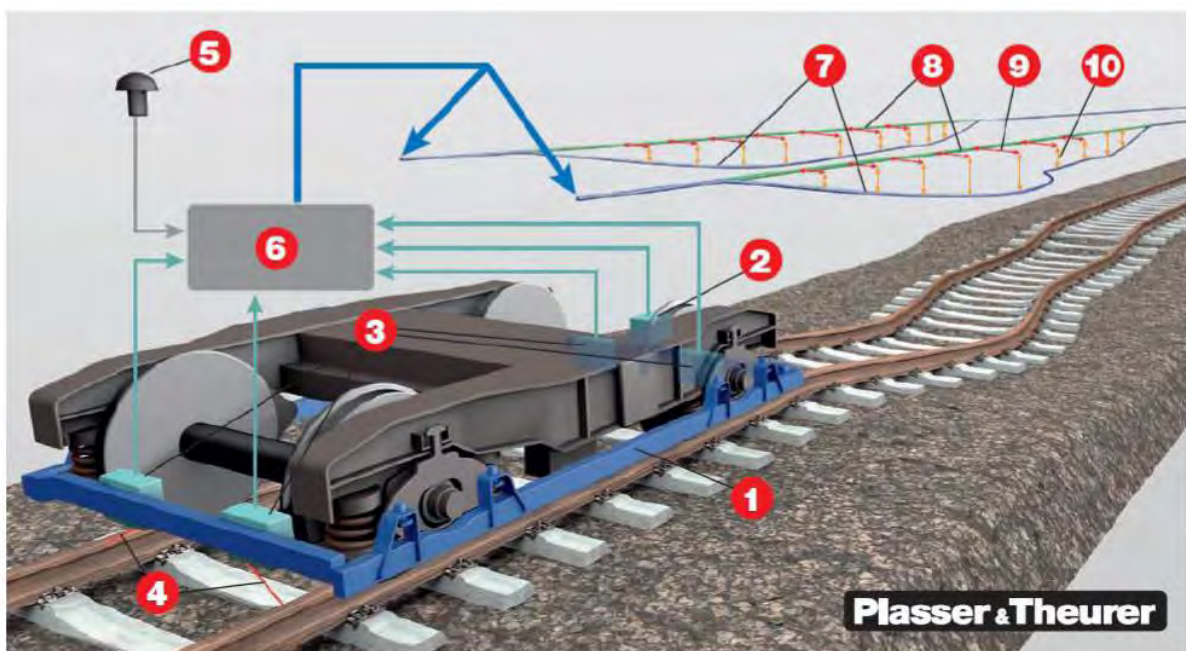


Figure 112 Recording cars: self-driving [left] [Plasser & Theurer 2013] or coupled to a train [right] [Hanreich 2004]

In recent years, both in response to the increase in high-speed routes and due to the increasing cost pressures in planning maintenance or reinvestment measures, the recorded track data has been subject to considerably more attention. Recording cars produce high precision measurements, and make it possible to take measurements while operating, either coupled to an existing train or in self-driving variants. [Auer 2013]

Annex 5 Recording track geometry

Recording the track geometry (POS/TG Position-Track Geometry Measurement System) is now standardized in Austria, using an inertial measurement unit (IMU), two optical track measurement systems (dual OGMS) and the navigation system (navigation computer with integrated GPS receiver and GPS antenna). For the actual recording, a measurement framework is coupled to the four axles of the chassis, to which the IMU and the four recording sensors for the double track gauge measurement are attached (see Figure 113). The measurement framework thus guarantees the consistent parallel alignment of the sensors and IMU in relation to the rail surface, so that these can be used as reference levels for the track measurement. With the three accelerometers and three rotary encoders which measure angular changes, it is possible to represent the motion as a 3-dimensional curve in terms of geographical coordinates. The angular changes are recorded in detail using three optical gyroscopes (rate gyros). The measurement system thus captures the translational and rotational motion, which can then be integrated twice to calculate the location of the recording vehicle and the track. The three-dimensional curve for the rails can be calculated separately from the track gauge measurements. [Hanreich 2004]



- | | |
|------------------------------------------------------------------------------------------------------------------------------------------------------------------------------------------------------------------------------------------------------------------------|----------------------------------------------------------------------------------------------------------------------------------------------------------------------------------------------------------------------------------------------------------------------------------------------------------------------------------------------------|
| <p>1 Messrahmen mit fixem vertikalen Abstand zu den Schienenoberflächen</p> <p>2 Inertial-Messeinheit IMU</p> <p>3 Messsensoren der Spurweitenmessung</p> <p>4 Laserstrahlen zur Abtastung der Spurweite</p> <p>5 GPS-Datenerfassung</p> <p>6 Navigations-Computer</p> | <p>7 Blaue Kurven: Raumkurven beider Schienen als Messergebnis, dem Gleisverlauf exakt folgend, mit GPS-Daten verortet</p> <p>8 Grüne Linien: Gleissolllage</p> <p>9 Rote Pfeile (horizontal): Richtungsfehler, aus der jeweiligen Raumkurve errechnet</p> <p>10 Orange Pfeile (vertikal): Höhenfehler, aus der jeweiligen Raumkurve errechnet</p> |
|------------------------------------------------------------------------------------------------------------------------------------------------------------------------------------------------------------------------------------------------------------------------|----------------------------------------------------------------------------------------------------------------------------------------------------------------------------------------------------------------------------------------------------------------------------------------------------------------------------------------------------|

Figure 113 How the Plasser & Thurer track geometry measurement system works

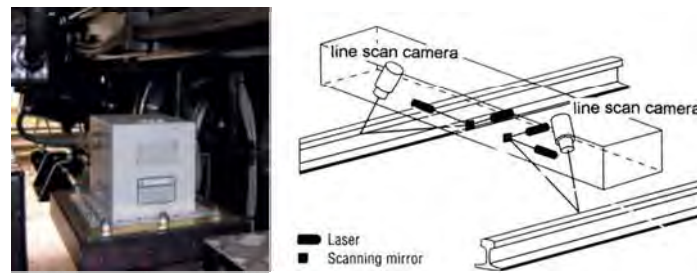


Figure 114 Inertial measurement unit [left] Measurement principles for the optical track gauge [right]

The optical measurement of the track gauge is based on determining the track gauge 14mm beneath the rail surface, using a laser triangulation with two lasers, two mirror galvanometers and two targeted cameras (see Figure 114). [Hanreich, Wogowitsch & Datler 2008]

The positioning system triggers the measurements, with 100 triggers per revolution. It is then possible to obtain all the required track geometry data, at the specified intervals (e.g. every 25cm), from the resulting 3-dimensional curve, and save it or retrieve it through the interface. During the recording, information will be supplied immediately when certain threshold values are exceeded. In addition to this, the evaluation software not only includes various algorithms for calculating indicators but also enables real-time capturing of the locations of the left and right rails, as calculated from the 3-d curve, in three different wavelengths and three different chord lengths. Historical data can thus be documented simultaneously with the recording data from other measurement systems.

Since the advent of recording, the problem of assigning the data to individual track kilometres with an appropriate accuracy in terms of reproducibility and repeatability according to EN-13005 or DIN 1219-1 has been an issue. Initially, the track geometry parameters were synchronized locally by the operator of the recording vehicle. In this way, the local start of the measurements was precisely documented, and as the recording continued, a synchronization button in the vehicle was pressed at the appropriate moment. This made it possible to establish a connection between, for example, the kilometre posts and the recorded data. However, this approach is subject to a loss of accuracy, particularly at high speeds. Consequently, a further development aimed to replace manual synchronization with magnets or beacons. This system was then developed further using encoded ALDs (Automatic Location Detectors). Each ALD is thus assigned to a unique identification number in the network, making it possible to capture the appropriate location data during the passage of the recording vehicle. However, due to the high price and high maintenance costs of the system, which are due to its sensibility to external influences, it was never installed. Instead, the development of satellite technology and an increase in the accuracy

of the entire system led Plasser American to develop a new system based on satellite data (GALS: GPS Aided Location Synchronization). This is a system which combines the data from differential GPS systems (in principle also possible with pure GPS, subject to a loss of accuracy) with the data from the POS/TG. The resulting Integrated Inertial Navigation algorithm (IIN) not only makes it possible to carry out the recording even during a brief failure of the differential GPS, but also increases the output of positional information to 200/s. A pure GPS system, by contrast, would only capture location data once per second. [Oberlechner, Metzger & Zywiel 2001]

The system described here normally exhibits an accuracy of less than 1mm within a speed range from 5km/h to 250km/h, making high-precision assignment of the recorded data possible. Even when the input data adheres to the specified standards, some processing is necessary, due to the fact that deviations of less than 2m, which occur as a result of irregularities in the recording (e.g. a long break in the GPS signal), may render the results unusable. To this end, final processing of the recording journey only uses one journey as a reference channel, and then divides the remaining journeys into 50m sections, which are subsequently shifted until the covariances of the data records approach 1. In other words, the individual recording journeys are shifted with respect to the reference channel until the individual journeys match up point for point (see Figure 115). [Hanreich, Wogowitsch & Datler 2008]

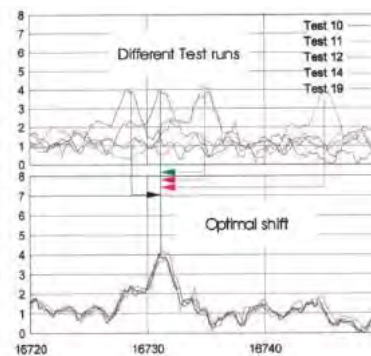


Figure 115 Comparison between the original recording journeys (above) and the recording journeys after processing (below) [Hanreich 2004]

Annex 6 Measuring rail profiles and abrasion

In order to obtain more precise information concerning the current condition of the rails, laser technology is combined with two recording cameras, which are mounted on each side of a chassis. In this way, the lasers act as detectors focused on the rail profile, making it possible to capture the entire cross-section of the rail from its base to the rail surface using the recording cameras. To this end, the laser units are precisely temperature-stabilized, in order to exclude the effects of ambient light as far as possible. Four lasers operating in the invisible frequency range scan the rails at intervals of $100\mu\text{s}$. It is possible to identify the equalized, precise cross-section profile from the rail surface to the rail foot using the resulting laser field and the two high-resolution cameras. The following parameters for the two rails can then be separately determined:

- Complete profile
- Rail elevation
- Rail-head width
- Rail inclination
- Track gauge and minimum track gauge

In addition, where known target profiles are available, the following parameters can be derived from the recorded values:

- Wear in height and width
- Wear of the rail surface, specified in square millimetres
- Rail wear at up to 9 user-specified points on the rail head

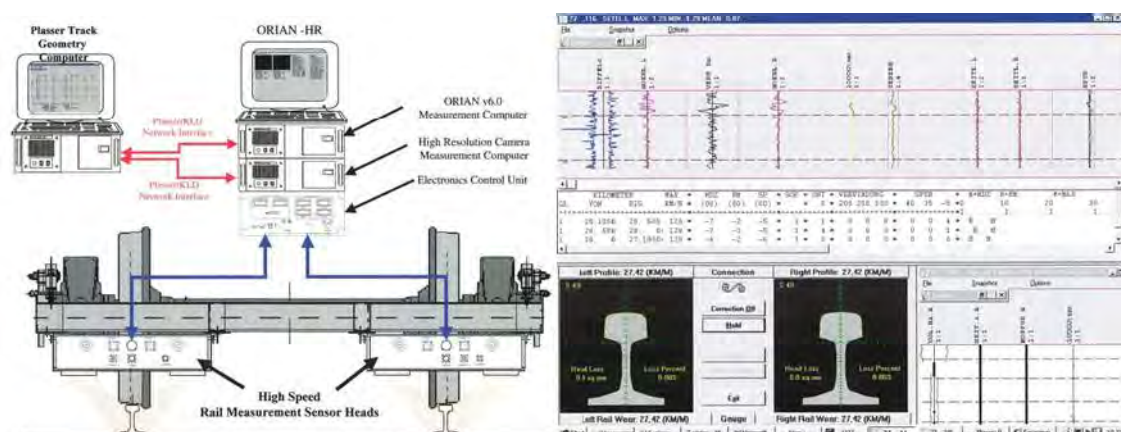


Figure 116 Recording rail profile and wear [Hanreich 2004]

If an additional camera is supplied, it is possible to determine the wheel-rail contact on the left and right rails, and then calculate the corresponding conicity with an additional algorithm. [Hanreich 2004]

Monographic Series TU Graz

Railway Research

Vol. 1 Stefan Marschnig

**iTAC – innovative Track
Access Charges**

2016

ISBN 978-3-85125-493-8

Vol. 2 Fabian Hansmann

**The Missing Link between Asset Data
and Asset Management**

2018

ISBN 978-3-85125-567-6